

**Inflammation of the Infrapatellar Fat Pad
and Knee Osteoarthritis:**

**Investigating the associations with other joint
pathologies and pain**

Hemalatha Urban

**A thesis submitted to fulfil requirements for the
degree of Doctor of Philosophy**

**Faculty of Medicine and Health
The University of Sydney**

November 2020

Statement of Originality

This statement is to certify that to the best of my knowledge; the content of this thesis is my own work. This thesis has not been submitted for any degree or other purposes except where listed below. I certify that the intellectual content of this thesis is the product of my own work and that all the assistance received in preparing this thesis and sources are acknowledged below:

My supervisors *Professor Christopher Little (CBL)* and *Professor David Hunter (DJH)* assisted in the designing of the various studies, data interpretation and thesis editing. Chapter 3 – 5 used samples from *Dr Carina Blaker's (CB)* PhD Thesis experiments. In these chapters, CBL performed all mouse surgeries with assistance from CB. CB also performed all the mechanical loading injuries with assistance from *Dr Elizabeth Clarke (EC)* as well as all animal care and tissue harvesting. *Ms Susan Smith* conducted all the histological tissue processing. I developed the adipose and fibrosis scoring system in consultation with CBL, which I scored along with the synovitis. CB carried out the remainder of the joint scoring. *Dr Sanaa Zaki* collected the von Frey data, and CB collected the incapacitance data. All histological and pain analysis was carried out by me with input from CBL. *Dr Cindy Shu* and *Ms Shihani Stoner* also provided training for real-time PCR which I conducted. *Dr Patrick Haubruck* provided training in FACS analysis from chapter 7 and guidance in the developing of the panel. All statistical analyses in this thesis were performed by myself with some assistance from *Dr Rachel O'Connell* (chapter 6).

Hemalatha Urban
BBioMedSc, MBioMedSc

10/09/2020

Authorship attribution statement

Chapter 1 of this thesis is published as a review: Urban, H. and C.B. Little, *The role of fat and inflammation in the pathogenesis and management of osteoarthritis*. Rheumatology (Oxford), 2018. **57**(suppl_4): p. iv10-iv21.

I designed the review and wrote the drafts of the manuscripts with input from my co-author.

Chapter 2 of this thesis has been submitted to Osteoarthritis and Cartilage Open as an original manuscript entitled: The impact of infrapatellar fat pad inflammation on pain in knee osteoarthritis: a systematic review and meta-analysis. **Urban, H.** Ashton, D. Ferreira, M F. Hunter, D J. Little, C B. Zaki, S.

I wrote the protocol with contributions from MLF, DJH, CBL and SZ to the development. I conducted the databases search and along with DA, screened all articles and extracted data. I wrote the drafts of the manuscripts, including the original with contributions from DA, MLF, DJH, CBL and SZ.

Chapter 6 of this thesis has been submitted to Arthritis, Care and Research as an original manuscript entitled: Hoffa-synovitis associated with centripetal adiposity, serum biomarkers of synovial inflammation and pain? **Urban, H.** Deveza, L. O'Connell, R. Little, C B. Hunter, D J.

All authors, including myself, contributed to the study conception and design. I acquired the data with assistance from LD and analysed the data with assistance from RO. I wrote the manuscripts, and all authors were involved in its interpretation and development.

In addition to the statements above, in cases where I am not the corresponding author of a published item, permission to include the published material has been granted by the corresponding author or appropriate publishing group.

Hemalatha Urban
BBioMedSc, MBioMedSc

10/09/2020

As the supervisors for the candidature upon which this thesis is based, I can confirm that the authorship attribution statements above are correct.

Christopher B Little
BVMS, PhD

10/09/2020

David J Hunter
MBBS, MSc (Clin Epi), MSpMed, PhD, FRACP (Rheumatology)

10/09/2020

Acknowledgements

The journey to my PhD started with someone taking a chance on me well before I enrolled in the course. Despite my inexperience, I landed a job with a wonderful manager and got to work with some of the most talented and inspiring researchers I've ever met. The opportunity introduced me to the world of clinical research in OA, helped me meet friends who've become like family and allowed me to become a better researcher. For that, I will be forever grateful.

I would firstly like to thank both of my supervisors, Chris Little and David Hunter, for their guidance and encouragement on this fantastic adventure. Your expertise, enthusiasm, support and drive for more have made this PhD journey one of the best experiences of my life. Chris, thank you for guiding me, believing in me when I didn't and helping discover my passion for lab work again. David, thank you for taking a chance on me all those years ago and all you've taught me during the seven years I've worked with you. I feel very fortunate to have been mentored by such inspiring individuals.

I also want to thank everyone from the GROW Team, Raymond Purves Laboratory and the broader Level 10 crew. Thank you all for the guidance, assistance and kindness over the past few years. I would be completely lost without all the help. In particular, I must thank Cindy Shu and Carina Blaker for all the guidance in the lab, with the samples and patience for my many questions. Thank you all for always having a minute to chat, for laughs, cake and wine (or Caipirinhas).

To my dear friends at work, Sarah, Leticia, Vicky, Manuela, Varshini, Jill, Carolina, Liz K and everyone else, thank you so much for always listening and encouraging me. It has honestly made going to work a joy every day, and I've missed it so much during Covid times.

This journey would have also been impossible without my family, near and far. Appa (Dad), thank you for always telling me nothing was impossible, for supporting me through my life and loving me. To my sisters, Gaya and Mona, thank you for keeping me going. I appreciate everything you've done for me throughout my life and all the things you've done from a distance, like keeping me company on my commutes home. My beautiful in-laws, Inger and Errol, thank you for everything you've done to support me. From attending my presentations to pick-ups from the station and chicken soup, so I don't have to cook. James, Nicole, and of course Floss, thank you for listening to me, all the kind words and scooter races. I love you all so very much and am nothing without you all.

Finally, and most importantly, I would like to thank my husband, Tom. Thank you for everything you've done to make this dream a reality. Thank you for all the pick-ups and drop-offs, the many cooked meals, all the motivation and belief in me. You are an amazing soul, and I am so grateful for you. You are truly my best friend, and I owe this all to you.

Also, thank you Brooklyn: for making me a cat person, interrupting zoom calls with meows and sitting next to me when I worked on this thesis.

Publications and Presentations

Publications arising from this thesis

1. **Urban, H.** Little, C B. **(2017)** The role of fat and inflammation in the pathogenesis and management of osteoarthritis. *Rheumatology (Oxford)*. 2018;57(suppl_4):iv10-iv21.
2. **Urban, H.** Eyles, J P. Huter, D J. Mills, K **(2018)** The relationship between pressure pain thresholds and anxiety in patellofemoral osteoarthritis: exploratory data. *Osteoarthritis and Cartilage*, Volume 26, S354 (Abstract)
3. **Urban, H.** Blaker, C. Shu, C. Clarke, E. Little, C B. **(2020)** Synovial inflammation in anterior cruciate ligament injury knees in mice: surgical vs non-surgical models. *Osteoarthritis and Cartilage*, Volume 28, S213 - S214 (Abstract)
4. **Urban, H.** Ashton, D. Ferreira, M F. Hunter, D J. Little, C B. Zaki, S. **(2020)** The impact of infrapatellar fat pad inflammation on pain in knee osteoarthritis: a systematic review and meta-analysis *Osteoarthritis and Cartilage Open* (Under review)
5. **Urban, H.** Deveza, L. O'Connell, R. Little, C B. Hunter, D J. **(2020)** Is Hoffa-synovitis associated with centripetal adiposity, serum biomarkers of synovial inflammation and pain? *Arthritis Care and Research* (Under review)

Infographics

1. What you need to know about Osteoarthritis and fat? **(2018)** 2018 Infographic Competition, NHMRC Musculoskeletal Centre for Research Excellence
 - *Runner up*

2. 5 Things to know about the Infrapatellar fat pad and OA. **(2019)** 2019 Infographic Competition, NHMRC Musculoskeletal Centre for Research Excellence

- *Winner*

Presentations

1. **Urban, H.** Hunter, D J. Little, C B. **(2017)** Inflammation of the Infrapatellar Fat Pad & Clinical Outcomes of the Knee: Thesis Proposal. Oral Presentation. Institute of Bone and Joint Research Seminar, Sydney, Australia

2. **Urban, H. (2017)** Fat Knees: The inflammation of the Infrapatellar Fat Pad and Clinical Outcomes of the Knee. Oral Presentation. Institute of Bone and Joint Research 2017 3 Minute Thesis Competition, Sydney, Australia

- *First place winner*

3. **Urban, H.** Hunter, D J. Little, C B. **(2017)** Inflammation of the Infrapatellar Fat Pad & Clinical Outcomes of the Knee: Protocol for an observational study. Oral Presentation. Sydney Musculoskeletal Network Scientific Meeting, 2017, Sydney, Australia

4. **Urban, H. (2018)** Fat Knees: The inflammation of the Infrapatellar Fat Pad and Clinical Outcomes of the Knee. Oral Presentation. Institute of Bone and Joint Research 2018 3 Minute Thesis Competition, Sydney, Australia

- *First place winner*

5. **Urban, H. (2018)** Fat Knees: The inflammation of the Infrapatellar Fat Pad and Clinical Outcomes of the Knee. Oral Presentation. Northern Clinical School, University of Sydney 2018 3 Minute Thesis Competition, Sydney, Australia

- *First place winner*

6. **Urban, H. (2018)** Fat Knees: The inflammation of the Infrapatellar Fat Pad and Clinical Outcomes of the Knee. Oral Presentation. Faculty of Medicine and Health, University of Sydney 2018 3 Minute Thesis Competition, Sydney, Australia
 - *First place winner*
7. **Urban, H. (2018)** Fat Knees: The inflammation of the Infrapatellar Fat Pad and Clinical Outcomes of the Knee. Oral Presentation. The University of Sydney, All Faculty 2018 3 Minute Thesis Competition, Sydney, Australia
 - *First place winner*
8. **Urban, H. (2018)** Fat Knees: The inflammation of the Infrapatellar Fat Pad and Clinical Outcomes of the Knee. Oral Presentation. The Asia Pacific 2018 3 Minute Thesis Competition, Brisbane, Australia
 - *Semi-finalist*
9. **Urban, H. Eyles, J. Hunter, D J. Mills, K. (2018)** The Relationship Between Pressure Pain Thresholds and Anxiety in Patellofemoral Osteoarthritis: Exploratory data. Poster Presentation, OARSI 2018 World Congress, Liverpool, United Kingdom
10. **Urban, H. (2018)** Fat Knees: The inflammation of the Infrapatellar Fat Pad and Clinical Outcomes of the Knee. Oral Presentation. The Royal Society of New South Wales, Sydney, Australia
 - *Invited presentation*

11. **Urban, H.** Eyles, J. Hunter, D J. Mills, K. **(2018)** The Relationship Between Pressure Pain Thresholds and Anxiety in Patellofemoral Osteoarthritis: Exploratory data. Poster Presentation, Australian Society for Medical Research NSW Scientific Meeting, 2018, Sydney, Australia
12. **Urban, H.** Hunter, D J. Little, C B. **(2018)** Inflammation of the Infrapatellar Fat Pad & Clinical Outcomes of the Knee: Protocol for an observational study. Poster Presentation. New Horizons Scientific Conference, Sydney, Australia
13. **Urban, H.** Hunter, D J. Little, C B. **(2018)** Inflammation of the Infrapatellar Fat Pad & Clinical Outcomes of the Knee. Oral Presentation. Kolling Institute of Medical Research, Level 10 Lab Seminar, Sydney, Australia
14. **Urban, H.** Hunter, D J. Little, C B. **(2018)** Inflammation of the Infrapatellar Fat Pad & Clinical Outcomes of the Knee. Oral Presentation. Royal North Shore Hospital, Rheumatology Research Department, Sydney, Australia
15. **Urban, H.** Ashton, D. Ferreira, M F. Hunter, D J. Little, C B. Zaki, S. **(2019)** Learning about systematic reviews: incorporating human and animal studies together. Oral Presentation. Kolling Institute of Medical Research, Level 10 Lab Seminar, Sydney, Australia
16. **Urban, H.** Blaker, C. Shu, C. Clarke, E. Little, C B. **(2019)** Inflammatory differences in the synovium of ACL deficient knees: surgical vs non-surgical injury. Oral Presentation. Matrix Biology Society of Australia and New Zealand 2019 Meeting, Sydney, Australia

Abstract

Osteoarthritis (OA) is a complex disease that involves mechanical, metabolic and inflammatory insults to its development. Obesity, one of the primary risk factors for OA, impacts all three of these mechanisms in disease development. In particular, the role of adipose tissue as an inflammatory organ, the involvement of adipose associated inflammation in OA and the proximity of the infrapatellar fat pad (IFP) to the synovial knee joint have driven research in recent years.

This thesis aimed to investigate the role of the IFP in knee OA with the surrounding structures and clinical manifestations of the disease. In **Chapter 2**, I systematically appraised the current literature to evaluate the relationship between IFP associated inflammation and pain in preclinical animal and human clinical studies.

A series of investigations evaluating the relationship between the IFP, surrounding joint tissues and pain in murine models are described and presented in chapter 3-5. **Chapter 4** identified strong correlations between IFP adiposity, synovitis and sub-synovial fibrosis but no associations to pain. **Chapter 5** built on that research by further evaluating the association of IFP adiposity and sub-synovial fibrosis to pathology in surrounding structures such as the cartilage, bone and meniscus.

The subsequent chapter builds on these animal model findings to evaluate the IFP in humans. **Chapter 6** showed increasing IFP(Hoffa)-synovitis was weakly correlated with lowering centripetal adiposity and serum markers of synovitis but not pain. The disassociation to pain was in stark contrast to the current literature and the findings of our systematic review.

Finally, **Chapter 7** presents the protocol of a proposed observational study to investigate the impact of IFP inflammation on clinical outcomes in an end-stage knee OA population and reports the feasibility of the study.

This thesis provides novel insights into the relationship of IFP adiposity and inflammation to the surrounding tissue structures and pain. The findings may help direct future research to 1) validate the associations identified in the preclinical studies of this thesis, 2) further understand the relationship of the IFP to other clinical manifestations including physical function, and 3) to determine if the IFP can be a potential therapeutic target.

Table of Contents

Statement of Originality.....	ii
Authorship attribution statement	iii
Acknowledgements.....	v
Publications and Presentations	vii
Publications arising from this thesis.....	vii
Infographics	vii
Presentations.....	viii
Abstract.....	xi
Table of Contents.....	xiii
List of Figures	xxi
List of Tables	xxiv
List of Abbreviations	xxvii
Chapter 1. Introduction and Literature Review.....	31
1.1 Introduction.....	31
1.2 Adipose tissue and its role in inflammation	34
1.3 Adipose tissue inflammation in OA	36
1.3.1 Systemic adipose derived inflammation in OA	36
1.3.2 Localised joint inflammation and adipose tissue	39

1.3.3 Adipo-derived inflammation and pain	42
1.4 Targeting adipose tissue in OA management.....	43
1.5 Research gaps and future directions	48
1.6 Research Objectives	49
Chapter 2. Systematic Review	52
2.1 Abstract.....	52
2.2 Introduction	54
2.3 Methods.....	56
2.3.1 Data sources and searches	56
2.3.2 Study Selection	57
2.3.3 Data Extraction and quality assessment	58
2.3.4 Data synthesis and analysis	59
2.4 Results.....	61
2.4.1 Included studies.....	61
2.4.2 Human imaging studies	61
2.4.3 Human tissue studies.....	76
2.4.4 Animal Studies	77
2.5 Discussion	81
2.6 Conclusion	86

2.7 Appendixes	87
2.7.1 PRISMA Checklist	87
2.7.2 PRISMA Abstract Checklist	89
2.7.3 PROSPERO Protocol	90
Chapter 3. Methodological Development	99
3.1 Introduction	99
3.2 Ethics.....	100
3.3 Animals	100
3.4 Knee injury models	101
3.4.1 Anaesthesia	101
3.4.2 Surgical models.....	101
3.4.3 Mechanical loading models	103
3.4.4 Non-operated controls	105
3.4.5 Randomization and blinding.....	105
3.4.6 Euthanasia	105
3.5 Histological sample processing.....	105
3.5.1 Sample processing	106
3.5.2 Histochemical staining.....	107
3.6 Histomorphometry assessment of IFP	107

3.7 Novel sub-synovial fibrosis scoring tool	110
3.7.1 Tool development.....	110
3.7.2 Sub-synovial fibrosis scoring tool	111
Chapter 4. Pre-clinical Study 1	119
4.1 Abstract.....	119
4.2 Introduction	122
4.3 Methods.....	125
4.3.1 Synovitis.....	125
4.3.2 Gene expression analysis.....	126
4.3.3 Pain behaviour testing.....	130
4.3.4 Statistical analysis.....	133
4.4 Results.....	136
4.4.1 Time and injury impacts on synovitis	136
4.4.2 Time and injury impacts on sub-synovial fibrosis	139
4.4.3 Time and injury impacts on IFP adiposity.....	141
4.4.4 Correlations between histological features	143
4.4.5 Impact of Synovitis, sub-synovial fibrosis and time on IFP adiposity.....	148
4.4.6 Gene expression analysis of the IFP and synovium unit	152
4.4.7 Changes in pain behaviour responses	158

4.5 Discussion	160
4.6 Conclusion	168
4.7 Appendix.....	169
Chapter 5. Pre-clinical Study 2	171
5.1 Abstract.....	171
5.2 Introduction	174
5.3 Methods.....	177
5.3.1 Joint pathology scoring.....	177
5.3.2 Statistical methods	180
5.4 Results.....	181
5.4.1 IFP adiposity and sub-synovial fibrosis are correlated to structural features	181
5.4.2 Strong associations to Cartilage and Bone/Enthesophyte pathology.....	182
5.4.3 Meniscal pathology associated with posterior fibrosis.....	188
5.4.4 Sub-chondral bone pathologies show little correlation to adiposity and fibrosis	188
5.5 Discussion	193
5.6 Conclusion	200
5.7 Appendix.....	201
5.7.1 IFP adiposity and structural features correlation.....	201
5.7.2 Sub-synovial fibrosis and structural features correlation	224

Chapter 6. Osteoarthritis Initiative Analysis	252
6.1 Abstract.....	252
6.2 Introduction	254
6.3 Methods.....	257
6.3.1 Study Participants.....	257
6.3.2 Semi-quantitative analysis of Hoffa's fat pad/IFP	257
6.3.3 Waist to height ratio.....	259
6.3.4 Pain	259
6.3.5 Biochemical markers	259
6.3.6 Statistical analysis.....	260
6.4 Results.....	262
6.4.1 Hoffa-synovitis is associated with WHtR	263
6.4.2 Hoffa-synovitis and WHtR associated with HA, MMP3 and pain.....	265
6.4.3 Assessment of WHtR and Hoffa-synovitis interaction on biomarkers and pain	268
6.5 Discussion	271
6.6 Conclusion	275
Chapter 7. Protocol for a Clinical Study	276
7.1 Abstract.....	276
7.2 Introduction	279

7.3 Methods.....	281
7.3.1 Study design.....	281
7.3.2 Participants.....	283
7.3.3 Screening	283
7.3.4 Study visit 1.....	284
7.3.5 Surgery.....	289
7.3.6 Tissue processing.....	290
7.3.7 Laboratory analysis.....	293
7.3.8 Statistical Methods.....	296
7.4 Preliminary Findings – study feasibility	299
7.4.1 Participants.....	299
7.4.2 Feasibility outcomes.....	300
7.4.3 Data and sample collection	300
7.5 Discussion	302
7.6 Conclusion	307
Chapter 8. Final considerations and conclusions	308
8.1 Summary of Main Findings.....	308
8.2 Strengths.....	316
8.2.1 Population.....	316

8.2.2 Outcome measures	318
8.3 Limitations	320
8.3.1 Inflammation	320
8.3.2 Animal study designs	320
8.3.3 IFP and synovium unit	321
8.3.4 Multiple testings	321
8.3.5 Unfeasible study	322
8.4 Future directions	323
8.5 Concluding remarks	325
References	326

List of Figures

Figure 1. A summary of the interaction between risk factors, systemic and local adipo-inflammatory pathways and biomechanics, with the structural and clinical features of osteoarthritis.....	45
Figure 2. The full search strategy used in Medline as an example for terms included	57
Figure 3. Flow chart of studies reporting pain and IFP inflammation	62
Figure 4. Pooled correlations of homogenous human imaging studies investigating pain and IFP inflammation.....	75
Figure 5. Rupture of the ACL by mechanical compression.....	104
Figure 6. Selection of scoring area for IFP adiposity.....	109
Figure 7. Differences in aspects of the scoring tool.	117
Figure 8. Total Synovitis Scores	136
Figure 9. Anterior synovitis.....	137
Figure 10. Posterior Synovitis	138
Figure 11. Sub-synovial fibrosis	140
Figure 12. IFP adiposity.....	142
Figure 13. PCR analysis of general inflammation and macrophage markers.....	155
Figure 14. PCR analysis of adipokines and T-cells.....	156
Figure 15. PCR analysis of MMPs, fibrosis markers and collagens.	157
Figure 16. von Frey and force plate outcomes of from baseline to 56 days.....	159
Figure 17. Different appearances of the IFP.....	163

Figure 18. Summary of strong significant associations between cartilage tissues and IFP adiposity percentage.	184
Figure 19. Summary of strong significant associations between cartilage tissues and total sub-synovial fibrosis.....	185
Figure 20. Summary of strong significant associations between osteophyte/enthesophyte tissues and IFP adiposity percentage.....	186
Figure 21. Summary of strong significant associations between osteophyte/enthesophyte tissues and total sub-synovial fibrosis.	187
Figure 22. Summary of strong significant associations between meniscus tissues and IFP adiposity percentage.	189
Figure 23. Summary of strong significant associations between meniscus tissues and total sub-synovial fibrosis.....	190
Figure 24. Summary of strong significant associations between subchondral bone tissues and IFP adiposity percentage.....	191
Figure 25. Summary of strong significant associations between subchondral bone tissues and total sub-synovial fibrosis.	192
Figure 26. Examples of grade 2 Hoffa-synovitis hyperintense signal changes within the infrapatellar region from Hunter et al. 2011 [207].....	258
Figure 27. Boxplot of waist to height ratio by Hoffa-synovitis category	265
Figure 28. Boxplot of serum HA, serum MMP3, overall WOMAC pain and WOMAC pain going upstairs by Hoffa-synovitis.....	268
Figure 29. Overview of the INTERLOCK study design	281

Figure 30. Tissue collection of cartilage on the tibial plateau. 290

Figure 31. Tissue collection of the lateral meniscus. 291

List of Tables

Table 1. Summary of adipokines and the associated effects in OA.....	33
Table 2. Thesis structure	50
Table 3. Human imaging study characteristics	63
Table 4. Human tissue study characteristics	76
Table 5. Study Characteristic – animal studies	78
Table 6. SYRCLE risk of bias – animal studies.....	80
Table 7. Description of each iteration of sub-synovial fibrosis scoring tool.....	111
Table 8. Cronbach’s Alpha for measuring the internal consistency of the scoring tool.....	118
Table 9. Gene groupings in mRNA expression analysis	127
Table 10. Variables used and the respective areas scored in the correlation analysis	134
Table 11. Correlation between adiposity measures in the IFP and synovitis scores.....	143
Table 12. Correlation between IFP adiposity and sub-synovial fibrosis.....	145
Table 13. Correlations between sub-synovial fibrosis and synovitis.....	146
Table 14. Linear regression of IFP adiposity percentage for synovitis, sub-synovial fibrosis and time in the different injury groups	150
Table 15. Details of gene primers analysed in RT-PCR	169
Table 16. OA pathology features scored in the different tissues and regions of the knee	179
Table 17. Spearman’s and partial correlation coefficients between the adipose percentage of the IFP and cartilage scores	201
Table 18. Spearman’s and partial correlation coefficients between the adipose percentage of the IFP and subchondral bone scores.....	203

Table 19. Spearman’s and partial correlation coefficients between the adipose percentage of the IFP and osteophyte/enthesophyte scores.....	204
Table 20. Spearman’s and partial correlation coefficients between the adipose percentage of the IFP and maximum osteophyte and enthesophyte scores	206
Table 21. Spearman’s and partial correlation coefficients between the adipose percentage of the IFP and meniscus scores	208
Table 22. Spearman’s and partial correlation coefficients between IFP adipose cell count, mean adipose cell size and cartilage scores	210
Table 23. Spearman’s and partial correlation coefficients between IFP adipose cell count, mean adipose cell size and subchondral bone	213
Table 24. Spearman’s and partial correlation coefficients between IFP adipose cell count, mean adipose cell size and osteophytes/enthesophytes.....	215
Table 25. Spearman’s and partial correlation coefficients between IFP adipose cell count, mean adipose cell size and meniscus tissue	221
Table 26. Spearman’s and partial correlation coefficients between total Sub-synovial fibrosis and cartilage scores	224
Table 27. Spearman’s and partial correlation coefficients between maximum sub-synovial fibrosis and cartilage scores.....	227
Table 28. Spearman’s and partial correlation coefficients between total sub-synovial fibrosis and subchondral bone scores.....	230
Table 29. Spearman’s and partial correlation coefficients between maximum sub-synovial fibrosis and subchondral bone scores	232

Table 30. Spearman’s and partial correlation coefficients between total sub-synovial fibrosis and osteophyte/enthesophyte scores.....	234
Table 31. Spearman’s and partial correlation coefficients between maximum sub-synovial fibrosis and osteophyte/enthesophyte scores.....	240
Table 32. Spearman’s and partial correlation coefficients between total sub-synovial fibrosis and meniscus scores.....	246
Table 33. Spearman’s and partial correlation coefficients between maximum sub-synovial fibrosis and meniscus scores.....	249
Table 34. Clinical and laboratory characteristics of study participants at baseline.....	262
Table 35. Simple linear regression of waist to height ratio (WHtR) and waist circumference on Hoffa-synovitis (x-variable).....	264
Table 36. Simple linear regression of WHtR and waist circumference on Hoffa-synovitis (x-variable) and their relationship with biomarkers of inflammation.....	266
Table 37. Two-way analysis of variance interaction model for the effect of WHtR and Hoffa-synovitis on serum HA and MMP3.....	269
Table 38. Clinical outcomes collected at study visit 1.....	284
Table 39. FACS analysis antibody selection.....	294
Table 40. Demographics.....	299
Table 41. Study milestones achieved by recruited patients.....	300

List of Abbreviations

α SMA	Alpha Smooth Muscle Actin
30s-CST	30 Second chair stand test
40m FPWT	40 Meter Fast Paced Walk Test
ACL	Anterior cruciate ligament
ACLR	ACL rupture
ACLT	ACL transection
BLOKS	Boston Leeds Osteoarthritis Knee Score
BMI	Body Mass Index
CI	Confidence Interval
COL	Collagen
Ctrp	C1q/TNF-related protease
DASS21	Depression, Anxiety and Stress Scale 21
dntps	Deoxyribonucleotide Triphosphates
DXA	Dual X-ray Absorptiometry
ELISA	Enzyme-Linked Immunosorbent Assays
FACS	Fluorescence-Activated Cell Sorting
GPNMB	Glycoprotein (Transmembrane) nmb

GRADE	Grading of Recommendations Assessment, Development and Evaluation
HA	Hyaluronan
HEPA	High-Efficiency Particulate Air
HFD	High Fat Diet
IFP	Infrapatellar Fat Pad
IGF1	Insulin-like Growth Factor-1
IHC	Immunohisto chemistry
IL	Interleukin
IQR	Inter-Quartile Range
K/L	Kellgren/Lawrence
KOOS	Knee Injury and Osteoarthritis Outcome Score
Mif	Macrophage Migration Inhibitory Factor
MiR	Micro-Ribonucleic Acid
MMP	Metalloproteinase
MOAKS	MRI Osteoarthritis Knee Score
mPD-Q	Modified PainDETECT
MRI	Magnetic Resonance Imaging
mRNA	Messenger- Ribonucleic Acid

NBF	Neutral Buffered Formalin
NOC	Non-Operated Control
NOSGEN	Newcastle-Ottawa Scale
OA	Osteoarthritis
OAI	Osteoarthritis Initiative
OARSI	Osteoarthritis Research Society International
PC	Percentage Change
PCL	Posterior Cruciate Ligament
PEO	Population, Exposure and Outcome
PKPM	Photographic Knee Pain Map
PPAR	Peroxisome Proliferator-Activated Receptor
PPT	Pressure Pain Threshold
PRISMA	Preferred Reporting Items for Systematic Reviews and Meta-Analyses
PROSPERO	The International Prospective Register of Systematic Reviews
PTOA	Post-Traumatic OA
ROM	Range of Motion
RT-PCR	Reverse Transcription Polymerase Chain Reaction
ScAT	Subcutaneous Adipose Tissue

SD	Standard Deviation
SE	Standard Error
SERPINE2	Serpin Peptidase Inhibitor Clade E Member 2
SF	Synovial Fluid
SHAM	Placebo surgery involving arthrotomy without ligament injury
Sirt	Sirtuin
Sra	Steroid Receptor RNA Activator
SYRCLE	Systematic Review Centre for Laboratory animal Experimentation
TGF	Transforming Growth Factor
TKA	Total Knee Arthroplasty
TNF	Tumour Necrosis Factor
Trpv	Transient Receptor Potential Vanilloid
UCP1	Uncoupling Protein-1
VAS	Visual Analogue scale
WHtR	Waist to Height Ratio
WISP2	WNT1 Inducible Signalling Protein 2
WOMAC	Western Ontario and McMaster Universities Osteoarthritis Index

Chapter 1. Introduction and Literature Review

Published as:

Urban H. Little CB. The role of fat and inflammation in the pathogenesis and management of osteoarthritis. Rheumatology (Oxford). 2018;57(suppl_4):iv10-iv21

1.1 Introduction

Osteoarthritis (OA) is a highly prevalent disease that is estimated to affect one in every eight adults and is a leading cause of chronic pain [1, 2]. It is one of the top contributors to global disability, with the knee being identified as one of the joints most commonly affected by OA [3]. Adding to the individual and societal burden of OA, current treatment options lack any approved disease modifying solutions and are limited to analgesic therapies to maintain joint function, and at end-stage, surgical joint replacement [4]. Traditionally defined as a result of ‘wear and tear’ affecting cartilage, OA is now better understood as a more complex disease involving mechanical, biochemical and biological processes that affect the whole joint [5, 6]. Specifically, OA is defined by the ‘Osteoarthritis Research Society International’ (OARSI) as a joint disorder with an initial manifestation of abnormal joint tissue metabolism followed by anatomical and/or physiological changes including cartilage degradation, bone remodelling, osteophyte formation, joint inflammation and loss of normal joint function [7].

Osteoarthritis has a multifactorial pathophysiology with mechanical, metabolic and inflammatory contributions to its aetiology, and recognised risk factors such as reduced muscle strength, joint injury, and obesity, among others [8, 9]. In particular, obesity is a prominent risk

factor due to increasing societal prevalence, and because it potentially contributes not only to the mechanical aspect by means of increasing joint load but also to the metabolic and inflammatory facets of the disease due to the role of fat as an endocrine organ secreting an array of pro-inflammatory mediators [10].

Increasingly, the role of inflammation in OA has become more clearly defined, with the identification of various soluble inflammatory mediators, such as cytokines, chemokines, adipokines, and lipids, associated with the pathophysiology of both the structural and symptomatic disease [6]. Histological examination has demonstrated complex inflammation in the synovium (synovitis) of the osteoarthritic joint which otherwise would be a thin layer of cells that are a source of hyaluronan and lubricin, key components of the synovial fluid [11]. There is a significant association between the presence and severity of synovitis and associated joint effusion, with both the incidence and progression of OA pain and structural pathology [11, 12]. A recent study demonstrated that despite being within the normal range, increasing levels of synovial fluid white blood cells were associated with increasing synovitis, cartilage loss and bone marrow lesions in patients with knee OA [13]. Increased levels of some cytokines including interleukin (IL)-6 and IL-8 in serum and synovial fluid have similarly been found in patients with OA [14-16]. Despite the sometimes unclear understanding of how these cytokines affect OA progression, it is generally accepted that they induce catabolic processes and inhibit anabolic processes in the joint [6]. Along with these traditional cytokines, a class of adipose derived molecules called adipokines have also been increasingly found to be associated with OA (Table 1) [17, 18]. The potential role of adipocyte-derived signalling molecules, in particular, has stimulated investigations not only on the role of systemic adipose tissue but also to examine

local articular adipose depots such as the infrapatellar fat pad (IFP), to further understand the role of adipose derived inflammation in OA [19, 20].

Table 1. Summary of adipokines and the associated effects in OA

Adipokines	Associated effects in OA	Levels in OA Patients	Association with pain
Adiponectin	↑ Cartilage degradation [89]	Higher in Plasma vs SF	↑ Plasma [132] ↓ SF [136]
	↑ in IFP vs subcutaneous fat [18, 20]		
Resistin	↑ Synovial fluid infiltration [18]	Higher in Plasma vs SF	↑SF [135]
	↑ Synovial hypertrophy [18]		
	↑ Cartilage degradation [93]		
	Correlated with bone marrow lesions [93]		
Leptin	↑ IGF1 and TGFβ [84]	Higher in SF vs Plasma	↑ SF, Serum [133, 136]
	↑ MMP2 and MMP9 [88]		
	↑ Cartilage degradation [113]		
Visfatin	↑ in IFP vs subcutaneous fat [20]	Higher in SF vs Plasma	↑ SF [136]
	↑ Cartilage degradation [113]		

In light of the increasing evidence, the aim of this narrative review is to discuss adipose-derived inflammation and its potential role in OA. Specifically, the role adipose-derived inflammation plays in the pathology of OA, and the contrast between systemic and local adipose-derived inflammation is examined. Finally, emerging evidence surrounding potential treatment applications targeting the adipo-inflammatory aspects of OA will be considered.

1.2 Adipose tissue and its role in inflammation

Historically characterised as an inert tissue for energy storage, adipose tissue has since been described as the largest endocrine organ in the body, consisting of adipocytes, nerve tissue and immune cells [21]. The discovery of Leptin, an adipose-derived inflammatory molecule, was the catalyst for the change in understanding of the inflammatory role played by adipose tissue [22]. Since then, significant strides have been made to implicate a variety of immune cells including macrophages, T-cells, B-cells and neutrophils in adipose-associated inflammation, which with increasing obesity results in an environment of low-grade systemic inflammation [23, 24].

Increasing amounts of adipose tissue affect the local and systemic populations of immune cells in terms of both quantity and cell types towards a more pro-inflammatory profile [24]. Within adipose tissue, this is characterised by the shift from alternatively activated (M2) macrophages in lean individuals to classically activated (M1) macrophages in the presence of obesity [25-28]. The M1 or M2 phenotypes of these adipose tissue macrophages are broadly classified as pro-inflammatory and anti-inflammatory respectively, with the former known to produce higher levels of pro-inflammatory cytokines such as IL-1, IL-6, and TNF α , and the latter anti-inflammatory/pro-anabolic molecules such as IL-10, IGF-1, and TGF- β [25, 27, 28]. Adipose

tissue macrophages are often found surrounding necrotic adipocytes with the purpose of consuming adipocyte debris in a process similar to foreign body tissue reaction, forming what is known as “crown-like structures” that increase in number in obesity [29, 30].

Inflammatory differences in the sub-types of brown (mainly found at the inter-scapular regions and associated with energy expenditure), white (mainly subcutaneous, intramuscular and visceral fat associated with obesity) and beige (brown adipocytes within white adipose tissue; the most common type of brown tissue in adult humans) adipose tissue, are affected by increasing adiposity [29, 31, 32]. In obese individuals, these differences include higher IL-6 production in brown adipose tissue associated with lower values of body fat percentages, and higher uncoupling protein-1 (UCP1) production in brown adipose tissue compared to white adipose tissue with an association to lower values of body mass index, body fat percentage and fat weight [33]. Additionally, brown adipose tissue in contrast to white is thought to down regulate the inflammatory profile of macrophages [34]. The relation of adipose tissue to inflammation is complex, given the effects of not only increasing obesity but the distinct types of adipose tissue. The differences in inflammatory profile between adipose tissue types have the capacity to differentially drive systemic and local inflammation through the accumulation and release of immune cells and inflammatory molecules [35]. Furthermore, recent pre-clinical studies have demonstrated cross-talk between different adipose tissue deposits with varying sensitivities to obesity-associated inflammation, and that removal of the most inflamed tissue can modify the response of the remainder [36].

1.3 Adipose tissue inflammation in OA

1.3.1 Systemic adipose derived inflammation in OA

The pathophysiological association between obesity and OA may manifest through several mechanisms. While biomechanical factors play a role in weight bearing joints through increased load, the established association of obesity to OA in non-weight bearing joints such as in the hand, implicates biochemical/biological mechanisms as a contributory factor [37]. Preclinical studies using high-fat-diet (HFD) induced obesity have shed light on the mechanical versus biological/inflammatory contribution to OA risk and pathophysiology. While HFD has been consistently demonstrated to increase body weight, fat mass, and spontaneous or injury-induced OA in mice, a number of studies have shown that OA severity is not correlated with body weight or joint loading [38-42]. Rather, OA incidence and/or severity in these and other *in vivo* studies [43-46] is associated with systemic and local joint inflammation, adipokine and cytokine levels. Interestingly, however, while genetically altered leptin signalling resulted in profound obesity, this was not associated with altered serum cytokine levels nor OA, suggesting increased fat mass alone is not disease-inducing [47]. The increased OA risk with HFD-induced fat mass may be associated with additional factors such as altered levels of cholesterol [48], specific fatty acids and lipoproteins [49-51], and gut microbiota [52]. Additionally, recent studies using combinations of HFD and unloading of the hind limbs, suggest that specific aspects of OA pathology (cartilage fibrillation and osteophyte size) require both adiposity and joint loading, while others (joint inflammation, chondrocyte apoptosis) occur with obesity alone [43].

Clearly, there is a complex interplay between biomechanical and both systemic and local biological effects of obesity and fat mass, as well as the initiating mechanisms of adiposity itself. The impact of these different pathways on the effect of obesity on OA may vary between joints. In load-bearing joints such as the knee, the association of obesity-related metabolic syndrome in OA patients is weakened when outcomes are adjusted for BMI, suggesting increased load as a result of obesity may play the greater role in the pathophysiology [53]. In contrast, inflammation might be expected to play a more important role than biomechanics in the association of obesity with hand OA documented in numerous populations and countries [37, 54-62]. However, a number of studies have failed to demonstrate an association between obesity and hand OA [63, 64], and as with knee OA indices of metabolic syndrome (other than hypertension) were not associated with hand OA after adjusting for BMI in a recent cohort study [65]. Furthermore, neither serum leptin levels, impaired blood glucose metabolism or type-2 diabetes were found to be associated with increased hand OA [66-68]. Together this may suggest a greater role for biomechanics in obesity-associated hand OA risk than previously thought, and/or that biological effect of obesity locally in joint tissues is more important than the systemic metabolic derangement in OA pathophysiology.

Adipose tissue is recognised as an endocrine organ that secretes a large number of inflammatory mediators including cytokines (IL-1, IL-6, IL-8, TNF α) and adipokines (leptin, adiponectin, resistin, visfatin) [10]. In addition to OA, adipose derived inflammation has been implicated in several other diseases including rheumatoid arthritis, diabetes and inflammatory bowel disease [69-71]. The increase of white adipose tissue in obesity is postulated to create a systemic environment of increased inflammation through the release of both cytokines and

pro-inflammatory adipokines such as leptin and visfatin, all of which have been all associated with OA [72-75]. The shift from M2 to M1 macrophage phenotypes in adiposity as previously discussed is also significant as it would enhance M1-cytokine driven cartilage degeneration and reduce the capacity for tissue repair and angiogenesis by M2 macrophage derived factors [25, 76]. The role of macrophages and their differential activation in OA is complex, however, and while loss of M2 activation has been associated with enhanced systemic inflammation following pan-macrophage depletion [77], M2 macrophages do not directly attenuate M1-driven cartilage catabolism [78], and TGF β produced by M2 macrophages can shift from being anabolic to pro-catabolic with ageing and OA [79, 80].

Adipokines are soluble molecules that predominantly originate from adipocytes and have been associated with obesity-related and metabolically induced inflammation, both of which have also been implicated in OA (Table 1) [81, 82]. While there is some contradictory evidence, leptin has generally been accepted as a major mediator in the construct of obesity and OA. It has been suggested that leptin mediates anabolic processes by the induction of insulin-like growth factor-1 (IGF1) and TGF β but also the expression of catabolic factors such as matrix metalloproteinase (MMP)-2 and MMP-9 [83, 84]. Leptin also stimulates the expression of IL-6 and IL-8 in synovial fibroblasts, alters the secretion of TGF β , osteocalcin, and collagen type I in subchondral osteoblasts, and decreases chondrogenesis while increasing osteogenesis in cartilage progenitor cells [85-88]. In addition to leptin, increased adiponectin and resistin have been associated with OA. Adiponectin is postulated to correlate to cartilage matrix degradation due to a positive association with circulating cartilage oligomeric matrix protein and increased MMP-3 [89]. However, adiponectin was found to be negatively associated with hand OA with

significantly lower levels in those with progression compared to those without [90]. Resistin, an adipokine that is variably reported to be increased in obese patients, was found to exacerbate adipose tissue inflammation and insulin resistance in mice, and induce an arthritic-like condition with synovial leukocyte infiltration and synovial hypertrophy after intra-articular administration [18, 81, 91, 92]. Serum levels of resistin have been positively associated with cartilage defects and bone marrow lesions in clinical studies [93].

1.3.2 Localised joint inflammation and adipose tissue

While the preceding evidence creates a construct for adiposity, systemic inflammation, adipokines and OA pathophysiology, studies have also shown elevated resistin, adiponectin and leptin occurring in knee synovial fluid compared to serum, which suggests a local adipogenic driver of pathology closer to the joint as opposed to just low-grade systemic inflammation [94, 95]. The infrapatellar fat pad (IFP) is a local adipose depot adjacent to the synovium in the knee joint. The IFP has been previously described to have a biomechanical role that contributes to load bearing, but emerging evidence also suggests a biochemical/biological contribution to the aetiology of knee OA [19, 96, 97]. The IFP is suggested to be the patellar tendons' source of blood supply contributing to a potential pain mechanism in the knee or perhaps specifically patella-femoral OA [19]. The roles of obesity as a risk factor and the implication of adipokines as well as synovitis in the pathophysiology of OA discussed above, coupled with the intra-synovial location of the IFP has created a potential knee OA pathophysiological construct that has become an increasing focus of research [20, 98], that is now also being investigated in other joints with an intra-articular fat deposit such as the hip [99]. In recent years, various clinical and

pre-clinical approaches have been used to investigate the relationship between inflammatory properties in the IFP to the signs, symptoms and structural OA.

While it is a white adipose tissue, the IFP has been found to behave differently and demonstrate different characteristics compared to other adipose tissues in response to HFD in the mouse [45, 100-102]. In addition to the development of OA features in these HFD models, an increase in total volume, adipocyte size, and blood vessels was found within the IFP [45, 100] as occurs in systemic fat deposits [101]. The increase IFP volume was found in one study to be positively associated with osteophyte area [45]. While some studies have shown that HFD increased production of inflammatory cytokines, growth factors and adipokines in the IFP similar to systemic fat deposits [43, 45, 101], others have suggested the IFP is protected from obesity driven inflammation despite concurrent OA induction [100]. Some of these changes observed in mice were also replicated clinically in end stage knee OA patients, where the IFP differed significantly from other peri-synovial adipose tissue with increased macrophages, toll-like-receptor (TLR)4 expression, and fibrosis in the latter, while both adipose tissues were influenced by BMI and showed an increase in adipocyte size and increased haematopoietic and M2 macrophage cell infiltration [103]. A recent clinical study in patients without OA found IFP volume to be positively associated with BMI [104]. This demonstrates sensitivity to diet/obesity-associated change in the IFP but whether it is predictive of subsequent joint disease or is protective as previously suggested [105] remains to be determined.

While the role and effect of obesity on the IFP remains to be completely defined, IFP inflammation as identified by change in magnetic resonance imaging (MRI) signal intensity has been linked to an increase in pain and correlated to radiographic abnormalities such as bone

marrow lesions and cartilage defects in knee OA patients [106-109]. On a cellular level, the IFP similar to surrounding synovial tissues in OA joints has an increase of inflammatory cell types and markers indicative of a localised role in inflammation[110]. Within the IFP, pro-inflammatory phenotypes of T-cells and macrophages were found to be the most abundant immune cells and compared to sub-cutaneous adipose tissue, higher percentages of mast cells and lower percentages T-cells were detected in the IFP of OA joints [20]. Inflammatory molecules including IL-6, visfatin, and adiponectin were also found in increased amounts in the IFP compared to sub-cutaneous fat [20, 98]. Additionally, new adipokines including serpin peptidase inhibitor clade E member 2 (SERPINE2), WNT1 inducible signalling protein 2 (WISP2) and glycoprotein (transmembrane) nmb (GPNMB) have been found to be produced by the IFP, with WISP2 increased in OA IFP [111].

The increase in inflammatory cells and synthesis and secretion of pro-inflammatory factors by the IFP can not only directly drive pathological change in joint tissues such as cartilage, but may modify the phenotype of other cells in the joint such as synovial fibroblasts [112-114]. The precise nature of the interaction between the IFP and surrounding tissues is not well-defined. In *in vitro* studies using conditioned media and IFP and synovial fibroblast co-cultures have suggested the IFP contributes to synovial fibrosis through release of one or more soluble factors [115], with IL-6 but not leptin or adiponectin implicated [116, 117]. In OA patients, adipokines involved in cartilage degradation, including leptin, chemerin and visfatin, are produced in both the synovial membrane and IFP [113]. Synovial fibroblasts produce an array of pro-inflammatory and pro-catabolic mediators when incubated with IFP, such as IL-8, IL-6, MMP1 and MMP3, and notably, these molecules were not produced in equivalent co-incubations with

sub-cutaneous fat [112]. More recently, a similar composition of immune cell populations in the synovial membrane and IFP have been characterised, providing further evidence for an interactive environment involving the IFP in knee OA [118].

While the relationship between obesity and the IFP has been extensively investigated as discussed earlier, the impact of the other well-recognised OA risk factors on the IFP, such as ageing and joint injury/trauma, has received less attention. In the rat, ageing has been associated with a decrease in IFP volume, increased IFP secretion of TNF α and IL-13, and decreased expression of M2 macrophage genes [119]. Clinically, however, ageing has been linked to increasing IFP volume in OA but not normal joints [120], with increased IFP cross-sectional area beneficially associated with both radiographic and symptomatic OA [105, 121]. Trauma and injury have also been linked to abnormalities in the IFP, with evidence of fibrous changes with strenuous exercise, anterior cruciate ligament injury, and post-arthroscopy [122-124]. How the OA risk factors of ageing, injury, and obesity interact to modify the IFP and its effects on joint homeostasis and pathology requires further investigation.

1.3.3 Adipo-derived inflammation and pain

The preceding discussion has largely focussed on the relationship between adipose tissue/adiposity/obesity and OA structural pathology, but there are also potentially direct links with pain. The association between inflammation and OA pain is well-established through the role of cytokines in the initiation and persistence of pain by directly activating nociceptive receptors in the joint [125-128]. Additionally, significant evidence implicates several pro-inflammatory molecules in peripheral and central sensitisation [125-128]. More recently, studies investigating adipose-derived inflammation and pain have emerged. In upper extremity

soft tissue disorders, visfatin and abdominal adiposity are associated with pain [129]. Furthermore, leptin and BMI were found to be positively associated self-reported generalised body pain in otherwise healthy post-menopausal women as well as musculoskeletal pain in patients with fibromyalgia [130].

Only a small number of studies have explored the association of adipokines to OA pain. Systemic adipokines levels (leptin and adiponectin) were associated with having an increased number of painful joints in women and positively correlated with pain [131-133]. Within the joint, levels of leptin, adiponectin and resistin in the synovial fluid were weakly correlated to patient-reported pain [134, 135]. However, a more recent and larger study showed pain was associated with intra-articular concentrations of various adipokines with joint specific differences: high levels of visfatin and leptin in the hip, and high levels of leptin and low levels of adiponectin in the knee [136]. Early data has also suggested no association between IFP derived CD4+ cells and pain [118]. While the inflammation and pain construct propose a natural role for adipokines/adipo-inflammation, the limited studies and conflicting evidence suggest a strong need for more well-designed studies.

1.4 Targeting adipose tissue in OA management

The above review clearly implicates the potential involvement of a number of systemic and local adipo-inflammatory pathways in OA structural and symptomatic disease, and these are summarised in Figure 1. While the precise role of different adipose tissues, specific adipose derived mediators and biological versus mechanical effects of obesity and adiposity in OA onset and progression has yet to be fully resolved, therapeutic avenues have already begun to

emerge. Numerous studies have established that weight reduction is beneficial to reducing OA symptoms [137-140], with persistent effects one year later even in the absence of weight loss maintenance [141] and reducing levels of inflammatory biomarkers with effects sustained at 24 months [142, 143]. Exercise and/or physical therapy even in the absence of significant weight loss has been shown to improve clinical outcome measures in OA patients [144, 145], and both symptoms and structure in pre-clinical animal models [40, 146, 147]. However, when directly compared, weight loss through diet or diet plus exercise results in superior clinical benefit than exercise alone [139], and conservative methods to target adiposity/obesity have therefore been incorporated into clinical guidelines for OA treatment [148].

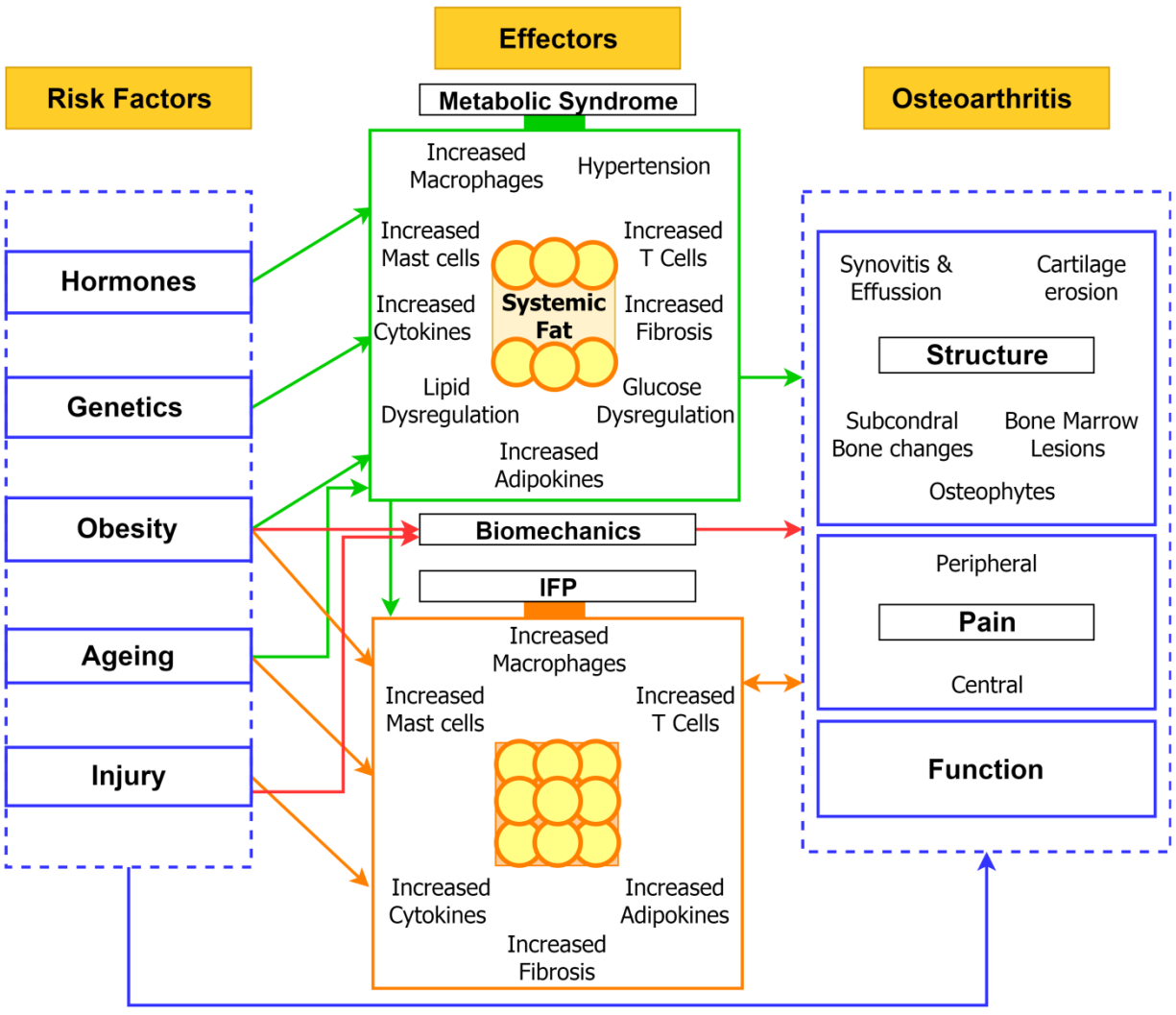


Figure 1. A summary of the interaction between risk factors, systemic and local adipoinflammatory pathways and biomechanics, with the structural and clinical features of osteoarthritis.

The mechanism whereby weight loss improves OA symptoms is less clear. Some studies have demonstrated a dose-dependent reduction in cartilage damage/loss with weight loss [149, 150] while others have not [151], which may be associated with the larger absolute mass change in the former studies. Weight loss is associated with reduced joint loading implicating biomechanics in the clinical improvement [152, 153]. However, patients in these studies also

experienced reduced serum IL-6 and C-reactive protein in association with reduced fat mass but independent of body mass, indicating reduced inflammation may play a role [139, 154]. In a pre-clinical mouse study, reduced OA structural damage in exercised animals was not associated with changes in body mass, fat mass or serum cytokines, suggesting other mechanisms may be more important [40]. A recent study demonstrated that changes in adiposity and weight as a result of diet and exercise in patients were correlated to reduced IFP volume [155] potentially implicating this local joint tissue effect in the clinical improvement.

The unique inflammatory characteristics of different adipose tissues, their response to obesity, and how these can be modified, may provide distinct therapeutic targets for OA. There are a number of studies using genetically modified mice that have identified molecular pathways that regulate both obesity and its inflammatory/metabolic consequences. Ablation of micro-RNA (miR)-34a [156], MMP-19 [157], lecithin:cholesterol acyltransferase (Lcat) [51], and transient receptor potential vanilloid (Trpv)-4 [158], all increased susceptibility to diet-induced obesity in mice. Evaluation of OA was only done in mice deficient in Lcat and Trpv-4 and showed concurrently increased obesity and structural pathology, while mice deficient in apolipoprotein A-I had similar HFD-induced obesity to wild-type animals but significantly worse OA suggesting a more direct role for HDL in the joint [51]. Decreased diet-induced obesity has been observed in mice with a deficiency in mast cells [159], ablation of steroid receptor RNA activator (Sra)-1 [160], and overexpression of C1q/TNF-related protease (Ctrp)-3 [161]. While none of these studies evaluated effects on OA, all reported decreased HFD-induced inflammatory cytokines such as IL-5, IL-6, and TNF. There is accumulating evidence from pre-clinical animal models especially using genetically modified mice, that targeting specific inflammatory pathways can

modify both post-traumatic and spontaneous age-associated OA (reviewed in [162-164]), but how this relates to changes in systemic or local adipose-inflammation has not been well-explored. One study has demonstrated a key role for macrophage migration inhibitory factor (Mif) in obesity-related white adipose tissue inflammation and metabolic syndrome despite no effect on adiposity itself [165]. An early pre-clinical study used dexamethasone to intervene in models of induced knee injury prior to the onset of OA, with results showing early improvements in the inflammation of the IFP that was not sustained at later time points and did not modify OA progression [166]. Mice deficient in sirtuin (Sirt)-6 were not more susceptible to HFD induced obesity but did have worse OA associated with increased synovitis and IFP inflammatory cytokine expression [167]. Resveratrol, which activates Sirt-1, has been shown to significantly reduce HFD-induced OA pathology in mice in association with reducing serum leptin and IL-1 β levels [168, 169].

There is great scope to therapeutically target the adipokines and inflammatory pathways that drive inflammation in the joint capsule, but to date, there has been limited translation of the specific targets identified in pre-clinical studies to patients. Adiponectin and leptin have been postulated to be potential therapeutic targets with suggestions of therapies likened to the anti-TNF α treatments [170]. The use of a peroxisome proliferator-activated receptor gamma (PPAR γ) agonist has recently been suggested as a potential novel treatment in response to the finding that PPAR γ expression was lower in the IFP of obese OA patients [103]. Similarly increased activated macrophages and increased IL-1 β associated with IFP activation and OA, could be targeted by existing therapeutics in obesity-associated OA [114, 171-174]. With the

emerging role of the IFP in knee OA, stratification of patients by MRI for locally applied intra-articular or even direct IFP injection of therapies may become a possibility.

1.5 Research gaps and future directions

While a great deal has been learned in recent years regarding the involvement of systemic and local adipose tissues in OA, there is still significant work to be done before therapeutics will be introduced into clinical practice. With regard to obesity itself, understanding the specific biomechanical, cellular and molecular pathways that link diet to adiposity and metabolic abnormalities, and these to particular diseases such as OA is in its infancy. In terms of systemic low-grade inflammation derived from adiposity, there is a need to define the key soluble signaling molecules (adipokines, cytokines, chemokines, and growth factors), their specific joint targets, and appropriate therapeutic approaches to target symptomatic and structural improvements in OA. Local to the knee joint, while existing research has implicated inflammation of the IFP in OA pathophysiology and symptoms, the detailed cellular and molecular mechanisms involved, the association between inflammation in the IFP and other synovial tissues, how these relate to clinical symptoms in patients, and whether these can be measured by MRI or other non-invasive tools have not been well-defined. The relationships between different risk factors for OA and the IFP and its role in structural and symptomatic disease have not been elucidated. While obesity and IFP have been increasingly investigated, very few studies have explored the role of ageing and joint injury, and we found no studies had looked at the impact of hormones or genetics on the IFP. Furthermore, no studies to our knowledge have investigated OA in the novel concept of “metabolically healthy obesity”, where

there is an absence of metabolic disorders in obese subjects, and such studies would be crucial when targeting obesity as a treatment. Finally, no studies to date have linked incident and progressive OA clinical symptoms or structural pathology in patients to the cellular and cytokine inflammatory profile of the IFP. This 'big picture' view of the inflammatory interaction between the IFP and the rest of the joint is needed to develop appropriate and patient- and OA-phenotype specific diagnostic, prognostic and therapeutic approaches [30]. Continued research and well-designed studies are required in both the pre-clinical and clinical sectors before the existing knowledge described in this review can be applied in the clinical environment.

1.6 Research Objectives

The research presented in this thesis aims to address some of the gaps identified in the literature by focusing on the relationship between IFP inflammation and clinical outcomes. As little is known about the detailed mechanisms involved, the association between inflammation and changes in the IFP and other pathology in other synovial tissues will also be investigated.

This thesis addresses the overarching aims, using a mixed methodology, in several stages. Firstly, the current literature was systematically assessed to evaluate the evidence between IFP inflammation and pain in animal and human studies. The associations between IFP adiposity to the surrounding tissue structures in the knee and pain were then evaluated in an animal study presented in chapter 3 – 5. The findings of the systematic review and animal studies were then assessed in a human population: using the Osteoarthritis Initiative, the relationship between IFP inflammation and centripetal adiposity was evaluated.

Finally based on the findings from the preceding chapters, the thesis presents a protocol and preliminary feasibility for an observational study in end-stage knee OA patients that uses a ‘bedside to bench’ approach with a multitude of clinical and laboratory assessments. The project described in this chapter would provide a comprehensive dataset that would further our understanding of how the IFP interacts within its micro and macro-environment to effect changes in clinical outcomes.

Table 2. Thesis structure

Chapter 1	Literature review and overview of the thesis
Chapter 2	This chapter presents the findings from a systematic review and meta-analysis evaluating the relationship between IFP inflammation and pain in the current literature. The review is comprehensive and assesses human imaging, human tissue and animal studies separately.
Chapter 3	Chapters 4 and 5 present the finding of animal studies carried out for this thesis. This chapter presents the methodology core to both the animal studies. As part of the methodology, the development of a novel sub-synovial histology scoring tool is described.
Chapter 4	Chapter 4 evaluates the relationship between IFP adiposity, synovitis, sub-synovial fibrosis and pain in preclinical mice models of post-traumatic OA.
Chapter 5	This chapter further assesses the role of IFP adiposity by evaluating the correlation with other structural features of knee OA in the animal models.

Table 2 continued

Chapter 6	Chapter 6 presents the results of a research study which evaluated the association between Hoffa-synovitis, centripetal adiposity, serum biomarkers of synovitis and pain in a nested cohort within the OAI database.
Chapter 7	The final results chapter in this thesis presents a protocol for an observational study that uses clinical and laboratory methodology to investigate IFP inflammation, its mechanisms of inflammation and associations to pain. As part of this chapter, the preliminary feasibility and learnings from this study are also presented.
Chapter 8	Chapter 8 provides an overall discussion and conclusion to the findings discussed in this doctoral thesis
References	All references are provided cumulatively at the end of the thesis.

Chapter 2. Systematic Review

Submitted for publication as:

Urban H, Ashton D, Ferreira ML, Hunter DJ, Little CB, Zaki S. The impact of infrapatellar fat pad inflammation on pain in knee osteoarthritis: a systematic review and meta-analysis. Osteoarthritis and Cartilage Open August 2020.

2.1 Abstract

Objective

The infrapatellar fat pad (IFP) is increasingly implicated in knee osteoarthritis (OA). However, the impact of IFP inflammation on pain, a key symptom of OA, is not well defined. We reviewed and appraised the literature on the relationship between IFP inflammation and pain in human and animal knee OA trials.

Methods

We conducted a systematic review of studies that reported pain and IFP inflammation in animal or human subjects with knee OA. Inclusion and exclusion were agreed independently by two reviewers. Searches were conducted in SCOPUS, Medline, Embase, and CINAHL databases using a pre-determined screening form up to the 3rd of July 2020. We evaluated the risk of bias of included studies using the Newcastle-Ottawa Scale and the Systematic Review Centre for Laboratory animal Experimentation tool. Correlation coefficients were pooled in R (version 3.6.2), using Fischer's z transformation.

Results

The search identified 20 articles (17 imaging, one human tissue, two animal). Nine imaging studies and one tissue-based study reported the correlation between pain and an IFP inflammation surrogate in 2680 and 42 participants, respectively. However, only three imaging studies were sufficiently homogenous to be included in the meta-analysis. The pooled results showed a positive correlation between pain and MOAK's Hoffa's synovitis of 0.25 (95% CI 0.1471 to 0.3462).

Conclusion

We showed a moderate quality (Grading of Recommendations Assessment, Development and Evaluation) positive correlation between IFP inflammation and pain. However, due to limited studies (3 included in meta-analysis), and the variability of outcome measures, more research is required.

PROSPERO Registration: CRD42019140267

Keywords: infrapatellar fat pad, pain, inflammation, osteoarthritis

2.2 Introduction

Osteoarthritis (OA) is one of the leading causes of chronic pain and affects approximately 1 in every eight adults[1, 2]. The OA Research Society International (OARSI) has defined the disease as a joint disorder which begins as abnormal joint tissue metabolism and subsequently results in anatomical and/or physiological changes such as joint inflammation and loss of normal joint function[7]. The multifactorial pathophysiology, which includes mechanical, metabolic and inflammatory aspects, and risk factors, such as joint injury and obesity, contribute to the complexity of OA [8, 9].

Obesity is implicated in OA due to the increased mechanical load on weight-bearing joints such as the hip and knee. [10]. In recent times, the biological role of adiposity as an endocrine organ that secretes a variety of inflammatory mediators has become more evident with associations in non-weight bearing joints such as those in the hand [175, 176]. Adipose tissue is comprised of adipocytes, neurovascular tissue and immune cells which contribute to low-grade systemic inflammation with increasing obesity[21, 23, 24]. Within OA, the role of inflammation and pain is well established but not fully understood with growing research demonstrating the association between systemic adipose-derived inflammation and pain[125, 127, 129-131, 177, 178]. The evidence of this relationship is predominantly from examinations of subcutaneous and abdominal adipose deposits.

In the knee joint, a local depot of adipose tissue is the infrapatellar fat pad (IFP). The IFP is located adjacent to the synovium and has well-defined biomechanical as well as potential biological roles in knee OA[19, 96, 97, 179]. Increased inflammation in the IFP within OA has been identified in clinical studies using a plethora of methods that range from cell composition

quantification using flow cytometry to magnetic resonance imaging (MRI) based scoring systems[20, 106, 110, 118]. In contrast to these clinical studies, basic science research has shown contradictory roles of the IFP in animal models with some studies indicating a high-fat diet increases inflammation in the IFP [43, 45] while others suggest that it is not affected by obesity driven inflammation despite OA development[100]. In line with this finding, one clinical study also identified dampened inflammatory characteristics in the IFP compared to peri-synovial adipose tissues in obese OA patients[180].

In addition to the uncertainty in basic research, clinical studies have also provided conflicting evidence when exploring the relationship between IFP inflammation and pain in OA. Ballegaard et al. showed a positive correlation between increasing levels of pain and IFP inflammation[106]. In contrast, Klein-Wieringa et al. showed no significant association between IFP CD4+ or CD8+ t cell, macrophage or mast cell numbers, and pain[118].

The current evidence available demonstrates a great deal of uncertainty about the inflammatory role of the IFP and its association with knee OA pain. This systematic review investigated the impact of IFP inflammation on pain in subjects (human and animal) with knee OA. We summarised the existing literature, categorised as human imaging-based, human tissue-based, or animal studies, while appraising the specific methods used to classify the outcomes measures as well as the statistical models used, to increase clarity on the relationship between localised adipose inflammation and pain.

2.3 Methods

This review used the 'PEO' (Population, Exposure and Outcome) acronym to devise the research question investigating IFP inflammation (Exposure) and pain (Outcome) in subjects (both human and animal) with knee OA (Population)

2.3.1 Data sources and searches

We prospectively registered this review with PROSPERO (registration number: CRD42019140267) on the 16th of September 2019.

Electronic searches were conducted in SCOPUS, Medline via Ovid, Embase via Ovid, and CINAHL via EBSCO-host databases. Search periods included the inception of the database to the 03rd of July 2020. Additional to the databases searched, we conducted citation tracking of the included studies, and relevant systematic reviews to ensure the inclusion of all relevant studies.

A combination of relevant keywords formed a search strategy to find publications that reported on OA, IFP and pain. Examples of these keywords include 'osteoarthritis', 'infrapatellar fat pad', 'Hoffa's synovitis', and 'pain' (Figure 2).

- 1 Osteoarthritis, Knee/
- 2 osteoart*.mp.
- 3 Arthroplasty, Replacement, Knee/
- 4 1 or 2 or 3
- 5 infrapatellar fat pad*.mp.
- 6 Patella/
- 7 Hoffas fat pad*.mp.
- 8 Hoffa* synovitis.mp.
- 9 effusion synovitis.mp.
- 10 IPFP maximal area.mp.

Figure 2. The full search strategy used in Medline as an example for terms included

2.3.2 Study Selection

We included case-control and cross-sectional studies which reported on inflammation of the IFP and pain in OA. This review did not place any restriction on the stage of the disease and included, both clinical and animal studies published in English. However, we excluded studies that focused on the use of IFP derived stem cells (rather than whole IFP or entire stromal vascular fraction), participants with any other inflammatory diseases (barring obesity) or pain measures that were only collected postoperatively. Additionally, we only included full original research publications, and excluded abstracts, protocols, feasibility papers, reviews and opinion articles.

Two independent reviewers (HU and DA) screened the titles/abstracts and full text using a piloted screening form based on the inclusion-exclusion criteria of this review. Disagreements at this screening stage were resolved by consultation with a third reviewer (SZ) if required.

2.3.3 Data Extraction and quality assessment

The same two independent reviewers (HU and DA) also extracted data and assessed the study quality using a standardised form. The data extraction form was based on the Cochrane Public Health Group – Data extraction and assessment template. Data retrieved included:

- study information (authors, year of publication, source of funding)
- study characteristics (design, aim, sample size, baseline imbalances, demographics, disease severity, body mass index (BMI), other outcome measures, missing data)
- pain and inflammation outcomes (measures used, scale, sample size, score and the validity of measures)
- Reported association for pain and IFP inflammation.

Included studies were primarily animal studies and human, case-control or cross-sectional studies. Appropriately, we selected tools to meet the needs of these different study designs. Risk of bias for animal studies was assessed using the SYRCLE (Systematic Review Centre for Laboratory animal Experimentation) tool[181]. For human case-control studies, the Newcastle-Ottawa Scale (NOSGEN) was used[182], and for cross-sectional studies, a modified version of the instrument was used[183]. However, due to the study designs – some questions were not applicable, and the risk of bias score presented is weighted against the maximum possible score for that study.

The GRADE (Grading of Recommendations Assessment, Development and Evaluation) system was used to evaluate the quality of the pooled analysis according to the four recommend levels of evidence[184]:

- high: authors have high confidence in the estimated effect or result
- moderate: authors believe the actual effect is close to the estimated effect
- low: authors believe the actual effect might be different from the estimated effect
- very low: very little confidence from authors regarding the estimated effect

The guidelines also recommend the quality of evidence is downgraded from 'high' if there were study design limitations, inconsistency of results, imprecision, indirectness, or publication bias[185, 186]. Study design limitations downgraded the quality of evidence if more than 25% of the sample were from 'high' risk of bias studies. Results were also lowered, for inconsistency if I² was greater than 50%, and for imprecision if the sample size was less than 200. Inconsistencies such as the use of surrogate measures also resulted in a downgrade. If an appropriate number of studies (>20 publications) were available, publication bias was assessed visually on a funnel plot.

2.3.4 Data synthesis and analysis

The included studies were evaluated in three sections: 1) human imaging studies, 2) human tissue studies and 3) animal studies. When more than one pain measure was reported, the Cochrane Musculoskeletal Network outcome recommendations were consulted, and the instrument that was ranked highest was used. For OA, 11 pain measures were ranked according

to preferred use as follows; 1) pain overall, 2) pain on walking, 3) WOMAC pain subscale, 4) pain on activities other than walking, 5) WOMAC global scale, 6) Lequesne OA index global score, 7) Other algofunctional scales, 8) Patient's global assessment, 9) Physician's global assessment, 10) Other outcomes, 11) No continuous outcome reported. The pain measures were synthesised into a 0 – 100 score, where zero is no pain, and 100 is extreme pain, based on the proportion of the score according to the original scale of the instrument.

Additionally, in an instrument with a scale of a different direction, scores were inverted to be comparable. Similarly, inflammation of the IFP in imaging studies with multiple measures reported had the validated or most common measure (used in OA research since there is no 'gold standard') obtained for this review. In non-imaging (tissue-based) studies, we used the levels of cytokine or inflammatory cell populations within the IFP.

This review pooled results from studies that showed methodological and design homogeneity for a meta-analysis of correlations. Statistical analysis was carried out in RStudio 1.2.5033 for R (version 3.6.2) using the '*meta*', '*metafor*' and '*dmetar*' packages designed for meta-analyses[187]. Correlation estimates were transformed into Fischer's Z and pooled for the meta-analysis. Based on the low between-study heterogeneity measured by I^2 (<40% based on the Cochrane Handbook for Systematic Reviews)[188], the combined results were reported in a fixed-effects model using the Sidik-Jonkman estimator.

2.4 Results

2.4.1 Included studies

Our search identified 5543 records across four databases. After excluding duplicates, we screened the titles and abstracts of 4789 unique publications and identified 181 potentially relevant articles which were then full text screened. Of the articles screened, 20 met the inclusion criteria; 17 imaging studies in humans, one tissue-based study in humans and two animal studies (Figure 3)[12, 106, 118, 189-205]. However, not all these studies reported the relationship between pain and IFP inflammation.

2.4.2 Human imaging studies

Seventeen studies reported pain and IFP associated inflammation in 2680 participants who were 62.70% female and on average 62 years old with a BMI of 30.14 (Table 3)[12, 106, 189-201, 204, 205]. This data excludes the studies by Mahler et al. as the mean data was not reported, and by Bernado-Bueno et al. for reporting the data for the number of knees in the study as opposed to the number of subjects[189, 196].

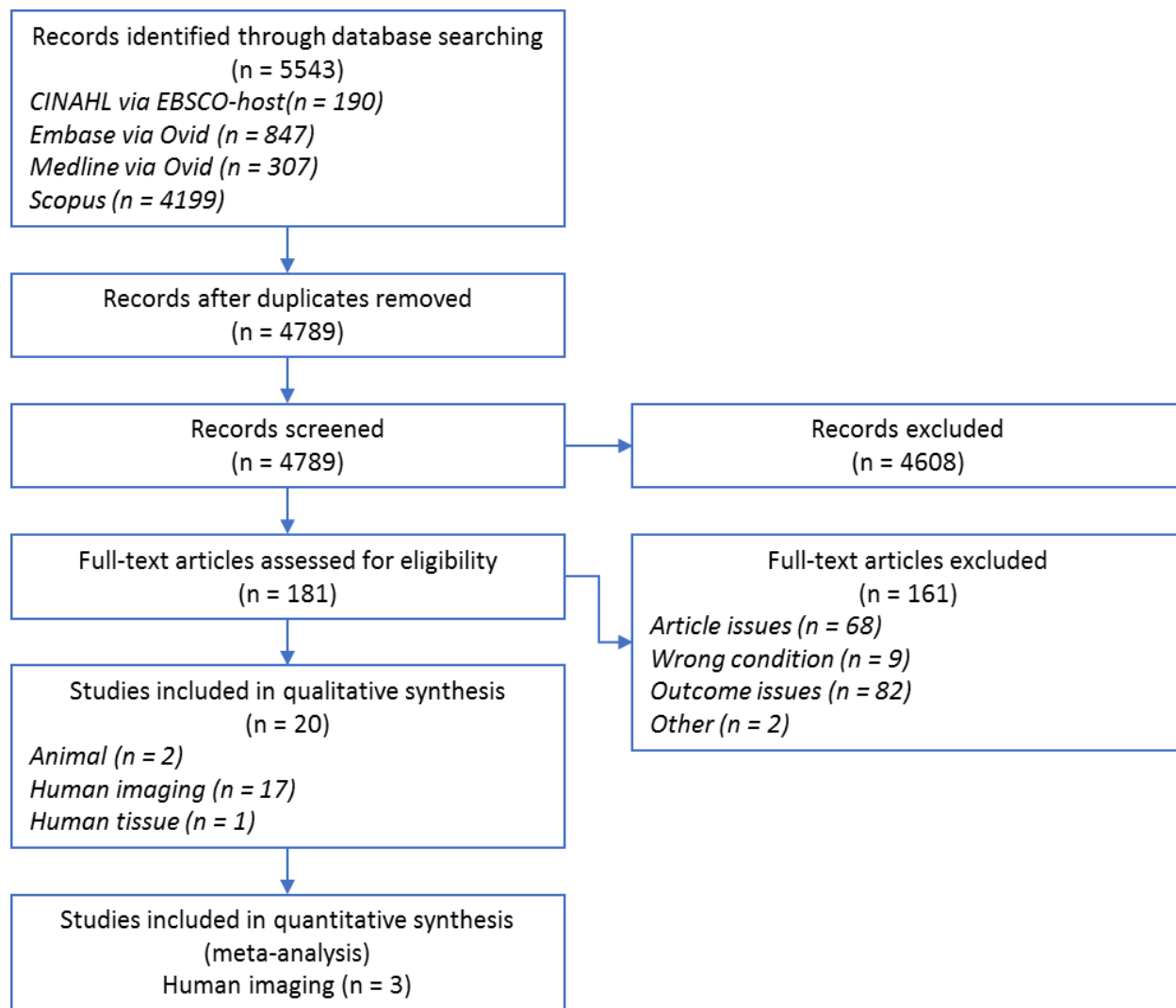


Figure 3. Flow chart of studies reporting pain and IFP inflammation

Table 3. Human imaging study characteristics

Study	Number of Participants	Participant Characteristics*	Pain Measure	IFP Inflammation measure	Statistical method	Results of association	Included in meta-analysis	Risk of Bias†
Ballegaard, 2014 [106]	95	Age – 65.3(6.5), Female – 82%, BMI – 32.3(3.7)	KOOS pain	MOAKS Hoffa’s synovitis	Spearman’s correlation	R = -0.21 P value = 0.046	Yes	7.78
Bernado-Bueno, 2017[189]	113 (226 eligible knees in two groups: Minimal pain n = 108, Substantial pain n = 118)	Overall Female – 81% Minimal pain Age – 65.4 (8.6), BMI – 26.8 (3) Substantial pain Age – 62.6(8), BMI – 26.9(2.9)	VAS	Sonographic Hoffa’s panniculitis	Univariate Logistic Regression	β = 0.629 P value = 0.383		8.89

Table 3 continued

Study	Number of Participants	Participant Characteristics*	Pain Measure	IFP Inflammation measure	Statistical method	Results of association	Included in meta-analysis	Risk of Bias†
Carotti, 2017 [190]	149	Age – 69.3(9.1), Female – 76%, BMI – 29.8(10.3)	WOMAC pain	MOAK’s Hoffa’s synovitis	Spearman correlation	R = 0.313 P value < 0.0001	Yes	8.89
Collins, 2016 [191][191]	Radiographic and pain progression cases – 194 Controls – 406	Cases Age – 62 (8.8), Female – 57%, BMI – 30.7(4.8) Controls Age – 61.3(8.9), Female – 60%, BMI – 30.7(4.8)	WOMAC pain	MOAK’s Hoffa’s synovitis	<i>Association not reported</i>			7.78

Table 3 continued

Study	Number of Participants	Participant Characteristics*	Pain Measure	IFP Inflammation measure	Statistical method	Results of association	Included in meta-analysis	Risk of Bias†
Cowan, 2015 [192]	Patellofemoral Joint OA (PFJOA) – 35 Controls – 11	PFJOA Age – 55(10), Female – 65%, BMI – 27(4) Controls Age – 53(5), Female – 63%, BMI – 25(2)	KOOS pain	IFP Volume	Univariate linear regression	R ² = 0.2018 P value <0.001		6.67
Gunbergesen, 2012 [193]	192	Age – 62.4(6.4), Female – 81%, BMI – 37.4(4.8)	KOOS pain	BLOKS	<i>Association not reported</i>			4.44

Table 3 continued

Study	Number of Participants	Participant Characteristics*	Pain Measure	IFP Inflammation measure	Statistical method	Results of association	Included in meta-analysis	Risk of Bias†
Hill, 2007 [12]	270	Age – 66.7(9.2), Female – 42%, BMI – 31.5(5.7)	VAS	Synovitis score (non-contrast MRI)	Generalised estimating equation	Estimate = 2.31 (95% CI -1.54, 6.16) P value = 0.24		8.89
Kaukinen, 2016 [194]	Cases – 80 Controls – 63	Cases Age – 59.9(7.8), Female – 61%, BMI – 29(4.3) Controls Age – 54.6(14.1), Female – 60%,	VAS	MOAK's Hoffa's synovitis	Poisson regression	Relative risk of pain = 2.48 (95% CI 1.77, 3.47)		6.67

Table 3 continued

Study	Number of Participants	Participant Characteristics*	Pain Measure	IFP Inflammation measure	Statistical method	Results of association	Included in meta-analysis	Risk of Bias†
		BMI – 24.8(3.2)						
Lo, 2009 [195]	160	Age – 61(9.9), Female – 50%, BMI – 30.3(4.7)	WOMAC pain	MRI synovitis hyperintense signal	Univariate Cox regression	Risk ratio of pain to synovitis score 1 - 1.9, 2 - 1.9, 3 - 2.3 P value = .20		8.89
Mahler, 2019 [196]	Total – 55 Low dose radiation therapy	LDRT Age – 62(9), Female -56%, BMI - 29 (25-30) [#]	WOMAC pain	MOAK's Hoffa's synovitis	<i>Association not reported</i>			10

Table 3 continued

Study	Number of Participants	Participant Characteristics*	Pain Measure	IFP Inflammation measure	Statistical method	Results of association	Included in meta-analysis	Risk of Bias†
	(LDRT) – 27 Sham – 28	Sham Age – 68(9), Female – 46%, BMI - 26 (24 - 31)#						
Oo, 2020 [205]	89	Overall age – 61 (7) Female – 54% BMI – 27 (6.4)	KOOS Pain	MOAK's Hoffa's synovitis	<i>Association not reported</i>			6.25
Petersen, 2016 [197]	Total cases – 61 (BLOKS 0 n=	BLOKS 0 Age – 67.9(62.0, 73.7)‡,	VAS	BLOKS	Pearson's correlation	R = 0.13 P value = 0.35		8.89

Table 3 continued

Study	Number of Participants	Participant Characteristics*	Pain Measure	IFP Inflammation measure	Statistical method	Results of association	Included in meta-analysis	Risk of Bias†
	16, BLOKS 1 n= 24, BLOKS 2 and 3 n= 21)	Female – 75%, BMI - 30.5(27.5, 33.5) † BLOKS 1 Age – 67.5(62.5, 72.4) †, Female – 46%, BMI - 30.7(28.1, 33.4) † BLOKS 2-3 Age – 69.1(65.0, 73.2) †, Female –						

Table 3 continued

Study	Number of Participants	Participant Characteristics*	Pain Measure	IFP Inflammation measure	Statistical method	Results of association	Included in meta-analysis	Risk of Bias†
		57%, BMI - 29.1(26.4, 31.8) ‡						
Radojic, 2017 [198]	104	Age – 66.8(7.2), Female – 61%, BMI – 30.4(5.2)	WOMAC pain	MOAK’s Hoffa’s synovitis	Spearman’s correlation	R = 0.19 P value = 0.059	Yes	5.56
Roemer, 2018 [199]	Severe OA – 125 No/mild OA – 46	Severe OA Age – 64.5 (8.8), Female – 55.2, BMI - 29.6 (4.7) No/mild OA Age – 64.7 (7.8),	WOMAC pain	MOAK’s Hoffa’s synovitis	<i>Association not reported</i>			8.89

Table 3 continued

Study	Number of Participants	Participant Characteristics*	Pain Measure	IFP Inflammation measure	Statistical method	Results of association	Included in meta-analysis	Risk of Bias†
		Female – 65.2, BMI - 29.8(4.2)						
Ruan, 2019 [204]	160	Overall Age – 55.4 Low IL-8 Female – 85% BMI – 25.6 (3.8) High IL-8 Female – 91% BMI – 25.5 (3.3)	WOMAC pain	IFP Signal intensity	<i>Association not reported</i>			7.78
Sofat, 2019 [200]	Controls – 6	Controls Age – 45(5.6),	WOMAC pain	MOAK’s Hoffa’s synovitis	<i>Association not reported</i>			9

Table 3 continued

Study	Number of Participants	Participant Characteristics*	Pain Measure	IFP Inflammation measure	Statistical method	Results of association	Included in meta-analysis	Risk of Bias†
	Mild – 42 Advanced – 78	Female – 100%, BMI – 23.3(3.6) Mild Age – 64.1(9.6), Female – 71%, BMI – 29.2(4.7) Advance Age – 68.9(7.7), Female – 64%, BMI – 32.3(5.6)						

Table 3 continued

Study	Number of Participants	Participant Characteristics*	Pain Measure	IFP Inflammation measure	Statistical method	Results of association	Included in meta-analysis	Risk of Bias†
Wu, 2017 [201]	Total – 146 (Low gherlin n = 74, High gherlin n = 72)	Low gherlin Age – 55.6 (8.1), Female – 88%, BMI– 26.3 (4.3) High gherlin Age – 56 (8.6), Female – 83%, BMI– 25.3 (3.1)	WOMAC pain	IFP Volume	<i>Association not reported</i>			8.89

These studies reported pain as the Western Ontario and McMaster Universities Osteoarthritis Index (WOMAC) pain subscale (9 studies), a visual analogue scale (VAS) (4 studies) or the Knee Injury and Osteoarthritis Outcome Score (KOOS) pain subscale (4 studies). Outcomes of the IFP were reported with less standardisation using a variety of surrogates for inflammation. The studies variably reported IFP signal alterations using the MRI Osteoarthritis Knee Score (MOAKS) Hoffa's Synovitis (10 studies), the Boston Leeds Osteoarthritis Knee Score (BLOKS) synovitis score in the IFP (2 studies), IFP volume (2 studies), and 1 study each using sonographic effusion in superficial and deep IFP, and IFP synovial thickening using a non-contrast MRI synovitis score. The methodological quality of the identified studies was predominantly high, with 12 studies scoring above seven on the NOSGEN scale (Table 3).

However, despite the data being available, only 9 of the 17 studies analysed and reported on the relationship between pain and IFP associated inflammation [12, 106, 189, 190, 192, 194, 195, 197, 198]. Five of the nine studies used unique statistical methods – univariate logistic regression, linear regression, generalised estimating equations, Poisson regression, and cox regression, and another study distinctively used a modified measure of IFP inflammation – BLOKS. These six studies demonstrated varying degrees of positive relationships between pain and IFP inflammation with very different statistical significances (Table 3). However, the studies were too dissimilar and thus, excluded from the meta-analysis.

The three remaining trials used homogenous methodologies (KOOS/WOMAC compared to MOAKS Hoffa’s synovitis score, analysed with Spearman’s correlation) to evaluate the correlation between pain and size of IFP signal intensity alteration in 348 participants[106, 190, 198]. Two of these studies had a low risk of bias while the remaining study by Radojic et al. had moderate risk. We identified “moderate-quality” evidence (GRADE) that showed a weak positive correlation between MOAKS Hoffa’s synovitis and pain of 0.25 (95% CI 0.1471, 0.3462) (p-value <0.0001) (Figure 4). The evidence was downgraded from ‘high’ to ‘moderate’ due to the use of a surrogate measure of inflammation.

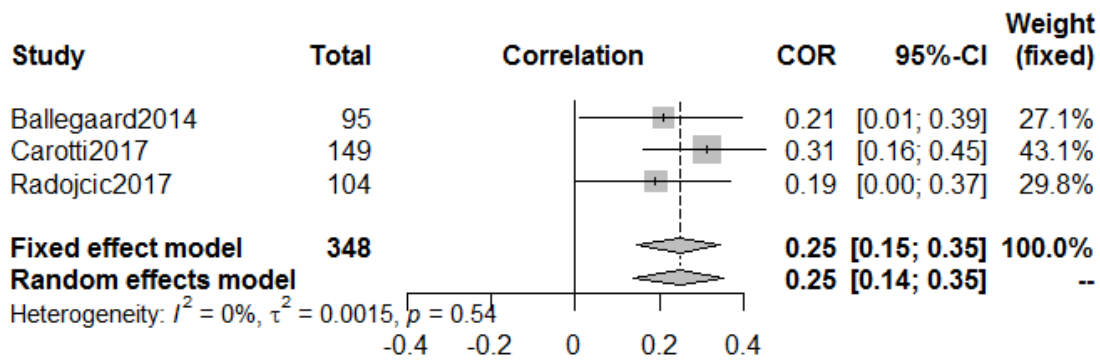


Figure 4. Pooled correlations of homogenous human imaging studies investigating pain and IFP inflammation

COR – Correlation value, CI – confidence interval, τ^2 – Tau-squared

2.4.3 Human tissue studies

Our review only identified one publication by Klein-Wieringa et al., which investigated tissue inflammation of the IFP based on number/percentage of different inflammatory cell populations[118]. This study reported findings from 42 participants with clinical data, of whom 52.4% were female, and on average, 63 years of age with a BMI of 28.9 (Table 4)[118]. The findings from the NOSGEN scale showed that it was not a study of high quality with a weighted score of 5.56.

Table 4. Human tissue study characteristics

Study	Number of Participants	Participant Characteristics	Pain Measure	IFP Inflammation measure	Was the association reported?	Risk of Bias†
Klein-Wieringa, 2016 [118]	76 (42 patients with clinical data)	Age – 63.3 (8.4) Female – 52.4% BMI – 28.9 (25.7 – 31) [#]	VAS	Flow Cytometry	Yes	5.56

[#] Median (interquartile range)

The study by Klein-Wieringa et al. presented the association of pain on a VAS to the percentages of immune cells in the IFP using linear regression analyses. Their study found that the percentage of IFP macrophages was moderately and positively associated to pain ($\beta = 0.36$,

95% CI -0.10 to 0.86)[118], with weaker positive associations between pain and CD4+ T cells percentage ($\beta = 0.19$, 95% CI -0.41 to 1.05) and mast cells percentage ($\beta = 0.20$, 95% CI -1.21 to 2.77), while the percentage of IFP CD8+ T cells was weakly negatively associated with pain ($\beta = -0.21$, 95% CI - 1.01 to 0.35) [118]. However, none of these associations were statistically significant.

2.4.4 Animal Studies

Two animal studies, both from the same research group and using a mono-iodoacetic acid-induced OA model in Wistar rats, met the inclusion criteria of this review (Table 5)[202, 203]. These studies reported pain findings using two methods: hind-limb weight-bearing asymmetry (incapacitance test) and distal pain sensitisation (allodynia, using a von Frey filament test) [202, 203]. Hoshino et al. reported inflammation in the IFP using a histopathological grading score that semi-quantitatively evaluated the cellularity and fibrosis,[202] whereas Inomata et al. reported macrophage infiltration as the average cell count of cells stained with ED-1 antibody in 3 separate areas of 3 independent sections[203]. Despite the trial's investigation of the two outcomes of interest, they did not evaluate the relationship between pain and IFP inflammation.

Table 5. Study Characteristic – animal studies

Study	Sample size	Sample characteristic	Model	Pain Measure	Inflammation measure	Association reported
Hoshino , 2018 [202]	Pain n=6 Histology Day 0 n=4 Day 1, 3, 5, 7 n=6	Male, Wistar Rats Charles river Japan	Mono- iodoace tic acid- induce d knee OA	Incapacit ance, Von Frey	Histology scoring	No
Inomata , 2019 [203]	36	Male, Wistar Rats Charles river Japan	Mono- iodoace tic acid- induce d knee OA	Incapacit ance, Von Frey	Macrophage infiltration	No

Using the SYRCLE risk of bias tool, we identified ambiguity in the selection bias domains regarding sequence generation and allocation concealment as well as performance bias regarding the housing of animals and blinding of caregivers and investigators (Table 6).

Table 6. SYRCLE risk of bias – animal studies

References	Selection bias (sequence generation)	Selection bias (baseline characteristics)	Selection bias (allocation concealment)	Performance bias (random housing)	Performance bias (blinding)	Detection bias (random outcome assessment)	Detection bias (blinding)	Attrition bias (incomplete outcomes)	Reporting bias (selective reporting)	Other sources of bias
Hoshino, 2018 [202]	No	Yes	NA	No	Unclear	No	Yes	Yes	Yes	Yes
Inomata, 2019 [203]	Unclear	Yes	No	Unclear	Unclear	Unclear	No	Yes	Yes	Yes

2.5 Discussion

This systematic review reports the appraisal of 17 human imaging, one human tissue and two animal studies which reported pain and IFP inflammation outcomes in subjects with knee OA.

Studies that evaluated IFP associated inflammation by imaging in humans showed high variability in the choices of outcome measures and statistical methods. Of the 17 publications included, nine studies reported a mostly positive association between pain and inflammation[12, 106, 189-201, 204, 205]. However, due to methodological inconsistencies, only three human imaging studies showed sufficient homogeneity to perform a meta-analysis[106, 190, 198]. Our results showed a statistically significant but weak correlation between inflammation identified by the MOAKS Hoffa's synovitis and knee pain in this small number of studies. Based on the GRADE methodology, this finding was of moderate quality.

Our review only identified a single clinical study that did not use an imaging surrogate but instead evaluated immune cell populations in the IFP and pain [118]. The results of the study, similar to our finding in imaging studies, tended to show a positive relationship. However, the statistical insignificance of their findings and the absence of similar studies prevents any definitive conclusions.

The final two studies identified in our review evaluated IFP tissue inflammation and pain in rat models of OA[202, 203]. However, as is common in animal research, the pain measures were continuously obtained from one set of animals and inflammatory outcomes achieved in a separate cohort. Thus, the direct association between IFP inflammation and pain was not evaluated.

To our knowledge, this is the first systematic review that evaluates the relationship between IFP inflammation (or surrogates thereof) and pain. Our systematic approach to identifying articles across several databases with broad criteria allowed us to identify articles that reported the outcomes of interest, even if the relationship was not analysed. Finding such articles helps us identify opportunities to utilise existing datasets to increase the productivity and utility of the data collected.

The main strength of this review is its inclusion of both clinical and animal studies. By not discriminating species, we were able to present the methods and findings of all relevant studies comprehensively.

Despite the strength of our study, there were some limitations. Inflammation is a broad term that can be defined by physiological and biological changes. Within OA, inflammation can include joint effusion, synovitis, increased population of immune cells or concentration of pro-inflammatory cytokines within the synovial fluid, synovial membrane and joint capsule[6]. Accordingly, the measures used to evaluate IFP inflammation in clinical studies are just as broad and range from volumetric to signal intensity analyses of the tissue[192, 195]. Quantitative measurements of synovitis using MRI rely on the rate of synovial enhancement when using an intravenous contrast agent in OA[206]. Contrast-enhanced MRIs are infrequently available due to the cost and potential adverse effects. Thus, a surrogate of signal changes in the IFP is more regularly utilised as a measure of synovitis[207, 208]. In semi-quantitative scoring methods, such as MOAKS and BLOKS, the size or signal intensity of the tissues contribute to a synovitis measure that is frequently represented as an indicator of inflammation [193, 197, 207, 209]. However, the caveat to these surrogate measures is the inability to discern what is actual tissue

inflammation from confounding pathologies that are a result of other causes such as surgery[210]. Hence, despite the merits, the variability and imprecision of these instruments require caution in interpreting the outcomes as “IFP inflammation”. The same variability of instruments also limits our meta-analysis by resulting in a low number of studies that could be combined and a result that should be cautiously interpreted.

Similarly, outcome measures for pain were also varied with studies using general measures such as a VAS or OA specific scales such as the WOMAC or its extension: KOOS[211, 212]. However, while the OA specific pain scales reduces the ambiguity of the VAS by using targeted questions, previous research has shown that the VAS is just as responsive as WOMAC[213]. Thus, pooling these measures did not face the same challenges as inflammation in clinical studies.

In a third of the articles included in our review, the relationship between pain and inflammation was not reported. In clinical studies, the reason for not reporting the association was due to the irrelevance to the study questions[191, 193, 196, 199-201, 204, 205]. While this is reasonable, it identifies an opportunity to reduce research data wastage.

In animal studies, the association was also not evaluated[202, 203]. As stated above, the outcomes were not obtained in the same animals, which is common in animal-based research where the measures of inflammation may require animal euthanasia (histopathology), thus precluding longitudinal evaluation. Acclimatising an increased number of animals to the testing methods for the sample size required to evaluate multiple outcomes at multiple timepoints poses an immense challenge. This challenge is not just intensive in labour hours but also comes with an increased financial cost that is not practical and ethical implications associated with the

use of additional animals. These limitations often result in studies with flawed methodologies and significance of findings. In our review, these limitations impact our ability to evaluate all available evidence adequately. Even in the absence of such study design issues, the pain outcome measures used in animals differ from those in patients making translation difficult.

Our results demonstrate some correlation between pain and IFP inflammation that could be a target for the treatment of knee OA. However, due to the limited number of studies and study types, further research is required.

Our key recommendation for imaging studies is the evaluation of methods used to determine IFP inflammation. The responsiveness and comparability of the measures should be investigated to enable future comparability of studies. Alternatively, a consensus of the most useful outcome measures should be identified by those in the OA research field to ensure their outputs can be consistent with other studies, as is done for physical performance measures by OARSI[214]. Ideally, the instrument would also be evaluated alongside measures of tissue inflammation, such as flow cytometric immune populations, cytokine levels in the tissues or joint fluids, or inflammatory gene expression analysis, to identify how comparable all clinical research could be and help identify a 'gold-standard' of IFP inflammation.

More human tissue and animal studies are required to understand the association with pain at a biological level despite the limitations of animal studies being likely to only inform on trends. To overcome that limitation, better designed pre-clinical studies that measure multiple outcomes in the same animals should also be carried out. Alignment of pain outcomes, such as evaluation of sensitization in patients and spontaneous activity-based measures in animals, would improve translation between pre-clinical and clinical studies. Finally, we recommend

the use of existing data where the outcomes are already present to increase the efficiency of the data collected.

2.6 Conclusion

The existing evidence identifies a weak correlation between IFP inflammation and pain in a small number of studies. The lack of studies evaluating inflammation at the cellular/molecular level in humans, and the paucity of animal studies suited to association analysis, highlight a need for further research and better-designed studies to understand better the relationship between the IFP and pain before its use as a potential therapeutic target can be evaluated.

2.7 Appendixes

2.7.1 PRISMA Checklist

Section/topic	#	Checklist item	Reported on page #
TITLE			
Title	1	Identify the report as a systematic review, meta-analysis, or both.	1
ABSTRACT			
Structured summary	2	Provide a structured summary including, as applicable: background; objectives; data sources; study eligibility criteria, participants, and interventions; study appraisal and synthesis methods; results; limitations; conclusions and implications of key findings; systematic review registration number.	3 – 4
INTRODUCTION			
Rationale	3	Describe the rationale for the review in the context of what is already known.	6 – 8
Objectives	4	Provide an explicit statement of questions being addressed with reference to participants, interventions, comparisons, outcomes, and study design (PICOS). Used (PEO – Participant, exposure, outcome)	9
METHODS			
Protocol and registration	5	Indicate if a review protocol exists, if and where it can be accessed (e.g., Web address), and, if available, provide registration information including registration number.	9
Eligibility criteria	6	Specify study characteristics (e.g., PICOS, length of follow-up) and report characteristics (e.g., years considered, language, publication status) used as criteria for eligibility, giving rationale.	10
Information sources	7	Describe all information sources (e.g., databases with dates of coverage, contact with study authors to identify additional studies) in the search and date last searched.	9
Search	8	Present full electronic search strategy for at least one database, including any limits used, such that it could be repeated.	Fig 1
Study selection	9	State the process for selecting studies (i.e., screening, eligibility, included in systematic review, and, if applicable, included in the meta-analysis).	10, 11
Data collection process	10	Describe method of data extraction from reports (e.g., piloted forms, independently, in duplicate) and any processes for obtaining and confirming data from investigators.	10, 11
Data items	11	List and define all variables for which data were sought (e.g., PICOS, funding sources) and any assumptions and simplifications made.	10, 11
Risk of bias in individual studies	12	Describe methods used for assessing risk of bias of individual studies (including specification of whether this was done at the study or outcome level), and how this information is to be used in any data synthesis.	11, 12

Section/topic	#	Checklist item	Reported on page #
Summary measures	13	State the principal summary measures (e.g., risk ratio, difference in means).	13
Synthesis of results	14	Describe the methods of handling data and combining results of studies, if done, including measures of consistency (e.g., I^2) for each meta-analysis.	12, 13
Risk of bias across studies	15	Specify any assessment of risk of bias that may affect the cumulative evidence (e.g., publication bias, selective reporting within studies).	11, 12
Additional analyses	16	Describe methods of additional analyses (e.g., sensitivity or subgroup analyses, meta-regression), if done, indicating which were pre-specified.	N/A
RESULTS			
Study selection	17	Give numbers of studies screened, assessed for eligibility, and included in the review, with reasons for exclusions at each stage, ideally with a flow diagram.	14, Fig 2
Study characteristics	18	For each study, present characteristics for which data were extracted (e.g., study size, PICOS, follow-up period) and provide the citations.	Table 1, 2, 3
Risk of bias within studies	19	Present data on risk of bias of each study and, if available, any outcome level assessment (see item 12).	14 – 18, Table 1, 2, 3, 4 ,
Results of individual studies	20	For all outcomes considered (benefits or harms), present, for each study: (a) simple summary data for each intervention group (b) effect estimates and confidence intervals, ideally with a forest plot.	Table 1, 2, 3
Synthesis of results	21	Present results of each meta-analysis done, including confidence intervals and measures of consistency.	15, 16
Risk of bias across studies	22	Present results of any assessment of risk of bias across studies (see Item 15).	15
Additional analysis	23	Give results of additional analyses, if done (e.g., sensitivity or subgroup analyses, meta-regression [see Item 16]).	N/A
DISCUSSION			
Summary of evidence	24	Summarize the main findings including the strength of evidence for each main outcome; consider their relevance to key groups (e.g., healthcare providers, users, and policy makers).	19
Limitations	25	Discuss limitations at study and outcome level (e.g., risk of bias), and at review-level (e.g., incomplete retrieval of identified research, reporting bias).	19 – 23
Conclusions	26	Provide a general interpretation of the results in the context of other evidence, and implications for future research.	22, 23
FUNDING			
Funding	27	Describe sources of funding for the systematic review and other support (e.g., supply of data); role of funders for the systematic review.	2

2.7.2 PRISMA Abstract Checklist

TITLE	CHECKLIST ITEM	REPORTED ON PAGE #
1. Title:	Identify the report as a systematic review, meta-analysis, or both.	1
BACKGROUND		
2. Objectives:	The research question including components such as participants, interventions, comparators, and outcomes.	3
METHODS		
3. Eligibility criteria:	Study and report characteristics used as criteria for inclusion.	3
4. Information sources:	Key databases searched and search dates.	3
5. Risk of bias:	Methods of assessing risk of bias.	3
RESULTS		
6. Included studies:	Number and type of included studies and participants and relevant characteristics of studies.	3
7. Synthesis of results:	Results for main outcomes (benefits and harms), preferably indicating the number of studies and participants for each. If meta-analysis was done, include summary measures and confidence intervals.	3
8. Description of the effect:	Direction of the effect (i.e. which group is favoured) and size of the effect in terms meaningful to clinicians and patients.	3
DISCUSSION		
9. Strengths and Limitations of evidence:	Brief summary of strengths and limitations of evidence (e.g. inconsistency, imprecision, indirectness, or risk of bias, other supporting or conflicting evidence)	4
10. Interpretation:	General interpretation of the results and important implications	4
OTHER		
11. Funding:	Primary source of funding for the review.	4
12. Registration:	Registration number and registry name.	4

2.7.3 PROSPERO Protocol

REVIEW TITLE AND TIMESCALE

1 Review title

The impact of infrapatellar fat inflammation on pain in knee osteoarthritis: a systematic review

2 Original language title

The impact of infrapatellar fat inflammation on pain in knee osteoarthritis: a systematic review

3 Anticipated or actual start date

July 01 2019

4 Anticipated completion date

July 01 2020

5 Stage of review at the time of this submission

The review has not yet started.

REVIEW TEAM DETAILS

6 Named contact

Hema Urban

7 Named contact email

Hemalatha.umapathy@sydney.edu.au

8 Named contact address

Level 10, Kolling Building, Royal North Shore Hospital, St Leonards, NSW 2065

9 Named contact phone number

+614 1277 2086

10 Organisational affiliation of the review

The University of Sydney

website address: <http://sydney.edu.au/>

11 Review team members and their organisational affiliations

Ms Hema Urban, Raymond Purves Bone and Joint Laboratory and Department of Rheumatology, Institute of Bone and Joint Research, The Kolling Institute, University of Sydney

Mr Dylan Ashton, Murray Maxwell Bone Laboratory, Institute of Bone and Joint Research, The Kolling Institute, University of Sydney

A/Prof Manuela Ferreira, Back Pain Group, Institute of Bone and Joint Research, The Kolling Institute, University of Sydney

Prof David Hunter, Department of Rheumatology, Institute of Bone and Joint Research, The Kolling Institute, University of Sydney

Prof Christopher Little, Raymond Purves Bone and Joint Laboratory, Institute of Bone and Joint Research, The Kolling Institute, University of Sydney

Dr Sanaa Zaki, Raymond Purves Bone and Joint Laboratory, Institute of Bone and Joint Research, The Kolling Institute, and Sydney School of Veterinary Science, University of Sydney

12 Funding sources/sponsors

N/A

13 Conflicts of interest

The authors declare no conflicts of interest

14 Collaborators

N/A

REVIEW METHODS

15 Review question(s)

Is infrapatellar fat pad (IFP) inflammation associated with pain changes in patients with knee osteoarthritis (OA)?

16 Searches

Electronic searches will be conducted in the following databases: SCOPUS, Medline via Ovid, Embase via Ovid, and CINAHL via EBSCO-host. The search strategy will be developed in consultation with a research librarian. Also, citation tracking of the included studies and relevant systematic reviews will be conducted. Search periods will include the inception of the database.

17 URL to the search strategy

N/A

18 Condition or domain being studied

Knee Osteoarthritis

19 Participants/population

Knee osteoarthritis or animal equivalent (Human and Animal studies)

20 Exposure(s)

Inflammation of the infrapatellar fat pad

Based on the study type inflammation will be measured as:

Human imaging studies

- MRI IFP signal intensity or imaging score for effusion-synovitis

Other human studies and animal studies

- Levels of cytokine, gene expression levels, inflammatory cell populations etc.

21 Comparator(s)/control

N/A

22 Types of study to be included

Case-control and cross-sectional studies that are published in English. Where analyses of the association between IFP inflammation and pain are available at baseline, cohort studies and randomised control trials will also be included. Both human and animal studies will be included.

23 Context

Studies with the following characteristics will be excluded: IFP derived stem cells, the inclusion of participants with inflammatory diseases and pain measures that were only collected

postoperatively. Additionally, protocol, feasibility, qualitative, review and opinion articles will be excluded.

24 Primary outcome(s)

Pain severity

In human studies, pain measured according to the Cochrane Musculoskeletal Network outcome recommendation, as listed below, will be used:

When more than one is reported, take the highest on the list*

- Pain overall
- Pain on walking
- WOMAC pain subscale
- Pain on activities other than walking
- WOMAC global scale
- Lequesne osteoarthritis index global score
- Other algofunctional scales
- Patient's global assessment
- Physician's global assessment

In animal studies, surrogate measures of pain reported will be used, such as the von Frey Test.

25 Secondary outcomes

Secondary outcomes include, but are not limited to, quality of life and physical function (if reported/available).

26 Data extraction (selection and coding)

Two independent reviewers (HU and DA) will screen titles/abstract and full text using a piloted screening form based on the inclusion-exclusion criteria of this review. Disagreement at this screening stage will be resolved by consensus of a third reviewer (SZ).

Two independent reviewers (HU and DA) will also extract data. The data extraction form is based on the Cochrane Public Health Group – Data extraction and assessment template. Data to be retrieved will include but is not limited to:

- study information (authors, year of publication)
- study characteristics (study type, location, participants, types of outcome measures)
- study details (study intention, methods, sample size, baseline imbalances, demographics, disease severity, body mass index, missing data)
- outcomes (inflammation measure, inflammation measure method, pain score, pain measure method, scale, the validity of measures)

Due to uncertainty regarding the nature and extent of information to be extracted, the data extraction form will be refined with discussions within the review team during the early stages of the review.

27 Risk of bias (quality) assessment

Studies for the systematic review are anticipated to be primarily animal studies and human, cohort or case-control, studies. Appropriately, tools to meet the needs of these study designs have been selected. Risk of bias for animal studies will be assessed using the SYRCLE (Systematic Review Centre for Laboratory animal Experimentation) tool[181]. For human case-

control studies, the Newcastle-Ottawa Scale will be used[182], and for cross-sectional studies, a modified version of the instrument will be used[183].

28 Strategy for data synthesis

Eligible studies will be evaluated in three sections: animal studies, human radiological studies and human tissue studies.

A meta-analysis will be used for similar studies (i.e., alike clinical diagnosis, inflammation measure and pain outcome assessment) and at low or moderate risk of bias. Estimates of association between IFP inflammation and pain will be pooled together.

If meta-analysis is not possible, a descriptive synthesis will be performed. An appraisal of each study will be included based on its risk of bias.

29 Analysis of subgroups or subsets

An attempt will be made to perform subgroup analyses based on disease severity and body mass index.

30 Type and method of review

Systematic review

31 Language

English

32 Country

Australia

33 Other registration details

N/A

34 Reference and/or URL for published protocol

I permit this file to be made publicly available.

35 Dissemination plans

The results of this review will be submitted to a peer-reviewed journal for publication and will be presented in national and international conferences.

36 Keywords

The following keywords with some variations according to the database to be searched will be included in the search strategy:

- 1 Osteoarthritis, Knee/
- 2 osteoart*.mp.
- 3 Arthroplasty, Replacement, Knee/
- 4 1 or 2 or 3
- 5 infrapatellar fat pad*.mp.
- 6 Patella/
- 7 Hoffas fat pad*.mp.
- 8 Hoffa* synovitis.mp.
- 9 effusion synovitis.mp.
- 10 IPFP maximal area.mp.
- 11 knee effusion.mp.
- 12 imaging score.mp.
- 13 Synovial tissue inflammation.mp.
- 14 5 or 6 or 7 or 8 or 9 or 10 or 11 or 12 or 13
- 15 exp Pain/
- 16 4 and 14 and 15

37 Details of any existing review of the same topic by the same authors

N/A

Chapter 3. Methodological Development

Investigating infrapatellar fat pad adiposity in pre-clinical models of post-traumatic osteoarthritis: core methods and development of a novel sub-synovial fibrosis scoring tool for murine models

3.1 Introduction

Chapter 3 describes the core methodologies used in the animal studies of this thesis presented in chapters 4 – 5. These studies utilized archival samples from a previous research project led by CB and SZ, and the relevant methodologies (Animals and Pain Behaviour Testing) are described below. Additionally, this chapter also describes methods specific to this thesis, such as the infrapatellar fat pad (IFP) adiposity assessment and novel sub-synovial fibrosis tools.

Fibrosis in the synovial tissues (sub-synovial loose connective tissue layer and joint capsule), is a prominent feature in OA[215]. However, there are limited validated tools for fibrosis assessments in existing histopathological scoring systems for pre-clinical animal studies, and these are often incorporated into an overall synovial health score[176, 216]. This chapter describes the development of a dedicated sub-synovial scoring tool for mice based on previous research and the experience of experts[203, 217]. Briefly, an iterative process of blinded scorings, discussions of shortfalls, further refinements and re-evaluations were used, until a final method that allowed for robust scoring was defined.

3.2 Ethics

The animal research conducted in chapters 3 – 5 were approved by the Northern Sydney Local Health District Animal Ethics Committee (protocol numbers: 1305-008A and RESP-15-126). The approvals were in accordance with the NSW Animal Research Act (1985), Animal Research Regulation (2010) and the Australian Code for the care and use of animal for scientific purposes (8th edition, 2013). All animals for this study were sourced and housed in the Kearns Facility of the Kolling Institute, St. Leonards, NSW, Australia.

3.3 Animals

Anterior cruciate ligament (ACL) injuries that markedly increase the risk of premature OA development humans are most common in adolescent males who are reaching skeletal maturity[218, 219]. This population was represented by using 10-week-old male C57/BL6 mice in this study. The C57BL/6 is the most common inbred mouse strain used in pre-clinical OA studies which will allow comparability to current literature[220, 221].

The mice were obtained from the Kearns Facility, C57BL/6 breeding colony at the Kolling Institute. Mice were housed in individually ventilated cages with high-efficiency particulate air (HEPA) filtered air, environmental enrichment, nesting material and Perspex housing, maintained in temperature-controlled rooms (19 – 22°C) with 12-hour light/dark cycles. Each cage housed 2 – 5 littermates with complete pelleted food and acidified water provided *ad libitum*.

3.4 Knee injury models

3.4.1 Anaesthesia

Vaporized Isoflurane was used to anaesthetize mice at either 2.5 % in oxygen (1 litre per minute), or 2 % in a combination of oxygen and nitrous oxide (1 and 2 litres per minute respectively: used where available in given procedure rooms in the animal house to reduce isoflurane exposure of operators and improve post-anaesthesia recovery and analgesia in mice). Mice were maintained in anaesthesia throughout the procedure using a nose cone and were monitored to ensure regular breathing, muscle relaxation and no reflexes. The process of joint injury only started when there no foot withdrawal reflex.

After each procedure, mice were transferred to clean cages upon heating pads to maintain body temperature. The animals regained consciousness and were ambulatory within 5 minutes after stopping anaesthesia. The mice were visually inspected to ensure that they were completely mobile with no weight-bearing changes to the injured limb and then returned to their pre-injury communal housing cages. The animals were not provided with any post-operative analgesia, and none displayed signs of general distress (e.g. isolation, coat roughening, weight loss, lack of spontaneous or evoked physical and exploratory activity) including overt evidence of pain (e.g. favouring the limb, not able to stand on hind limbs, not using the leg while climbing), requiring veterinary intervention or humane euthanasia.

3.4.2 Surgical models

Transection of the ACL in surgery is a frequent model of arthritis in several different species of animals[222, 223]. The ACL transection (ACLT) model in this study was performed using a

previously published protocol[224]. The right hind limb of anaesthetized mice was prepped for surgery by shaving and cleaning the skin with 80% ethanol. All surgeries were performed using an operating microscope by CBL, a board-certified specialist veterinary surgeon with extensive experience in the appropriate procedures. Briefly, following a 5mm skin incision on the medial side of the patella, the joint capsule was opened medial to the patella extending from the patella tendon attachment on the tibia to the vastus medialis muscle 2 mm proximal to the patella. The internal structures of the knee were then exposed by laterally luxating the patella, flexing the joint and bluntly reflecting the IFP distally. Minimal bleeding occurs during this approach (when present usually from the IFP) and was controlled by applying direct pressure with surgical swabs. The ACL was then visualized by identifying the ligament attached anteriorly on the tibia and posteriorly on the lateral femoral condyle. Surgical control (SHAM) animals did not progress beyond the visualization. The ACL transection was carried out under direct microscopic visualization using a 15-degree blade angled ophthalmic incision scalpel (Feather® Micro Scalpels, Cologne, Germany). The successful transection was confirmed visually and by the increased posterior translation of the femur relative to the tibia. Joints in both ACLT and SHAM were then flushed with sterile saline (to remove any blood or tissue debris), the patella manually repositioned and the incision anatomically closed in 3 layers: ophthalmic grade 8/0 absorbable suture material (Vicryl, Ethicon Inc., Somerville, NJ, USA) for the joint capsule (simple continuous) and subcutaneous tissue (mattress), and VetBond tissue glue for the skin (3M, Maplewood, MN, USA).

3.4.3 Mechanical loading models

The other injury models used in this study utilized compressive mechanical loads to rupture the ACL. Naturally occurring joint injuries are neither confined to the failure of a unique structure, nor do they come with surgical incisions that can activate immune responses. The use of a non-invasive rupture model overcomes these limitations to more closely replicate the nature of traumatic ACL injuries in humans. The established ACL rupture (ACLR) model used in this study was developed by Blaker et al. and is based off the findings from Christiansen et al. who showed that loading of the flexed knee joint in resulted in posterior translation and external rotation of the femur relative to the tibia, and with sufficient load, ACL rupture[225, 226].

Anaesthetized animals were positioned on the custom-made loading apparatus with the right hind-limb flexed to allow the tibia to be vertically fit between the fixtures (Figure 5 A-B). The limb was pre-loaded to 0.5N to ensure correct and secure alignment. A single compressive load (1mm/s) was applied to the joint and continuously monitored with an in-line load cell until a 1 N decrease within 0.25 seconds was detected to indicate the rupture of the ligament, at which point limb loading was automatically stopped to avoid excessive joint luxation and direct tibial loading (Figure 5 C).

In addition to the ACLR group, a sub-critical mechanical load model was developed to evaluate the impact of joint injury without ACL rupture. The loading was carried out identically to the ACLR model but ceased before the rupture by loading the joint to 9 N which was approximately 75% of the joint load target (12 N) that was previously established to cause ACL rupture in similar aged and gendered mice[225, 227, 228].

The mechanical injuries were performed by CB and EC who were experienced operators while EC assisted in ensuring blinding of group status was maintained.

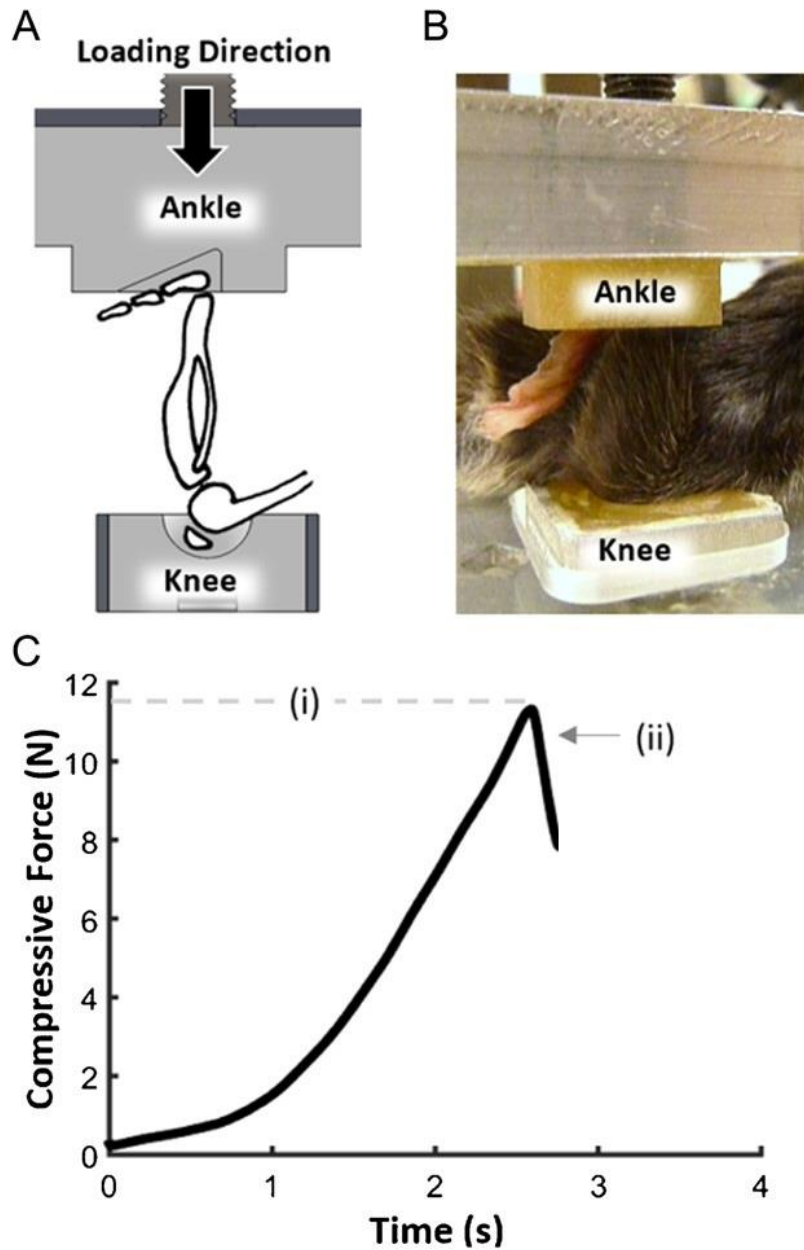


Figure 5. Rupture of the ACL by mechanical compression.

(A and B) demonstrate the positioning of the joint in the apparatus. (C) The force vs time curve shows (i) the load required for rupture of the ACL ligament and (ii) the detection of the ACL rupture. This image is reprinted from Blaker et al. [226] with permission from John Wiley and Sons.

3.4.4 Non-operated controls

Naïve mice with no procedures carried out were included as a non-operated control (NOC) group in this study to ensure any normal changes, due to age or development, are not incorrectly attributed to the injury models.

3.4.5 Randomization and blinding

Animals in each cage were assigned an injury group and post-injury time point using a random number generator. The allocation included conditions to ensure each cage contained mice of different injury groups, time points and were unlikely to lead to single-housing isolation. To reduce bias during the injury procedures, the researcher applying the trauma was blinded until either the ACL was exposed (ACLT or Sham) or the hind limb was appropriately positioned with the loading apparatus (ACLR or sub-critical). All procedures were carried out on the right hind limb for additional consistency.

3.4.6 Euthanasia

Mice were euthanized by sustained exposure to CO₂ or cervical dislocation under anaesthesia at the designated post-injury time points.

3.5 Histological sample processing

At each pre-determined post-injury time point (1, 2, 4 or 8 weeks), seven animals from each injury group (ACLT, Sham, ACLR and sub-critical) along with six naïve mice were allocated for histological joint pathology assessment.

3.5.1 Sample processing

Following euthanasia, the intact knee joint capsule excluding skin and any surrounding tissue was isolated from the animal by mid-shaft cuts on the tibia and femur. The joint was fixed in 10% (v/v) neutral buffered formalin for 24 hours before storage in 70% (v/v) ethanol.

The samples were decalcified by gentle agitation in 10% (v/v) formic acid and 5% (v/v) formalin at room temperature for 24 hours. The joints were washed in distilled water for 15 minutes before further 24-hour storage in 70% (v/v) ethanol.

The samples were then dehydrated for an hour each in increasing concentrations of ethanol (70%, 75%, 85%, 95% and triplicate of 100% (v/v)). Three 2-hour immersions in chloroform then removed ethanol and the joint received three two-hour changes and one six-hour change of paraffin wax under vacuum.

The joints were embedded in paraffin blocks with the medial side facing down to allow sagittal sections. Following trimming on the microtome to the beginning of the exposure of articular cartilage, 4 μ m thick sagittal sections were cut and mounted on Superfrost Plus slides. The slides, each with three serial sections, were collected every 84 μ m in the medial tibiofemoral compartment and every 48 μ m in the patellofemoral and lateral tibiofemoral compartments to ensure capture and visualization of the smaller focal areas of damage that were previously reported[229-231]. Lastly, slides were dried at 85°C for 30 minutes and 55°C overnight to ensure the sections adhered.

3.5.2 Histochemical staining

Before staining, the paraffin was removed from the sections using 3 x 5-minute washes in xylene followed by rehydration through graded ethanol (100-50%) and finally water for 15 minutes. The slides were then drained well and stained for 10 minutes in 0.04% (w/v) Toluidine Blue O in 0.1M sodium acetate buffer (pH 4). Sections were rinsed in tap water, counterstained for 2 minutes in 0.1% (w/v) Fast Green and rinsed again. The slides were then dehydrated in three changes of isopropyl alcohol and then xylene. Finally, Euckitt® (O. Kindler & ORSAtec, Freiburg, BW, Germany), a mounting resin and a glass coverslip was applied to complete the staining.

3.6 Histomorphometry assessment of IFP

Previous histological characterizations of the adiposity within IFP have been evaluated in cadaveric human samples, rats and mice[96, 100, 119, 203]. These pre-clinical characterizations have focused mainly on ageing or obesity-induced models of OA. Based on the methodology from Inomata et al. and Fu et al., we evaluate the adipose cell count, mean adipocyte cell size and percentage adiposity within a prespecified field of view that was centralized on the IFP[119, 203].

Adiposity of the IFP was evaluated on a single section within the medial tibiofemoral compartment where synovitis and sub-synovial fibrosis were scored as well. The criteria for the slide chosen, to facilitate using the same anatomical location in all joints, included initial signs of the ACL attachment to the femur (Figure 6A) and without any visualization of the patella. Once the slide was selected, the field of view was focused on the IFP in increasing magnifications. Ideally, the field of view consisted mainly of the IFP with little or no presence of

the meniscus or patellar tendon and included a small section of synovium above the fat pad (Figure 6 B). The images were captured on the Leica DMLB Fluorescence Microscope (Leica, Wetzlar, Germany) using a 40X objective and 10X eyepiece for a total of 400X magnification.

Using the ImageJ software, the overall IFP area and adipocyte area were manually isolated and measured in separate outcomes. The number of adipose cells were also manually counted.

Using these variables, we determined adiposity percentage (total adipocyte area/ overall IFP area) and mean adipose cell size (adipocyte area/adipocyte count) for use in our analyses.

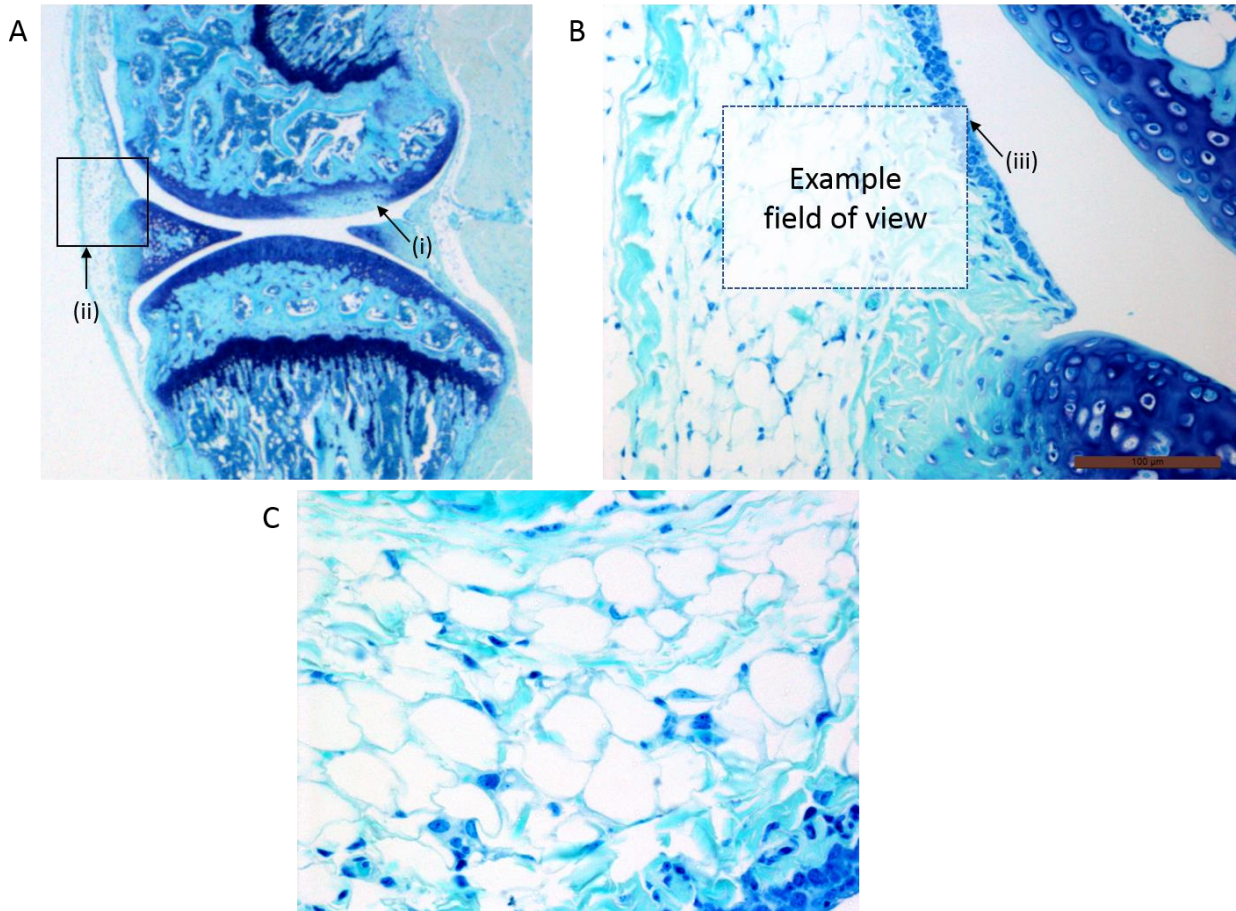


Figure 6. Selection of scoring area for IFP adiposity

(A) (i) Identifies the first sign of the ACL attachment to the femur. (A) (ii) and (B) Shows the approximate scoring area including on 1.6X and 20X magnification, respectively. (B) (iii) An example of the inclusion of the synovium. (C) Shows the final image captured for analysis at 40X magnification.

3.7 Novel sub-synovial fibrosis scoring tool

Fibrosis is a prominent feature of osteoarthritic joints that worsens with disease severity[215]. The accumulation of excessive collagen-rich fibres contributes significantly to clinical manifestations, such as stiffness, and potentially also pain[12, 232]. Fibrotic changes often result from injuries and microtrauma, and within the knee affect the synovium and adjacent spaces, including the IFP[233]. Despite fibrosis in synovial-adjacent tissues and the involvement of all joint tissues in OA, reporting of fibrosis is often integrated into the gradings for synovial health [176, 216]. Some studies have developed fibrosis scoring systems for sheep, rats and humans[203, 217, 234]. However, there is no current validated sub-synovial fibrosis scoring tool for mice despite this species being one of the most commonly used for pre-clinical models of OA[235].

3.7.1 Tool development

The sub-synovial fibrosis scoring tool was developed in an iterative process in consultation with a senior scientist (CBL) with extensive experience in evaluating histopathology in pre-clinical models. A primary criterion and scoring tool were decided upon before independent scoring of 10 unique and randomized specimens by both assessors (HU and CBL) in the first instance. During each follow-up consultation round, assessors discussed the merits and difficulties of the scoring guidelines in terms of validity, feasibility and consistency. The modified tool from each consultation round was audited again by independent scoring of 10 further unique and randomized samples. This process was repeated until both assessors were satisfied with the integrity and reproducibility of the scoring system. The inter-rater reliability of the scoring

system at each iteration was statistically evaluated using Cronbach’s alpha. The analysis was performed using IBM SPSS Statistics, version 26 (IBM Corporation, Armonk, NY, USA).

This thesis presents fibrosis scores assessed by HU while blinded to the injury and time point status of the samples in Chapter 4 and 5 based on the final iteration of the scoring tool described below.

3.7.2 Sub-synovial fibrosis scoring tool

The first iteration of the sub-synovial scoring tool was a crude scoring of the fibrotic thickness in the posterior and anterior of the joint. The thickness was assessed relatively to the thickest normal section of calcified and uncalcified cartilage within the same slide. Each subsequent consultation resulted in a new iteration of the instrument to overcome any identified challenges (Table 1). Several aspects of the fibrosis were eventually included in the final iteration, including the thickness, density and spread of the changes (Figure 3).

Table 7. Description of each iteration of sub-synovial fibrosis scoring tool

Iteration	Description of tool	Challenges
1	<p>→Scoring the maximum thickness of fibrosis</p> <p>0 – less than 1/3 the thickness of the cartilage</p> <p>1 – between 1/3 – 2/3 the thickness of the cartilage</p> <p>2 – between 2/3 – 1 X the thickness of the cartilage</p> <p>3 – more than 1X the thickness of the cartilage</p>	<p>The thickness of fibrosis varies a great deal along the span of synovium visible on each section</p>

Table 7 continued

<p>2</p>	<p>→ Scoring the maximum thickness of fibrosis</p> <p>0 – less than 1/3 the thickness of the cartilage</p> <p>1 – between 1/3 – 2/3 the thickness of the cartilage</p> <p>2 – between 2/3 – 1 X the thickness of the cartilage</p> <p>3 – more than 1X the thickness of the cartilage</p> <p>→ Scoring total fibrosis as the sum of the products of the percentage and thickness of fibrosis</p> <p>0 – less than 20%</p> <p>1 – more than 21% and less than 40%</p> <p>2 – more than 41% and less than 60%</p> <p>3 – more than 61% and less than 80%</p> <p>4 – more than 80%</p>	<p>The density of the fibrosis varies</p>
<p>3</p>	<p>→ Scoring the maximum thickness of fibrosis</p> <p>0 – less than 1/3 the thickness of the cartilage <i>densely packed</i></p>	<p>Downgrading scores based on density was not an accurate</p>

Table 7 continued

	<p><i>fibres or 1/3 – 2/3 the thickness of the cartilage loosely packed</i></p> <p>1 – between 1/3 – 2/3 the thickness of the cartilage <i>densely packed fibres or 2/3 – 1 X the thickness of the cartilage loosely packed</i></p>	<p>representation of the severity</p> <p>The area to score</p>
	<p>2 – between 2/3 – 1 X the thickness of the cartilage <i>densely packed fibres or more than 1 X the thickness of the cartilage loosely packed</i></p> <p>3 – more than 1X the thickness of the cartilage <i>densely packed fibres</i></p> <p>→ Scoring total fibrosis as the sum of the products of the percentage (as in iteration 2) and thickness of fibrosis</p>	<p>is not well defined</p>
<p>4</p>	<p><i>Area to score – Superior to the meniscal remnant to halfway to the synovial attachment to the bone</i></p> <p>→ Scoring the maximum thickness of fibrosis</p> <p>0 – less than 1/3 the thickness of the cartilage densely packed</p>	<p>The area to score is not well defined</p>

Table 7 continued

	<p>fibres</p> <p>1 – between 1/3 – 2/3 the thickness of the cartilage loosely packed</p> <p>2 – between 1/3 – 2/3 the thickness of the cartilage densely packed fibres</p> <p>3 – between 2/3 – 1 X the thickness of the cartilage loosely packed</p> <p>4 – between 2/3 – 1 X the thickness of the cartilage densely packed fibres</p> <p>5 – more than 1 X the thickness of the cartilage loosely packed</p> <p>6 – more than 1X the thickness of the cartilage densely packed fibres</p> <p>→ Scoring total fibrosis as the sum of the products of the percentage (as in iteration 2) and thickness of fibrosis</p>	
--	---	--

Table 7 continued

<p>5</p>	<p>1 – between 1/3 – 2/3 the thickness of the cartilage loosely packed</p> <p>2 – between 1/3 – 2/3 the thickness of the cartilage densely packed fibres</p> <p>3 – between 2/3 – 1 X the thickness of the cartilage loosely packed</p> <p>4 – between 2/3 – 1 X the thickness of the cartilage densely packed fibres</p> <p>5 – more than 1 X the thickness of the cartilage loosely packed</p> <p>6 – more than 1X the thickness of the cartilage densely packed fibres</p> <p>→ Scoring total fibrosis as the sum of the products of the percentage (as in iteration 2) and thickness of fibrosis</p>	
<p>6</p>	<p><i>Area to score – Superior to the meniscal remnant up to the margin of the growth plate</i></p> <p>→ Scoring the maximum thickness of fibrosis</p>	<p>High consistency scoring on the same slides, but the selection of slides was not</p>

Table 7 continued

	<p>0 – less than 1/3 the thickness of the cartilage densely packed fibres</p> <p>1 – between 1/3 – 2/3 the thickness of the cartilage loosely packed</p> <p>2 – between 1/3 – 2/3 the thickness of the cartilage densely packed fibres</p> <p>3 – between 2/3 – 1 X the thickness of the cartilage loosely packed</p> <p>4 – between 2/3 – 1 X the thickness of the cartilage densely packed fibres</p> <p>5 – more than 1 X the thickness of the cartilage loosely packed</p> <p>6 – more than 1X the thickness of the cartilage densely packed fibres</p> <p>→Scoring total fibrosis as the sum of the products of the percentage (as in iteration 2) and thickness of fibrosis</p>	<p>always matched between assessors.</p>
--	---	--

At each iteration, the inter-rater reliabilities were calculated and used to inform the need to refine the scoring tool (Table 2). Despite iteration 2 having a high Cronbach's alpha (maximum fibrosis = 0.854, total fibrosis = 0.931) the scientific basis of the instrument required modification. After several rounds, the Cronbach's alpha once again showed high consistency (maximum fibrosis = 0.886, total fibrosis = 0.911). The consistency was finally audited in prechosen slides, and assessors maintained a high alpha of 0.683 for maximum fibrosis and alpha of 0.807 for total fibrosis.

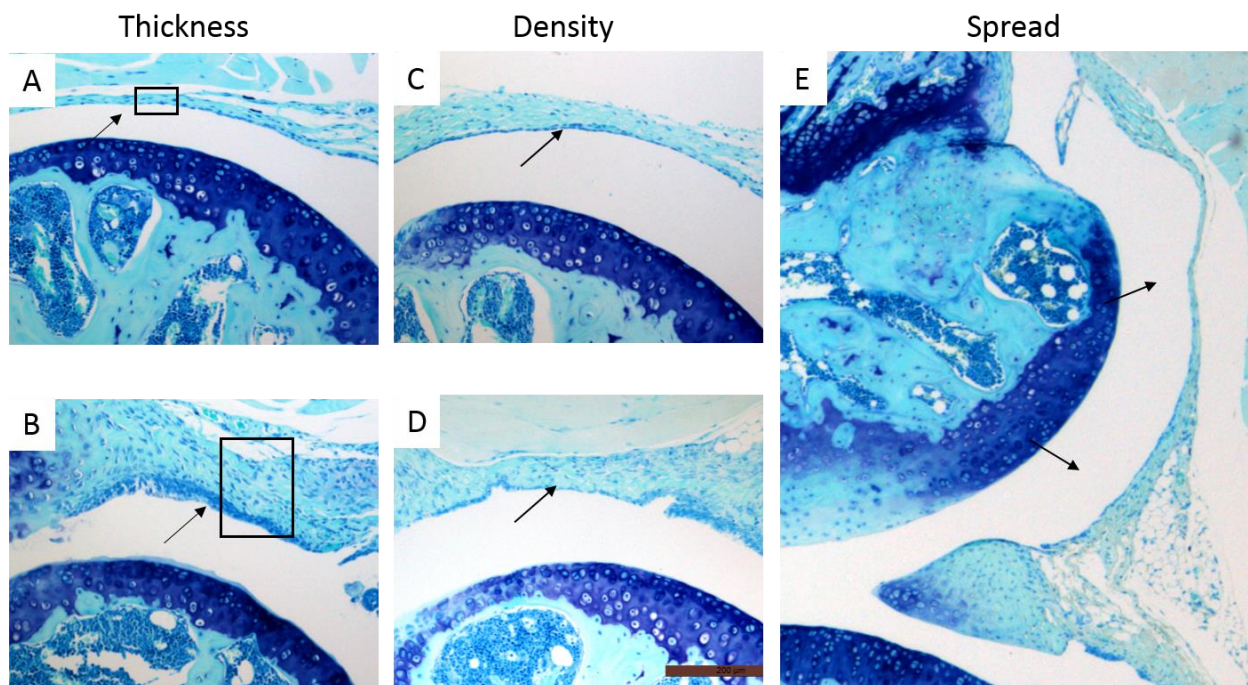


Figure 7. Differences in aspects of the scoring tool.

(A) and (B) show the differences in a grade 1 vs grade 6 score of thickness, respectively. (C) and (D) show the density difference in a loosely packed network with small white spaces versus densely packed fibrosis. (E) Shows the variation of thickness spread across the scoring area.

Table 8. Cronbach's Alpha for measuring the internal consistency of the scoring tool

Instrument	Cronbach's Alpha		
	Fibrosis	Maximum Fibrosis	Total Fibrosis
Iteration 1	0.648		
Iteration 2		0.854	0.931
Iteration 3		0.447	0.433
Iteration 4		0.799	0.895
Iteration 5		0.568	0.779
Iteration 6		0.886	0.911
Final Development Audit		0.683	0.807

Chapter 4. Pre-clinical Study 1

Written as a manuscript in preparation for submission:

Urban, H. Blaker, C. Shu, C. Clarke, E. Little, C B. Investigating IFP adiposity, synovitis, sub-synovial fibrosis and pain in pre-clinical models of post-traumatic osteoarthritis. Osteoarthritis and Cartilage

4.1 Abstract

Background

As seen in chapters 1 and 2, little is known about changes in IFP adiposity, its relationship to the synovium or pain in preclinical models. There is virtually no current literature of these mechanisms in models of post-traumatic osteoarthritis (PTOA) despite the history of injuries accounting for more than 12% of knee OA incidence. This study aims to investigate the relationship between features of IFP adiposity, synovitis and sub-synovial fibrosis in preclinical models of ACL injury.

Methods

As described in Chapter 3, 10-week old male C57Bl/6 mice were assigned to ACL-transection (ACLT), SHAM surgery, ACL-rupture (ACLR), sub-critical ACL injury or non-operated control groups and studied for 1, 2, 4- or 8-weeks post-injury. In addition to the histological methods described in chapter 3, synovitis was also assessed on the following domains; 1) pannus formation, 2) bone erosion, 3) synovial hyperplasia, 4) sub-synovial infiltrate and 5) synovial exudate. The IFP, anterior-synovium and joint capsule were harvested en bloc for RNA

extraction and quantitative real-time polymerase chain reaction (RT-PCR) analysis of a spectrum of molecules implicated in synovial inflammation and fibrosis. The genes evaluated can be broadly categorised into five groups:

- 1) Pro-inflammatory cytokines (*Il6, Il18*)
- 2) Macrophages (*Tnf, Itgam, Itgax, Mrc1*)
- 3) Adipokines (*Adipoq, Lep*)
- 4) T-cells (*Cd4, Cd8a*)
- 5) Fibrosis (*Mmp3, Mmp9, Mmp13, Acta2, Col1a, Col3a*)

Additionally, a separate set of animals underwent pain behaviour testing at baseline and 1, 2, 4, and 8-weeks post-injury (n=5-7/group/time point) using von Frey Filaments (to quantify tactile allodynia) and an incapitance unit (to determine static hind limb weight distribution). Differences between the treatment groups at different time points were assessed using a mixed-effects model with Geisser-Greenhouse correction and Tukey's multiple comparison test. Spearman's correlation was used to evaluate the association between histological adiposity, synovitis and sub-synovial fibrosis.

Findings

The reduced adiposity measures of the IFP were associated with increased levels of synovitis and sub-synovial fibrosis histologically in preclinical models of ACL injury. This relationship impacted local pathology as well as the whole joint as seen by correlations to posterior pathology. The pro-inflammatory changes in surgical models appeared to be linked to CD4 T-

cell and M1 macrophage pathways. However, reduced IFP adiposity appeared to reduce adipokine activity. No trends between changes in IFP adiposity and pain were ascertained.

Conclusion

Changes of IFP adiposity of the various PTOA models were associated with local and whole joint presentations of synovitis and sub-synovial fibrosis histologically. In general, pro-inflammatory changes in surgical models were connected to CD4 T-cell and M1 macrophage pathways. Additionally, the reduced adiposity of the IFP appeared to be related to lower adipokine activity. Future studies are needed to understand the relationship of IFP adiposity to other pathological changes in the joint as well as to confirm the inflammatory pathways identified in this study.

4.2 Introduction

Osteoarthritis (OA) is a complex disease that involves all joint structures, including the synovium in its pathophysiology[236]. In its healthy state, the synovial lining is 1-2 cells thick and functions to maintain tissue surfaces as well as the composition and volume of synovial fluid[237]. Despite out-dated definitions of OA as a cartilage disease, there has been strong evidence of synovitis in osteoarthritic joints for many years [238, 239]. Since then with the advent of more advanced imaging methods, synovial changes have been found to precede the development of radiographic OA and contribute to the progression of structural as well as symptomatic disease [240, 241].

Synovitis in OA is histologically characterised as hyperplasia of the synovial lining and thickening of the subintima, along with sub-synovial fibrosis, vascularisation and focal inflammatory cell infiltration [242]. The molecular mechanisms of synovitis are far more complicated with the involvement of multiple immune cells such as macrophages, T-cells and B-cells along with a myriad of other inflammatory mediators including cytokines, chemokines and intact and degraded matrix molecules (acting as damage-associated-molecular-patterns; DAMPs) [11, 118, 243, 244]. The products of this inflammatory response in the tissues lining the joint are often released into the synovial fluid, which in turn drives further damage in intra-articular structures (cartilage, meniscus) as well as propagating more widespread synovitis: a vicious cycle that worsens structural damage and disease progression [241, 245].

The infrapatellar fat pad (IFP) is an innervated piece of adipose tissue adjacent to the synovium, which contributes to the inflammation of the joint[19, 176]. Evidence of increased levels of adipokines, such as adiponectin and leptin, in the synovial fluid of the knee compared to other

joints, have suggested the IFP plays a symbiotic role with the other tissues in knee OA pathophysiology[94, 95]. Inflammation in the IFP is often used as a surrogate for “synovitis” when evaluating MRI's in clinical trials[197, 207]. However, the relationship between the IFP and the synovium/synovial-tissue more broadly is not well investigated.

Despite the uncertain interaction, both tissues have been investigated separately for their association with pain. The relationship between synovitis and pain is well-established with evidence of significant correlation and increasing pain associated with greater synovitis[246, 247]. Several studies further established the relationship by identifying that fluctuations in pain were closely linked to the variation in synovial effusion[195, 248, 249]. The association between IFP inflammation and pain is less well-established, with conflicting results reported, as highlighted in chapter 2. Consistent with findings from our systematic review (submitted/Chapter 2), Ballegaard et al. showed a positive correlation between pain and IFP inflammation defined by MRI[106]. In contrast, Klein-Wieringa et al. showed no significant association between IFP inflammation as defined by the accumulation of different immune cell types, and knee pain[118].

Despite the theoretical construct created by the proximity of the IFP and synovium and their association to pain, there remains a significant gap in the current understanding of the potential cellular and molecular mechanisms that connect the IFP, synovium and pain. This study aims to investigate the relationship between IFP adiposity and synovitis in preclinical models of post-traumatic OA (PTOA). It is estimated that 12% of lower limb OA incidence is linked to a history of joint trauma[250]. Within the knee, the anterior cruciate ligament (ACL) is most commonly injured, and 50% of the injuries lead to PTOA development within 10 – 20

years[251-254]. However, the IFP has not been well studied in the context of traumatic injuries despite the critical relation to disease incidence. Findings from two recent studies have demonstrated that surgical destabilisation of the medial meniscus results in increased inflammation and fibrosis in the IFP[255, 256]. In the present study, we have used well-established mouse models of ACL injury, to first evaluate if IFP adiposity is correlated to synovitis or sub-synovial fibrosis in the medial tibiofemoral compartment of the murine knee joint using histological scores. We also explored the changes at different stages of PTOA development in IFP adiposity, synovitis and fibrosis individually using histopathological methods and by gene expression analysis of the synovium-IFP tissue unit. Finally, we compared those findings to temporal changes in pain measures to discern if any of the biological changes observed have an impact on symptoms.

4.3 Methods

The methodology for animal work, sample processing, histological adiposity and histological fibrosis scoring is detailed in Chapter 3. Joints were studied at 7, 14, 28- and 56-days post-injury for histopathological scoring and gene analysis. Behavioural pain studies were conducted on a separate set of animals and studied longitudinally for 56 days as described below (Section 4.7).

4.3.1 Synovitis

Synovial inflammation was assessed in the medial tibiofemoral compartment using previously published methods (n=7/group/timepoint) [257]. The synovial tissues in the anterior and posterior regions of the joint were scored separately in slides consistent to IFP adiposity and sub-synovial fibrosis scoring. Serial toluidine-blue/fast-green stained sagittal sections every 40 microns through the width of the medial femorotibial joint compartment were examined to define a standardised anatomical location to score synovitis in all joints. Previous studies determined that the optimum location for evaluating synovitis is in the medial femorotibial joint is toward the axial margin of the compartment at the point when the femoral enthesis of the ACL first becomes apparent (Chapter 3, Figure 6 A)[221, 257, 258]. At this location, articular cartilage is still visualised on the anterior and posterior femur with a clear osteochondral margin and a prominent proximal synovial reflection without the intrusion of the patella in the anterior or fabella in the posterior of the joint. If as a result of imperfect sagittal positioning in the paraffin block a single section fulfilling these criteria could not be identified, separate sections were used to score anterior and posterior joint regions to comply with the above criteria. This synovial scoring system assessed pannus formation, cortical bone erosion, synovial lining hyperplasia, sub-synovial inflammation on a 0 – 3 scale of increasing severity, as well as

the presence of synovial exudate (0 – absent, 1 – present)[221, 257, 258]. The scores of the individual components were also summed to provide a total synovitis score for the joint. All slides were scored by an assessor (HU) blinded to the injury group and post-injury timepoint. Five sets of 10 randomly chosen animals were also assessed by a senior scientist (CBL) with extensive experience with the synovitis scoring system to ensure the reliability of the scoring. On average, across five separate scorings, assessors achieved a Cronbach's alpha of 0.8, which is generally regarded as high consistency[259].

4.3.2 Gene expression analysis

The mRNA expression of a variety of molecules in the combined synovium/IFP tissue of different treatment groups at different time points was evaluated (n=6/group/time point). The molecules chosen for this study included inflammatory cytokines as well as markers of macrophage, adipokine, t-cell and fibrosis activity (Table 9). Additionally, GAPDH and 18s were evaluated as housekeeping genes.

Table 9. Gene groupings in mRNA expression analysis

Inflammatory Cytokines	Macrophages	Adipokines	T-cells	Fibrosis
<ul style="list-style-type: none"> • <i>Il6</i> • <i>Il1b</i> 	<ul style="list-style-type: none"> • <i>Tnf</i> • <i>Itgam</i> • <i>Itgax (M1)</i> • <i>Mrc1 (M2)</i> 	<ul style="list-style-type: none"> • <i>Adipoq</i> • <i>Lep</i> 	<ul style="list-style-type: none"> • <i>Cd4</i> • <i>Cd8a</i> 	<ul style="list-style-type: none"> • <i>Col1a</i> • <i>Col3a</i> • <i>Acta2</i> • <i>Mmp3</i> • <i>Mmp9</i> • <i>Mmp13</i>

Sample processing

Following euthanasia, the synovial tissue (comprising the joint capsule and synovial lining anterior to the collateral ligaments plus the IFP) was surgically excised en bloc under microscopy as previously described[258, 260], immediately frozen in liquid nitrogen and stored at -80°C until required. The samples were pulverised using the MIKRO – Dismembrator S (Braun, Melsungen, Germany) and processed, as per manufacturer instructions, using TRIzol reagent (Invitrogen, VIC, Australia).

RNA extraction and quantification

The extraction of RNA from the processed samples was carried out using RNeasy Kits (Qiagen, VIC, Australia) by following the manufacturer guidelines. Samples were incubated with 300 µl of

chloroform and then centrifuged at 12,000 rpm (speed used for the following step in extraction) for 15 minutes to separate the aqueous (containing the RNA) and organic phases. The aqueous phase was then retrieved and combined with an equal volume of 70% ethanol. After a gentle inversion to ensure mixing, each sample was loaded into separate RNeasy spin columns and centrifuged for 20 seconds. The capacity of the columns was 600 μ l, and hence, the previous step was repeated until the sample was depleted. Samples were incubated at room temperature for 5 minutes with 350 μ l of RW1 buffer and then centrifuged again for 20 seconds.

The collection tubes under the column were replaced at this stage. An on-column DNase application (80 μ l in RDD buffer) was applied, centrifuged for 20 seconds and then re-applied. Samples were then incubated at 37°C for an hour and washed once with 350 μ l of RW1 buffer and twice with 500 μ l of RDD buffer. To ensure, no remaining traces of ethanol, samples were then centrifuged for an additional 2 minutes. After which RNA was collected by loading 30 μ l of RNase free water and centrifuging for one minute.

The quantity of RNA was measured on a Nanodrop spectrophotometer (Thermo Fisher Scientific, Waltham, MA, USA).

Reverse transcription (RT)

All RNA samples were reverse transcribed to cDNA at the same time using the GoScript Kit (Promega, Madison, WI, USA) according to manufacturer instructions. The reverse transcription master-mix contained the following for each reaction:

- From the kit:
 - 1µl RT enzyme
 - 10 µl 5 X RT buffer
 - 3 µl of MgCl₂
- 2 µl deoxyribonucleotide triphosphates (dNTPs)
- 2 µl random primers
- 2 µl RNase inhibitor

Sample volumes equivalent to 500ng of RNA were calculated and added to RNase free water for a final amount of 30ul. Each diluted sample then received 20 µl of master-mix and was spun down quickly in the centrifuge. Samples were then incubated at 37°C for 3 hours, followed by 5 minutes at 93°C and cooled on ice for five minutes. Finally, samples were diluted with 75 µl of water and stored at 4°C while in use for the next step.

Polymerase Chain Reaction (RT-PCR)

Quantification for gene expression was carried out using the Rotor-Gene 6000 System (Corbett Life Sciences, Sydney, NSW, Australia). Due to the number of samples, the reactions were executed in two separate batches per gene (using 72 sample rings) with an equal distribution of treatment groups and time points across the two batches.

A master-mix for each reaction contained Immomix, forward and reverse primers (as described in the appendix) and SYBR Green 1 dye in RNase free water. Each reaction tube contained 12 µl of master-mix along with 3 µl of cDNA sample (that was normalised to 500 ng of total RNA used in for RT in all samples) or standard. The standards used in this experiment were an

amalgamation of 5 µl of cDNA from each sample which was then serially diluted for four standards (1 in 1, 4, 16 and 64 dilutions). Additionally, RNase free water was used as a negative control and all controls were run in duplicates. The reactions were carried out using the following thermal profile:

- Denaturation for 10 minutes at 95°C
- 45 cycles of
 - 95°C for 10 seconds
 - Primer specific annealing temperature for 15 seconds (Appendix 4)
 - 72°C for 20 seconds
- Melt curve generation

A melt curve analysis was done to confirm the specificity of the product from the reaction. The use of two separate batches/gene resulted in two independent outputs that had to be appropriately quantified for comparison. In order to achieve this, the standard curve thresholds were manually adjusted until the cycling threshold of the standards were almost identical. All gene analysis results are presented as the relative fluorescence units.

4.3.3 Pain behaviour testing

Pain behaviour testing was conducted at baseline as well as 7, 14, 28, and 56-days post-injury (n=5-7/group/time point). Two separate outcomes were measured; the withdrawal response to a distal mechanical stimulus (using von Frey Filaments); and change in right (ipsilateral) versus left (contra-lateral) static hind limb weight-bearing (using an incapitance machine). Before baseline testing, all mice were acclimatised to the testing equipment during at least two

sessions on separate days. The animals were placed in the von Frey and incapacitance testing chambers and allowed to acclimatise for 30 minutes or 1 – 3 minutes, respectively.

We evaluated the four injury groups for pain behaviours: sham surgery, ACLT, ACLR and sub-critical injury. Measures were collected at baseline before the injury to serve as an internal uninjured control. Assessors were blinded to the injury groups by having an independent researcher randomise and assign coded identification tags to mice and cages.

Von Frey Filament Testing

Mechanical allodynia was evaluated with von Frey filaments (Ugo Basile, Italy) using a pre-established protocol[261-264]. Testing began after each mouse had been acclimatised to the individual testing chambers with wire mesh floors and had reduced their exploratory and grooming behaviours. An intermediate filament (size 3.61, log units = 0.4g of force) was used at the first instance and followed by a series of different sizes to determine the paw withdrawal threshold. As per protocol, the stimulus was applied for up to 3 seconds using the filament perpendicular to the plantar surface of the hind paw until the instrument buckled, indicating maximum force had been reached. A positive response of changed behaviours, such as biting, licking, shaking or withdrawal of the paw tested, was recorded and followed with more testing using smaller filaments. A negative response, with no behaviour's changes, was also recorded but the following stimulus was carried out with increasingly larger filaments instead (known as the “up-down” method). In total, six stimuli were applied to determine the 50% paw withdrawal threshold based on the calculations by Chaplan et al. [264].

The animals were tested on both hind-limbs – with the uninjured paw first followed by the injured limb, in duplicate. The 50% paw withdrawal threshold was calculated for each round and leg separately, and the average score for the limb recorded. All von Frey data presented in this chapter was collected by an experienced and blinded assessor (SZ), and the analysis and interpretation were carried out by HU.

Incapacitance

Variations in static hind-limb weight-bearing behaviour were evaluated in a custom incapacitance tester which included a chamber, separate force plates for each limb, data acquisition software (USB-6008, National Instruments, Austin, Texas, USA) and a customised LabVIEW program (LabVIEW Run-Time Engine 2009 Software, National Instruments, Austin, Texas, USA).

Weight-bearing behaviour was recorded following the acclimatisation period in the chamber and only while the mouse was in the correct position. The appropriate testing position required the mouse to:

1. have fore-paws placed on the front of the chamber;
2. with each hind-limb resting on the respective force plates;
3. without any weight support from the walls of the testing chamber and;
4. tail positioned outside the chamber and slightly elevated to avoid contact with the force plates.

Measurements were recorded for a total period of 30 seconds which excluded any breaks where the animal was not in the correct position (during which testing was paused until the

right placement was resumed). The data collected provided the weight distribution ratio of the injured over the un-injured limb.

4.3.4 Statistical analysis

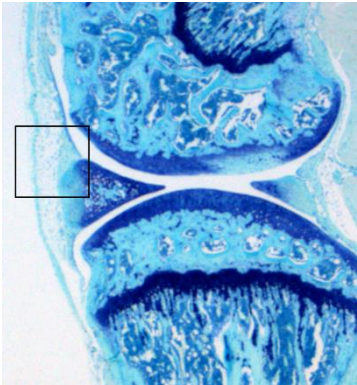
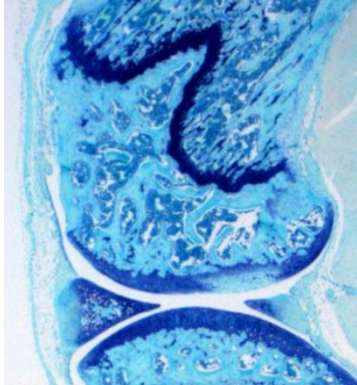
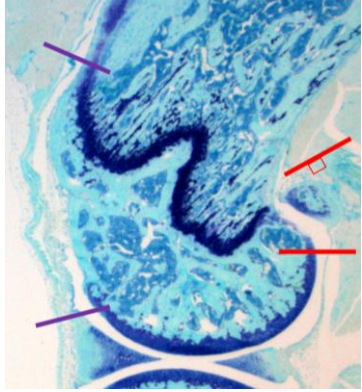
The histology and gene expression differences between the treatment groups at different time points were evaluated using a mixed-effects model with Geisser-Greenhouse correction. The differences were further investigated to each group using Tukey's multiple comparison test.

Similarly, the differences in pain outcomes were evaluated using a mixed-effect model with Geisser-Greenhouse correction. However, the differences were compared to the internal baseline control, and thus, Dunnet's multiple comparison test was used post-hoc.

Spearman's correlation was used to evaluate the strength and direction of the association between histological adiposity, synovitis and sub-synovial fibrosis (Table 10). All samples, including those of different timepoints were included into a single analysis. Correlation coefficients ≤ 0.29 represented weak association; between 0.30 and 0.49 moderate and ≥ 0.50 strong association[265]. Multiple linear regression was also used to evaluate if synovitis, sub-synovial fibrosis and time points could predict IFP adiposity percentage in each injury group separately. The overall fit of each model (R^2) and the β coefficient for each variable are presented in the results.

A nominal significance level of 0.05 was used. Correlation and regression analyses were performed using IBM SPSS Statistics, version 26 (IBM Corporation, Armonk, NY, USA) and GraphPad Prism version 8.4.2 (GraphPad Software, Inc., San Diego, CA, USA) for all other statistical analyses and figures.

Table 10. Variables used and the respective areas scored in the correlation analysis

Adiposity	Synovitis	Sub-synovial Fibrosis
		
<ul style="list-style-type: none"> • Adiposity percentage • Adipose cell count • Mean adipose cell size 	<ul style="list-style-type: none"> • Whole joint synovitis • Total anterior synovitis • Anterior pannus • Anterior cortical bone erosion • Anterior synovial lining hypertrophy • Anterior sub-synovial inflammation • Anterior synovial exudate • Total posterior synovitis • Posterior pannus 	<ul style="list-style-type: none"> • Maximum anterior fibrosis • Total anterior fibrosis • Maximum posterior fibrosis • Total posterior fibrosis

	<ul style="list-style-type: none">• Posterior cortical bone erosion• Posterior synovial lining hypertrophy• Posterior sub-synovial inflammation• Posterior synovial exudate	
--	--	--

4.4 Results

4.4.1 Time and injury impacts on synovitis

There was no change in total synovitis score in NOC or sub-critically injured mice over time (Figure 8). In contrast, total synovitis score was increased from day 7 in SHAM, ACLT and ACLR animals. These changes were still present on day 56 in ACLT and ACLR, while synovitis levels in SHAM animals reduced back to NOC levels by that stage.

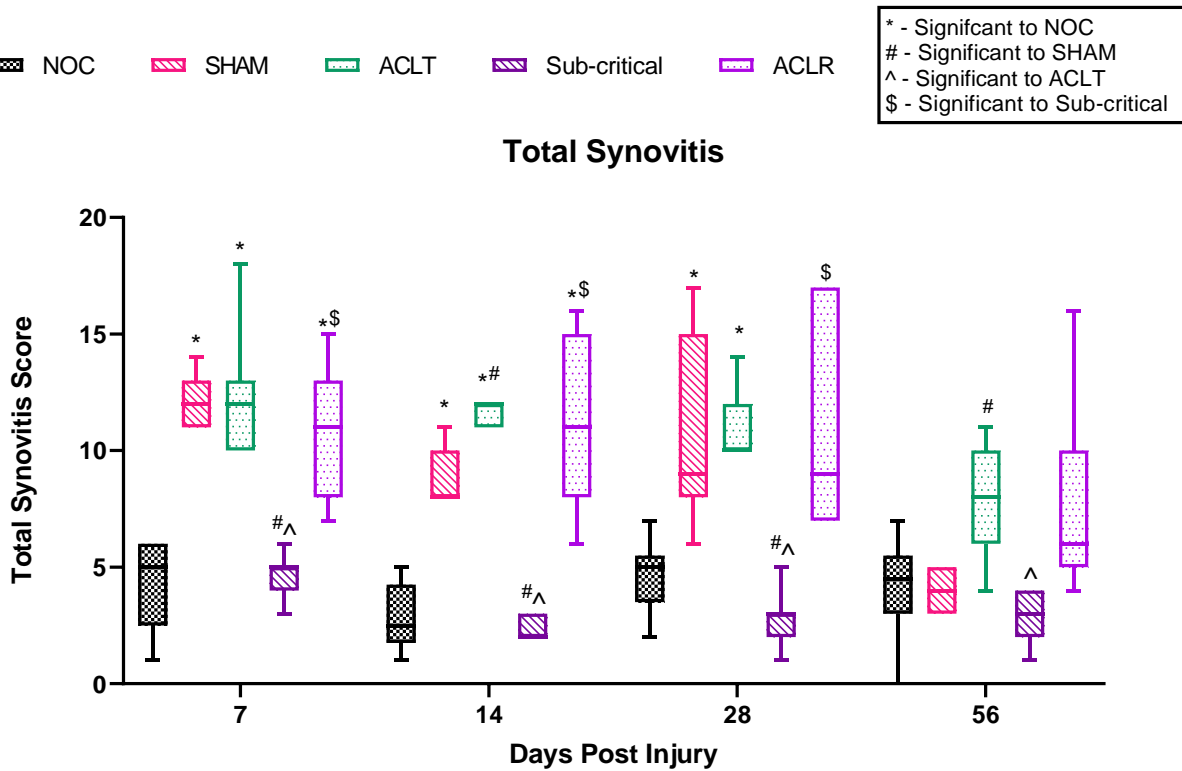


Figure 8. Total Synovitis Scores

Overall, the temporal and injury-group patterns were similar when total anterior and posterior synovitis were evaluated separately (Figure 9 and 10, respectively). Of the individual domains of

synovitis, only synovial hyperplasia, sub-synovial inflammation and synovial exudate discriminated between the different models, and this was true both anterior and posterior. Pannus formation and bone erosion were not statistically different between any of the groups at any time in either region.

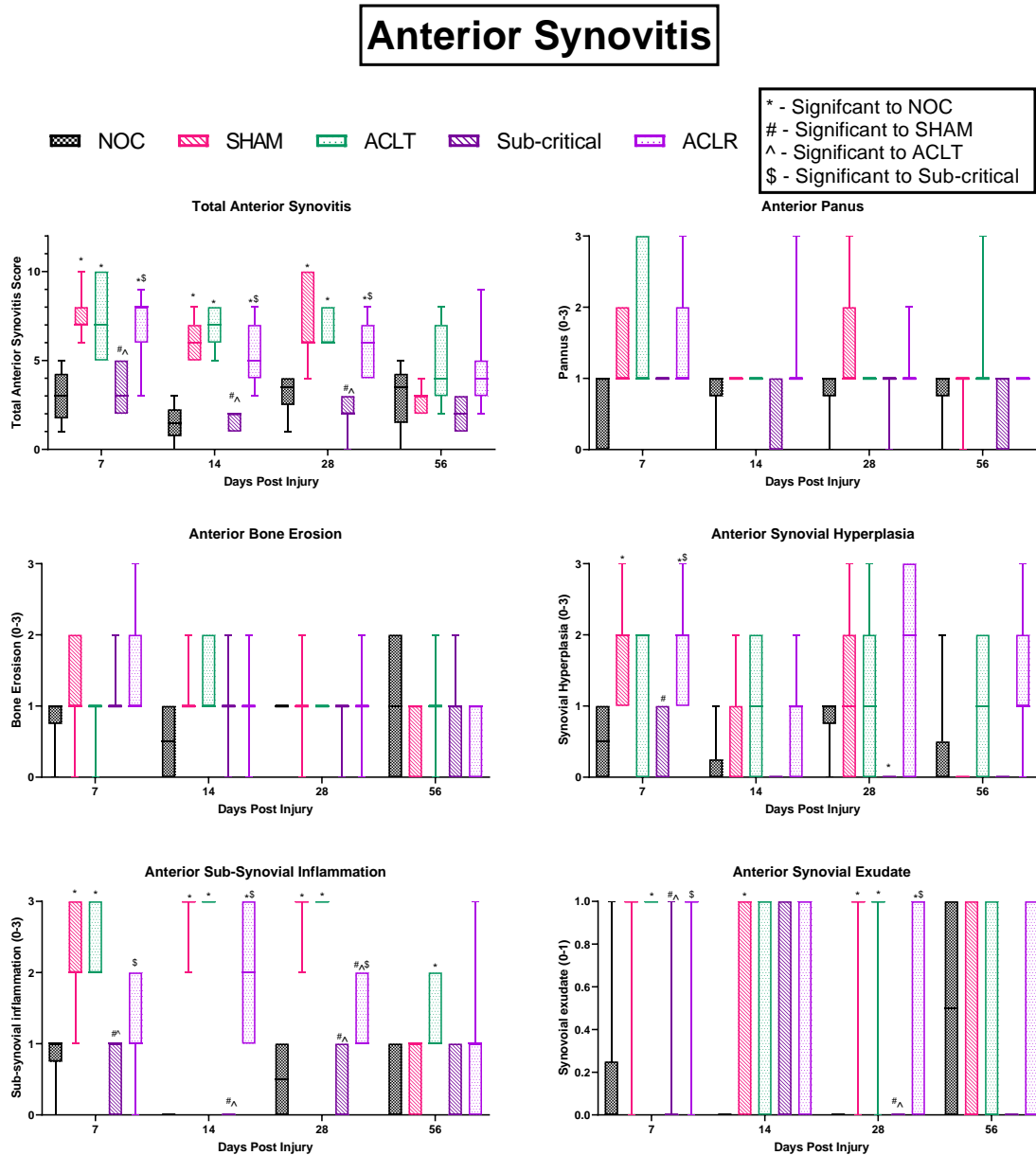


Figure 9. Anterior synovitis

Posterior Synovitis

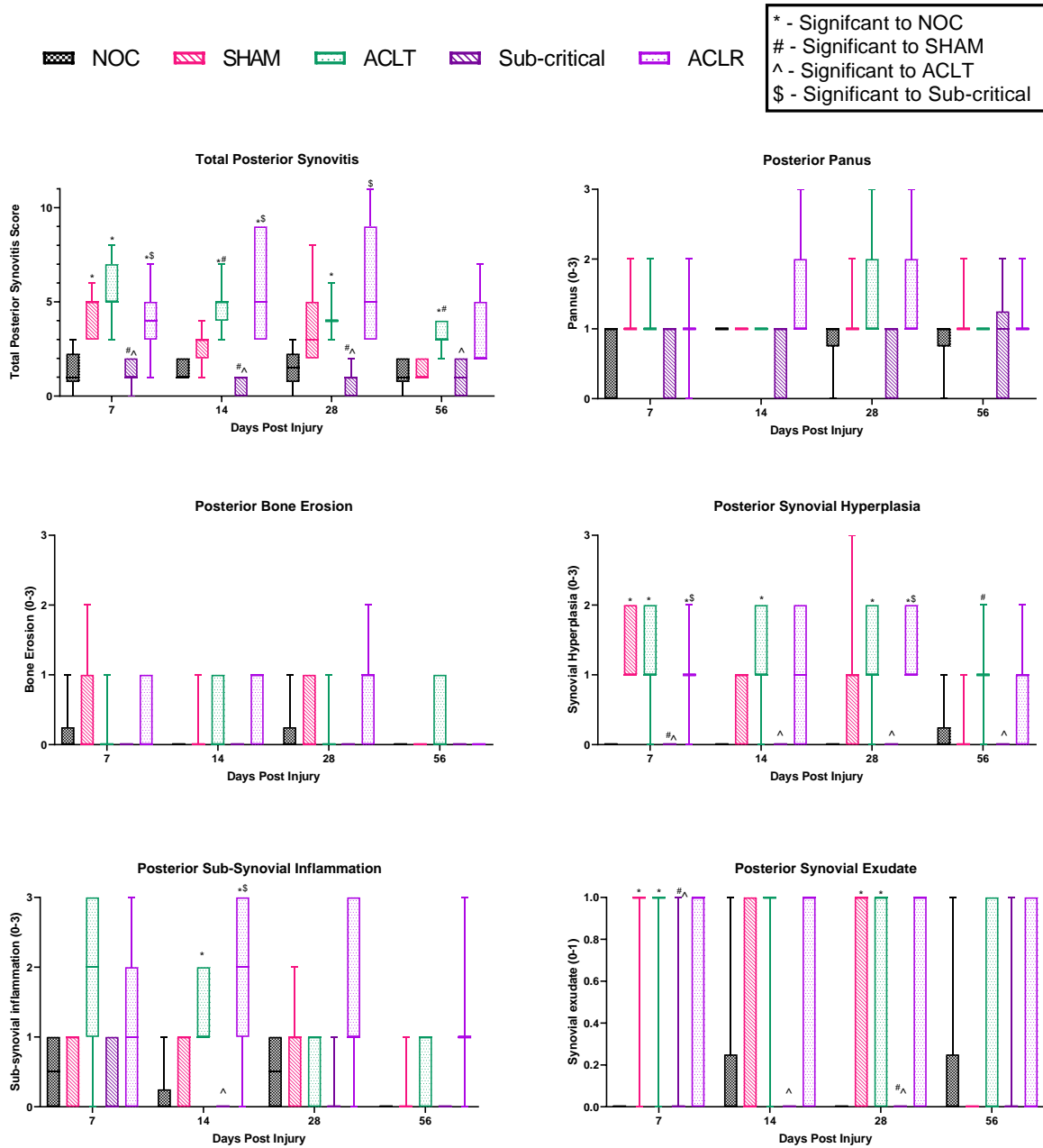


Figure 10. Posterior Synovitis

4.4.2 Time and injury impacts on sub-synovial fibrosis

Maximum fibrosis scores showed little difference between groups or with time in the anterior of the joint, other than an increase in ACLR at day 7 compared with NOC (Figure 11). Posterior maximal fibrosis scores were lower than anterior in NOC and remained low at all times. There was no effect of sub-critical injury on maximum posterior fibrosis, while increases were seen in SHAM, ACLT and ACLR from day 7. While the fibrotic changes appeared to be sustained to day 56 in the ACL deficient knees (ACLT and ACLR), posterior fibrosis resolved in SHAM-operated animals returning to levels similar to NOCs.

In contrast to maximum scores, total fibrosis score, which included a measure of the spread or percentage of joint capsule affected, was increased in both anterior and posterior joint regions in response to injury. Models with complete loss of ACL integrity (ACLT, ACLR) showed increased total anterior and posterior fibrosis from day seven, which tended to normalise by day 28 and 56, respectively (Figure 11). There was an increase in total fibrosis score in SHAM-operated joints from day-14 onwards albeit not statistically significant compared with NOC, and only in the anterior joint. Fibrosis increased more rapidly in ACLR compared with ACLT in both anterior and posterior joint regions, and the increase tended to be more sustained.

Sub-Synovial Fibrosis

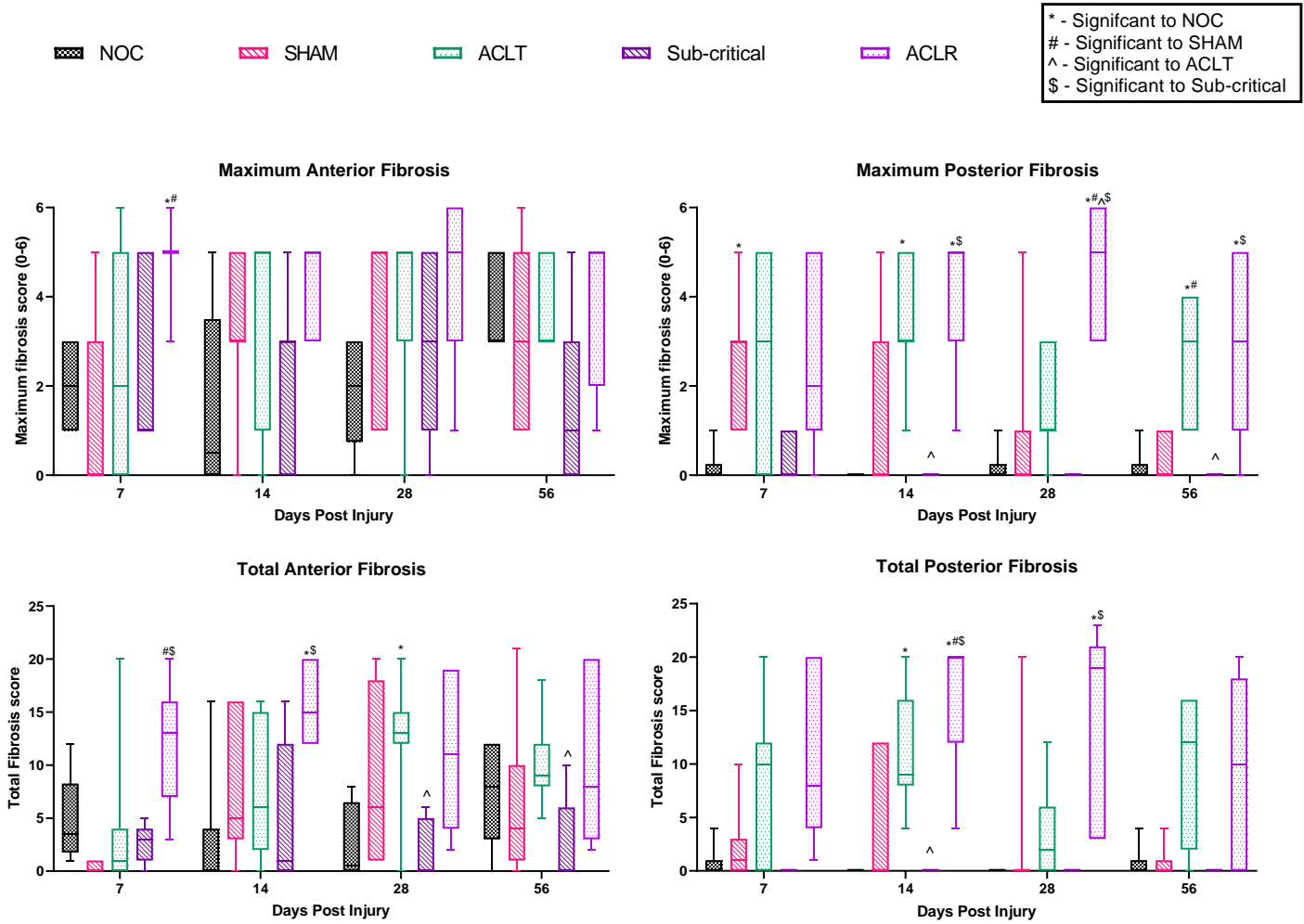


Figure 11. Sub-synovial fibrosis

4.4.3 Time and injury impacts on IFP adiposity

There was no change in adiposity measures of the IFP (adipose percentage, cell count and mean cell size) in naïve (NOC) joints over time (Figure 12). All three IFP adiposity measures were markedly impacted by joint surgery (SHAM, ACLT; Figure 12). In both SHAM and ACLT, there was a notable decrease in all measures from day seven, which further deteriorated to demonstrate a significant difference compared to NOC in both models from day 14. Adiposity percentage and cell count remained significantly lower in both surgical models at 56 days after surgery, whereas, adipose cell size began to increase and was no longer statistically lower than NOCs at day 56. There was no effect of sub-critical mechanical injury on any IFP adiposity measures at any time. However, while less severe than surgical injury, all three IFP adiposity measures were affected by ACLR with a different temporal pattern compared to the surgical models. Adipose percentage and cell count in ACLR were unchanged at 7 days, decreased at days 14 and 28 before returning to be the same as NOC by day 56. Mean adipocyte size also showed a transient decrease in ACLR but only at day 14, returning to NOC levels by day 28.

Adiposity in the IFP

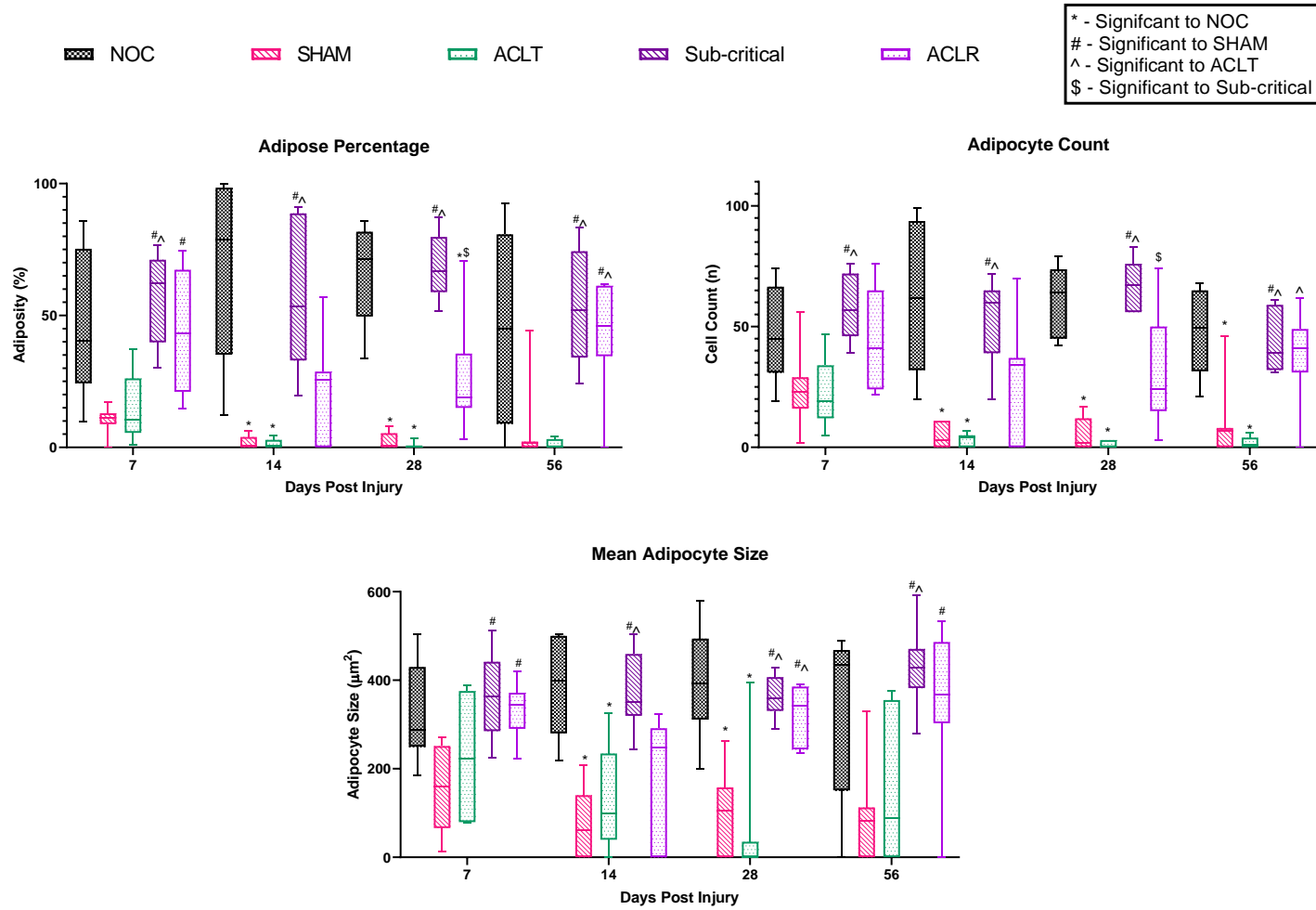


Figure 12. IFP adiposity

4.4.4 Correlations between histological features

The above findings revealed temporal, regional and model-specific changes in synovitis, sub-intimal fibrosis and IFP adiposity. To further explore how changes in these individual measures may be inter-related correlation analysis was conducted.

Reduced adiposity in the IFP was strongly correlated with higher whole joint, total anterior and total posterior synovitis scores (Table 11). In the anterior, percentage adiposity was weakly negatively correlated to pannus formation, moderately negatively correlated to the presence of synovial exudate and strongly negatively correlated with sub-synovial inflammation in the anterior of the joint. Correlations to the posterior features were somewhat different with weak correlations to bone erosion and sub-synovial inflammation, and moderate correlations to pannus formation, synovial hyperplasia and synovial exudate. Similar findings were found when assessing the correlation between synovitis and number of adipose cells or their mean size.

Table 11. Correlation between adiposity measures in the IFP and synovitis scores

Spearman's Rho	Percentage adiposity	Adipose Cell count	Mean adipose cell size
Whole Joint Synovitis	-0.552	-0.521	-0.465
P value	<0.001	<0.001	<0.001
Total Anterior	-0.535	-0.506	-0.469
P value	<0.001	<0.001	<0.001
Anterior Pannus	-0.219	-0.157	-0.265

Table 11 continued

Spearman's Rho	Percentage adiposity	Adipose Cell count	Mean adipose cell size
P value	0.010	0.068	0.002
Anterior Bone Erosion	-0.043	-0.047	-0.036
P value	0.621	0.592	0.680
Anterior Synovial Hyperplasia	-0.168	-0.163	-0.107
P value	0.051	0.058	0.218
Anterior Sub-synovial inflammation	-0.702	-0.690	-0.615
P value	<0.001	<0.001	<0.001
Anterior Synovial exudate	-0.446	-0.377	-0.419
P value	<0.001	<0.001	<0.001
Total Posterior	-0.515	-0.486	-0.417
P value	<0.001	<0.001	<0.001
Posterior Pannus	-0.310	-0.303	-0.227
P value	<0.001	<0.001	0.008
Posterior Bone Erosion	-0.214	-0.216	-0.173
P value	0.012	0.012	0.045
Posterior Synovial Hyperplasia	-0.451	-0.435	-0.341
P value	<0.001	<0.001	<0.001

Table 11 continued			
Spearman's Rho	Percentage adiposity	Adipose Cell count	Mean adipose cell size
Posterior Sub-synovial inflammation	-0.276	-0.267	-0.239
P value	0.001	0.002	0.005
Posterior Synovial exudate	-0.438	-0.415	-0.305
P value	<0.001	<0.001	<0.001

IFP adiposity was also moderately but negatively correlated to total sub-synovial fibrosis in both anterior and posterior regions of the joint (Table 12). The maximum fibrosis score in the anterior medial tibial compartment showed lesser association with IFP adiposity measures, while moderate negative correlations were seen with maximal posterior fibrosis.

Table 12. Correlation between IFP adiposity and sub-synovial fibrosis

Spearman's Rho	Percentage adiposity	Adipose Cell count	Mean adipose cell size
Max Anterior Fibrosis	-0.182	-0.141	-0.120
P value	0.034	0.102	0.167
Total Anterior Fibrosis	-0.299	-0.326	-0.189
P value	<0.001	<0.001	0.028

Table 12 continued			
Spearman's Rho	Percentage adiposity	Adipose Cell count	Mean adipose cell size
Max Posterior Fibrosis	-0.370	-0.343	-0.306
P value	<0.001	<0.001	<0.001
Total Posterior Fibrosis	-0.329	-0.328	-0.241
P value	<0.001	<0.001	0.005

Finally, maximum and total anterior fibrosis was correlated to whole joint, anterior and posterior synovitis along with some of the individual features in a positive but weak relationship (Table 13). Anterior pannus formation and bone erosion along with posterior bone erosion showed no correlation to anterior fibrosis. In contrast, posterior fibrosis (maximum and total) showed mainly strong and positive correlations to whole joint, anterior and posterior synovitis. The only feature that was not correlated to posterior fibrosis was anterior bone erosion.

Table 13. Correlations between sub-synovial fibrosis and synovitis

Spearman's Rho	Max Anterior Fibrosis	Total Anterior Fibrosis	Max Posterior Fibrosis	Total Posterior Fibrosis
Whole Joint Synovitis	0.261	0.317	0.683	0.627
P value	0.002	<0.001	<0.001	<0.001

Table 13 continued

Spearman's Rho	Max Anterior Fibrosis	Total Anterior Fibrosis	Max Posterior Fibrosis	Total Posterior Fibrosis
Total Anterior	0.264	0.276	0.607	0.535
P value	0.002	0.001	<0.001	<0.001
Anterior Pannus	0.114	0.070	0.360	0.257
P value	0.186	0.417	<0.001	0.003
Anterior Bone Erosion	0.060	0.111	0.144	0.144
P value	0.491	0.199	0.095	0.096
Anterior Synovial Hyperplasia	0.188	0.149	0.526	0.459
P value	0.028	0.084	<0.001	<0.001
Anterior Sub-Synovial Inflammation	0.216	0.279	0.482	0.415
P value	0.012	0.001	<0.001	<0.001
Anterior Synovial Exudate	0.270	0.209	0.424	0.394
P value	0.001	0.014	<0.001	<0.001
Total Posterior	0.206	0.316	0.672	0.651
P value	0.016	<0.001	<0.001	<0.001
Posterior Pannus	0.200	0.254	0.345	0.337

Table 13 continued				
Spearman's Rho	Max Anterior Fibrosis	Total Anterior Fibrosis	Max Posterior Fibrosis	Total Posterior Fibrosis
P value	0.020	0.003	<0.001	<0.001
Posterior Bone Erosion	0.021	0.168	0.325	0.366
P value	0.809	0.051	<0.001	<0.001
Posterior Synovial Hyperplasia	0.170	0.270	0.658	0.625
P value	0.048	0.001	<0.001	<0.001
Posterior Sub-Synovial Inflammation	0.127	0.196	0.485	0.493
P value	0.139	0.022	<0.001	<0.001
Posterior Synovial Exudate	0.190	0.200	0.436	0.394
P value	0.027	0.019	<0.001	<0.001

4.4.5 Impact of Synovitis, sub-synovial fibrosis and time on IFP adiposity

Despite the correlations, when synovitis, sub-synovial fibrosis and time points were used to predict IFP adipose percentage in the individual injury groups, only the OA pathology models (ACLR, ACLT) showed some involvement of synovitis and time (Table 14). In the ACLR group, synovitis significantly predicted IFP adipose percentage ($\beta = -2.549$ (95% CI: -4.770, -0.328), $R^2 = 0.369$) and was still significant when the time point variable was added to the model. In the ACLT group, neither synovitis nor fibrosis were significant predictors but the timepoint was ($\beta =$

-0.247 (95% CI: -0.477, -0.014), $R^2 = 0.265$). Sub-synovial fibrosis was not a significant predictor in any of the models.

Table 14. Linear regression of IFP adiposity percentage for synovitis, sub-synovial fibrosis and time in the different injury groups

Injury Group	Synovitis		Sub-Synovial Fibrosis		Timepoint		R ² (Overall model fit)
	β (95% CI)	P-value	β (95% CI)	P-value	β (95% CI)	P-value	
NOC	-1.183 (-8.345, 5.979)	0.735	0.245 (-2.940, 2.450)	0.852			0.007
	-1.024 (-8.378, 6.329)	0.774	-0.065 (-2.931, 2.801)	0.963	-0.173 (-0.936, 0.589)	0.640	0.019
SHAM	-0.176 (-1.143, 0.791)	0.711	-0.247 (-0.698, 0.204)	0.270			0.055
	-0.323 (-1.731, 1.086)	0.641	-0.237 (-0.703, 0.229)	0.304	-0.041 (-0.319, 0.238)	0.766	0.059
Sub-critical	1.106 (-5.389, 7.602)	0.729	-0.146 (-2.196, 1.905)	0.885			0.006
	0.987 (-5.968, 7.942)	0.772	-0.161 (-2.273, 1.951)	0.877	-0.027 (-0.502, 0.447)	0.906	0.006

Table 14 continued

Injury Group	Synovitis		Sub-Synovial Fibrosis		Timepoint		R ² (Overall model fit)
	β (95% CI)	P-value	β (95% CI)	P-value	β (95% CI)	P-value	
ACLR	-2.549 (-4.770, -0.328)	0.026	-0.443 (-1.218, 0.331)	0.249			0.369
	2.755 (-5.109, -0.400)	0.024	-0.447 (-1.233, 0.339)	0.252	-0.123 (-0.533, 0.286)	0.539	0.379
ACLT	0.322 (-0.970, 1.614)	0.612	-0.296 (-0.659, 0.068)	0.106			0.114
	-0.901 (-2.557, 0.756)	0.273	-0.207 (-0.556, 0.141)	0.232	-0.247 (-0.477, -0.014)	0.036	0.265

4.4.6 Gene expression analysis of the IFP and synovium unit

General inflammation as measured by *Il6* and *Il1β* expression in the synovium/IFP tissue unit, was increased acutely (day 7) in response to surgery (SHAM, ACLT) irrespective of ACL injury, remained elevated for 14 -28 days and then normalised by day 56 (Figure 13). The milder increase in *Il6* on day 7 and 14 following ACLR in comparison to both NOC and the sub-critical injury was not statistically significant.

General macrophage activation markers *Tnf* and *Itgam* were slightly elevated in all injury models (SHAM, ACLT, sub-critical, ACLR) compared to NOC for the first two weeks but these differences were not statistically significant other than SHAM vs NOC at day-14 (Figure 13). The M1 macrophage marker *Itgax* was significantly increased in SHAM, ACLT and ACLR compared with NOC at day 7. Expression of *Itgax* progressively decreased from day 14 in ACLR, while it remained elevated in SHAM through day 28 and in ACLT through to day 56. Expression of the M2 macrophage marker *Mrc1* was also increased in SHAM, ACLT and ACLR compared with NOC at day 7, and the difference in SHAM reached statistical significance. By day 28 *Mrc1* expression in SHAM, ACLT and ACLR was similar to NOC. The temporal change in expression of all macrophage markers tended to be different in sub-critically injured joints compared with other injury groups, with a delayed (day 14 – 28) increase followed by a day 56 decline.

There were distinct differences between groups in the temporal pattern of adipokine expression (Figure 14). In both NOC and sub-critically injured mice, expression of both *Adipoq* and *Lep* increased from day 7 to 28 and then declined at day 56. In contrast, expression of both adipokines remained relatively static in SHAM, ACLT, and ACLR, with levels generally lowest in

the surgically injured joints (SHAM, ACLT). This reduction was particularly the case for *adipoq* in the first 28 days.

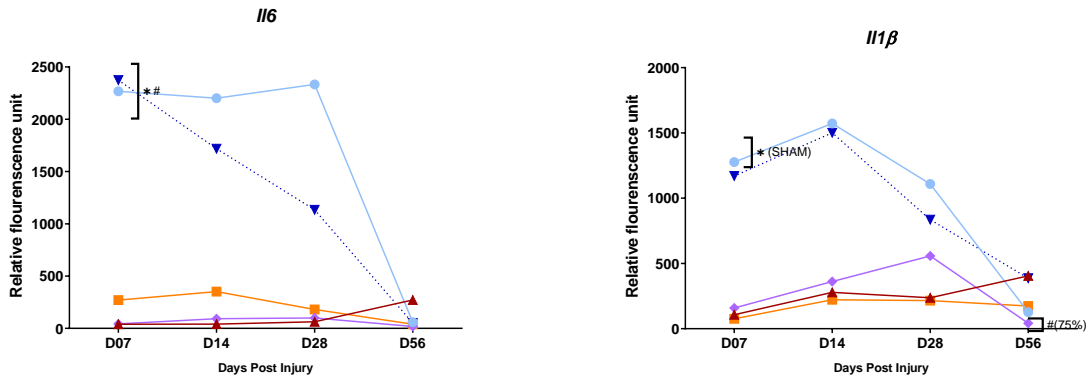
The T-helper cell marker *Cd4* was elevated after surgery (SHAM, ACLT) compared to ACLR and NOC at day 7 and 14 (Figure 14). However, *Cd4* was also increased in ACLR compared with NOC on day 7 and 14, albeit to a lesser degree than surgically injured joints. *Cd4* remained elevated in SHAM and ACLT compared with NOC at day 28 and 56, but this was not statistically significant. While all injury models had higher expression of the cytotoxic T-cell marker *Cd8a* than NOC at day 7, these differences were not significant. In NOC and sub-critically injured joints, *Cd8a* showed a similar temporal pattern to the adipokines (increasing to day 28 then decreasing at day 56). In all other groups, *Cd8a* expression tended to remain consistent over time, except for day 56 in ACLT, where it increased to be significantly higher than NOC.

Expression of genes associated with fibrosis and matrix deposition (*Col1a*, *Col3a*), turnover (*Mmp3*, *Mmp9*, *Mmp13*), and pro-fibrotic cellular metaplasia (*Acta2* - myofibroblast marker), showed different temporal and injury- associated changes (Figure 15). The two major fibrosis-associated collagens (*Col1a*, *Col3a*) showed very similar expression patterns: acute post-injury increase (day 7 and 14) compared with NOC in SHAM, ACLT and ACLR, followed by a return to normal at day 28. The rise in expression of both collagens was most marked in SHAM where expression increased from day 7-14 before declining, with very similar and somewhat lower expression in ACLT and ACLR than SHAM from day 7-28. In contrast, while expression of *Mmp3* and *Mmp13* were increased in the same three injury models, it was higher in SHAM and ACLT compared with ACLR and remained elevated through day 28 before declining in all groups. There was no significant or consistent temporal or injury-associated change in *Mmp9*

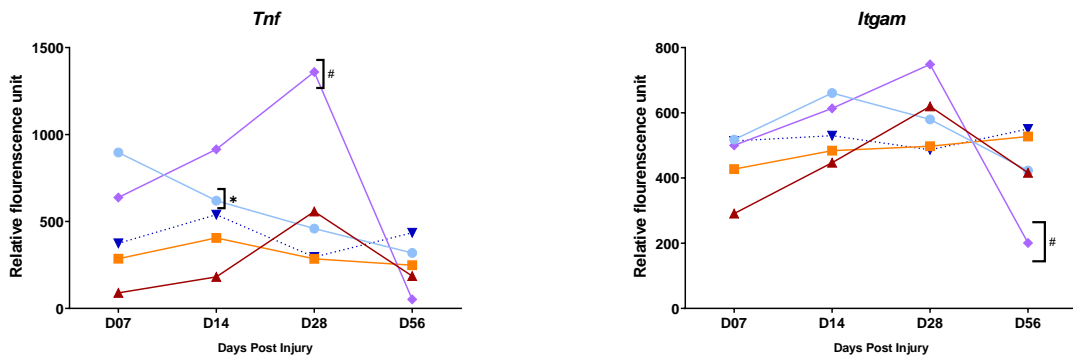
expression, and while *Acta2* expression was higher in SHAM, ACLT and ACLR compared with NOC at day 7, these differences were not significant and were not maintained at later times.



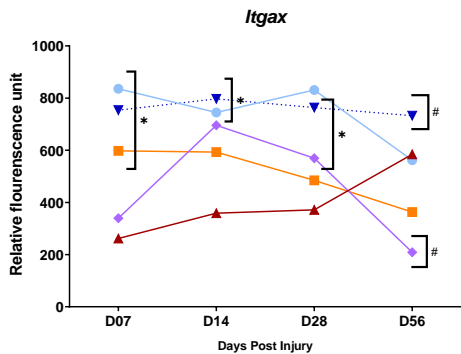
General Inflammation



Macrophage markers



M1



M2

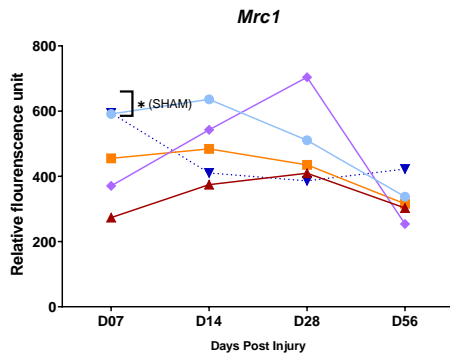
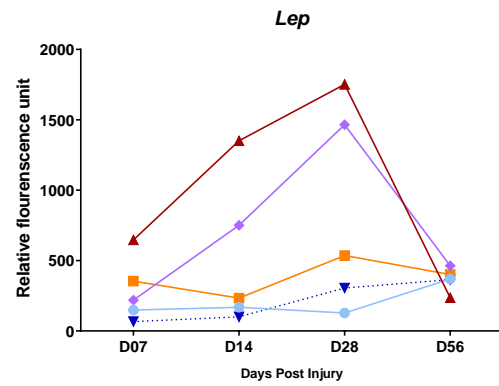
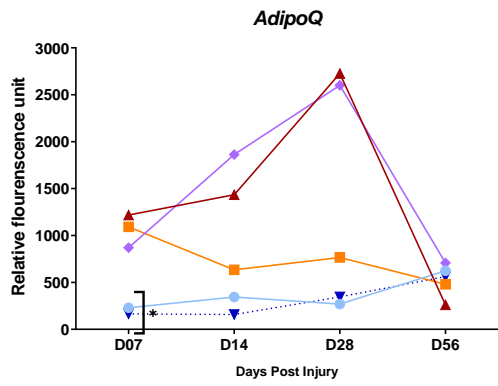


Figure 13. PCR analysis of general inflammation and macrophage markers



Adipokines



T-Cells

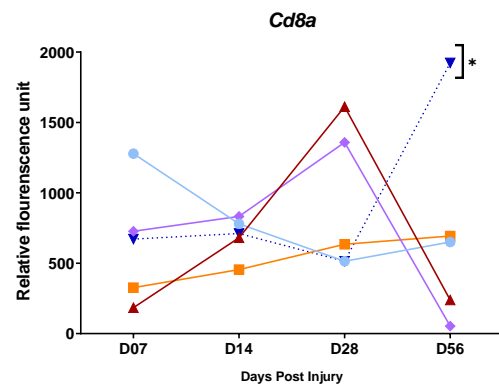
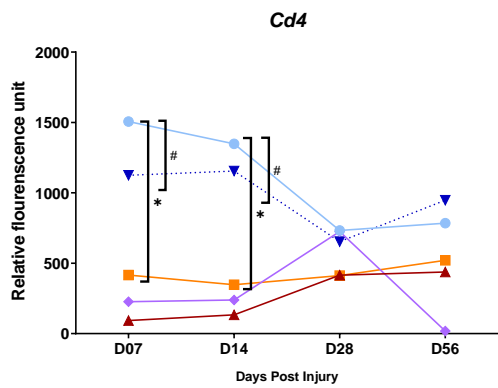


Figure 14. PCR analysis of adipokines and T-cells

▲ NOC
 ● SHAM
 ▼ ACLT
 ■ ACLR
 ◆ Sub-critical

*Significant to NOC
 #Significant to ACLR

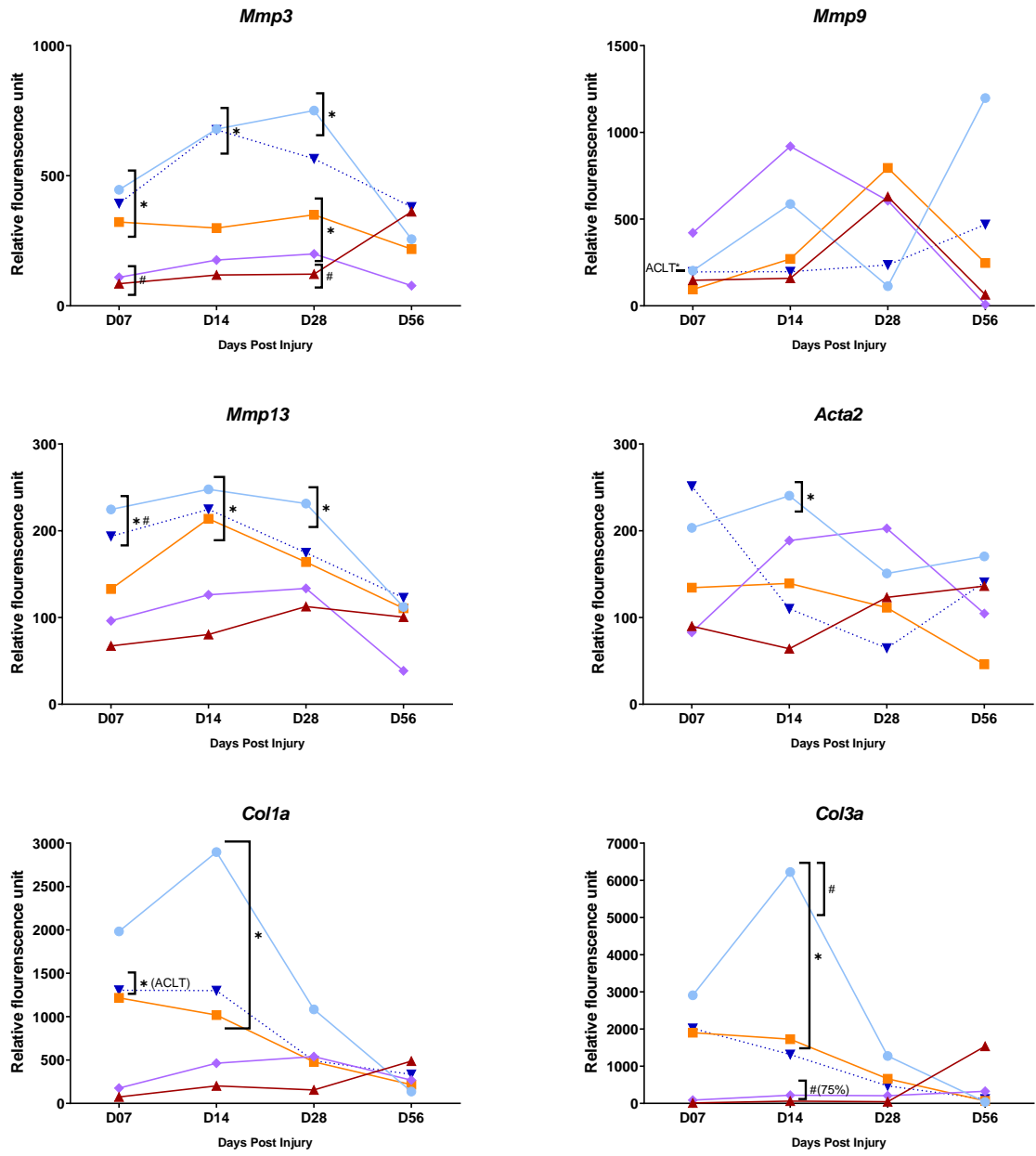


Figure 15. PCR analysis of MMPs, fibrosis markers and collagens.

4.4.7 Changes in pain behaviour responses

Compared to baseline measures, von Frey analysis showed a significant reduction in paw withdrawal threshold in all four injury groups irrespective of surgery or ACL integrity ($P < 0.001$; Figure 16). Between-group analysis showed no differences at any time point.

Force plate analysis showed SHAM-operated, and sub-critically injured animals to have no significant changes from baseline at any time point (Figure 16). All other groups showed reduced weight-bearing on the injured (right) leg (i.e. lower R/L weight distribution ratios) in the first few weeks post-injury, but these changes became less consistent by week 8. Between-group analysis showed that at week 1 in comparison with sub-critically injured animals, ACLT and ACLR groups had a lower R/L weight-bearing ratio (mean difference = -0.38, p -value = 0.006 and mean difference = -0.42, p -value = 0.005 respectively). This difference was maintained at week 2 for ACLR versus sub-critically injured animals (mean difference = -0.26, p -value = 0.009). At week 4 ACLT animals had a significantly lower R/L weight-bearing ratio compared to both SHAM and sub-critically injured groups (mean difference = -0.39, p -value = 0.01 and mean difference = -0.38, p -value = 0.01 respectively).

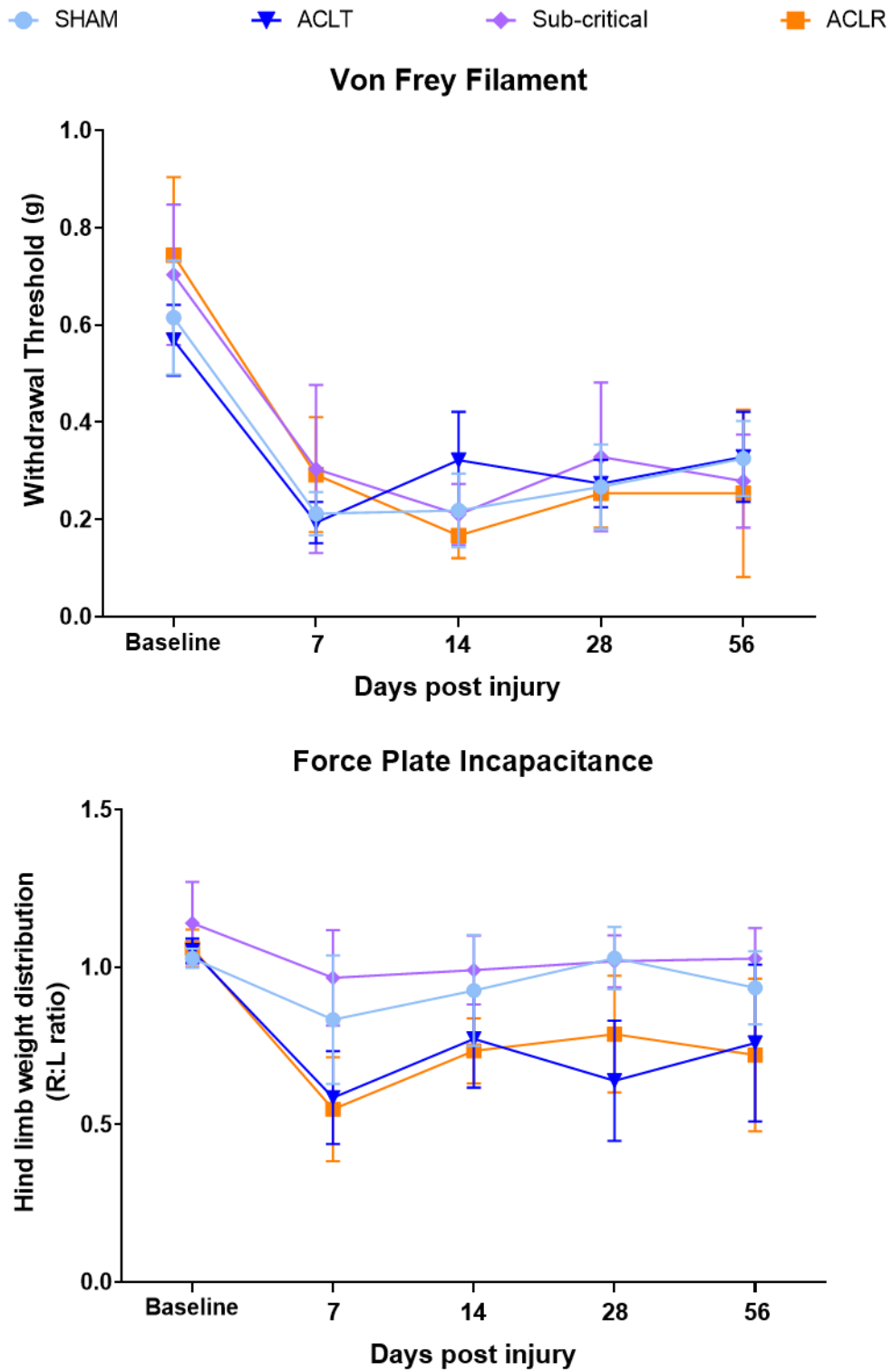


Figure 16. von Frey and force plate outcomes of from baseline to 56 days.

4.5 Discussion

This study describes the relationship of IFP adiposity to synovitis, sub-synovial fibrosis, and pain using histopathological, gene-expression and behaviour assessment methods. Our findings show evidence of a relationship between IFP adiposity and synovitis as well as with sub-synovial fibrosis. However, visually, no apparent trends linked the changes in IFP adiposity measures to pain behaviour outcomes.

The histological IFP adipose measures used in this study indicated that surgical models (SHAM and ACLT) were most impacted from day 7 and did not recover from the insult by the last time point. The microscopic visualisation of the tissue showed the IFP adipose to be often replaced with either fibrotic tissue or cellular infiltrate (Figure 17), which is consistent with previous findings[99]. Interestingly, the surgery protocol of this study took care to reflect the IFP away from the arthrotomy incision rather than dissect through it, suggesting that the changes were a result of the localised molecular response to the adjacent surgical injury and its repair/resolution, rather than direct IFP tissue damage. However, the mechanical ACL rupture group also showed a reduction in all 3 IFP adiposity measures, albeit to a lesser degree, that was slower in onset (day 14) and appeared to recover by day 56. This difference suggests that some at least some of the IFP adiposity changes are not related to surgical trauma and that they can resolve despite progressive OA and associated synovitis and sub-synovial fibrosis. While recovery of normal IFP adiposity is possible, it may be worsened and more permanent with surgical intervention, which is a novel finding that may have implications with regard to clinical management of patients with joint injury and OA.

The three IFP adipose measures (adipose percentage, cell count and average cell size) were all similarly negatively correlated to histological synovitis in the joint. Surgically impacted mice showed more significant synovitis from day 7, while ACLR as well as sub-critical to a lesser degree, showed more synovitis in the posterior of the joint. While histological synovitis trended inversely overall to adiposity in the different groups, the regression model showed that it was only involved in predicting IFP adiposity in the ACL rupture group. This association between IFPs with greater adiposity, larger and more cells to less severe synovitis was consistent with the literature in patients that showed knees with increased IFP volumes to be protected from joint damage and osteoarthritis[105, 266, 267]. However, a study by Fu et al. partly contradicted our results by showing increasing adipocyte size in the IFP of rats to be associated to increased synovial thickening, although less OA when considering cartilage loss[119]. This may reflect the differences in species and/or OA phenotypes in the two studies, post-traumatic versus age-associated, with potential for confounding by injury-associated inflammation in the former and systemic adiposity in the latter.

The most curious finding when evaluating IFP adiposity and synovitis in the current study was the strong correlation to posterior synovial health. The existing constructs indicate that anatomical proximity contributes to the interaction between the synovium and IFP[110, 176]. Given that, it would be logical only to see associations and changes with the anterior of the joint. Our findings question that association and postulate that the molecular impact of the local adipose tissue is more impactful than the anatomical location of the IFP. Alternatively, the changes in IFP adiposity could be a result from the pathological changes in the synovium and be

a surrogate signal of worse joint disease which is observed in the models examined with increasing whole joint synovitis and fibrosis.

Lower IFP adiposity was also correlated to increasing sub-synovial fibrosis. In the anterior portion of the joint, this was a logical association given that the IFP is often replaced with fibrotic tissues[99, 100, 268, 269]. The increased fibrosis in the IFP may drive OA development given a previous study postulating that it worsens cartilage damage in knees that have been surgically treated after ACL rupture[270]. As with synovitis, posterior fibrosis was also negatively correlated to adiposity, further suggesting that these changes are more likely attributed to the global progression of disease severity rather than the localised synovial exacerbation. This finding was noteworthy but not entirely unexpected, given the scoring area of anterior sub-synovial fibrosis includes the region of the IFP. Our fibrosis scoring tool assesses a much wider area of the joint and adiposity in the IFP is not replaced by fibrous tissue alone but by often densely packed cells as well (Figure 17). While cellular infiltration in IFP was observed in this study, it was not characterized and would be important to be further assessed in the future.

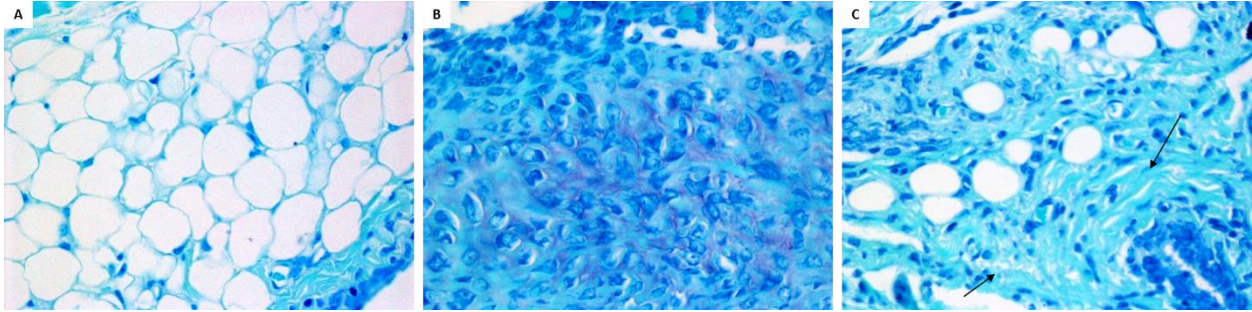


Figure 17. Different appearances of the IFP.

A) shows an IFP with a high adipose percentage whereas B) the area can be filled with B) cellular infiltrate or C) collagen fibres as indicated by the cyan staining.

The gene expression analysis results of this study revealed that surgical insult alone, irrespective of ACL damage and subsequent OA onset, induced acute inflammation (increased *IL6* and *IL1 β* expression) which resolved by eight weeks. This inflammatory response may be driven by CD4⁺ T cells and involve M1 macrophage pathways, given the similar temporal increase in markers for these inflammatory cell types. These inflammatory pathways were most upregulated in surgical models that also had the greatest change in IFP adiposity, suggesting they may be related. The involvement of macrophage activity would not be unexpected given the well-described development of crown-like structures (a ring of macrophage cells) in the microenvironment of dying adipose tissues [28], which the reduced adiposity in the surgical animals could possibly indicate. Although, this suggestion is less supported if the reduced adiposity were a result of the previously established trans-differentiation of adipose cells to myofibroblasts[271]. However, the CD4 T-cell pathway, which includes IL6 as a mediator regulates the M2 pathway in epididymal fat pad rather than the pro-inflammatory M1 that we

observed[272]. The caveat to our findings is that we only used a single marker to evaluate the activation of these complex macrophage polarisation pathways and if not limited by sample volume, it would have been beneficial to include analysis of other M2 markers such as *CD163* or *CD301*[273, 274]. Further evaluation of temporal cellular changes in the IFP in the different injury models using flow-cytometry to quantitate the different cell types would also help to resolve the extent of their involvement[258, 260].

The reduction in adiposity of the IFP in SHAM and ACLT was associated with much lower expression of adipokines compared to the other groups, particularly *adipoq* in the first four weeks post-injury. This decrease in adipokines was evident in the ACLR group as well to a lesser degree, consistent with the intermediate decrease in IFP adiposity in this injury model and suggesting mechanical damage plays a role in biological changes to the IFP. These temporal and injury-specific associations with IFP adiposity confirm local regulation of adipokine expression. Previous literature has indicated increasing levels of adipokines with worse OA severity [275], which was not the case in our study where despite increasing OA pathology with time in ACLT and ACLR (see chapter 5) adipokine expression remained low. This discrepancy may be due to direct damage to the adipose tissue in post-traumatic OA models as opposed to spontaneous age- and obesity-associated OA, but if present injured IFP may further stimulate inflammatory mechanisms. The reason for the higher and increasing levels of *adipoq* and *lep* expression through day 28 before sharply decreasing at day 56 in non-operated and sub-critically injured controls is unclear. These temporal changes were not related to any change in IFP adiposity measures in healthy joints. There was similarly no evidence of synovitis, and at 18 weeks C57Bl/6 mice have not developed any spontaneous OA (see data in chapter 5) that is generally

seen at 12-18 months of age. There was no difference in body weight in these mice compared with joint injury groups that would implicate systemic diet/obesity-related regulation. None of the mice in this study received medication, and the expression changes were similar in the two control groups despite only sub-critically injured animals having anaesthesia. Previous studies in rats have not reported increased adipokine (leptin) expression or secretion with increasing age [119].

Despite the interesting revelations from histology and gene analysis, the pain behaviour assessment revealed much less. Both our assessments demonstrated increased pain behaviours in the ACLT and ACLR groups, and to a lesser degree sub-critically injured mice, that was sustained for the duration of the study. However, there were no clear trends in terms of temporal association with IFP adiposity. A limitation of these assessments was that the time and cost constraint prevented the assessments from being carried out in mice assigned for histological or gene analysis. Thus, we were unable to conduct any meaningful statistical correlation analyses to understand the relationship further. This limitation is also applicable to our correlations of gene and histological studies, which by necessity due to the size limitation of mouse joints must be done in separate animals (i.e. no ability for biopsy in histologically evaluated IFPs).

On the other hand, a key strength of this study is the separate histological evaluation of the IFP and synovium. The two issues are often evaluated as one functional unit given the suggestions of cross talk and anatomical proximity as well as the IFP being used in human imaging studies as a surrogate for synovial inflammation[207, 276]. This approach has prevented existing research from elucidating the intricacies of the relationship between these two neighbouring but distinct

tissues. Our study histologically evaluated the tissues separately but together as a functional unit for gene expression which allows better comparison to existing literature while overcoming some of their challenges.

Another limitation of this study was the selection of male mice only despite women disproportionately developing knee OA[277]. In light of that evidence, it will be important to determine if the relationships observed in this study remain or if there are gender-specific variances, such as the known differences in the risk of OA development and pain regulation, that would modify the outcomes[277-279].

The selection of an ACL-injury PTOA model was also a limitation in this study. Injuries to the ACL create a great deal of instability within the joint which could drive fibrosis development. Other PTOA models, such as a meniscal destabilisation (DMM) result in much less instability but still develops progressive OA[280]. The impact of joint stability on outcomes evaluated in the study will be interesting to explore. Furthermore, this study has a lack of models representing spontaneous OA or ageing disease development. As previously mentioned, a history of traumatic injury only accounts for 12% of lower limb OA incidence[250]. In a clinical setting, OA development is far less precise, and these investigations need to be carried out in a manner that facilitates the 'bench to bedside' knowledge translation philosophy [281]. The knowledge transfer in those scenarios is also dependant on macroscopic views of the disease. By evaluating the microenvironments of just the IFP and synovium in a whole joint disease neglects the involvement of surrounding structures[236]. Thus, future studies evaluating the associations between IFP adiposity and the other features of OA are needed.

Additionally, the IFP scoring system in this study relies on a single sagittal section in the medial compartment of the joint and it is uncertain how representative this section is of the rest of the tissue. A future study that validates the use of a single slide to represent the whole IFP should be carried out to improve confidence in the scoring system.

New studies should also focus on increasing data productivity with a better study design that would include the correlation of features within the same animal where possible. These studies should incorporate other models of different OA phenotypes to have outcomes applicable to more of the OA population.

4.6 Conclusion

Adiposity changes in the IFP of various models of PTOA were associated with levels of synovitis and sub-synovial fibrosis histologically. This relationship extended from local effects to whole joint effects as seen by correlations to posterior pathology. While the pro-inflammatory changes in surgical models appeared to be linked to CD4 T-cell and M1 macrophage pathways, the reduced adiposity of the IFP seemed to be connected to lower adipokine activity. Future studies are needed to understand the relationship of IFP adiposity to other pathological changes in the joint as well as to confirm the inflammatory pathways identified in this study.

4.7 Appendix

Table 15. Details of gene primers analysed in RT-PCR

Target gene	Sequence Accession number	Sequence	Annealing temperature (°C)	Product size, (base pairs)
<i>Ilf6</i>	NM_031168.2	F – CTT CCA TCC AGT TGC CTT CTT G R – TGT TGG GAG TGG TAT CCT CTG TG	55	104
<i>Ilf1b</i>	NM_008361.4	F – ACC TGT TCT TTG AAG TTG ACG GAC R – TCT TGT TGA TGT GCT GCT GCG AG	55	117
<i>Tnf</i>	NM_013693	F – GCA GGT CTA CTT TGG AGT CAT TGC R – CAC TGT CCC AGC ATC TTG TGT TTC	56	222
<i>Iltgam</i> (Cd11b)	NM_001082960.1	F – GCA GTC ATC TTG AGG AAC CGT G R – ATG TCC ACA GAG CAA AGG GAG G	56	173
<i>Iltgax</i> (Cd11c)	BC057200.1	F – TTG GGG TAG GAC ACA AAG ATG G R – AAG GCA GCA GGA GAT GAG AAA AG	55	106
<i>Mrc1</i> (Cd206)	NM_008625.2	F – ACC TGG GGA CCT GGT TGT ATT C R – TTG CCG TCT GAA CTG AGA TGG	56	217
<i>Adipoq</i>	NM_009605.5	F – GAG AAG GGA GAG AAA GGA GAT G R – ATA CAC ATA AGC GGC TTC TCC	55	144
<i>Lep</i>	NM_008493.3	F – CAGGGAGGAAAATGTGCTGGA R – CCCTCTGCTTGGCGGATAC	56	180
<i>Cd4</i>	NM_013488.3	F – TGT GCC GAG CCA TCT CTC TTA G R – ATG CTG CCC CAG AAT CTT CCT C	58	197

Table 15 continued

Target gene	Sequence Accession number	Sequence	Annealing temperature (°C)	Product size, (base pairs)
<i>Cd8a</i>	NM_001081110.2	F – TTA TCC TGG GGA GTG GAG AAG C R – AGC ATC CTT GCG AAA CGG AC	56	132
<i>Mmp3</i>	NM_010809.1	F – GCT GAG GAC TTT CCA GGT GTT G R – GGT CAC TTT TTT GGC ATT TGG GTC	53	120
<i>Mmp9</i>	NM_013599.4	F – TGG CTT TTG TGA CAG GCA CTT C R – CGG TGG TGT TCT CCA ATG TAA GAG	55	223
<i>Mmp13</i>	NM_008607.2	F – CCA TCC CGT GAC CTT ATG TT R – GAG GCG GGG ATA ATC TTT GT	54	237
<i>Acta2</i>	NM_007392.3	F – ATA GGT GGT TTC GTG GAT GCC R – GAG CGT GAG ATT GTC CGT GAC	55	225
<i>Col1a1</i>	NM_007742.4	F – TCA GAA GAT GTA GGA GTC GAG G R – ATA GCC ATA GGA CAT CTG GGA	59	189
<i>Col3a1</i>	NM_009930.2	F – TTC TAC ACC TGC TCC TGT GCT TC R – CAT TCC TCC CAC TCC AGA CTT G	58	229

Chapter 5. Pre-clinical Study 2

Written as a manuscript in preparation for submission:

Urban, H. Blaker, C. Shu, C. Clarke, E. Little, C B. Correlations of IFP adiposity and sub-synovial fibrosis with other histological pathologies in murine PTOA. Osteoarthritis and Cartilage

5.1 Abstract

Background

The previous chapter investigated the relationship between the synovium and the infrapatellar fat pad (IFP). However, osteoarthritis (OA) is a multifactorial joint disease that includes all structures of the joint, and there is little research investigating the interaction between IFP adiposity and structural osteoarthritic pathologies in the joint. Chapter 5 aims to address this gap by exploring the correlations between IFP adiposity and sub-synovial fibrosis with features of cartilage, subchondral bone, osteophytes, enthesophytes and meniscal pathology in murine models of post-traumatic OA (PTOA)

Methods

As in chapter 4, this study evaluated 10-week old male C57Bl/6 mice that were assigned to ACL-transection (ACLT), SHAM surgery, ACL-rupture (ACLR), sub-critical ACL injury or non-operated control (NOC) groups at 1, 2, 4- or 8-weeks post-injury. In addition to IFP adiposity and sub-synovial fibrosis scoring described in chapter 3, cartilage, subchondral bone, osteophyte, enthesophyte and meniscus pathologies in the medial tibiofemoral compartment were evaluated using an established protocol. Spearman's correlation was used to assess the

association between IFP adiposity and sub-synovial fibrosis with the individual features of tissue-specific pathology. Partial correlation was to control for surgery status (SHAM and ACLT) in the whole sample and in mice with injuries that develop structural joint pathologies (sub-critical, ACLR and ACLT).

Findings

Adiposity of the IFP was significantly and negatively correlated to many of the pathologies in cartilage, bone and meniscal tissues in varying degrees. The significant correlations were strengthened when adjusted for surgery status in the whole sample and even more in injury models. All histopathological features of cartilage (structural damage, proteoglycan loss and chondrocyte hypertrophy), osteophytes and enthesophytes (size, maturity and severity) and meniscus (structural damage, proteoglycan loss and bone formation) were strongly and negatively correlated to IFP adiposity in injury models when adjusted for surgery status.

Similar findings were observed for sub-synovial fibrosis, but the correlations were positive, indicating more fibrosis was associated with higher disease severity. Interestingly, many of the strong associations with sub-synovial fibrosis were in the posterior of the joint.

Conclusion

Our findings show IFP adiposity is closely correlated to many of the surrounding histopathological features of OA. The increased correlation strength in the posterior of the joint suggests a more significant role for altered anterior-posterior joint mechanics/stability in fibrosis development. As this study is hypothesis-generating, future research is required to

validate these findings in additional preclinical models before investigating how they can be manipulated to improve the treatment of the disease.

5.2 Introduction

Osteoarthritis (OA) is a complex joint disease initiated by micro- and macro-injuries that result in the activation of structural, mechanical and biological pathways which culminate in impaired joint tissue metabolism [7, 282]. The interplay between the various local and systemic impairments is followed by changes to the joint anatomy and physiology including articular cartilage degradation, bone remodelling, development of osteophytes and meniscal damage and dysfunction [7, 279, 283].

The loss of articular cartilage is one of the key hallmarks of OA[284]. In healthy joints, cartilage covers the end of the bones and comprises of chondrocytes within a network of collagen fibers with proteoglycans and glycoproteins[285]. The embedded chondrocytes play a significant role in producing and maintaining the surrounding extracellular matrix by communicating through mechano-transduction and the release of cytokines, chemokines and growth factors[286, 287]. In OA, the cartilage homeostasis is disrupted by a combination of biological and mechanical insults which results in the release of inflammatory molecules and breakdown products[288, 289]. This release increases the production of proteolytic enzymes from chondrocytes as well as from surrounding tissues resulting in the breakdown of cartilage proteins and proteoglycans[288, 289]. The damaged cartilage from these insults results in a vicious cycle of further load-induced mechanical damage and cellular injury in OA[290].

Changes to the bone is another structural hallmark of OA[284]. The subchondral bone plate is a layer of cortical bone that lies directly beneath the cartilage and separates it from the trabecular bone and associated marrow spaces [291]. Subchondral bone contains osteocytes, osteoblast and osteoclasts, and these cells respond to load by remodeling the extracellular

matrix with both increased resorption and formation of bone to optimise its structure[292]. The process is impaired in osteoarthritic joints as demonstrated with changes in the balance between osteoclasts which drive bone reabsorption in the early stages of the disease, and bone formation driven by increased osteoblasts which predominates in later stages[293, 294]. Changes to the subchondral bone also include increased adiposity, cyst formations and focal areas of inflammation/necrosis (seen as bone marrow lesions on MRI)[295-297]. In addition to subchondral bone changes, bony outgrowths, both osteophytes and enthesophytes, are a pathognomonic feature in OA. Osteophytes, which develop at the margin of the joint, and enthesophytes, which form at the osseous insertion of ligaments, tendons and the joint capsule, both develop through a process of endochondral ossification[298, 299]. This process starts by increasing cell proliferation and chondroid metaplasia and is thought to be a response to abnormal loads and joint biomechanics[300].

The meniscus is another structure within the healthy knee joint that functions to manage and distribute loads[301]. The menisci are semilunar shaped fibrocartilaginous tissues located between the distal femur and proximal tibia and are comprised of fibro-chondrocytes, collagens, proteoglycans and other glycoproteins[301]. As with the chondrocytes in the cartilage, meniscal cells play a significant role in maintaining the proteins of their extracellular matrix. The similarities with articular cartilage also extend to the type of changes observed in OA; the menisci are prone to proteoglycan loss, matrix degradation, cellular proliferation and macroscopic structural defects such as fissures and tears[302, 303]. The breakdown of the meniscal tissues results in an upregulation of inflammatory and proteolytic factors and impair

load management which eventuates to worsen the joint pathology through biological and mechanical mechanisms[304, 305].

As with synovitis in the previous chapter, there is little research in general, and none in PTOA, investigating the associations between the manifestation of OA in these multiple joint tissues to the infrapatellar fat pad (IFP) or sub-synovial fibrosis. An existing study in patients suggests that increased IFP volume (which is associated with increased pain[192]) is associated with worse cartilage health[266, 306]. Similarly, in rats, adipocyte size within the IFP was significantly associated with cartilage damage in an age-dependent manner[119]. An ex-vivo study also showed that IFP conditioned media aggravated pre-injured cartilage explants by increasing gene expression of cyclooxygenase-2, inducible nitric oxide synthase, and interleukin-6[117]. In contrast, a separate study demonstrated that a co-culture of healthy IFP and healthy cartilage or meniscus did not stimulate proteoglycan degradation but instead stimulated sulphated glycosaminoglycan production[307].

Despite these findings, little is known about the association between the IFP and sub-synovial fibrosis to structures such as cartilage, subchondral bone, bone growths and meniscus in OA. The previous chapter described the joint interactions between synovitis and IFP adiposity as well as sub-synovial fibrosis, but a fuller understanding of the association requires also evaluating the relationship with broader OA pathological changes, which can independently impact on synovitis[221]. This chapter aims to address these gaps by investigating the correlation between IFP adiposity and sub-synovial fibrosis with the other structural pathologies of OA in the medial compartment in murine post-traumatic OA (PTOA) models. In addition to assessing the correlations in a full heterogeneous sample including controls, partial

correlations were carried out to evaluate the impact of surgery (regardless of disease development (SHAM operated and anterior cruciate ligament-transection (ACLT))) in the full sample and separately in only models that develop the structural disease (sub-critically injured, ACL-rupture (ACLR) and ACLT).

5.3 Methods

The methodology for animal work, sample processing, histological IFP adiposity and histological sub-synovial fibrosis scoring is detailed in Chapter 3. Joints were studied at 1, 2, 4- and 8-weeks post-injury for histopathological scoring.

5.3.1 Joint pathology scoring

As previously mentioned, OA is a whole joint disease, but the current literature has tended to focus primarily on changes to articular cartilage with far less evaluation of other structural pathologies in mouse models[7, 220]. The scoring matrix used in this chapter to assess the OA histopathology was developed within the Raymond Purves Bone and Joint Laboratory based on existing guidelines for murine models[257, 308-312]. Additionally, observed features that were not addressed in the previously published guidelines, such as osteocyte cell loss and osteochondral damage, and a new scoring matrix for murine meniscal pathology, were included in the global OA pathology matrix following an iterative development process by senior scientists involved in the previous publications (CBL, MJ, CS) as part of the PhD of Dr Carina Blaker (CB, University of Sydney 2019). Specific pathological changes were assessed in the relevant regions of the medial tibiofemoral compartment as detailed in Table 16. By scoring

tissues in sequential slides, a maximum pathology score and well as total score (sum of scores) were generated to measure both severity and progression/spread, respectively.

Table 16. OA pathology features scored in the different tissues and regions of the knee

Tissues	Articular Cartilage	Subchondral Bone	Osteophyte/ Enthesophyte Formation	Menisci
Features	<ul style="list-style-type: none"> • Structural damage • Proteoglycan loss • Chondrocyte hypertrophy • Total score (sum of features) 	<ul style="list-style-type: none"> • Osteocyte loss • Sclerosis • Vascular invasion • Osteochondral damage • Total score (sum of features) 	<ul style="list-style-type: none"> • Maturity • Size • Severity (maturity X size) 	<ul style="list-style-type: none"> • Structural damage • Proteoglycan loss • Bone formation • Total score (sum of features)
Regions	<ul style="list-style-type: none"> • Tibia • Femur • The summed score of regions 	<ul style="list-style-type: none"> • Tibia 	<ul style="list-style-type: none"> • Anterior tibia and femur • Posterior tibia and femur 	<ul style="list-style-type: none"> • Anterior meniscus • Posterior meniscus • The summed score of regions

All slides were coded and randomized, and scored by a single observer (CB), who was thus blinded to the injury group and timepoints of the specimens.

5.3.2 Statistical methods

Spearman's correlation was used to evaluate the strength and direction of the association between histological adiposity, sub-synovial fibrosis and the other histopathological scores in all the samples together (articular cartilage, subchondral bone, osteophyte and enthesophyte formation, and menisci). Partial correlation was also used to adjust the analyses for surgical intervention in the whole sample and in models that develop joint pathologies (sub-critically injured, ACLR and ACLT). Correlation coefficients ≤ 0.29 represented weak association; between 0.30 and 0.49 moderate; and ≥ 0.50 strong association [265]

A nominal significance level of 0.05 was used. Correlation analyses were performed using IBM SPSS Statistics, version 26 (IBM Corporation, Armonk, NY, USA).

5.4 Results

As all IFP adiposity measures (adipose percentage, adipose cell count, mean adipose cell size) were similarly associated to structural features and due to the overwhelming amount of data, only correlations to the adipose percentage of the IFP are presented in the results section below, with the remaining data in Appendix 5. Similarly, only total sub-synovial fibrosis scores are presented, with maximum fibrosis scores detailed in Appendix 5.

5.4.1 IFP adiposity and sub-synovial fibrosis are correlated to structural features

IFP adiposity and sub-synovial fibrosis were significantly correlated, in varying degrees, to many of the total and maximum scores for the different histopathological features. All adiposity correlations were negative – indicating higher adiposity in the IFP was correlated to lower pathology scores, whereas all fibrosis scores were positively associated (more severe fibrosis – more severe OA features).

When evaluating IFP adiposity in the whole sample, most of the significant correlations were of a low-moderate strength (Appendix 5, Table 17 – 25). These negative correlations (bar some enthesophyte pathologies) strengthened when the sample was adjusted for surgical intervention and increased again when limited to pathological models. For example, the correlation between IFP adipose percentage and total summed cartilage score in the whole sample was $\rho = -0.31$, increased to $\rho = -0.61$ when adjusted for surgery and again to $\rho = -0.61$ when limited to models that develop joint injuries (Appendix 5, Table 17). As a result, the strong correlations between the structural features and adiposity were only evident in injury/OA models.

Similarly, most of the significant positive correlations between fibrosis and OA pathology in the whole sample were of moderate strength (Appendix 5, Table 26 – 33). However, unlike adiposity, the associations did not appear to strengthen as much or as consistently when adjusted for surgical intervention in the whole sample or just in pathological animals (e.g. total anterior fibrosis and total summed cartilage scores in the whole sample: $\rho = 0.50$, surgical models only: $\rho = 0.44$ and in pathological models: $\rho = 0.47$) (Appendix 5, Table 26). The most prominent overarching finding was that many of the strong correlations observed were only to posterior fibrosis, while only a few strong associations with anterior fibrosis were found and only when adjusted for surgery in OA models.

5.4.2 Strong associations to Cartilage and Bone/Enthesophyte pathology

In both, IFP adiposity and sub-synovial fibrosis, the individual features of pathology in cartilage and bone/enthesophyte tissues showed the greatest number of strong correlations. These strong and therefore more likely biologically significant inter-tissue pathology associations are presented graphically in Figure 18 – 21. Of the cartilage features, proteoglycan loss was most strongly correlated with IFP adiposity percentage (OA animals adjusted for surgery, $\rho = -0.61$, p -value < 0.01) and total posterior fibrosis (whole sample, $\rho = 0.70$, p -value < 0.01) (Figure 18, 19; Appendix 5, Table 17, 26).

All summed characteristics of osteophytes and enthesophytes showed strong negative correlations to adiposity only in OA animals when adjusted for surgical intervention, whereas the associations were more complex with fibrosis (Figure 20 and 21, respectively). Many of the strong positive correlations for both types of marginal bone formation were associated with total posterior fibrosis, while each enthesophyte feature was also strongly correlated to

anterior fibrosis. Despite the many strong correlations from both bone outgrowth types to adiposity and fibrosis, summed enthesophytes scores showed much stronger correlations compared to osteophytes (Figure 21). As an example, the correlation of summed osteophyte maturity to total posterior fibrosis was $\rho = 0.58$, whereas, for enthesophytes, it was $\rho = 0.74$ (Appendix 5, Table 30). This trend was similar for IFP adiposity, with $\rho = -0.21$ and $\rho = -0.39$ for osteophytes and enthesophytes, respectively (Appendix 5, Table 19).

When evaluating the separate regions of the joint, IFP adiposity and sub-synovial fibrosis also showed distinct variations to the anterior and posterior of the joint (Appendix 5, Table 19 and 30 respectively). Both outcomes were significantly correlated to osteophyte features in the anterior of the joint but posterior enthesophyte development. As an example, in the joint pathology only analysis, the correlation of osteophyte maturity to IFP adipose percentage in the anterior of the joint was $\rho = -0.51$ but only $\rho = 0.10$ in the posterior. Inversely, the correlation of enthesophyte maturity to IFP adipose percentage in the anterior was only $\rho = -0.08$ but was $\rho = -0.56$ in the rear of the joint. The same findings were observed in sub-synovial fibrosis with the correlation between osteophyte maturity and fibrosis in the anterior of the joint $\rho = 0.46$ and posterior of the joint $\rho = 0.07$ while in enthesophyte $\rho = 0.18$ (anterior) and $\rho = 0.57$ (posterior).

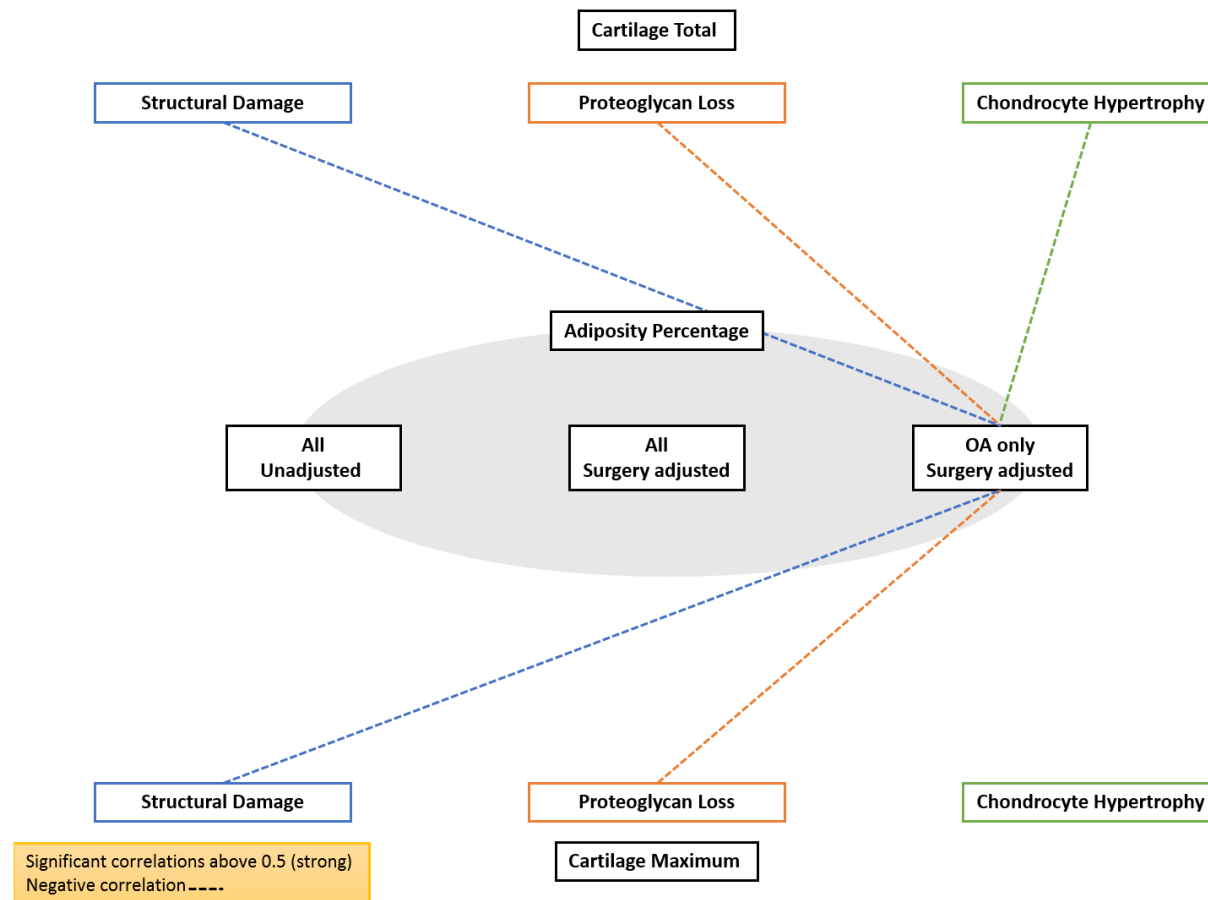


Figure 18. Summary of strong significant associations between cartilage tissues and IFP adiposity percentage. Significant and strong correlated associations observed in the whole sample (“All”) or sub-critically injured, ACLT and ACLR joints only (“OA only”) based on Spearman’s correlation coefficients and partial correlation coefficients which were adjusted for surgical intervention (Appendix 5, Table 17).

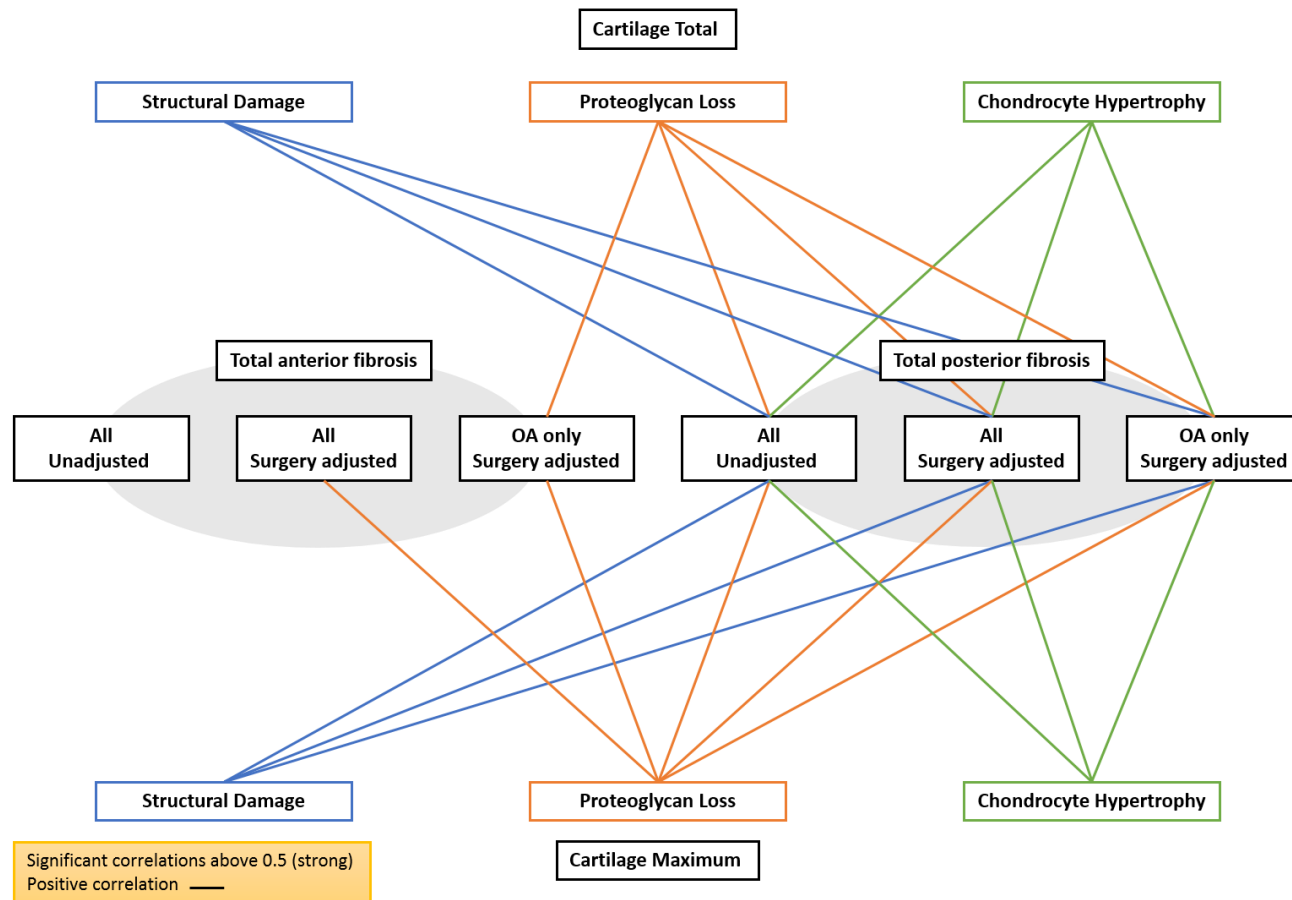


Figure 19. Summary of strong significant associations between cartilage tissues and total sub-synovial fibrosis. Significant and strong correlated associations observed in the whole sample (“All”) or sub-critically injured, ACLT and ACLR joints only (“OA only”) based on Spearman’s correlation coefficients and partial correlation coefficients which were adjusted for surgical intervention (Appendix 5 Table 26).

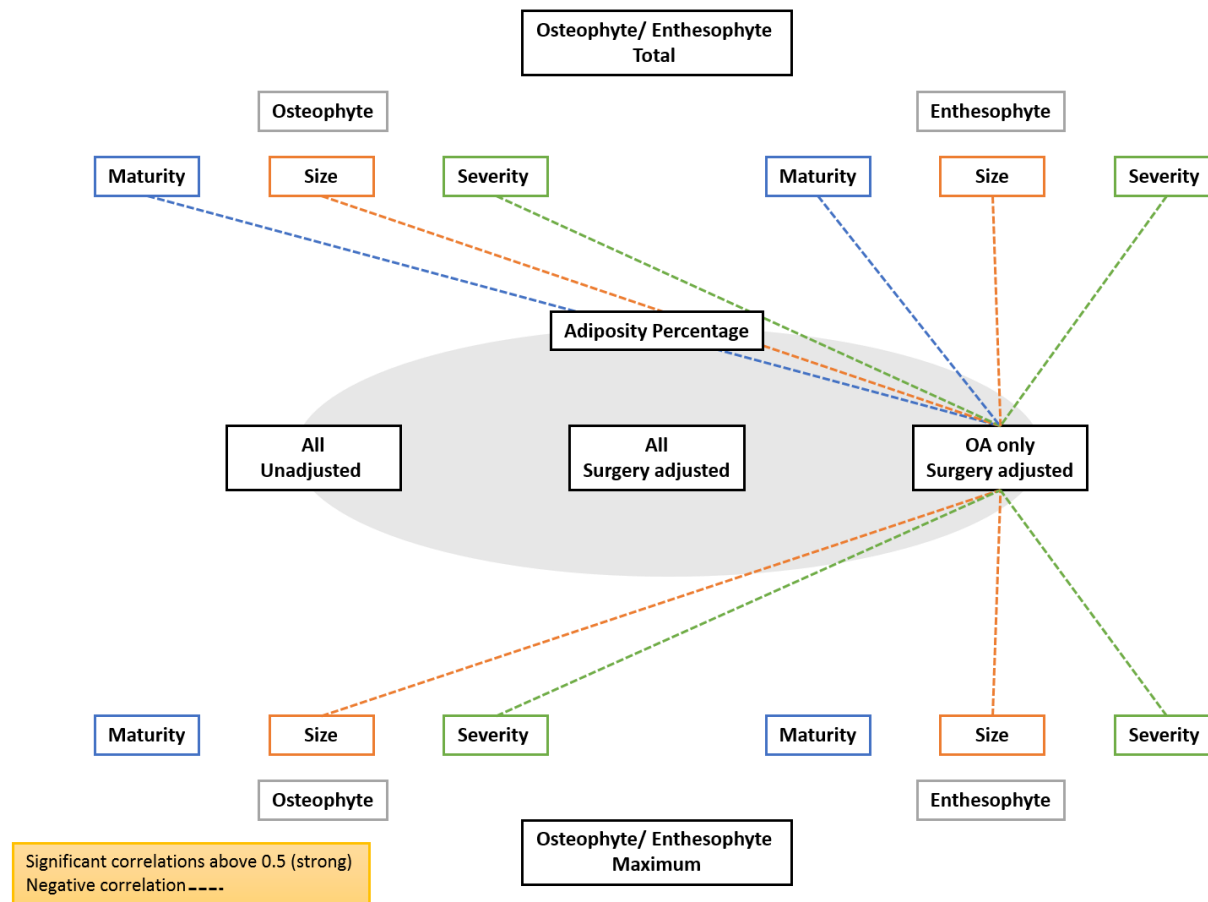


Figure 20. Summary of strong significant associations between osteophyte/enthesophyte tissues and IFP adiposity percentage.

Significant and strong correlated associations observed in the whole sample (“All”) or sub-critically injured, ACLT and ACLR joints only (“OA only”) based on Spearman’s correlation coefficients and partial correlation coefficients which were adjusted for surgical intervention (Appendix 5 Table 19).

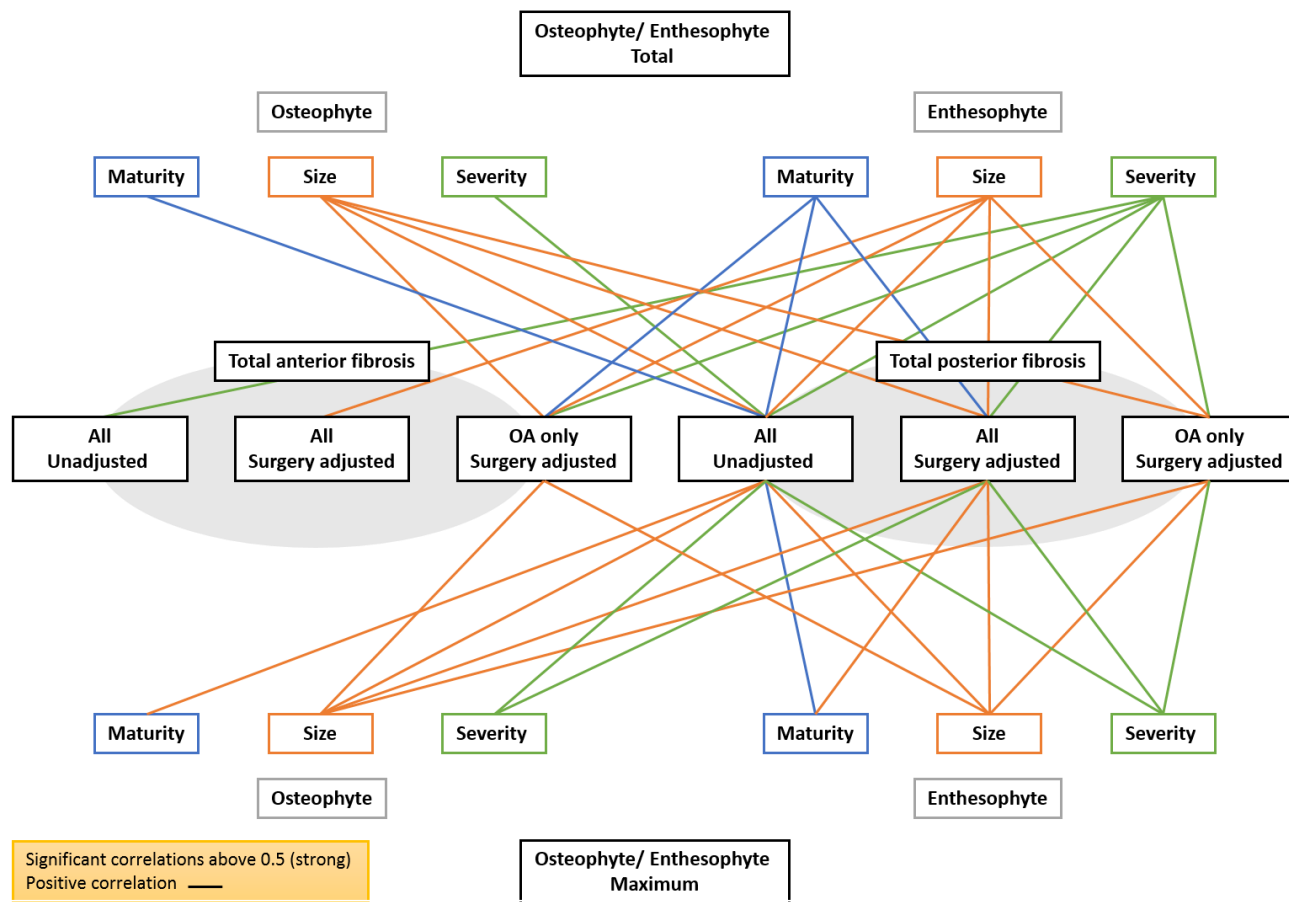


Figure 21. Summary of strong significant associations between osteophyte/enthesophyte tissues and total sub-synovial fibrosis.

Significant and strong correlated associations observed in the whole sample (“All”) or sub-critically injured, ACLT and ACLR joints only (“OA only”) based on Spearman’s correlation coefficients and partial correlation coefficients which were adjusted for surgical intervention (Appendix 5 Table 30).

5.4.3 Meniscal pathology associated with posterior fibrosis

As with the other pathologies, meniscal changes showed a strong negative correlation to adiposity in OA only models adjusted for surgery (Figure 22). Total posterior and summed meniscal tissue structural damage in surgery adjusted pathological animals were one of the high correlations in the adiposity analysis ($r = -0.6$, $p\text{-value} < 0.001$ and $r = -0.6$, $p\text{-value} < 0.001$ respectively) (Appendix 5 Table 21). All the meniscal pathology features were also strongly correlated to posterior fibrosis, but only structural damage and bone formation were strongly correlated to anterior fibrosis in OA surgery adjusted mice (Figure 23) (Appendix 5 Table 32).

5.4.4 Sub-chondral bone pathologies show little correlation to adiposity and fibrosis

In contrast to other joint tissue pathologies, those in sub-chondral bone showed very few correlations to adiposity or fibrosis (Figure 24, 25) (Appendix 5 Table 18, 28). Osteochondral damage was the only feature that showed a strong negative correlation to adiposity percentage in pathological animals ($\rho = -0.52$, $p\text{-value} < 0.01$). In sub-synovial fibrosis, correlations to posterior fibrosis were positive and of a low to moderate strength when present and were more robust compared to anterior fibrosis. However, osteocyte loss was the only feature strongly correlated with total posterior fibrosis ($\rho = 0.51$, $p\text{-value} < 0.01$) (Appendix 5 Table 28).

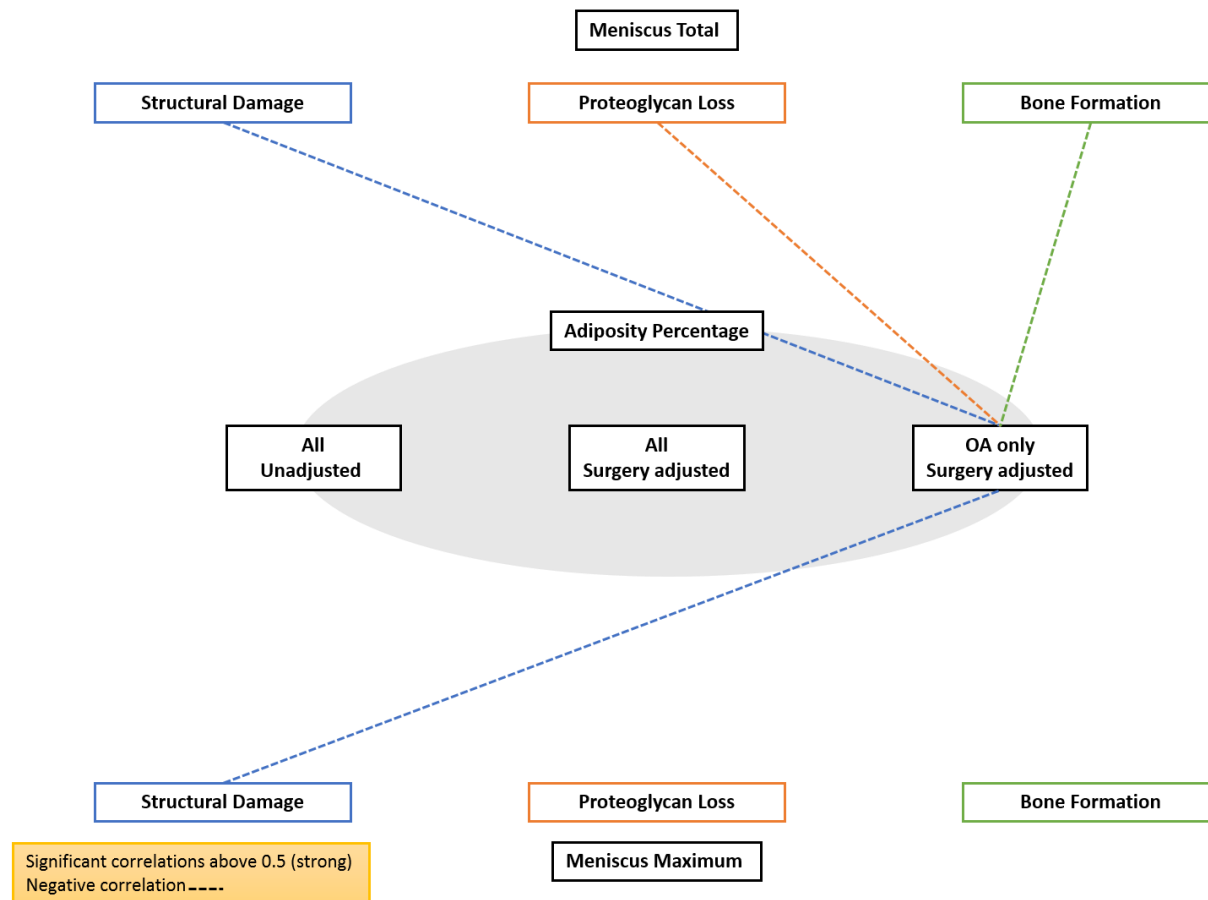


Figure 22. Summary of strong significant associations between meniscus tissues and IFP adiposity percentage. Significant and strong correlated associations observed in the whole sample (“All”) or sub-critically injured, ACLT and ACLR joints only (“OA only”) based on Spearman’s correlation coefficients and partial correlation coefficients which were adjusted for surgical intervention (Appendix 5 Table 21).

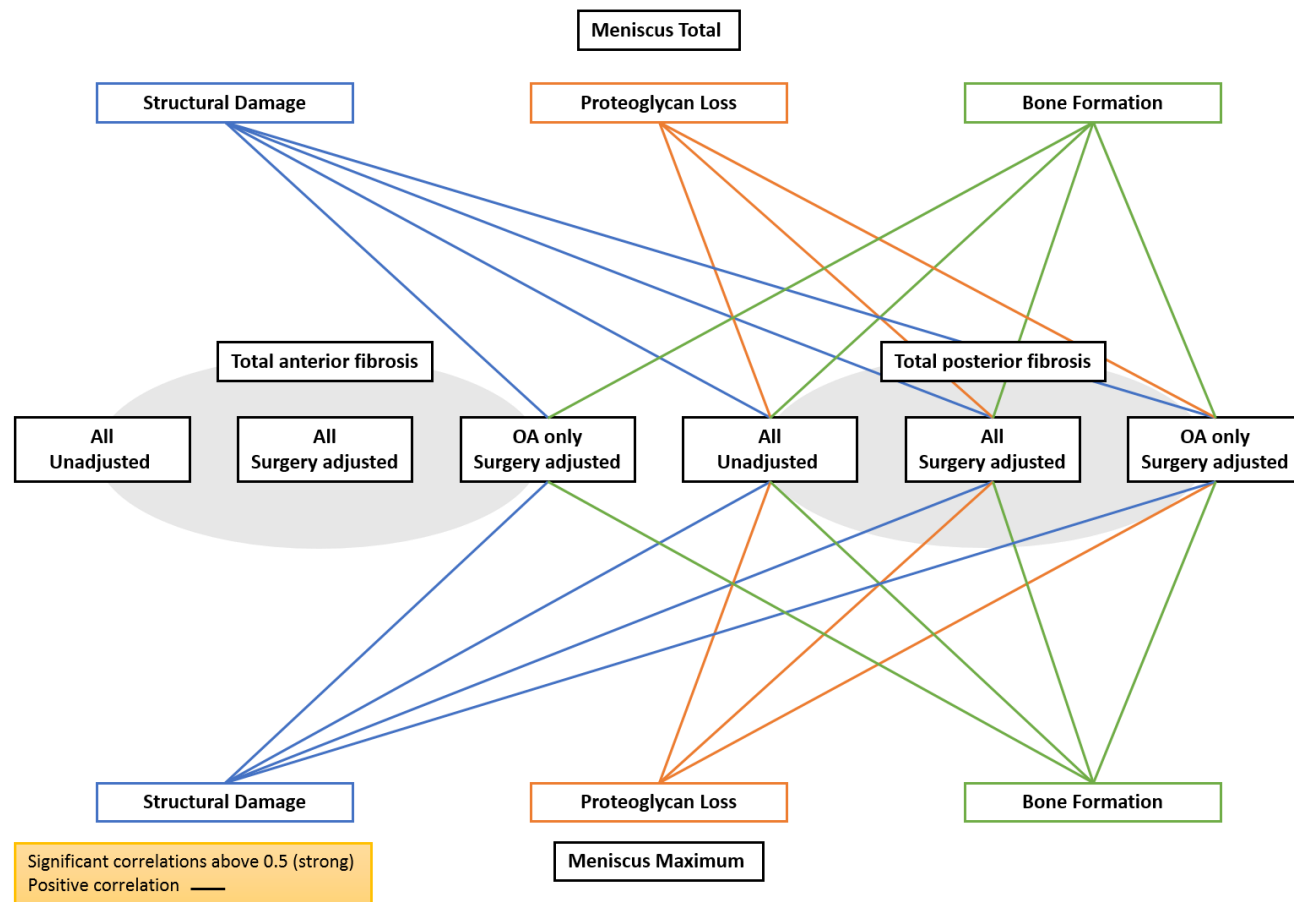


Figure 23. Summary of strong significant associations between meniscus tissues and total sub-synovial fibrosis. Significant and strong correlated associations observed in the whole sample (“All”) or sub-critically injured, ACLT and ACLR joints only (“OA only”) based on Spearman’s correlation coefficients and partial correlation coefficients which were adjusted for surgical intervention (Appendix 5 Table 32).

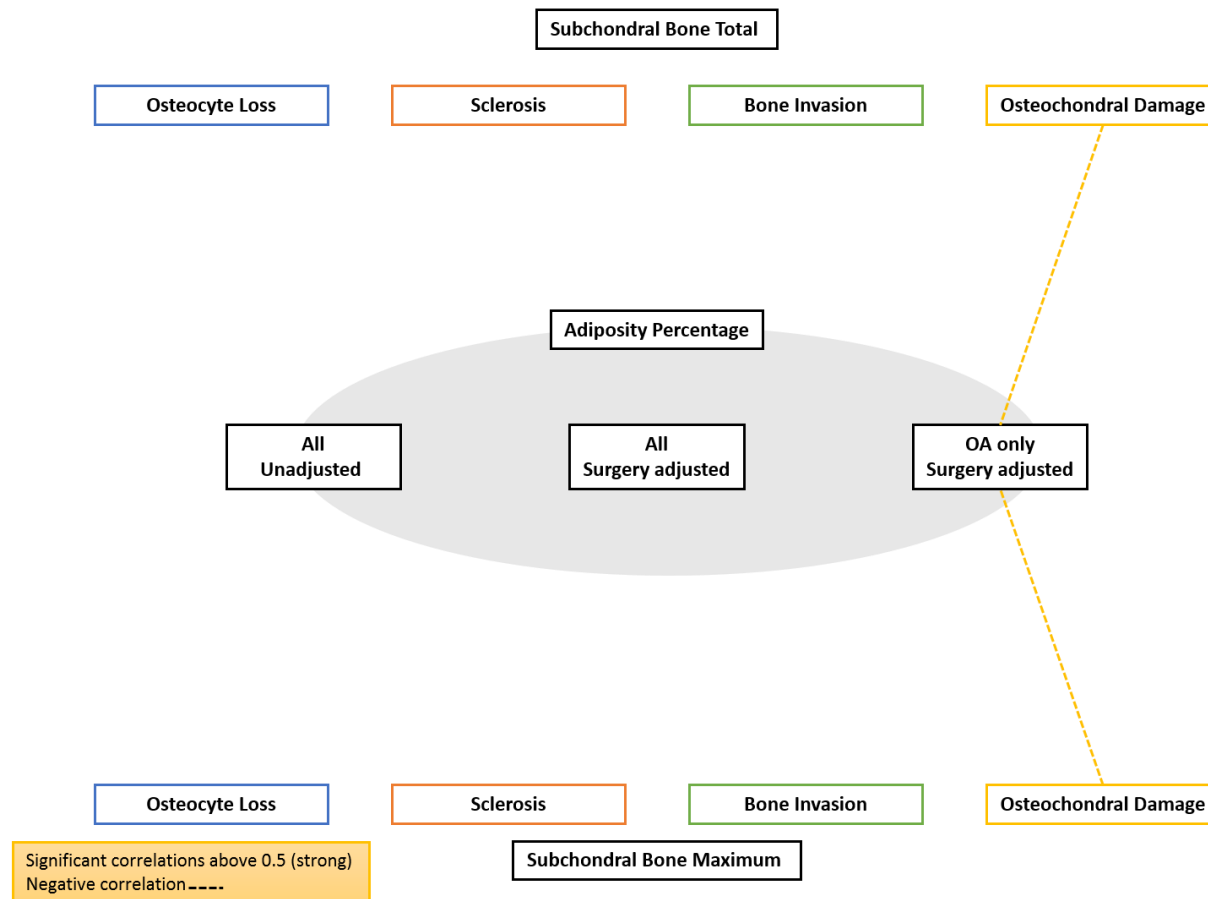


Figure 24. Summary of strong significant associations between subchondral bone tissues and IFP adiposity percentage. Significant and strong correlated associations observed in the whole sample (“All”) or sub-critically injured, ACLT and ACLR joints only (“OA only”) based on Spearman’s correlation coefficients and partial correlation coefficients which were adjusted for surgical intervention (Appendix 5 Table 18).

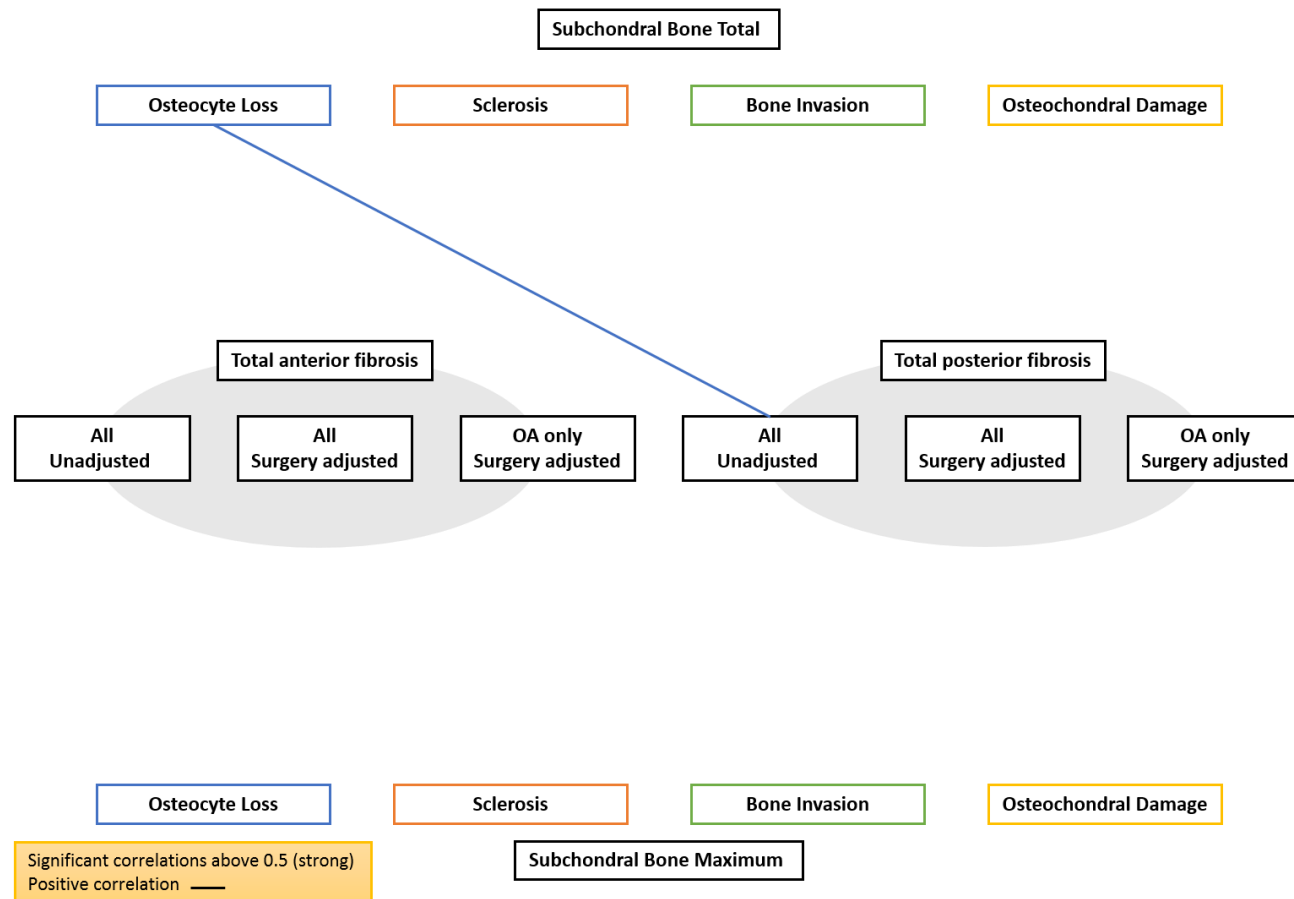


Figure 25. Summary of strong significant associations between subchondral bone tissues and total sub-synovial fibrosis. Significant and strong correlated associations observed in the whole sample (“All”) or sub-critically injured, ACLT and ACLR joints only (“OA only”) based on Spearman’s correlation coefficients and partial correlation coefficients which were adjusted for surgical intervention (Appendix 5 Table 28).

5.5 Discussion

This chapter explores the correlations between IFP adiposity and sub-synovial fibrosis with features of OA pathology in the medial tibiofemoral compartment of the murine knee joint. The structures investigated included the cartilage, subchondral bone, osteophyte and enthesophyte development, and meniscus. Many correlations were identified, but strong and therefore most likely biologically-relevant relationships were most evident for cartilage, osteophyte, enthesophyte and meniscus pathology to adiposity in OA models and posterior sub-synovial fibrosis. Very few significant correlations between subchondral bone and IFP adiposity or sub synovial fibrosis were identified, and of those present, many were of low strength.

In general, adiposity of the IFP was significantly and negatively correlated to many of the histopathological features of OA. The negative correlations indicated that lower or unhealthier adiposity in the IFP was associated with higher joint disease activity indicated by higher pathology scores. These correlations were also strengthened when tested only in OA/pathology-inducing models suggesting the involvement of the disease-causing mechanisms in IFP adiposity loss or vice versa. The adiposity findings matched the consensus in current literature in patients that the maximal area of the IFP is protective or associated with less joint pathology[121]. Studies have shown that larger IFPs in older adults with or without OA were associated with lesser cartilage defects, joint space narrowing presence of osteophytes and bone marrow lesions[105, 121, 266, 267]. Similarly, a study in rats showed declining IFP weights in ageing mice while OA pathology increased in severity, although the relationship was not statistically evaluated[119]. This chapter now demonstrates the same relationship between the IFP and OA pathology in a PTOA model.

Within the OA models examined, reduced IFP adiposity was strongly correlated to features of cartilage pathology, osteophytes, enthesophytes and meniscal disease/damage. Proteoglycan loss in cartilage and meniscus, overall cartilage score and structural damage in the posterior meniscus showed the strongest correlations to adiposity. The extracellular matrix of adipose tissue contains proteoglycans, including aggrecan which is associated with early adipose development but is increasingly degraded and has lower production in models of genetic obesity[313]. Hence, in mice, proteoglycans may contribute to the regulation of lipid uptake in adipocytes and obesity[313]. In humans, intra-articular injections of micro-fragmented adipose tissues also stimulate proteoglycan synthesis in cartilage[314, 315]. The bi-directional interaction between adipose and proteoglycans is further supported by evidence of a synergistic effect observed in co-cultures of bovine IFP and cartilage, that resulted in increased production of proteoglycan (sGAG) compared to isolated cultures indicating that a healthy IFP contributes to maintaining joint homeostasis[307]. The correlations identified in our study, in conjunction with the literature postulates an adipose driven protection/maintenance-of cartilage and meniscus proteoglycan levels and thus tissue health. This suggestion is supported by the strong correlations between IFP adiposity and the total and maximum summed cartilage, total and maximum summed meniscus scores, and strong to moderate correlations observed in the other domains of cartilage and meniscus histopathology (structural damage and chondrocyte hypertrophy).

Loss of IFP adiposity was also associated with the increased presence of anterior osteophytes and posterior enthesophytes in our models of PTOA. This finding was contrary to a recent study of mice fed a high-fat diet, which showed a positive correlation between maximal IFP volume

and osteophyte size in obesity/metabolic-OA[45]. It is unclear how changes in IFP adiposity might influence osteophyte development. One possibility is that the loss of IFP volume could contribute to more micro-instability and stress through the joint leading to increase marginal endochondral ossification[179, 316]. The IFP not only has a biomechanical role in the joint but, as a piece of secretory adipose tissue, it can also affect the biological microenvironment[176]. Many recent studies have used adipose-derived stem cells to seed the regenerations of osteochondral bone and cartilage with success[317-319]. Additionally, osteophytes are suggested to be derived from mesenchymal stem cells from adjacent sources such as the synovium or periosteum[298, 320, 321]. The loss of adiposity in the IFP may cause the dispersion/release and activation of the stem cells within the tissue potentially contributing to the development of osteophytes in the anterior (but not the posterior) of the joint as observed[322]. However, a separate body of evidence indicates that adipose tissue and its associated factors, such as leptin, are not effective in stimulating osteogenesis in healing fractures[323-325]. The lack of clarity indicates the strong need for further studies to describe better and understand the relationship between adiposity in the IFP and the development of osteophytes or enthesophytes.

Sub-synovial fibrosis was also significantly correlated, in varying degrees, to many of the structural pathologies. The positive correlations logically indicated that increased fibrosis severity was associated with increased histological changes. A similar finding in ovine models showed meniscectomy to induce OA resulted in a more than 10-fold increase in subintimal fibrosis and triple the depth compared to non-operated controls[326]. Our findings also showed strong correlations to sub-synovial fibrosis were most apparent with cartilage, osteophyte and

enthesophyte, and meniscal tissue changes, indicating potential common biological or biomechanical pathways. Interestingly, the relationships were more likely and much more robust in the posterior of the joint, which may implicate biomechanical stressors as the key link. The ACL functions as a stabiliser that prevents posterior subluxation of the femur relative to the tibia[327, 328]. The loss/impairment of the ACL in the models in the current study therefore manifests as instability in the posterior of the joint while the intact posterior cruciate ligament (PCL) maintains anterior stability. This culminates in stress to the posterior joint tissues with a fibrotic response representing an attempt to stabilise the joint[327]. As highlighted in the introduction, osteophyte and enthesophyte development are also thought to be a response to abnormal load stress[300]. Additionally, damage to the cartilage and meniscus results in impaired mechanical load management[304, 305]. Together these changes create a cycle of insults with injured structures synthesizing and releasing factors (e.g. metalloproteinases) that further degrade nearby structures, impaired structural responses, and alter loading mechanisms that eventuate in even further injury to the structures[329].

Similar findings of greater correlation to posterior pathology were also seen in the enthesophyte and meniscal tissues when evaluating adiposity. Considering the anterior location of the IFP, it is curious that posterior pathology, instead of the anatomically closer anterior structures, were more highly correlated. This association highlights the multifactorial nature of the disease and of the roles the IFP plays. Changes closer to the IFP may represent the biological drivers of the disease such as a response to released enzymes, growth factors and cytokines, while posterior meniscus and enthesophyte correlations highlight that despite the increased focus on biochemical changes which may be present in the extracellular matrix, the

mechanical manifestation of joint injury could be worsened by the loss of the IFP and its protective mechanical role[330]. Additionally, the changes to the IFP might confound the development of anterior sub-intimal fibrosis which in turn may impact any observations of correlations with the other joint pathologies.

An interesting finding is the lack of correlations between IFP adiposity or synovial fibrosis and subchondral bone pathology despite existing evidence of strong correlations between subchondral bone changes and cartilage health [221, 331]. Within this chapter, IFP adiposity and sub-synovial fibrosis are shown to be highly correlated to cartilage pathologies. However, the disconnect to subchondral bone changes could be attributed to joint mechanics. Both subchondral bone and cartilage have a dynamic role in managing compressive load through the joint[332, 333]. However, the models evaluated in this study appear to have a more significant role for mechanical instability, as evident by the correlation to posterior enthesophyte pathology observed. Alternatively, this discrepancy could be more associated with the molecular breakdown of the IFP. Given the increasing understanding about the biological role of the IFP, the molecular products from IFP breakdown could potentially have a more significant impact on mesenchymal stem cell activation, which is more critical to osteophyte and enthesophyte formation than subchondral bone pathology. However, further research to determine if the lack of association to subchondral bone pathology is biomechanical or biological is needed.

A key strength of this study was the broad “patient” sample that represented different OA/joint-pathology trajectories and severities using multiple models and different time points. In addition to non-operated controls, the sample included mice that were injured but did

eventuate in any (SHAM) or progressive OA-like (sub-critical) structural pathology, and two distinct ptOA-inducing ACL injury types that develop different disease phenotypes/trajectories (more rapid and severe in ACLR than ACLT). The inclusion of the sub-critical mechanical injury that causes focal non-progressive osteochondral lesions but not other typical OA pathologies (no synovitis or osteophytes), and controls for the effect of supra-physiological compressive loading in common real-world non-OA-inducing injuries. This diverse sample improves our understanding of the impact of the biomechanics, surgical intervention and progressive OA disease, on the relationships.

Another strength was the analysis of the different structural features in this study. Instead of evaluating overall cartilage changes or bony growths, the individual characteristics such as structural damage, chondrocyte hypertrophy, or osteophyte size and locations (femur, tibia, etc.) were evaluated separately for the correlations. The individual features of these “tissue pathologies” have different mechanisms and pathways, and by not considering the features based on the just the tissue or anatomical location this study aids in identifying potential commonalities and differences. However, the drawback of this approach is the multiple testing’s conducted that may have resulted in false significances identified. While it was possible to statistically correct for this disadvantage, this study was intending to be exploratory and to facilitate the generation of hypothesis. Hence, the findings should be confirmed in future studies, that can be appropriately powered for the *a priori* nominated/defined outcomes. Another limitation is also the lack of evaluation and correlation to clinical manifestations of the disease (pain/disability), which reduced the impact the study could have on disease modification and translation to patients.

These limitations do provide an opportunity for novel future studies. The strong correlations identified could be investigated in relevant models. For example, the relationships between IFP adiposity and cartilage damage could be evaluated in Bsl2 deficient mice which have dramatically lower adipose mass[334]. It would be essential to structure the study in a manner that allows testing and confirming of the hypotheses. Such a study would involve evaluating the different outcomes in the same sets of animals to enable statistical analyses such as correlations or regression models. Similarly, studies should be carried out in human populations to evaluate if similar findings are present. Such a study could be through existing databases such as the osteoarthritis initiative or in new studies to understand the clinical impact of these relationships.

5.6 Conclusion

In summary, this chapter identified several negative strong correlations between IFP adiposity and multiple features of OA pathology in cartilage, osteophyte and enthesophyte development and meniscal tissue but not sub-chondral bone within the medial tibiofemoral compartment of the murine knee joint in mice that develop post-traumatic OA. Similar findings were identified in sub-synovial fibrosis and the structural features showing positive correlations. Most interestingly, many of the associations with sub-synovial fibrosis and meniscus to IFP adiposity were to the posterior of the joint. These findings postulate there is a robust mechanical role that aggravates the abnormal biological environment.

5.7 Appendix

Please note that given the length of the tables – table number is indicated in the top-left cell throughout this section to assist in keeping track.

5.7.1 IFP adiposity and structural features correlation

Table 17. Spearman's and partial correlation coefficients between the adipose percentage of the IFP and cartilage scores

Table 17	All models				Joint pathology only	
	Unadjusted		Adjusted for surgery		Adjusted for surgery	
	ρ	p value	ρ	p value	ρ	p value
Cartilage Scores						
Total Score						
Structural damage						
Tibia	-0.18	0.03	-0.47	<0.01	-0.58	<0.01
Femur	-0.11	0.21	-0.48	<0.01	-0.59	<0.01
Summed	-0.17	0.05	-0.48	<0.01	-0.59	<0.01
Proteoglycan loss						
Tibia	-0.35	<0.01	-0.46	<0.01	-0.58	<0.01
Femur	-0.25	<0.01	-0.48	<0.01	-0.61	<0.01
Summed	-0.34	<0.01	-0.49	<0.01	-0.61	<0.01
Chondrocyte hypertrophy						
Tibia	-0.14	0.10	-0.35	<0.01	-0.47	<0.01
Femur	-0.21	0.01	-0.41	<0.01	-0.50	<0.01
Summed	-0.20	0.02	-0.41	<0.01	-0.51	<0.01

Table 17	All models				Joint pathology only	
	Unadjusted		Adjusted for surgery		Adjusted for surgery	
Cartilage Scores	ρ	p value	ρ	p value	ρ	p value
Summed Cartilage Score	-0.31	<0.01	-0.50	<0.01	-0.61	<0.01
Maximum Score						
Structural damage						
Tibia	-0.18	0.03	-0.48	<0.01	-0.58	<0.01
Femur	-0.11	0.20	-0.48	<0.01	-0.59	<0.01
Summed	-0.17	0.05	-0.48	<0.01	-0.59	<0.01
Proteoglycan loss						
Tibia	-0.38	<0.01	-0.41	<0.01	-0.56	<0.01
Femur	-0.25	<0.01	-0.44	<0.01	-0.58	<0.01
Summed	-0.36	<0.01	-0.46	<0.01	-0.61	<0.01
Chondrocyte hypertrophy						
Tibia	-0.13	0.14	-0.24	<0.01	-0.33	<0.01
Femur	-0.21	0.02	-0.37	<0.01	-0.47	<0.01
Summed	-0.20	0.02	-0.37	<0.01	-0.46	<0.01
Summed Cartilage Score	-0.29	<0.01	-0.50	<0.01	-0.62	<0.01

Table 18. Spearman's and partial correlation coefficients between the adipose percentage of the IFP and subchondral bone scores

Table 18	All models				Joint pathology	
	Unadjusted		Adjusted for surgery		Adjusted for surgery	
Subchondral Bone Scores	ρ	p value	ρ	p value	ρ	p value
Total Scores						
Osteocyte loss	-0.28	<0.01	-0.23	0.01	-0.28	0.01
Sub-chondral sclerosis	0.05	0.56	-0.13	0.14	-0.15	0.19
Sub-chondral bone invasion	-0.13	0.14	-0.21	0.02	-0.35	<0.01
Osteochondral damage	-0.11	0.21	-0.42	<0.01	-0.52	<0.01
Summed Subchondral Bone Score	-0.14	0.11	-0.43	<0.01	-0.53	<0.01
Maximum score						
Osteocyte loss	-0.25	<0.01	-0.23	0.01	-0.25	0.02
Sub-chondral sclerosis	0.15	0.08	-0.01	0.87	0.05	0.65
Sub-chondral bone invasion	-0.06	0.46	-0.03	0.71	-0.11	0.31
Osteochondral damage	-0.11	0.21	-0.44	<0.01	-0.53	<0.01
Summed Subchondral Bone Score	-0.09	0.29	-0.43	<0.01	-0.53	<0.01

Table 19. Spearman's and partial correlation coefficients between the adipose percentage of the IFP and osteophyte/enthesophyte scores

Table 19	All models				Joint pathology only	
	Unadjusted		Adjusted for surgery		Adjusted for surgery	
	ρ	p value	ρ	p value	ρ	p value
Total Scores						
Osteophyte						
Maturity						
Anterior	-0.21	0.01	-0.41	<0.01	-0.51	<0.01
Posterior	0.01	0.91	-0.09	0.30	-0.10	0.36
Summed	-0.21	0.01	-0.42	<0.01	-0.51	<0.01
Size						
Anterior	-0.21	0.02	-0.47	<0.01	-0.58	<0.01
Posterior	0.01	0.91	-0.09	0.30	-0.10	0.36
Summed	-0.21	0.02	-0.47	<0.01	-0.58	<0.01
Severity						
Anterior	-0.21	0.01	-0.42	<0.01	-0.52	<0.01
Posterior	0.01	0.91	-0.09	0.30	-0.10	0.36
Summed	-0.21	0.01	-0.42	<0.01	-0.52	<0.01
Enthesophyte						
Maturity						
Anterior	-0.44	<0.01	-0.08	0.37	-0.08	0.47
Posterior	-0.31	<0.01	-0.43	<0.01	-0.56	<0.01

Table 19	All models				Joint pathology only	
	Unadjusted		Adjusted for surgery		Adjusted for surgery	
Total Scores	ρ	p value	ρ	p value	ρ	p value
Summed	-0.41	<0.01	-0.37	<0.01	-0.50	<0.01
Size						
Anterior	-0.43	<0.01	-0.08	0.34	-0.09	0.44
Posterior	-0.27	<0.01	-0.43	<0.01	-0.57	<0.01
Summed	-0.37	<0.01	-0.41	<0.01	-0.55	<0.01
Severity						
Anterior	-0.44	<0.01	-0.07	0.39	-0.08	0.48
Posterior	-0.31	<0.01	-0.44	<0.01	-0.56	<0.01
Summed	-0.39	<0.01	-0.41	<0.01	-0.52	<0.01

Table 20. Spearman's and partial correlation coefficients between the adipose percentage of the IFP and maximum osteophyte and enthesophyte scores

Table 20	All models				Joint pathology only	
	Unadjusted		Adjusted for surgery		Adjusted for surgery	
	ρ	p value	ρ	p value	ρ	p value
Maximum Scores						
Osteophyte						
Maturity						
Anterior	-0.21	0.02	-0.36	<0.01	-0.47	<0.01
Posterior	0.01	0.91	-0.09	0.29	-0.10	0.36
Summed	-0.20	0.02	-0.37	<0.01	-0.47	<0.01
Size						
Anterior	-0.20	0.02	-0.45	<0.01	-0.57	<0.01
Posterior	0.01	0.91	-0.09	0.29	-0.10	0.36
Summed	-0.20	0.02	-0.45	<0.01	-0.56	<0.01
Severity						
Anterior	-0.21	0.01	-0.42	<0.01	-0.52	<0.01
Posterior	0.01	0.91	-0.09	0.29	-0.10	0.36
Summed	-0.21	0.01	-0.42	<0.01	-0.52	<0.01
Enthesophyte						
Maturity						
Anterior	-0.43	<0.01	-0.11	0.22	-0.12	0.29
Posterior	-0.33	<0.01	-0.38	<0.01	-0.52	<0.01

Table 20	All models				Joint pathology only	
	Unadjusted		Adjusted for surgery		Adjusted for surgery	
Maximum Scores	ρ	p value	ρ	p value	ρ	p value
Summed	-0.44	<0.01	-0.33	<0.01	-0.47	<0.01
Size						
Anterior	-0.42	<0.01	-0.12	0.16	-0.14	0.20
Posterior	-0.30	<0.01	-0.39	<0.01	-0.53	<0.01
Summed	-0.41	<0.01	-0.35	<0.01	-0.51	<0.01
Severity						
Anterior	-0.43	<0.01	-0.12	0.16	-0.14	0.21
Posterior	-0.32	<0.01	-0.42	<0.01	-0.54	<0.01
Summed	-0.41	<0.01	-0.38	<0.01	-0.51	<0.01

Table 21. Spearman's and partial correlation coefficients between the adipose percentage of the IFP and meniscus scores

Table 21	All models				Joint pathology	
	Unadjusted		Adjusted for surgery		Adjusted for surgery	
Meniscus Scores	ρ	p value	ρ	p value	ρ	p value
Total Score						
Tissue Structural damage						
Anterior	-0.16	0.06	-0.45	<0.01	-0.54	<0.01
Posterior	-0.14	0.10	-0.49	<0.01	-0.60	<0.01
Summed	-0.18	0.04	-0.49	<0.01	-0.60	<0.01
Superficial Proteoglycan Loss						
Anterior	-0.16	0.07	-0.42	<0.01	-0.52	<0.01
Posterior	-0.14	0.12	-0.39	<0.01	-0.48	<0.01
Summed	-0.16	0.07	-0.41	<0.01	-0.51	<0.01
Bone Formation						
Anterior	-0.28	<0.01	-0.43	<0.01	-0.52	<0.01
Posterior	-0.27	<0.01	-0.37	<0.01	-0.46	<0.01
Summed	-0.33	<0.01	-0.42	<0.01	-0.51	<0.01
Summed Meniscal Score	-0.24	<0.01	-0.48	<0.01	-0.59	<0.01

Table 21	All models				Joint pathology	
	Unadjusted		Adjusted for surgery		Adjusted for surgery	
	ρ	p value	ρ	p value	ρ	p value
Meniscus Scores						
Maximum Score						
Tissue Structural damage						
Anterior	-0.15	0.08	-0.39	<0.01	-0.45	<0.01
Posterior	-0.13	0.12	-0.44	<0.01	-0.54	<0.01
Summed	-0.16	0.06	-0.44	<0.01	-0.52	<0.01
Superficial Proteoglycan Loss						
Anterior	-0.16	0.07	-0.22	0.01	-0.39	<0.01
Posterior	-0.15	0.09	-0.33	<0.01	-0.44	<0.01
Summed	-0.17	0.05	-0.31	<0.01	-0.46	<0.01
Bone Formation						
Anterior	-0.30	<0.01	-0.36	<0.01	-0.48	<0.01
Posterior	-0.31	<0.01	-0.33	<0.01	-0.45	<0.01
Summed	-0.35	<0.01	-0.37	<0.01	-0.48	<0.01
Summed Meniscal Score	-0.25	<0.01	-0.44	<0.01	-0.55	<0.01

Table 22. Spearman's and partial correlation coefficients between IFP adipose cell count, mean adipose cell size and cartilage scores

Table 22	IFP Adipose Cell Count						Mean IFP Adipose Cell Size					
	All				Joint pathology		All				Joint pathology	
	Unadjusted		Adjusted for surgery		Adjusted for surgery		Unadjusted		Adjusted for surgery		Adjusted for surgery	
	ρ	p value	ρ	p value	ρ	p value	ρ	p value	ρ	p value	ρ	p value
Total Cartilage Scores												
Structural damage												
Tibia	-0.19	0.03	-0.48	0.34	-0.58	<0.01	-0.08	0.34	-0.31	<0.01	-0.39	<0.01
Femur	-0.15	0.08	-0.49	0.90	-0.58	<0.01	0.01	0.90	-0.31	<0.01	-0.39	<0.01
Summed	-0.18	0.04	-0.49	0.53	-0.58	<0.01	-0.05	0.53	-0.31	<0.01	-0.39	<0.01
Proteoglycan loss												
Tibia	-0.37	<0.01	-0.46	<0.01	-0.53	<0.01	-0.25	<0.01	-0.26	<0.01	-0.37	<0.01
Femur	-0.28	<0.01	-0.50	0.08	-0.60	<0.01	-0.15	0.08	-0.30	<0.01	-0.40	<0.01
Summed	-0.36	<0.01	-0.49	0.01	-0.58	<0.01	-0.23	0.01	-0.29	<0.01	-0.39	<0.01

Table 22	IFP Adipose Cell Count						Mean IFP Adipose Cell Size					
	All				Joint pathology		All				Joint pathology	
	Unadjusted		Adjusted for surgery		Adjusted for surgery		Unadjusted		Adjusted for surgery		Adjusted for surgery	
	ρ	p value	ρ	p value	ρ	p value	ρ	p value	ρ	p value	ρ	p value
Chondrocyte hypertrophy												
Tibia	-0.16	0.07	-0.35	0.63	-0.42	<0.01	-0.04	0.63	-0.15	0.09	-0.22	0.05
Femur	-0.22	0.01	-0.39	0.26	-0.45	<0.01	-0.10	0.26	-0.19	0.03	-0.28	0.01
Summed	-0.21	0.01	-0.40	0.29	-0.46	<0.01	-0.09	0.29	-0.19	0.03	-0.27	0.01
Summed Cartilage Score	-0.33	<0.01	-0.50	0.02	-0.59	<0.01	-0.20	0.02	-0.30	<0.01	-0.39	<0.01
Maximum Cartilage scores												
Structural damage												
Tibia	-0.18	0.04	-0.47	<0.01	-0.56	<0.01	-0.09	0.31	-0.27	<0.01	-0.34	<0.01
Femur	-0.15	0.07	-0.50	<0.01	-0.59	<0.01	0.01	0.89	-0.24	<0.01	-0.33	<0.01

Table 22	IFP Adipose Cell Count						Mean IFP Adipose Cell Size					
	All				Joint pathology		All				Joint pathology	
	Unadjusted		Adjusted for surgery		Adjusted for surgery		Unadjusted		Adjusted for surgery		Adjusted for surgery	
	ρ	p value	ρ	p value	ρ	p value	ρ	p value	ρ	p value	ρ	p value
Summed	-0.18	0.04	-0.49	<0.01	-0.59	<0.01	-0.06	0.51	-0.26	<0.01	-0.34	<0.01
Proteoglycan loss												
Tibia	-0.40	<0.01	-0.41	<0.01	-0.50	<0.01	-0.28	<0.01	-0.20	0.02	-0.32	<0.01
Femur	-0.27	<0.01	-0.44	<0.01	-0.54	<0.01	-0.16	0.06	-0.29	<0.01	-0.40	<0.01
Summed	-0.38	<0.01	-0.47	<0.01	-0.55	<0.01	-0.26	<0.01	-0.27	<0.01	-0.39	<0.01
Chondrocyte hypertrophy												
Tibia	-0.14	0.09	-0.24	<0.01	-0.28	0.01	-0.04	0.67	-0.06	0.50	-0.10	0.37
Femur	-0.20	0.02	-0.33	<0.01	-0.39	<0.01	-0.11	0.20	-0.20	0.02	-0.30	0.01
Summed	-0.21	0.02	-0.33	<0.01	-0.39	<0.01	-0.09	0.28	-0.16	0.06	-0.25	0.02
Summed Cartilage Score	-0.31	<0.01	-0.51	<0.01	-0.60	<0.01	-0.18	0.03	-0.29	<0.01	-0.38	<0.01

Table 23. Spearman's and partial correlation coefficients between IFP adipose cell count, mean adipose cell size and subchondral bone

Table 23	IFP Adipose Cell Count						Mean IFP Adipose Cell Size					
	All				Joint pathology		All			Joint pathology		
	Unadjusted		Adjusted for surgery		Adjusted for surgery		Unadjusted		Adjusted for surgery		Adjusted for surgery	
	P	p value	ρ	p value	ρ	p value	P	p value	ρ	p value	ρ	p value
Total Subchondral Bone Scores												
Osteocyte loss	-0.26	<0.01	-0.19	0.03	-0.20	0.07	-0.21	0.01	-0.18	0.03	-0.27	0.01
Sub-chondral sclerosis	0.06	0.52	-0.14	0.10	-0.20	0.07	0.05	0.58	-0.12	0.15	-0.18	0.10
Sub-chondral bone invasion	-0.08	0.33	-0.12	0.18	-0.23	0.04	-0.21	0.02	-0.21	0.02	-0.38	<0.01
Osteochondral damage	-0.15	0.09	-0.45	<0.01	-0.54	<0.01	-0.03	0.74	-0.30	<0.01	-0.37	<0.01
Summed Subchondral Bone Score	-0.11	0.20	-0.44	<0.01	-0.54	<0.01	-0.13	0.12	-0.33	<0.01	-0.42	<0.01

Table 23	IFP Adipose Cell Count						Mean IFP Adipose Cell Size					
	All				Joint pathology		All			Joint pathology		
	Unadjusted		Adjusted for surgery		Adjusted for surgery		Unadjusted		Adjusted for surgery		Adjusted for surgery	
	P	p value	p	p value	p	p value	p	p value	p	p value	p	p value
Maximum Subchondral Bone Scores												
Osteocyte loss	-0.22	0.01	-0.20	0.02	-0.24	0.03	-0.18	0.04	-0.15	0.09	-0.19	0.09
Sub-chondral sclerosis	0.19	0.03	0.02	0.80	0.07	0.54	0.07	0.41	-0.10	0.25	-0.13	0.25
Sub-chondral bone invasion	-0.02	0.84	0.07	0.44	-0.02	0.83	-0.18	0.04	-0.15	0.08	-0.27	0.02
Osteochondral damage	-0.14	0.09	-0.45	<0.01	-0.54	<0.01	-0.03	0.74	-0.28	<0.01	-0.35	<0.01
Summed Subchondral Bone Score	-0.05	0.57	-0.39	<0.01	-0.51	<0.01	-0.12	0.16	-0.34	<0.01	-0.44	<0.01

Table 24. Spearman's and partial correlation coefficients between IFP adipose cell count, mean adipose cell size and osteophytes/enthesophytes

Table 24	IFP Adipose Cell Count						Mean IFP Adipose Cell Size					
	All				Joint pathology		All				Joint pathology	
	Unadjusted		Adjusted for surgery		Adjusted for surgery		Unadjusted		Adjusted for surgery		Adjusted for surgery	
	P	p value	ρ	p value	ρ	p value	ρ	p value	ρ	p value	ρ	p value
Total score												
Osteophyte												
Maturity												
Anterior	-0.20	0.02	-0.41	<0.01	-0.48	<0.01	-0.16	0.07	-0.31	<0.01	-0.41	<0.01
Posterior	0.00	0.97	-0.09	0.33	-0.09	0.40	0.02	0.78	-0.02	0.86	-0.01	0.90
Summed	-0.20	0.02	-0.41	<0.01	-0.48	<0.01	-0.16	0.07	-0.31	<0.01	-0.41	<0.01
Size												
Anterior	-0.19	0.02	-0.45	<0.01	-0.54	<0.01	-0.16	0.07	-0.36	<0.01	-0.48	<0.01
Posterior	0.00	0.97	-0.09	0.33	-0.09	0.40	0.02	0.78	-0.02	0.86	-0.01	0.90

Table 24	IFP Adipose Cell Count						Mean IFP Adipose Cell Size					
	All				Joint pathology		All				Joint pathology	
	Unadjusted		Adjusted for surgery		Adjusted for surgery		Unadjusted		Adjusted for surgery		Adjusted for surgery	
	P	p value	ρ	p value	ρ	p value	ρ	p value	ρ	p value	ρ	p value
Summed	-0.19	0.02	-0.45	<0.01	-0.54	<0.01	-0.16	0.07	-0.36	<0.01	-0.48	<0.01
Severity												
Anterior	-0.20	0.02	-0.43	<0.01	-0.50	<0.01	-0.15	0.08	-0.32	<0.01	-0.43	<0.01
Posterior	0.00	0.97	-0.09	0.33	-0.09	0.40	0.02	0.78	-0.02	0.86	-0.01	0.90
Summed	-0.20	0.02	-0.43	<0.01	-0.50	<0.01	-0.15	0.08	-0.32	<0.01	-0.42	<0.01
Enthesophyte												
Maturity												
Anterior	-0.46	<0.01	-0.15	0.09	-0.13	0.26	-0.35	<0.01	-0.07	0.40	-0.15	0.18
Posterior	-0.34	<0.01	-0.45	<0.01	-0.56	<0.01	-0.16	0.06	-0.21	0.02	-0.33	<0.01
Summed	-0.45	<0.01	-0.43	<0.01	-0.52	<0.01	-0.26	<0.01	-0.20	0.02	-0.34	<0.01

Table 24	IFP Adipose Cell Count						Mean IFP Adipose Cell Size					
	All			Joint pathology			All			Joint pathology		
	Unadjusted		Adjusted for surgery		Adjusted for surgery		Unadjusted		Adjusted for surgery		Adjusted for surgery	
	P	p value	ρ	p value	ρ	p value	ρ	p value	ρ	p value	ρ	p value
Size												
Anterior	-0.45	<0.01	-0.14	0.10	-0.12	0.27	-0.33	<0.01	-0.08	0.34	-0.17	0.13
Posterior	-0.29	<0.01	-0.42	<0.01	-0.50	<0.01	-0.15	0.08	-0.22	0.01	-0.34	<0.01
Summed	-0.39	<0.01	-0.42	<0.01	-0.50	<0.01	-0.24	0.01	-0.22	0.01	-0.37	<0.01
Severity												
Anterior	-0.46	<0.01	-0.13	0.12	-0.12	0.28	-0.35	<0.01	-0.08	0.35	-0.15	0.19
Posterior	-0.33	<0.01	-0.46	<0.01	-0.54	<0.01	-0.18	0.04	-0.23	0.01	-0.33	<0.01
Summed	-0.42	<0.01	-0.44	<0.01	-0.52	<0.01	-0.25	<0.01	-0.23	0.01	-0.35	<0.01
Maximum Scores												

Table 24	IFP Adipose Cell Count						Mean IFP Adipose Cell Size					
	All			Joint pathology			All			Joint pathology		
	Unadjusted		Adjusted for surgery		Adjusted for surgery		Unadjusted		Adjusted for surgery		Adjusted for surgery	
	P	p value	ρ	p value	ρ	p value	ρ	p value	ρ	p value	ρ	p value
Osteophyte												
Maturity												
Anterior	-0.20	0.02	-0.35	<0.01	-0.43	<0.01	-0.15	0.08	-0.24	<0.01	-0.34	<0.01
Posterior	0.00	0.97	-0.09	0.33	-0.09	0.40	0.02	0.78	-0.02	0.85	-0.01	0.90
Summed	-0.20	0.02	-0.36	<0.01	-0.44	<0.01	-0.15	0.09	-0.24	<0.01	-0.33	<0.01
Size												
Anterior	-0.19	0.03	-0.42	<0.01	-0.50	<0.01	-0.14	0.10	-0.31	<0.01	-0.42	<0.01
Posterior	0.00	0.97	-0.09	0.33	-0.09	0.40	0.02	0.78	-0.02	0.85	-0.01	0.90
Summed	-0.18	0.03	-0.42	<0.01	-0.50	<0.01	-0.14	0.10	-0.30	<0.01	-0.41	<0.01
Severity												

Table 24	IFP Adipose Cell Count						Mean IFP Adipose Cell Size					
	All				Joint pathology		All				Joint pathology	
	Unadjusted		Adjusted for surgery		Adjusted for surgery		Unadjusted		Adjusted for surgery		Adjusted for surgery	
	P	p value	ρ	p value	ρ	p value	ρ	p value	ρ	p value	ρ	p value
Anterior	-0.20	0.02	-0.41	<0.01	-0.49	<0.01	-0.15	0.07	-0.30	<0.01	-0.41	<0.01
Posterior	0.00	0.97	-0.09	0.33	-0.09	0.40	0.02	0.78	-0.02	0.85	-0.01	0.90
Summed	-0.20	0.02	-0.41	<0.01	-0.49	<0.01	-0.15	0.08	-0.30	<0.01	-0.40	<0.01
Enthesophyte												
Maturity												
Anterior	-0.45	<0.01	-0.17	0.05	-0.15	0.18	-0.34	<0.01	-0.02	0.85	-0.08	0.45
Posterior	-0.36	<0.01	-0.41	<0.01	-0.51	<0.01	-0.19	0.03	-0.17	0.05	-0.31	<0.01
Summed	-0.47	<0.01	-0.38	<0.01	-0.48	<0.01	-0.29	<0.01	-0.13	0.13	-0.29	0.01
Size												
Anterior	-0.44	<0.01	-0.17	0.05	-0.14	0.20	-0.33	<0.01	-0.07	0.43	-0.16	0.14

Table 24	IFP Adipose Cell Count						Mean IFP Adipose Cell Size					
	All				Joint pathology		All				Joint pathology	
	Unadjusted		Adjusted for surgery		Adjusted for surgery		Unadjusted		Adjusted for surgery		Adjusted for surgery	
	P	p value	ρ	p value	ρ	p value	ρ	p value	ρ	p value	ρ	p value
Posterior	-0.31	<0.01	-0.37	<0.01	-0.45	<0.01	-0.17	0.05	-0.16	0.06	-0.30	0.01
Summed	-0.42	<0.01	-0.36	<0.01	-0.44	<0.01	-0.26	<0.01	-0.15	0.08	-0.32	<0.01
Severity												
Anterior	-0.45	<0.01	-0.18	0.04	-0.17	0.13	-0.34	<0.01	-0.06	0.49	-0.13	0.23
Posterior	-0.34	<0.01	-0.43	<0.01	-0.52	<0.01	-0.18	0.03	-0.22	0.01	-0.34	<0.01
Summed	-0.43	<0.01	-0.42	<0.01	-0.50	<0.01	-0.27	<0.01	-0.20	0.02	-0.34	<0.01

Table 25. Spearman's and partial correlation coefficients between IFP adipose cell count, mean adipose cell size and meniscus tissue

Table 25	IFP Adipose Cell Count						Mean IFP Adipose Cell Size					
	All				Joint pathology		All				Joint pathology	
	Unadjusted		Adjusted for surgery		Adjusted for surgery		Unadjusted		Adjusted for surgery		Adjusted for surgery	
	P	p value	ρ	p value	ρ	p value	ρ	p value	ρ	p value	ρ	p value
Total Meniscus Scores												
Tissue Structural damage												
Anterior	-0.16	0.07	-0.42	<0.01	-0.48	<0.01	-0.10	0.25	-0.29	<0.01	-0.36	<0.01
Posterior	-0.15	0.07	-0.46	<0.01	-0.54	<0.01	-0.07	0.44	-0.31	<0.01	-0.40	<0.01
Summed	-0.19	0.03	-0.46	<0.01	-0.54	<0.01	-0.08	0.38	-0.31	<0.01	-0.40	<0.01
Superficial Proteoglycan Loss												
Anterior	-0.18	0.03	-0.35	<0.01	-0.42	<0.01	-0.06	0.49	-0.23	0.01	-0.29	0.01
Posterior	-0.14	0.11	-0.34	<0.01	-0.38	<0.01	-0.08	0.34	-0.21	0.02	-0.29	0.01
Summed	-0.18	0.04	-0.35	<0.01	-0.40	<0.01	-0.07	0.42	-0.22	0.01	-0.30	0.01

Table 25	IFP Adipose Cell Count						Mean IFP Adipose Cell Size					
	All				Joint pathology		All				Joint pathology	
	Unadjusted		Adjusted for surgery		Adjusted for surgery		Unadjusted		Adjusted for surgery		Adjusted for surgery	
	P	p value	ρ	p value	ρ	p value	ρ	p value	ρ	p value	ρ	p value
Bone Formation												
Anterior	-0.29	<0.01	-0.42	<0.01	-0.49	<0.01	-0.17	0.05	-0.23	0.01	-0.31	0.01
Posterior	-0.28	<0.01	-0.36	<0.01	-0.40	<0.01	-0.14	0.12	-0.17	0.05	-0.26	0.02
Summed	-0.34	<0.01	-0.41	<0.01	-0.47	<0.01	-0.22	0.01	-0.21	0.02	-0.30	0.01
Summed Meniscal Score	-0.26	<0.01	-0.44	<0.01	-0.52	<0.01	-0.13	0.13	-0.28	<0.01	-0.37	<0.01
Maximum Meniscus Scores												
Tissue Structural damage												
Anterior	-0.15	0.08	-0.35	<0.01	-0.38	<0.01	-0.09	0.31	-0.22	0.01	-0.29	0.01
Posterior	-0.15	0.09	-0.41	<0.01	-0.46	<0.01	-0.06	0.52	-0.23	0.01	-0.31	0.01

Table 25	IFP Adipose Cell Count						Mean IFP Adipose Cell Size					
	All				Joint pathology		All				Joint pathology	
	Unadjusted		Adjusted for surgery		Adjusted for surgery		Unadjusted		Adjusted for surgery		Adjusted for surgery	
	P	p value	ρ	p value	ρ	p value	ρ	p value	ρ	p value	ρ	p value
Summed	-0.17	0.04	-0.40	<0.01	-0.44	<0.01	-0.06	0.47	-0.23	0.01	-0.31	<0.01
Superficial Proteoglycan Loss												
Anterior	-0.17	0.05	-0.18	0.03	-0.29	0.01	-0.10	0.26	-0.05	0.57	-0.15	0.18
Posterior	-0.15	0.09	-0.26	<0.01	-0.34	<0.01	-0.08	0.35	-0.12	0.19	-0.21	0.06
Summed	-0.18	0.04	-0.26	<0.01	-0.35	<0.01	-0.09	0.30	-0.10	0.27	-0.20	0.07
Bone Formation												
Anterior	-0.32	<0.01	-0.36	<0.01	-0.44	<0.01	-0.18	0.04	-0.10	0.26	-0.18	0.11
Posterior	-0.33	<0.01	-0.35	<0.01	-0.43	<0.01	-0.16	0.06	-0.12	0.18	-0.25	0.03
Summed	-0.36	<0.01	-0.38	<0.01	-0.45	<0.01	-0.21	0.01	-0.11	0.20	-0.21	0.06
Summed Meniscal Score	-0.27	<0.01	-0.40	<0.01	-0.47	<0.01	-0.14	0.10	-0.20	0.02	-0.30	0.01

5.7.2 Sub-synovial fibrosis and structural features correlation

Table 26. Spearman's and partial correlation coefficients between total Sub-synovial fibrosis and cartilage scores

Table 26	Anterior Total						Posterior Total					
	All				Joint pathology		All				Joint pathology	
	Unadjusted		Adjusted for surgery		Adjusted for surgery		Unadjusted		Adjusted for surgery		Adjusted for surgery	
	ρ	p value	ρ	p value	ρ	p value	ρ	p value	ρ	p value	ρ	p value
Total Cartilage Scores												
Structural damage												
Tibia	0.36	<0.01	0.39	<0.01	0.42	<0.01	0.51	<0.01	0.55	<0.01	0.54	<0.01
Femur	0.36	<0.01	0.39	<0.01	0.43	<0.01	0.62	<0.01	0.59	<0.01	0.59	<0.01
Summed	0.34	<0.01	0.39	<0.01	0.43	<0.01	0.56	<0.01	0.57	<0.01	0.56	<0.01
Proteoglycan loss												
Tibia	0.46	<0.01	0.45	<0.01	0.50	<0.01	0.67	<0.01	0.59	<0.01	0.55	<0.01
Femur	0.46	<0.01	0.49	<0.01	0.53	<0.01	0.62	<0.01	0.63	<0.01	0.60	<0.01
Summed	0.48	<0.01	0.48	<0.01	0.53	<0.01	0.70	<0.01	0.63	<0.01	0.59	<0.01

Table 26	Anterior Total						Posterior Total					
	All				Joint pathology		All				Joint pathology	
	Unadjusted		Adjusted for surgery		Adjusted for surgery		Unadjusted		Adjusted for surgery		Adjusted for surgery	
	ρ	p value	ρ	p value	ρ	p value	ρ	p value	ρ	p value	ρ	p value
Chondrocyte hypertrophy												
Tibia	0.46	<0.01	0.47	<0.01	0.43	<0.01	0.55	<0.01	0.49	<0.01	0.58	<0.01
Femur	0.42	<0.01	0.40	<0.01	0.41	<0.01	0.60	<0.01	0.62	<0.01	0.59	<0.01
Summed	0.47	<0.01	0.46	<0.01	0.44	<0.01	0.62	<0.01	0.60	<0.01	0.61	<0.01
Summed Cartilage Score	0.50	<0.01	0.44	<0.01	0.47	<0.01	0.70	<0.01	0.61	<0.01	0.60	<0.01
Maximum Cartilage Scores												
Structural damage												
Tibia	0.35	<0.01	0.44	<0.01	0.49	<0.01	0.50	<0.01	0.62	<0.01	0.60	<0.01
Femur	0.36	<0.01	0.41	<0.01	0.45	<0.01	0.62	<0.01	0.65	<0.01	0.64	<0.01
Summed	0.33	<0.01	0.43	<0.01	0.48	<0.01	0.54	<0.01	0.64	<0.01	0.63	<0.01

Table 26	Anterior Total						Posterior Total					
	All				Joint pathology		All				Joint pathology	
	Unadjusted		Adjusted for surgery		Adjusted for surgery		Unadjusted		Adjusted for surgery		Adjusted for surgery	
	ρ	p value	ρ	p value	ρ	p value	ρ	p value	ρ	p value	ρ	p value
Proteoglycan loss												
Tibia	0.46	<0.01	0.48	<0.01	0.55	<0.01	0.65	<0.01	0.60	<0.01	0.61	<0.01
Femur	0.40	<0.01	0.45	<0.01	0.52	<0.01	0.54	<0.01	0.59	<0.01	0.56	<0.01
Summed	0.47	<0.01	0.51	<0.01	0.57	<0.01	0.66	<0.01	0.65	<0.01	0.62	<0.01
Chondrocyte hypertrophy												
Tibia	0.36	<0.01	0.36	<0.01	0.30	0.01	0.43	<0.01	0.32	<0.01	0.33	<0.01
Femur	0.42	<0.01	0.38	<0.01	0.41	<0.01	0.59	<0.01	0.60	<0.01	0.58	<0.01
Summed	0.46	<0.01	0.42	<0.01	0.41	<0.01	0.58	<0.01	0.56	<0.01	0.55	<0.01
Summed Cartilage Score	0.49	<0.01	0.49	<0.01	0.53	<0.01	0.67	<0.01	0.66	<0.01	0.63	<0.01

Table 27. Spearman's and partial correlation coefficients between maximum sub-synovial fibrosis and cartilage scores

Table 27	Anterior Maximum						Posterior Maximum					
	All				Joint pathology		All				Joint pathology	
	Unadjusted		Adjusted for surgery		Adjusted for surgery		Unadjusted		Adjusted for surgery		Adjusted for surgery	
	ρ	p value	ρ	p value	ρ	p value	ρ	p value	ρ	p value	ρ	p value
Total Cartilage Scores												
Structural damage												
Tibia	0.26	<0.01	0.21	0.01	0.20	0.07	0.50	<0.01	0.53	<0.01	0.53	<0.01
Femur	0.31	<0.01	0.23	0.01	0.22	0.04	0.56	<0.01	0.57	<0.01	0.57	<0.01
Summed	0.29	<0.01	0.22	0.01	0.21	0.06	0.52	<0.01	0.55	<0.01	0.55	<0.01
Proteoglycan loss												
Tibia	0.37	<0.01	0.33	<0.01	0.32	<0.01	0.63	<0.01	0.60	<0.01	0.57	<0.01
Femur	0.42	<0.01	0.34	<0.01	0.33	<0.01	0.56	<0.01	0.62	<0.01	0.59	<0.01
Summed	0.42	<0.01	0.35	<0.01	0.34	<0.01	0.65	<0.01	0.63	<0.01	0.60	<0.01
Chondrocyte hypertrophy												

Table 27	Anterior Maximum						Posterior Maximum					
	All				Joint pathology		All				Joint pathology	
	Unadjusted		Adjusted for surgery		Adjusted for surgery		Unadjusted		Adjusted for surgery		Adjusted for surgery	
	ρ	p value	ρ	p value	ρ	p value	ρ	p value	ρ	p value	ρ	p value
Tibia	0.34	<0.01	0.33	<0.01	0.29	0.01	0.51	<0.01	0.48	<0.01	0.58	<0.01
Femur	0.37	<0.01	0.29	<0.01	0.27	0.01	0.53	<0.01	0.62	<0.01	0.61	<0.01
Summed	0.38	<0.01	0.33	<0.01	0.29	0.01	0.56	<0.01	0.60	<0.01	0.62	<0.01
Summed Cartilage Score	0.43	<0.01	0.28	<0.01	0.26	0.02	0.64	<0.01	0.60	<0.01	0.59	<0.01
Maximum Cartilage Scores												
Structural damage												
Tibia	0.24	<0.01	0.25	<0.01	0.23	0.04	0.50	<0.01	0.62	<0.01	0.61	<0.01
Femur	0.30	<0.01	0.26	<0.01	0.25	0.02	0.56	<0.01	0.63	<0.01	0.63	<0.01
Summed	0.27	<0.01	0.26	<0.01	0.24	0.03	0.51	<0.01	0.63	<0.01	0.63	<0.01
Proteoglycan loss												

Table 27	Anterior Maximum						Posterior Maximum					
	All				Joint pathology		All				Joint pathology	
	Unadjusted		Adjusted for surgery		Adjusted for surgery		Unadjusted		Adjusted for surgery		Adjusted for surgery	
	ρ	p value	ρ	p value	ρ	p value	ρ	p value	ρ	p value	ρ	p value
Tibia	0.35	<0.01	0.36	<0.01	0.35	<0.01	0.62	<0.01	0.58	<0.01	0.60	<0.01
Femur	0.37	<0.01	0.35	<0.01	0.36	<0.01	0.51	<0.01	0.58	<0.01	0.57	<0.01
Summed	0.40	<0.01	0.38	<0.01	0.38	<0.01	0.63	<0.01	0.64	<0.01	0.62	<0.01
Chondrocyte hypertrophy												
Tibia	0.25	<0.01	0.26	<0.01	0.23	0.04	0.39	<0.01	0.32	<0.01	0.36	<0.01
Femur	0.37	<0.01	0.32	<0.01	0.34	<0.01	0.54	<0.01	0.62	<0.01	0.61	<0.01
Summed	0.37	<0.01	0.34	<0.01	0.34	<0.01	0.54	<0.01	0.57	<0.01	0.58	<0.01
Summed Cartilage Score	0.43	<0.01	0.33	<0.01	0.31	<0.01	0.61	<0.01	0.65	<0.01	0.63	<0.01

Table 28. Spearman's and partial correlation coefficients between total sub-synovial fibrosis and subchondral bone scores

Table 28	Anterior Total						Posterior Total					
	All		Joint pathology		All		Joint pathology					
	Unadjusted	Adjusted for surgery	Adjusted for surgery	Adjusted for surgery	Unadjusted	Adjusted for surgery	Adjusted for surgery	Adjusted for surgery				
	ρ	p value	ρ	p value	ρ	p value	ρ	p value	ρ	p value		
Total Subchondral Bone Scores												
Osteocyte loss	0.29	<0.01	0.22	0.01	0.18	0.11	0.51	<0.01	0.44	<0.01	0.40	<0.01
Sub-chondral sclerosis	0.11	0.19	0.17	0.05	0.19	0.09	0.01	0.93	0.07	0.44	0.11	0.30
Sub-chondral bone invasion	0.11	0.21	0.17	0.05	0.23	0.03	0.39	<0.01	0.35	<0.01	0.30	0.01
Osteochondral damage	0.24	0.01	0.26	<0.01	0.28	0.01	0.42	<0.01	0.42	<0.01	0.42	<0.01
Summed Subchondral Bone Score	0.24	0.01	0.30	<0.01	0.32	<0.01	0.39	<0.01	0.47	<0.01	0.46	<0.01
Maximum Subchondral Bone Scores												

Table 28	Anterior Total						Posterior Total					
	All				Joint pathology		All				Joint pathology	
	Unadjusted		Adjusted for surgery		Adjusted for surgery		Unadjusted		Adjusted for surgery		Adjusted for surgery	
	ρ	p value	ρ	p value	ρ	p value	ρ	p value	ρ	p value	ρ	p value
Osteocyte loss	0.27	<0.01	0.24	<0.01	0.22	0.05	0.48	<0.01	0.46	<0.01	0.44	<0.01
Sub-chondral sclerosis	0.00	0.99	0.03	0.76	0.03	0.81	-0.13	0.13	-0.09	0.32	-0.14	0.20
Sub-chondral bone invasion	0.04	0.67	0.03	0.71	0.10	0.37	0.23	0.01	0.17	0.05	0.17	0.12
Osteochondral damage	0.24	0.01	0.28	<0.01	0.30	0.01	0.42	<0.01	0.47	<0.01	0.47	<0.01
Summed Subchondral Bone Score	0.22	0.01	0.31	<0.01	0.34	<0.01	0.41	<0.01	0.52	<0.01	0.51	<0.01

Table 29. Spearman's and partial correlation coefficients between maximum sub-synovial fibrosis and subchondral bone scores

Table 29	Anterior Maximum						Posterior Maximum					
	All				Joint pathology		All				Joint pathology	
	Unadjusted		Adjusted for surgery		Adjusted for surgery		Unadjusted		Adjusted for surgery		Adjusted for surgery	
	ρ	p value	ρ	p value	ρ	p value	ρ	p value	ρ	p value	ρ	p value
Total Subchondral Bone Scores												
Osteocyte loss	0.20	0.02	0.15	0.08	0.08	0.48	.47	<0.01	0.43	<0.01	0.39	<0.01
Sub-chondral sclerosis	0.02	0.78	0.06	0.47	0.07	0.54	0.01	0.89	0.09	0.31	0.16	0.15
Sub-chondral bone invasion	0.06	0.52	0.09	0.32	0.12	0.28	.41	<0.01	0.33	<0.01	0.26	0.02
Osteochondral damage	0.09	0.30	0.10	0.24	0.08	0.47	.43	<0.01	0.40	<0.01	0.40	<0.01
Summed Subchondral Bone Score	0.13	0.13	0.13	0.13	0.11	0.34	.41	<0.01	0.46	<0.01	0.45	<0.01

Table 29	Anterior Maximum						Posterior Maximum					
	All				Joint pathology		All				Joint pathology	
	Unadjusted		Adjusted for surgery		Adjusted for surgery		Unadjusted		Adjusted for surgery		Adjusted for surgery	
	ρ	p value	ρ	p value	ρ	p value	ρ	p value	ρ	p value	ρ	p value
Maximum Subchondral Bone Scores												
Osteocyte loss	0.20	0.03	0.18	0.04	0.09	0.43	.43	<0.01	0.38	<0.01	0.35	<0.01
Sub-chondral sclerosis	-0.08	0.33	-0.05	0.58	0.01	0.92	-0.07	0.44	-0.05	0.55	-0.08	0.48
Sub-chondral bone invasion	0.01	0.90	-0.01	0.94	0.01	0.91	.24	<0.01	0.13	0.12	0.07	0.55
Osteochondral damage	0.09	0.30	0.11	0.19	0.09	0.44	.43	<0.01	0.45	<0.01	0.45	<0.01
Summed Subchondral Bone Score	0.09	0.32	0.12	0.16	0.10	0.37	.42	<0.01	0.48	<0.01	0.47	<0.01

Table 30. Spearman's and partial correlation coefficients between total sub-synovial fibrosis and osteophyte/enthesophyte scores

Table 30	Anterior Total						Posterior Total					
	All				Joint pathology		All				Joint pathology	
	Unadjusted		Adjusted for surgery		Adjusted for surgery		Unadjusted		Adjusted for surgery		Adjusted for surgery	
	ρ	p value	ρ	p value	ρ	p value	ρ	p value	ρ	p value	ρ	p value
Total Scores												
Osteophyte												
Maturity												
Anterior	0.46	<0.01	0.42	<0.01	0.46	<0.01	0.57	<0.01	0.49	<0.01	0.43	<0.01
Posterior	0.07	0.40	0.07	0.41	0.07	0.52	0.13	0.14	0.16	0.06	0.16	0.14
Summed	0.46	<0.01	0.42	<0.01	0.46	<0.01	0.57	<0.01	0.49	<0.01	0.44	<0.01
Size												
Anterior	0.46	<0.01	0.46	<0.01	0.50	<0.01	0.59	<0.01	0.58	<0.01	0.54	<0.01
Posterior	0.07	0.40	0.07	0.41	0.07	0.52	0.13	0.14	0.16	0.06	0.16	0.14

Table 30	Anterior Total						Posterior Total					
	All				Joint pathology		All				Joint pathology	
	Unadjusted		Adjusted for surgery		Adjusted for surgery		Unadjusted		Adjusted for surgery		Adjusted for surgery	
	ρ	p value	ρ	p value	ρ	p value	ρ	p value	ρ	p value	ρ	p value
Summed	0.46	<0.01	0.45	<0.01	0.50	<0.01	0.59	<0.01	0.58	<0.01	0.55	<0.01
Severity												
Anterior	0.46	<0.01	0.40	<0.01	0.43	<0.01	0.58	<0.01	0.49	<0.01	0.44	<0.01
Posterior	0.07	0.40	0.07	0.41	0.07	0.52	0.13	0.14	0.16	0.06	0.16	0.14
Summed	0.46	<0.01	0.40	<0.01	0.43	<0.01	0.58	<0.01	0.49	<0.01	0.44	<0.01
Enthesophyte												
Maturity												
Anterior	0.19	0.02	0.19	0.02	0.17	0.13	0.32	<0.01	0.07	0.39	-0.03	0.76
Posterior	0.47	<0.01	0.46	<0.01	0.52	<0.01	0.75	<0.01	0.65	<0.01	0.61	<0.01
Summed	0.49	<0.01	0.46	<0.01	0.51	<0.01	0.73	<0.01	0.55	<0.01	0.48	<0.01

Table 30	Anterior Total						Posterior Total					
	All				Joint pathology		All				Joint pathology	
	Unadjusted		Adjusted for surgery		Adjusted for surgery		Unadjusted		Adjusted for surgery		Adjusted for surgery	
	ρ	p value	ρ	p value	ρ	p value	ρ	p value	ρ	p value	ρ	p value
Size												
Anterior	0.20	0.02	0.20	0.02	0.19	0.09	0.35	<0.01	0.13	0.13	<0.01	0.98
Posterior	0.46	<0.01	0.50	<0.01	0.57	<0.01	0.75	<0.01	0.72	<0.01	0.71	<0.01
Summed	0.49	<0.01	0.51	<0.01	0.59	<0.01	0.76	<0.01	0.68	<0.01	0.65	<0.01
Severity												
Anterior	0.20	0.02	0.20	0.02	0.18	0.10	0.33	<0.01	0.08	0.36	-0.02	0.87
Posterior	0.47	<0.01	0.46	<0.01	0.51	<0.01	0.74	<0.01	0.64	<0.01	0.61	<0.01
Summed	0.50	<0.01	0.47	<0.01	0.52	<0.01	0.74	<0.01	0.58	<0.01	0.52	<0.01
Maximum Scores												
Osteophyte												

Table 30	Anterior Total						Posterior Total					
	All				Joint pathology		All				Joint pathology	
	Unadjusted		Adjusted for surgery		Adjusted for surgery		Unadjusted		Adjusted for surgery		Adjusted for surgery	
	ρ	p value	ρ	p value	ρ	p value	ρ	p value	ρ	p value	ρ	p value
Maturity												
Anterior	0.45	<0.01	0.41	<0.01	0.44	<0.01	0.55	<0.01	0.45	<0.01	0.39	<0.01
Posterior	0.07	0.40	0.07	0.41	0.07	0.52	0.13	0.14	0.16	0.06	0.16	0.14
Summed	0.45	<0.01	0.41	<0.01	0.44	<0.01	0.56	<0.01	0.47	<0.01	0.41	<0.01
Size												
Anterior	0.46	<0.01	0.46	<0.01	0.51	<0.01	0.60	<0.01	0.58	<0.01	0.54	<0.01
Posterior	0.07	0.40	0.07	0.41	0.07	0.52	0.13	0.14	0.16	0.06	0.16	0.14
Summed	0.46	<0.01	0.45	<0.01	0.50	<0.01	0.59	<0.01	0.59	<0.01	0.55	<0.01
Severity												
Anterior	0.45	<0.01	0.40	<0.01	0.43	<0.01	0.56	<0.01	0.47	<0.01	0.42	<0.01

Table 30	Anterior Total						Posterior Total					
	All				Joint pathology		All				Joint pathology	
	Unadjusted		Adjusted for surgery		Adjusted for surgery		Unadjusted		Adjusted for surgery		Adjusted for surgery	
	ρ	p value	ρ	p value	ρ	p value	ρ	p value	ρ	p value	ρ	p value
Posterior	0.46	<0.01	0.46	<0.01	0.50	<0.01	0.59	<0.01	0.59	<0.01	0.55	<0.01
Summed	0.45	<0.01	0.42	<0.01	0.45	<0.01	0.57	<0.01	0.50	<0.01	0.45	<0.01
Enthesophyte												
Maturity												
Anterior	0.19	0.03	0.21	0.02	0.16	0.15	0.32	<0.01	0.14	0.09	0.03	0.77
Posterior	0.47	<0.01	0.44	<0.01	0.50	<0.01	0.74	<0.01	0.60	<0.01	0.55	<0.01
Summed	0.46	<0.01	0.42	<0.01	0.47	<0.01	0.70	<0.01	0.50	<0.01	0.45	<0.01
Size												
Anterior	0.20	0.02	0.23	0.01	0.20	0.06	0.35	<0.01	0.24	0.01	0.12	0.30
Posterior	0.45	<0.01	0.46	<0.01	0.54	<0.01	0.74	<0.01	0.70	<0.01	0.69	<0.01

Table 30	Anterior Total						Posterior Total					
	All				Joint pathology		All				Joint pathology	
	Unadjusted		Adjusted for surgery		Adjusted for surgery		Unadjusted		Adjusted for surgery		Adjusted for surgery	
	ρ	p value	ρ	p value	ρ	p value	ρ	p value	ρ	p value	ρ	p value
Summed	0.46	<0.01	0.46	<0.01	0.54	<0.01	0.75	<0.01	0.64	<0.01	0.62	<0.01
Severity												
Anterior	0.48	<0.01	0.47	<0.01	0.55	<0.01	0.74	<0.01	0.64	<0.01	0.62	<0.01
Posterior	0.44	<0.01	0.42	<0.01	0.49	<0.01	0.72	<0.01	0.56	<0.01	0.52	<0.01
Summed	0.48	<0.01	0.45	<0.01	0.48	<0.01	0.73	<0.01	0.57	<0.01	0.51	<0.01

Table 31. Spearman's and partial correlation coefficients between maximum sub-synovial fibrosis and osteophyte/enthesophyte scores

Table 31	Anterior Maximum						Posterior Maximum					
	All				Joint pathology		All				Joint pathology	
	Unadjusted		Adjusted for surgery		Adjusted for surgery		Unadjusted		Adjusted for surgery		Adjusted for surgery	
	ρ	p value	ρ	p value	ρ	p value	ρ	p value	ρ	p value	ρ	p value
Total Scores												
Osteophyte												
Maturity												
Anterior	0.37	<0.01	0.32	<0.01	0.33	<0.01	0.51	<0.010	0.51	<0.01	0.47	<0.01
Posterior	-0.01	0.90	<0.01	1.00	-0.02	0.88	0.13	0.14	0.15	0.08	0.15	0.17
Summed	0.37	<0.01	0.32	<0.01	0.32	<0.01	0.51	<0.01	0.51	<0.01	0.47	<0.01
Size												
Anterior	0.37	<0.01	0.32	<0.01	0.32	<0.01	0.53	<0.01	0.54	<0.01	0.51	<0.01
Posterior	-0.01	0.90	<0.01	1.00	-0.02	0.88	0.13	0.14	0.15	0.08	0.15	0.17

Table 31	Anterior Maximum						Posterior Maximum					
	All				Joint pathology		All				Joint pathology	
	Unadjusted		Adjusted for surgery		Adjusted for surgery		Unadjusted		Adjusted for surgery		Adjusted for surgery	
	ρ	p value	ρ	p value	ρ	p value	ρ	p value	ρ	p value	ρ	p value
Summed	0.37	<0.01	0.32	<0.01	0.32	<0.01	0.53	<0.01	0.54	<0.01	0.51	<0.01
Severity												
Anterior	0.37	<0.01	0.28	<0.01	0.28	0.01	0.52	<0.01	0.48	<0.01	0.44	<0.01
Posterior	-0.01	0.90	<0.01	1.00	-0.02	0.88	0.13	0.14	0.15	0.08	0.15	0.17
Summed	0.37	<0.01	0.28	<0.01	0.28	0.01	0.52	<0.01	0.48	<0.01	0.44	<0.01
Enthesophyte												
Maturity												
Anterior	0.13	0.12	0.11	0.20	-0.01	0.96	0.31	<0.01	0.03	0.74	-0.10	0.38
Posterior	0.39	<0.01	0.35	<0.01	0.36	<0.01	0.68	<0.01	0.62	<0.01	0.58	<0.01
Summed	0.41	<0.01	0.33	<0.01	0.29	0.01	0.67	<0.01	0.50	<0.01	0.43	<0.01

Table 31	Anterior Maximum						Posterior Maximum					
	All				Joint pathology		All				Joint pathology	
	Unadjusted		Adjusted for surgery		Adjusted for surgery		Unadjusted		Adjusted for surgery		Adjusted for surgery	
	ρ	p value	ρ	p value	ρ	p value	ρ	p value	ρ	p value	ρ	p value
Size												
Anterior	0.16	0.07	0.12	0.15	0.04	0.74	0.33	<0.01	0.09	0.32	-0.07	0.54
Posterior	0.37	<0.01	0.38	<0.01	0.39	<0.01	0.69	<0.01	0.67	<0.01	0.66	<0.01
Summed	0.40	<0.01	0.37	<0.01	0.37	<0.01	0.71	<0.01	0.62	<0.01	0.58	<0.01
Severity												
Anterior	0.13	0.12	0.10	0.27	0.01	0.91	0.32	<0.01	0.03	0.71	-0.08	0.47
Posterior	0.38	<0.01	0.33	<0.01	0.33	<0.01	0.68	<0.01	0.61	<0.01	0.58	<0.01
Summed	0.41	<0.01	0.32	<0.01	0.29	0.01	0.68	<0.01	0.53	<0.01	0.47	<0.01
Maximum Scores												
Osteophyte												

Table 31	Anterior Maximum						Posterior Maximum					
	All				Joint pathology		All				Joint pathology	
	Unadjusted		Adjusted for surgery		Adjusted for surgery		Unadjusted		Adjusted for surgery		Adjusted for surgery	
	ρ	p value	ρ	p value	ρ	p value	ρ	p value	ρ	p value	ρ	p value
Maturity												
Anterior	0.36	<0.01	0.32	<0.01	0.33	<0.01	0.50	<0.01	0.54	<0.01	0.52	<0.01
Posterior	-0.01	0.90	<0.01	1.00	-0.02	0.88	0.13	0.14	0.15	0.08	0.15	0.17
Summed	0.36	<0.01	0.31	<0.01	0.32	<0.01	0.50	<0.01	0.55	<0.01	0.53	<0.01
Size												
Anterior	0.37	<0.01	0.35	<0.01	0.35	<0.01	0.53	<0.01	0.59	<0.01	0.56	<0.01
Posterior	-0.01	0.90	<0.01	1.00	-0.02	0.88	0.13	0.14	0.15	0.08	0.15	0.17
Summed	0.37	<0.01	0.33	<0.01	0.34	<0.01	0.53	<0.01	0.59	<0.01	0.57	<0.01
Severity												
Anterior	0.36	<0.01	0.30	<0.01	0.30	0.01	0.51	<0.01	0.55	<0.01	0.53	<0.01

Table 31	Anterior Maximum						Posterior Maximum					
	All				Joint pathology		All				Joint pathology	
	Unadjusted		Adjusted for surgery		Adjusted for surgery		Unadjusted		Adjusted for surgery		Adjusted for surgery	
	ρ	p value	ρ	p value	ρ	p value	ρ	p value	ρ	p value	ρ	p value
Posterior	0.37	<0.01	0.34	<0.01	0.35	<0.01	0.53	<0.01	0.59	<0.01	0.57	<0.01
Summed	0.37	<0.01	0.31	<0.01	0.31	<0.01	0.51	<0.01	0.53	<0.01	0.50	<0.01
Enthesophyte												
Maturity												
Anterior	0.13	0.14	0.13	0.14	-0.04	0.70	0.31	<0.01	0.08	0.36	-0.06	0.57
Posterior	0.38	<0.01	0.34	<0.01	0.35	<0.01	0.67	<0.01	0.55	<0.01	0.49	<0.01
Summed	0.38	<0.01	0.31	<0.01	0.25	0.03	0.63	<0.01	0.43	<0.01	0.34	<0.01
Size												
Anterior	0.14	0.10	0.14	0.10	0.02	0.85	0.34	<0.01	0.18	0.04	0.03	0.77
Posterior	0.36	<0.01	0.35	<0.01	0.35	<0.01	0.70	<0.01	0.69	<0.01	0.69	<0.01

Table 31	Anterior Maximum						Posterior Maximum					
	All				Joint pathology		All				Joint pathology	
	Unadjusted		Adjusted for surgery		Adjusted for surgery		Unadjusted		Adjusted for surgery		Adjusted for surgery	
	ρ	p value	ρ	p value	ρ	p value	ρ	p value	ρ	p value	ρ	p value
Summed	0.38	<0.01	0.33	<0.01	0.31	<0.01	0.70	<0.01	0.61	<0.01	0.59	<0.01
Severity												
Anterior	0.39	<0.01	0.35	<0.01	0.33	<0.01	0.68	<0.01	0.60	<0.01	0.57	<0.01
Posterior	0.36	<0.01	0.30	<0.01	0.24	0.03	0.67	<0.01	0.52	<0.01	0.47	<0.01
Summed	0.39	<0.01	0.30	<0.01	0.25	0.02	0.66	<0.01	0.52	<0.01	0.45	<0.01

Table 32. Spearman's and partial correlation coefficients between total sub-synovial fibrosis and meniscus scores

Table 32	Anterior Total						Posterior Total					
	All				Joint pathology		All				Joint pathology	
	Unadjusted		Adjusted for surgery		Adjusted for surgery		Unadjusted		Adjusted for surgery		Adjusted for surgery	
	ρ	p value	ρ	p value	ρ	p value	ρ	p value	ρ	p value	ρ	p value
Total Meniscus Scores												
Tissue Structural damage												
Anterior	0.41	<0.01	0.45	<0.01	0.51	<0.01	0.62	<0.01	0.52	<0.01	0.49	<0.01
Posterior	0.42	<0.01	0.44	<0.01	0.49	<0.01	0.59	<0.01	0.61	<0.01	0.60	<0.01
Summed	0.45	<0.01	0.46	<0.01	0.51	<0.01	0.61	<0.01	0.61	<0.01	0.59	<0.01
Superficial Proteoglycan Loss												
Anterior	0.30	<0.01	0.40	<0.01	0.43	<0.01	0.63	<0.01	0.56	<0.01	0.50	<0.01
Posterior	0.35	<0.01	0.43	<0.01	0.46	<0.01	0.61	<0.01	0.61	<0.01	0.56	<0.01
Summed	0.36	<0.01	0.42	<0.01	0.46	<0.01	0.66	<0.01	0.60	<0.01	0.55	<0.01
Bone Formation												

Table 32	Anterior Total						Posterior Total					
	All				Joint pathology		All				Joint pathology	
	Unadjusted		Adjusted for surgery		Adjusted for surgery		Unadjusted		Adjusted for surgery		Adjusted for surgery	
	ρ	p value	ρ	p value	ρ	p value	ρ	p value	ρ	p value	ρ	p value
Anterior	0.49	<0.01	0.46	<0.01	0.49	<0.01	0.73	<0.01	0.58	<0.01	0.55	<0.01
Posterior	0.46	<0.01	0.44	<0.01	0.48	<0.01	0.73	<0.01	0.60	<0.01	0.54	<0.01
Summed	0.49	<0.01	0.47	<0.01	0.50	<0.01	0.79	<0.01	0.61	<0.01	0.56	<0.01
Summed Meniscal Score	0.44	<0.01	0.48	<0.01	0.53	<0.01	0.74	<0.01	0.64	<0.01	0.61	<0.01
Maximum Meniscus Scores												
Tissue Structural damage												
Anterior	0.42	<0.01	0.48	<0.01	0.53	<0.01	0.61	<0.01	0.56	<0.01	0.51	<0.01
Posterior	0.42	<0.01	0.46	<0.01	0.52	<0.01	0.57	<0.01	0.60	<0.01	0.58	<0.01
Summed	0.45	<0.01	0.49	<0.01	0.55	<0.01	0.60	<0.01	0.60	<0.01	0.58	<0.01
Superficial Proteoglycan Loss												

Table 32	Anterior Total						Posterior Total					
	All				Joint pathology		All				Joint pathology	
	Unadjusted		Adjusted for surgery		Adjusted for surgery		Unadjusted		Adjusted for surgery		Adjusted for surgery	
	ρ	p value	ρ	p value	ρ	p value	ρ	p value	ρ	p value	ρ	p value
Anterior	0.19	0.03	0.17	0.05	0.27	0.01	0.52	<0.01	0.46	<0.01	0.47	<0.01
Posterior	0.32	<0.01	0.37	<0.01	0.43	<0.01	0.60	<0.01	0.61	<0.01	0.61	<0.01
Summed	0.28	<0.01	0.31	<0.01	0.39	<0.01	0.63	<0.01	0.61	<0.01	0.60	<0.01
Bone Formation												
Anterior	0.48	<0.01	0.48	<0.01	0.53	<0.01	0.72	<0.01	0.60	<0.01	0.56	<0.01
Posterior	0.44	<0.01	0.45	<0.01	0.52	<0.01	0.71	<0.01	0.61	<0.01	0.56	<0.01
Summed	0.48	<0.01	0.49	<0.01	0.55	<0.01	0.77	<0.01	0.63	<0.01	0.58	<0.01
Summed Meniscal Score	0.42	<0.01	0.50	<0.01	0.57	<0.01	0.74	<0.01	0.67	<0.01	0.64	<0.01

Table 33. Spearman's and partial correlation coefficients between maximum sub-synovial fibrosis and meniscus scores

Table 33	Anterior Total						Posterior Total					
	All				Joint pathology		All				Joint pathology	
	Unadjusted		Adjusted for surgery		Adjusted for surgery		Unadjusted		Adjusted for surgery		Adjusted for surgery	
	ρ	p value	ρ	p value	ρ	p value	ρ	p value	ρ	p value	ρ	p value
Total Meniscus Scores												
Tissue Structural damage												
Anterior	0.30	<0.01	0.32	<0.01	0.34	<0.01	0.59	<0.01	0.56	<0.01	0.55	<0.01
Posterior	0.29	<0.01	0.28	<0.01	0.27	0.01	0.56	<0.01	0.60	<0.01	0.60	<0.01
Summed	0.31	<0.01	0.30	<0.01	0.30	0.01	0.57	<0.01	0.61	<0.01	0.61	<0.01
Superficial Proteoglycan Loss												
Anterior	0.26	<0.01	0.27	<0.01	0.26	0.02	0.57	<0.01	0.59	<0.01	0.55	<0.01
Posterior	0.32	<0.01	0.31	<0.01	0.29	0.01	0.60	<0.01	0.62	<0.01	0.59	<0.01
Summed	0.32	<0.01	0.30	<0.01	0.28	0.01	0.62	<0.01	0.62	<0.01	0.59	<0.01
Bone Formation												

Table 33	Anterior Total						Posterior Total					
	All				Joint pathology		All				Joint pathology	
	Unadjusted		Adjusted for surgery		Adjusted for surgery		Unadjusted		Adjusted for surgery		Adjusted for surgery	
	ρ	p value	ρ	p value	ρ	p value	ρ	p value	ρ	p value	ρ	p value
Anterior	0.39	<0.01	0.31	<0.01	0.27	0.01	0.69	<0.01	0.57	<0.01	0.56	<0.01
Posterior	0.37	<0.01	0.32	<0.01	0.30	0.01	0.69	<0.01	0.63	<0.01	0.60	<0.01
Summed	0.40	<0.01	0.32	<0.01	0.29	0.01	0.73	<0.01	0.62	<0.01	0.59	<0.01
Summed Meniscal Score	0.36	<0.01	0.32	<0.01	0.31	<0.01	0.69	<0.01	0.65	<0.01	0.63	<0.01
Maximum Meniscus Scores												
Tissue Structural damage												
Anterior	0.31	<0.01	0.38	<0.01	0.41	<0.01	0.58	<0.01	0.57	<0.01	0.55	<0.01
Posterior	0.30	<0.01	0.34	<0.01	0.34	<0.01	0.54	<0.01	0.59	<0.01	0.59	<0.01
Summed	0.32	<0.01	0.37	<0.01	0.39	<0.01	0.57	<0.01	0.61	<0.01	0.60	<0.01
Superficial Proteoglycan Loss												

Table 33	Anterior Total						Posterior Total					
	All				Joint pathology		All				Joint pathology	
	Unadjusted		Adjusted for surgery		Adjusted for surgery		Unadjusted		Adjusted for surgery		Adjusted for surgery	
	ρ	p value	ρ	p value	ρ	p value	ρ	p value	ρ	p value	ρ	p value
Anterior	0.14	0.11	0.12	0.16	0.18	0.11	0.48	<0.01	0.46	<0.01	0.45	<0.01
Posterior	0.27	<0.01	0.28	<0.01	0.28	0.01	0.59	<0.01	0.57	<0.01	0.54	<0.01
Summed	0.22	0.01	0.23	0.01	0.26	0.02	0.60	<0.01	0.59	<0.01	0.55	<0.01
Bone Formation												
Anterior	0.40	<0.01	0.40	<0.01	0.40	<0.01	0.68	<0.01	0.62	<0.01	0.63	<0.01
Posterior	0.36	<0.01	0.35	<0.01	0.36	<0.01	0.66	<0.01	0.59	<0.01	0.55	<0.01
Summed	0.41	<0.01	0.40	<0.01	0.40	<0.01	0.72	<0.01	0.64	<0.01	0.62	<0.01
Summed Meniscal Score	0.33	<0.01	0.38	<0.01	0.40	<0.01	0.69	<0.01	0.67	<0.01	0.65	<0.01

Chapter 6. Osteoarthritis Initiative Analysis

Submitted for publication as:

Urban H, Deveza L, O'Connell R, Little CB, Hunter DJ. Is Hoffa-synovitis associated with centripetal adiposity, systemic markers of synovial inflammation and pain?

Arthritis Care & Research Submitted September 2020

6.1 Abstract

Objective

To investigate the relationship between infrapatellar fat pad (IFP) inflammation (Hoffa-synovitis) and central adiposity (waist-to-height ratio: WHtR) in knee osteoarthritis (OA), and the effect of that interplay on serum biomarkers of synovial inflammation and pain.

Design

We obtained data from all participants of the Foundation for the National Institutes of Health OA Biomarkers Consortium within the Osteoarthritis initiative (n=600). Baseline Hoffa-synovitis measured on non-contrast-enhanced MRIs and scored according to the MRI OA Knee score (MOAKS), serum Hyaluronan (HA) and Matrix Metalloproteinase-3 (MMP3) levels, and Western Ontario and McMaster Universities Osteoarthritis Index (WOMAC) pain data were extracted for this study. We assessed the relationship between Hoffa-synovitis, WHtR, HA, MMP3, and WOMAC pain (overall and ascending stairs) using linear regression and Spearman's correlation, and the effect of the Hoffa-synovitis and WHtR interplay on serum biomarkers or pain using two-way analysis of variance and logistic regression.

Results

Hoffa-synovitis and WHtR were inversely associated: with moderate/severe Hoffa-synovitis (score 2/3) having lower WHtR on average compared to patients with a physiologic Hoffa-synovitis (score 0), even after adjustment for age and sex (β (95% CI): -0.028 (-0.051, -0.005), $P = 0.017$). There was an increasing linear trend in serum HA levels (logged) with higher Hoffa-synovitis severity which remained after adjustment for age and sex (Percentage Change (PC) per unit increase (95% CI) = 11% (2%, 21%), $P = 0.017$). WHtR demonstrated a positive linear relationship with serum HA (logged) which also remained after adjustment for age and sex (PC per 0.10 increase: 12% (4%, 20%), $P = 0.004$). Both Hoffa-synovitis and WHtR were associated with MMP3 in univariate analysis but not after adjustment for age and sex. Hoffa-synovitis was not correlated with pain; however, increased adiposity was associated with increased pain overall and pain going upstairs. There was no interaction effect between Hoffa-synovitis and WHtR on serum biomarkers or pain.

Conclusion

Hoffa-synovitis and centripetal adiposity are inversely associated with each other. However, the lack of effect of the interaction on pain and systemic biomarkers indicate that Hoffa-synovitis and central adiposity act independently in terms of their relationship to OA knee pain and more generalised synovitis. Future studies using more specific measures of IFP inflammation are required to validate our findings.

6.2 Introduction

Adipose tissue is increasingly recognised as an endocrine organ consisting of adipocytes, various immune cell types, and neurovascular tissue[21]. The immune cells in adipose tissue, which include macrophages, T-cells, B-cells and neutrophils, have been implicated in the production of inflammatory mediators, such as adipokines and cytokines, and contribute to a state of low-grade systemic inflammation in obesity[23, 24]. In OA, pre-clinical models have further established the biological role of adiposity by showing that disease severity is associated with levels of inflammation rather than just bodyweight or joint loading in obese mice[39, 43]. Increased levels of adipokines, such as leptin, adiponectin and resistin, have also further supported the role of adipogenic inflammation in the pathogenesis of OA[176].

Studies in knee OA patients have also identified increased adipokine levels in the synovial fluid compared to serum levels which suggest a local driver of adipogenic inflammation in the joint[133, 136]. Both leptin and visfatin are increased in the synovial fluid, with the latter also raised in a local depot of adipose tissue adjacent to the synovium in the knee: the infrapatellar fat pad (IFP)[20, 136]. In obese mice that develop OA, physiological properties such as adipocyte size, volume and vasculature, and levels of inflammatory mediators have been found to be increased within the IFP[45]. In contrast, other studies have suggested that the IFP may be protected from the effects of obesity-associated inflammation, even when OA develops[100].

While the role of obesity in IFP inflammation remains uncertain, a small number of studies have begun to investigate the association between IFP inflammation and joint or OA pain. Consistent with other adipose tissues, the IFP contains nociceptive nerve fibres that produce substance P,

which has been implicated in anterior knee pain[335]. Studies have evaluated this logical construct using a variety of surrogates for IFP inflammation, such as MRI signal intensity or ultrasonographic effusion, and found increased inflammation to be associated with increased pain[106, 189]. However, the few available studies vary significantly in methodologies of evaluating IFP inflammation, pain and statistical methods. Hence, there remains ambiguity in understanding the IFP inflammation and pain relationship.

In addition to the literature gaps outlined above, few studies have investigated the role of systemic adiposity and the IFP. Several studies have found no association between IFP volume and BMI[336, 337]. However, interpreting BMI as a measure of adiposity is inaccurate as it does not account for differences in body composition[338]. BMI is now regarded as a poor predictor of adiposity, with recent studies recommending other methods such as the waist to hip or waist to height ratios (WHtR) which measure centripetal adiposity[339]. In particular, the WHtR was found to have a much stronger correlation to fat mass ($r=0.706$) compared to BMI or waist to hip ratio ($r = -0.003$ and -0.146 , respectively) [340]. WHtR was also found to be a more useful anthropometric tool in metabolic syndrome, cardiovascular health and weight loss compared to other measures[340-342]. To date, there has been no published evaluation of the association between WHtR and the IFP, nor the impact of their interaction on OA-related knee pain.

Our study addresses these gaps by evaluating the association between IFP inflammation and WHtR using the Osteoarthritis Initiative (OAI) database. We used Hoffa-synovitis score from the MRI OA Knee Score (MOAKS) tool as a surrogate measure for IFP inflammation[208]. Additionally, we investigated the relationship between Hoffa-synovitis, WHtR, serum Hyaluronan (HA) and Matrix Metalloproteinase 3 (MMP3) and WOMAC pain (overall and

ascending stairs). Both serum HA and MMP3 are biomarkers indicative of synovial inflammation, and serum HA has also previously been established as a surrogate for systemic inflammation[343-345]. Finally, we investigated the effect of the interplay between Hoffa-synovitis and WHtR on serum HA and MMP3, and WOMAC pain.

6.3 Methods

The Osteoarthritis Initiative (OAI) is a multicentre observational study of 4796 adults between 45 – 79 years of age with or at risk of OA. The OAI study collected various outcomes including clinical assessments, self-reported questionnaires and imaging measures which are publicly available. Our research examined the baseline data of the Foundation of the National Institute of Health (FNIH) Biomarkers Consortium within the broader OAI sample[346].

6.3.1 Study Participants

Briefly, participants of the FNIH Biomarkers consortium had baseline Kellgren/Lawrence (K/L) grade of 1, 2 or 3 on standardised posteroanterior weight bearing x-rays of their index knee, as well as available clinical data, stored biological specimens, and knee imaging measures (x-rays and MRIs) at baseline and 24 months[347]. We evaluated data from all 600 participants of the FNIH Biomarkers Consortium in this study.

Demographic and clinical data were collected and assessed in all participants at baseline. Baseline imaging measures, x-ray and MRI, were obtained at the same time and examined independently by two central readers to determine K/L grade. Additional details regarding imaging acquisitions have been previously described [348].

6.3.2 Semi-quantitative analysis of Hoffa's fat pad/IFP

Non-contrast MRIs were acquired using 3 T systems (Siemens Trio) and a dedicated quadrature transmit/receive knee coil at the four clinical sites of the OAI[349]. As previously described, the protocol included three sequences; 1) coronal intermediate weighted 2-dimensional turbo spin-

echo sequence, 2) sagittal intermediate-weight fat-suppressed turbo spin-echo sequence, and 3) a sagittal 3-dimensional dual-echo steady-state sequence[349].

The acquired MRIs were interpreted by two radiologists with more than thirteen and fifteen years of experience, respectively, who were blinded to clinical data, including case or control status[349]. The images were evaluated using the validated MRI OA Knee Score (MOAKS) to determine the score of various joint structures, including Hoffa-synovitis [207]. Changes in the signal intensity in the intercondylar region of the IFP was scored either 0 (physiological amount), 1 (mild), 2 (moderate) or 3 (severe) (figure 26). While this score is commonly used as a surrogate for chronic synovitis, it is non-specific and can have other causes such as Hoffa's disease[207].

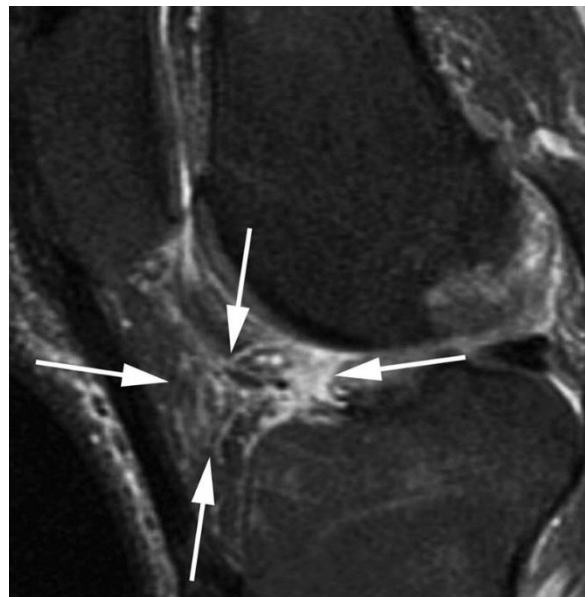


Figure 26. Examples of grade 2 Hoffa-synovitis hyperintense signal changes within the infrapatellar region from Hunter et al. 2011 [207]

6.3.3 Waist to height ratio

The waist to height ratio (WHtR) was determined by dividing the waist circumference by height. Increasing values of the ratio indicated increasing central adiposity, with a prior study identifying 0.59 as the required cut-off score, for both men and women, to predict visceral obesity [339]. The anthropometric measures used were collected at baseline. Height was measured using a calibrated wall-mounted stadiometer without shoes and in light clothing. Waist circumference was measured while the participant was standing upright, on bare skin, using a tape measure.

6.3.4 Pain

We used the Western Ontario and McMaster Universities Osteoarthritis Index (WOMAC) pain subscale to determine overall pain[212]. The subscale consisted of five-items whose combined scores ranged from 0-20, where 20 was extreme pain. We also used the item 'pain going upstairs', which was on a 0-4 scale (4 being the worst pain) as an indicator of anterior knee pain.

6.3.5 Biochemical markers

Morning blood samples were collected after an overnight fast during the relevant study visit, and specimens were delivered to a commercial biobank for storage at -70°C following a standardised protocol[350]. As previously described, enzyme-linked immunosorbent assays (ELISAs) with low inter-plate coefficients of variation (HA – 7.4% and MMP3 – 9.6%) were used to measure the biochemical markers in duplicate[350]. In our study, we evaluated MMP3 and HA as systemic markers of synovial inflammation, and the latter as a surrogate for systemic inflammation[345, 351, 352]. We used an interpolated value from the standard curve extension

of the lowest standard to zero in cases where the concentration of the analyte was below the limit of detection.

6.3.6 Statistical analysis

Linear regression was used to evaluate the relationship between Hoffa-synovitis and WHtR and each with natural log-transformed HA and MMP3. Models were fitted unadjusted and with adjustment for age and sex. For Hoffa-synovitis, deviation from linearity was assessed using orthogonal polynomial contrast coefficients and the variable fitted as a categorical where necessary. Since WHtR is a ratio variable, an alternative set of models was fitted using waist circumference instead with hip circumference included as an adjustment variable as recommended by Kronmal et al. [353]. The pain variables were not normally distributed, and an appropriate transformation was not available. Hence, Spearman's rank-order correlation was used to evaluate the strength and direction of the association between Hoffa-synovitis and WHtR to pain overall as well as pain going upstairs. Correlation coefficients ≤ 0.29 represented weak association; between 0.30 and 0.49 moderate; and ≥ 0.50 strong association[265].

Two-way analysis of variance was used to investigate the interaction between Hoffa-synovitis and WHtR and effect on serum HA and MMP3. Due to non-normality, HA and MMP3 were natural log-transformed, and geometric means and standard error factors presented. Two zero values for MMP3 were imputed as half the value between zero and the next smallest value (0.95/2) to allow inclusion in the log-transformed analysis. Logistic regression was used to assess any interaction between Hoffa-synovitis and WHtR on the outcomes overall pain and pain going up stairs which were dichotomised as no pain (score of 0) vs at least some pain (score of ≥ 1).

For these analyses, we dichotomised WHtR into two groups, healthy and increased adiposity, with a cut off of 0.59 based on the findings of Swainson et al. [339]. By dichotomising the WHtR, we were able to produce results that were more clinically meaningful. In the ANOVA, Hoffa-synovitis was analysed using three groups: normal, mild and 'moderate and severe' (combined due to low numbers in the latter two groups). The interaction effect was evaluated unadjusted for other covariates, and in models adjusted for sex and age. In the absence of interaction, models were subsequently refitted, including only the main effects.

The Cochran-Armitage test was used to test for trend amongst binomial proportions across levels of Hoffa-synovitis.

A nominal significance level of 0.05 was used. We used IBM SPSS statistics software, version 26 for all statistical analyses and GraphPad Prism 8 for figures.

6.4 Results

The demographic and clinical characteristics of the participants are described in Table 34. Participants included in our study were, on average, 61.6 years old and predominantly female with a K/L grade of at least 2. Most participants were 'obese' with a mean BMI of 30.2 kg/m². Consistent with BMI, the mean WHtR was 0.64, and when using a validated cut-off score of 0.59, a high proportion of participants (>70%) had increased centripetal adiposity. Hoffa-synovitis was present in 58.9% of participants. However, only 52 (8.6%) of those participants had moderate to severe Hoffa-synovitis. The remaining 91% of subjects had either no or mild Hoffa-synovitis.

Table 34. Clinical and laboratory characteristics of study participants at baseline

		<i>n</i>
Age, years, mean (SD)	61.6 (8.9)	
Female, n (%)	353 (58.8%)	
Left/Right index knee, n	322 / 278	
KL grade, n (%)		
1	75 (12.5%)	
2	306 (51%)	
3	219 (36.5%)	
Adiposity		
Body mass index, kg/m ² , mean (SD)	30.2 (4.8)	599
Abdominal circumference, cm, mean (SD)	107.3 (12.4)	595

Table 34 continued		
		<i>n</i>
WHtR, mean (SD)	0.64 (0.08)	595
Healthy (<0.59), n (%)	175 (29.4%)	
Increased adiposity (>0.6), n (%)	420 (70.6%)	
Hoffa-synovitis score, n (%)		
Normal (HS = 0)	246 (41%)	
Mild (HS = 1)	302 (50.3%)	
Moderate (HS = 2)	47 (7.8%)	
Severe (HS = 3)	5 (0.8%)	
Serum biomarker, ng/ml, mean (SD)		
HA	47.7 (43.8)	599
MMP3	17.8 (15.3)	599
WOMAC, median (IQR)		
Pain overall (0-20)	1 (0, 4)	600
Pain ascending stairs (0-4)	1 (0, 1)	599

6.4.1 Hoffa-synovitis is associated with WHtR

Hoffa-synovitis was associated with WHtR in that patients with moderate/severe Hoffa-synovitis (score 2/3) had lower WHtR on average compared to patients with a physiologic amount (score 0). This difference remained after adjustment for age and sex (Table 35, Figure 27). In an alternative model predicting waist circumference instead and including adjustment

for hip circumference, the finding was consistent whereby patients with moderate/severe Hoffa-synovitis patients had lower waist circumference.

Table 35. Simple linear regression of waist to height ratio (WHtR) and waist circumference on Hoffa-synovitis (x-variable)

Analysis:	Y = WHtR	β coefficient (95% CI)	p	P (Factor)	R ²
Crude	Hoffa Synovitis:				
	Physiologic amount	Ref		0.002	0.021
	Mild	-0.00004 (-0.014,	0.99		
	Moderate/Severe	0.014)	0.001		
	-0.042 (-0.067, -0.018)				
Adjusted*	Hoffa Synovitis:				
	Physiologic amount	Ref		0.033	0.149
	Mild	0.002 (-0.011, 0.014)	0.82		
	Moderate/Severe	-0.028 (-0.051, -0.005)	0.017		
	Y = Waist (cm)				
Adjusted*	Hoffa Synovitis:				
	Physiologic amount	Ref		0.015	0.033
	Mild	0.198 (-1.884, 2.279)	0.852		
	Moderate/Severe	-5.065 (-8.78, -1.351)	0.008		
	Hip circumference [‡]	1.988 (0.501, 3.476)	0.009		

*Adjusted for age and sex

‡Per 10cm increase

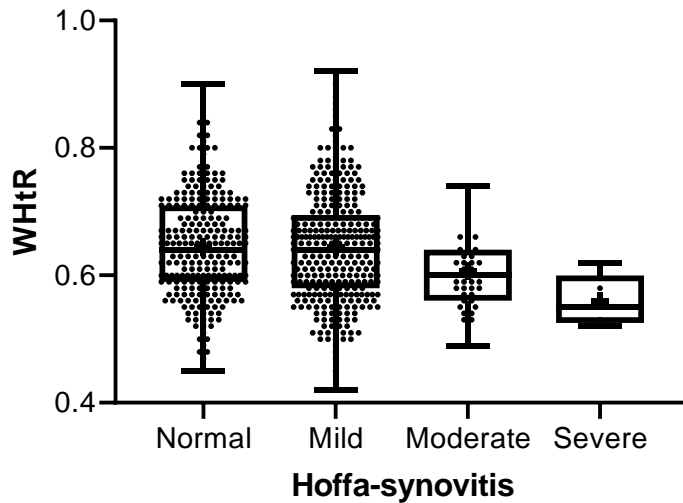


Figure 27. Boxplot of waist to height ratio by Hoffa-synovitis category

6.4.2 Hoffa-synovitis and WHtR associated with HA, MMP3 and pain

Higher severity of Hoffa-synovitis was associated with an increasing linear trend in serum levels of HA and MMP3 (log-transformed) (Table 36, Figure 28); however, after adjustment for age and sex, only the association with HA remained (percentage change (95% CI): 11% (2%, 21%), $p = 0.017$). Similarly, WHtR demonstrated a positive linear relationship with HA and MMP3 (log-transformed), and again after adjustment only the relationship with HA remained (per 0.10 increase: 12% (4%, 20%), $p = 0.004$). These results were consistent in an alternative set of models in which waist circumference was found to be linearly related with HA after adjustment for hip circumference, age and sex (per 10cm increase: 7% (3%, 12%), $p = 0.002$).

No correlation was found between the severity of Hoffa-synovitis and WOMAC overall pain ($r_s = 0.07$, $p = 0.085$) or pain going upstairs ($r_s = 0.03$, $p = 0.41$) (Figure 28). WHtR was positively correlated with overall pain ($r_s = 0.11$, $p = 0.006$) and pain going upstairs ($r_s = 0.24$, $p < 0.001$).

Table 36. Simple linear regression of WHtR and waist circumference on Hoffa-synovitis (x-variable) and their relationship with biomarkers of inflammation.

Analysis:	Y = HA[†]	β coefficient (95% CI)	Percentage Change (95% CI)[§]	p	R²
Crude	Hoffa-synovitis	0.136 (0.04, 0.232)	15% (4%, 26%)	0.006	0.013
Adjusted*	Hoffa-synovitis	0.107 (0.019, 0.194)	11% (2%, 21%)	0.017	0.188
Crude	WHtR (per 0.10)	0.093 (0.017, 0.169)	10% (2%, 18%)	0.016	0.01
Adjusted*	WHtR (per 0.10)	0.109 (0.035, 0.183)	12% (4%, 20%)	0.004	0.189
Crude	Hip circumference [‡]	-0.05 (-0.113, 0.014)	-5% (-11%, 1%)	0.13	0.011
	Waist circumference [‡]	0.055 (0.005, 0.105)	6% (1%, 11%)	0.031	
Adjusted*	Hip circumference [‡]	-0.023 (-0.109, 0.062)	-2% (-10%, 6%)	0.593	0.19
	Waist circumference [‡]	0.071 (0.025, 0.117)	7% (3%, 12%)	0.002	
Analysis:	Y = MMP3[†]	β coefficient (95% CI)	Percentage Change (95% CI)[§]	p	R²
Crude	Hoffa-synovitis	0.125 (0.044, 0.206)	13% (4%, 23%)	0.002	0.015
Adjusted*	Hoffa-synovitis	0.060 (-0.009, 0.129)	6% (-1%, 14%)	0.089	0.296
Crude	WHtR (per 0.10)	-0.136 (-0.199, - 0.072)	-13% (-18%, - 7%)	<0.001	0.029
Adjusted*	WHtR (per 0.10)	0.026 (-0.033, 0.084)	3% (-3%, 9%)	0.389	0.292

Table 36 continued

Crude	Hip circumference [‡]	0.240 (0.189, 0.291)	27% (21%, 34%)	<0.001	0.128
	Waist circumference [‡]	-0.015 (-0.055, 0.025)	-1% (-5%, 3%)	0.47	
Adjusted*	Hip circumference [‡]	-0.023 (-0.090, 0.045)	-2% (-9%, 5%)	0.512	0.293
	Waist circumference [‡]	0.014 (-0.023, 0.05)	1% (-2%, 5%)	0.464	

†Log-transformed

*Adjusted for age and sex

‡Per 10cm increase

§Percentage Change = $100 \times [\exp(\beta) - 1]$

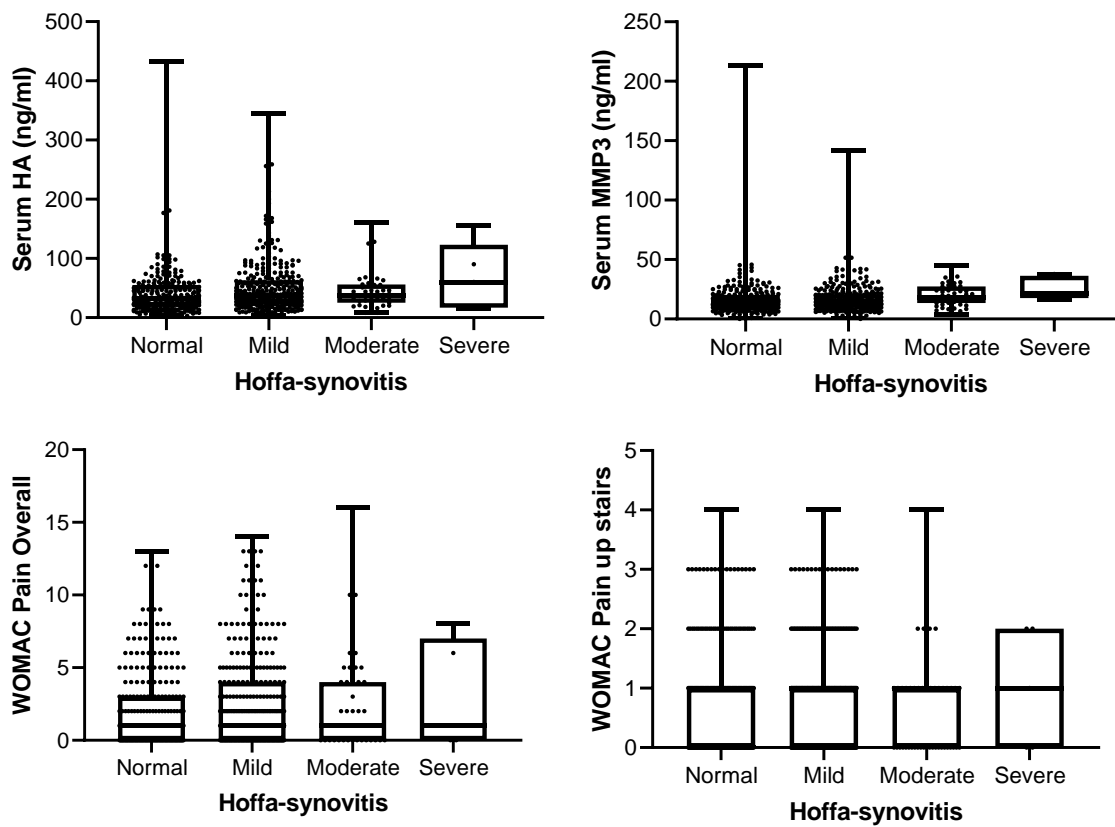


Figure 28. Boxplot of serum HA, serum MMP3, overall WOMAC pain and WOMAC pain going upstairs by Hoffa-synovitis

6.4.3 Assessment of WHtR and Hoffa-synovitis interaction on biomarkers and pain

No significant interaction between the effects of Hoffa-synovitis and WHtR were found for either serum biomarker in unadjusted models or after adjustment for age and sex (Table 37). In subsequent additive models, significant main effects for both Hoffa-synovitis and WHtR on HA and MMP3 were shown with higher severity associated with higher mean biomarker levels, and increased adiposity associated with higher HA but lower MMP3. After adjustment for age and sex, only the main effect for Hoffa-synovitis on serum HA remained significant ($F(2, 588) = 3.4$, $p = 0.034$).

Table 37. Two-way analysis of variance interaction model for the effect of WHtR and Hoffa-synovitis on serum HA and MMP3

WHtR	Hoffa-synovitis	HA†		MMP3†	
		n	Geometric Mean (SE)	n	Geometric Mean (SE)
Healthy	0	63	27.9 (1.1)	63	16.2 (1.08)
	1	88	33.3 (1.09)	88	15.5 (1.07)
	2-3	24	36.3 (1.17)	24	19.4 (1.14)
Increased adiposity	0	178	33.0 (1.06)	178	12.4 (1.05)
	1	213	40.2 (1.05)	213	13.9 (1.05)
	2-3	28	40.5 (1.16)	28	17.8 (1.13)
Unadjusted	Interaction effect	$F(2, 588) = 0.060$, $p = 0.94$		$F(2, 588) = 0.968$, $p = 0.38$	
	Main effect for WHtR	$F(1, 588) = 3.219$, $p = 0.07$		$F(1, 588) = 4.496$, $p = 0.03$	
	Main effect for Hoffa-synovitis	$F(2, 588) = 3.829$, $p = 0.02$		$F(2, 588) = 3.630$, $p = 0.03$	

†Log-transformed

Table 37 continued			
Adjusted for age and sex	Interaction effect	F (2, 586) = 0.023, p = 0.98	F (2, 586) = 0.827 p = 0.44
	Main effect for WHtR	F (1, 586) = 2.099, p = 0.15	F (1, 586) = 0.023, p = 0.88
	Main effect for Hoffa-synovitis	F (2, 586) = 2.663, p = 0.07	F (2, 586) = 1.307, p = 0.27

†Log-transformed

Logistic regression analysis of the outcome "overall pain" did not reveal an interaction effect for Hoffa-synovitis and WHtR, although the test of interaction only just failed to meet significance (p = 0.051). However, there was a significant main effect for WtHR with increased adiposity associated with the presence of any pain (= 1.77, 95% CI: 1.23 – 2.55, p = 0.002). Within the healthy adiposity patients (WHtR < 0.59), there was a significant increasing trend in the proportions with the presence of pain by higher Hoffa-synovitis severity (p = 0.009).

Logistic regression analysis revealed no interaction effect for Hoffa-synovitis and WHtR on the outcome "pain going upstairs" (p = 0.10). However, there was a significant main effect for WtHR with increased adiposity associated with having 84% higher odds of reporting pain going upstairs compared to patients with normal adiposity (odds Ratio = 1.84, 95% CI: 1.28 – 2.64, p = 0.0009). Within the healthy adiposity patients, there was an increasing trend in the proportions with pain going upstairs by higher Hoffa-synovitis severity (p = 0.024). WtHR remained associated with overall pain and pain going upstairs after adjustment for age and sex.

6.5 Discussion

Our study found that increasing Hoffa-synovitis was correlated with lower centripetal adiposity as measured by the WHtR. This association did not change when the relationship was adjusted for age or sex. Increasing Hoffa-synovitis was also weakly correlated to increased serum HA and MMP3 levels but not pain. Additionally, the interaction between Hoffa-synovitis and centripetal adiposity did not impact serum HA and MMP3 levels, nor overall pain or pain going upstairs.

The inverse correlation between Hoffa-synovitis and centripetal obesity was unexpected. While it was statistically significant, the weakness of the relationship may render the finding clinically negligible[265]. The possibility of an insignificant correlation may be supported by a recent publication that suggested no association between adiposity measured on whole-body dual x-ray absorptiometry (DXA) scans and synovitis (including the infrapatellar region)[354]. However, those results were based on a model adjusted for BMI and when unadjusted, visceral adiposity was associated with synovitis[354]. Within the IFP specifically, several pre-clinical studies have demonstrated that obesity-induced by a high-fat diet is associated with increased inflammation with higher levels of cytokines, adipokines and growth factors in the IFP[43, 45, 101]. Similarly, clinical studies have shown the IFP to be impacted by BMI and have increased macrophage infiltration[180, 203, 355]. In contrast, a recent study reported the IFP was protected from adipogenic inflammation in obesity-induced early OA in mice[100]. Additionally, volumetric analyses in patients have also proposed that larger and healthier IFP's are positively associated with increasing BMI[180, 356]. This evidence supports our findings that indicate increasing obesity might have a protective role in maintaining the health of the IFP[356]. A recent clinical study carried out in humans also showed inflammatory characterisations, such as

lymphocyte infiltration or IL-6 immunohistochemical grading, in IFP tissue samples were not correlated with BMI, further supporting our finding[234]. The disconnect between central adiposity and IFP inflammation could also be due to the inflammatory variations between brown (associated with energy expenditure) and white (associated with obesity) adipose tissue which are altered by increasing obesity[29, 31]. Pre-clinical studies have shown that these different adipose deposits have varying responses to obesity-associated inflammation [36]. Additionally, in anorexia nervosa, patients experiencing systemic adipose tissue loss, concurrently experience an increase in bone marrow fat[357]. These variations in adipose type in conjunction with our findings postulate that the IFP may behave more like brown adipose tissue, and this hypothesis needs further study.

Hoffa-synovitis was weakly but positively correlated to the serum biomarkers in our cohort, as previously shown[358]. Both HA and MMP3 are markers of synovial inflammation [343, 344]. The correlation between these variables indicates a potential interaction between inflammation in the IFP and more generalised synovitis in joint regions distant from the IFP. Studies have demonstrated that the factors released from the IFP can promote fibrosis and cellular infiltration of further-removed synovium[115, 179]. Additionally, HA is associated with a systemic marker of inflammation, C-reactive Protein, while MMP3 has been correlated to levels adiponectin[89, 345]. These findings, alongside the correlation found in this study, suggest that the low-grade systemic adipose-derived inflammation may play a role in driving changes within the IFP. However, when we evaluated the impact of Hoffa-synovitis and WHtR on the inflammation biomarkers, we found that the variables acted independently from each other.

This result suggests that while there may be a relationship between the IFP and synovitis, or adipogenic inflammation, it is not affected by centripetal adiposity.

We found no correlation between Hoffa-synovitis and overall pain or pain going upstairs. Our findings are supported by a body of evidence that suggests that IFP inflammation is not associated with pain. In particular, studies by Radojic et al. and Petersen et al. using very similar measures to our study found no associations between pain and IFP inflammation[197, 198]. Additionally, a tissue-based study in humans, as opposed to the imaging studies mentioned, also showed no association between the number of immune cells such as T-cells, macrophages or mast cells in the IFP and pain [118]. However, these findings were in contrast to two previous studies which found significant correlations between increasing Hoffa-synovitis score (MOAKS) and increasing pain (Spearman's Correlation = 0.42 and 0.31)[106, 190]. While using similar measures to our analyses, these studies had much smaller sample sizes (n = 95 and 113). Another critical difference in the study from Ballegaard et al. was their use of contrast-enhanced MRI, which was not the case in the OAI cohort[106]. Contrast-enhanced MRIs identify synovitis with higher specificity and may explain the discrepancy in the findings[359, 360].

Centripetal adiposity measured by WHtR was correlated to pain. There was no interaction between Hoffa-synovitis and WHtR and the effect on pain, indicating that the variables were acting independently in that relationship to pain. Thus despite adiposity impacting OA knee pain as previously shown, we found no evidence that centripetal adiposity engages with IFP inflammation to worsen pain[361, 362].

Our study has several strengths that include a large sample as well as the use of a more appropriate measure of adiposity as opposed to the conventional method of BMI. However,

there are some limitations, as well. Despite having a sample size of 600, less than 10% had moderate or severe Hoffa-synovitis. To overcome this challenge, we modified our analyses by grouping the higher severity groups and hence reduced the sensitivity of our analysis. Furthermore, the original biomarkers component of the OAI is a case-control study, and thus there are inherent biases in the participant selection that may influence our results. The use of non-contrast MRI is also not ideal, given the findings that contrast-enhanced MRIs are superior in identifying synovitis[360]. Finally, the investigation of serum biomarkers posed several limitations. We were unable to exclude the possibility of other contributing sources to inflammatory changes such as hip or spine OA given the systemic nature of the sample. The biomarkers analysed, as part of the OAI, also did not include any adipogenic inflammatory mediators. Hence, we were unable to directly investigate the relationship between adipose-derived systemic inflammation and IFP inflammation.

6.6 Conclusion

Our finding indicates that there is a weak and negative correlation between Hoffa-synovitis and centripetal adiposity. Hoffa-synovitis was also weakly correlated to serum HA and MMP3. Most importantly, our study found no relationship between Hoffa-synovitis and pain in this large cohort. The interaction between IFP inflammation and adiposity also did not affect changes in serum markers of synovial inflammation and pain. Taken together, these findings indicate that Hoffa-synovitis and central adiposity act independently in terms of their relationship to OA knee pain and more generalised synovitis. Future studies using different and more accurate measures of IFP inflammation, such as contrast-enhanced MRIs and IFP tissue analysis, are required to validate our findings.

Chapter 7. Protocol for a Clinical Study

Inflammation of the infrapatellar fat pad and clinical outcomes in knee osteoarthritis (The INTERLOCK Study): protocol and process evaluation

This protocol was submitted to the Northern Sydney Local Health District Human Research Ethics Committee (RESP/17/221), received ethical approval on the 22nd of November 2017 and governance approval on the 7th of August 2018. This study was initially intended to make up the majority of this doctoral thesis. However, this was not possible due to challenges in recruitment. Thus, the study is presented as a protocol with preliminary feasibility findings.

7.1 Abstract

Background

The previous chapters of this thesis have highlighted that there is insufficient research to clarify the molecular and clinical role of the infrapatellar fat pad (IFP) in knee osteoarthritis (OA). This final chapter describes a prospective study protocol to address this deficiency and assesses the feasibility of the proposed INTERLOCK study. This study aims to investigate the relationship between cellular and molecular inflammation in the IFP, and clinical outcomes, such as disability and pain (physical and self-reported measures), in patients with end-stage knee osteoarthritis

Methods

The INTERLOCK Study is a cross-sectional trial carried out at a single site. Participants will attend a single study visit before total knee arthroplasty, where tissue samples will be collected. During the study visit, participants will complete a variety of self-reported questionnaires, physical measures and imaging tests that will evaluate pain, function and disability. The tissues obtained during surgery, including the IFP, will be subjected to a variety of analyses to assess the inflammatory status. The study will correlate these measures to establish the role of the IFP in knee OA. The primary feasibility measure evaluated in this chapter is the recruitment rate which aims to include at least 1 participant per week on average.

Findings

A total of 9 patients who had an INTERLOCK study surgeon listed as their admitting physician and visited the surgical pre-admission clinic at the Royal North Shore Hospital were eligible for screening. Of the nine patients, four agreed to participate and were more likely to be female, and on average, 64 years of age, and body mass index (BMI) of 29.75 kg/m². The recruitment rate of this study was 0.13 participants per week. This rate was much lower than anticipated (1 patient/per week) and, thus, recruitment was concluded after 30 weeks.

Conclusion

The INTERLOCK study aimed to reconcile clinical and laboratory findings to increase the understanding of how the biological state of the IFP impacts the surrounding tissues and relates to the disease experience of people with knee OA. The protocol also intended to evaluate multiple aspects of the disease, such as pain and disability against various conventional methods used to assess inflammation in the fat pad to connect research to the clinical experience. While the recruitment rate of this study was inadequate, the few participants

recruited allowed testing of the methodology, which was deemed feasible. However, significant strides to the recruitment strategy will need to be made to achieve the required sample size.

7.2 Introduction

Osteoarthritis (OA) is a highly prevalent disease that is estimated to affect one in every eight adults and is a leading cause of chronic pain [1, 2, 363]. The inflammatory role of adipose tissue and involvement of adipose associated inflammation in OA coupled with the synovial adjacent location of the infrapatellar fat pad (IFP) has been of great interest to the OA research community in recent years[364]. However, as seen in chapter 2, there are very few published studies that evaluate IFP inflammation and clinical manifestations of the disease.

Research in recent years has investigated the structural and inflammatory properties of the IFP alongside the signs and symptoms of OA. The various studies utilised multiple techniques, such as imaging and cellular/molecular tissue analysis, to IFP inflammation. As mentioned in Chapter 2, the variations between the techniques, lack of validity and understanding of the comparability of the different methods make it challenging to reconcile the literature. Those studies, despite the methodological variations, showed that IFP inflammation and size identified by MRI is linked to increases in clinical symptoms such as pain[365-367]. However, this research in this thesis showed contradictory evidence. Chapter 2 showed that Hoffa-synovitis in a small meta-analysis was positively correlated to pain (correlation = 0.25, 95% CI 0.1471, 0.3462) (p-value <0.0001). However, when using the much larger nested case-control population of 600 participants in the FNIH OAI biomarkers consortium (Chapter 5), no correlation was found between Hoffa-synovitis severity and WOMAC overall pain ($r_s = 0.07$, $p = 0.085$). This discrepancy identified the need for further study to clarify the relationship.

Prior investigations on a cellular level of the IFP also indicated, similar to surrounding synovial tissues, an increase of inflammatory cell types and markers [368-371]. However, there is still a

disconnect in the current understanding mechanisms that connect the IFP, synovium and clinical outcomes. Chapter 4 demonstrated that adiposity of the IFP was inversely correlated to synovitis and sub-synovial fibrosis – indicated that less healthy fat pads (with smaller adipocytes) were associated with more severe OA pathology. This work was done in a preclinical model investigating PTOA as a result of ACL injury and requires further study in a human population.

While previous research, published and of this thesis, have implicated inflammation in the IFP in OA pathophysiology and symptoms, the detailed cellular and molecular mechanisms involved still lack clarity in human populations. Furthermore, the association between inflammation in the IFP and other synovial tissues, as well as how these relate to clinical symptoms in patients is not well-defined.

This chapter aims to describe the protocol and assess the feasibility of the proposed INTERLOCK study. The proposed research seeks to address the gaps in the literature mentioned above by investigating cellular and molecular inflammation in the IFP in relation to clinical outcomes such as disability and pain (physical and self-reported measures) in patients with end-stage knee osteoarthritis. This project also aims to define the relationship between the localised inflammation of the IFP measured by clinically relevant imaging methods with that determined directly in the IFP tissues ex-vivo and in-vitro using multiple outcome measures.

7.3 Methods

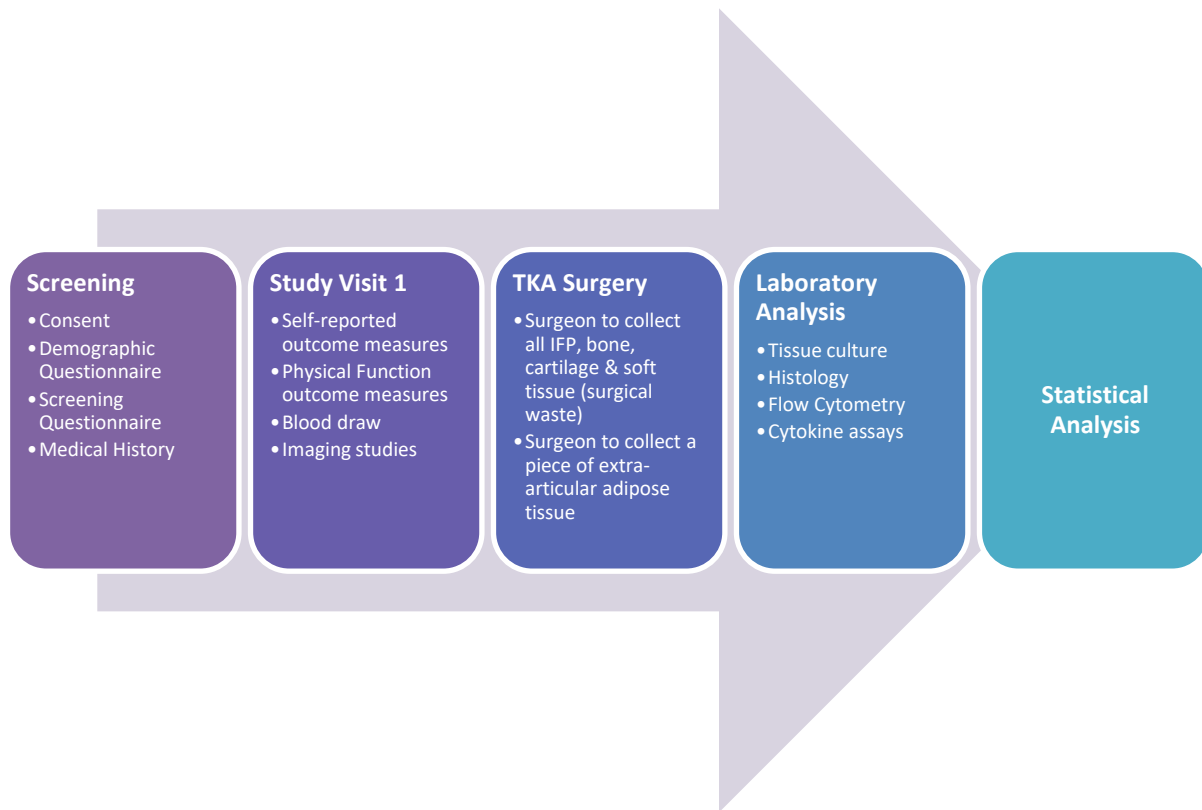


Figure 29. Overview of the INTERLOCK study design

7.3.1 Study design

The INTERLOCK study is a single-centre cross-sectional investigation of the relationship between cellular, molecular and imaging measures of inflammation of the IFP and clinical outcomes of the knee that include, pain and function (Figure 29). The study consists of a single study visit before total knee arthroplasty for participants. Tissues collect during surgery are then subjected to a series of experimental analyses to characterise the IFP alongside other tissues. Clinical outcomes obtained during the study visit and will be related to the findings of the laboratory experiments.

The INTERLOCK study protocol, all study documents and subsequent amendments have approval from the Northern Sydney Local Health District Human Ethics and Governance Committee (HREC/17/HAWKE/297).

Primary Objective

To investigate tissue inflammation (IL-1 β and IL-6 as measured by Multiplex cytokine assay in pg/ml) in the IFP compared to the pain in end-stage knee OA patients scheduled for total knee replacement (TKA).

Secondary Objectives

- 1) To investigate the relationship between inflammation in the IFP and physical function
- 2) To investigate the relationship between inflammation in the IFP identified by ex-vivo methods and inflammation in the IFP detected by ultrasound
- 3) To compare inflammation identified by histological grading versus ultrasound imaging of the synovium
- 4) To investigate the relationship between inflammation in the IFP to subcutaneous adipose tissue and systemic inflammation
- 5) To investigate the effects of IFP inflammation on the inflammation of the synovium

7.3.2 Participants

We aim to recruit 52 participants from the pool of patients visiting the Royal North Shore Hospital surgical pre-admission clinic before scheduled total knee arthroplasty. Eligible participants will meet the following criteria:

- Knee osteoarthritis as diagnosed according to the American College of Rheumatology Criteria [372]
- Scheduled for total knee arthroplasty with a surgeon involved in the trial
- Able to complete questionnaires in English
- Willing to provide written consent to participate in the study
- Willing to complete study assessments
- Willing to stop anti-inflammatory medications for one week before study visit and surgery

The exclusion criteria included any of the following:

- Autoimmune rheumatic diseases
- Contraindications for any study measure
- Women lactating, pregnant or of childbearing potential who are not willing to avoid pregnancy during the study

7.3.3 Screening

Before the screening session, potential participants will be provided with an information sheet to contemplate their involvement in the study. The patients are encouraged to ask any questions and discuss with family members before providing written consent. During the

screening process, participants will be assessed based on the inclusion and exclusion criteria of the study, and basic demographic and medical history data will be collected.

7.3.4 Study visit 1

Study visit one will occur within a two-week window before the scheduled TKA. The visit will collect clinical outcome measures to evaluate against the laboratory findings of the joint tissues. The assessments include self-reported measures, physical function measures and clinical measures as described in Table 38.

Table 38. Clinical outcomes collected at study visit 1

Instrument	Description
Self-Reported	
Knee injury and osteoarthritis outcome score (KOOS)	The KOOS is a validated questionnaire used to assess patient-reported outcomes about their knee OA and associated difficulties[373]. The KOOS is patient-administered and includes five subscales: pain, symptoms, function in daily living, function in sport and recreation and knee-related quality of life. A visual analogue scale will also evaluate pain.

Table 38 continued

Instrument	Description
Self-Reported	
Photographic knee pain map (PKPM)	The PKPM is a validated instrument used to determine the location of pain and has been subsequently used in an Australian OA population [374, 375]. Participants will mark the areas of their pain directly onto a photographic representation over which a transparency template with distinct knee regions will be placed.
Modified PainDETECT (mPD-Q)	The mPD-Q is a self-reported instrument used to distinguish neuropathic pain and is based on a validated low back pain questionnaire [376, 377]. The modification involved changes to specify the questions towards an OA population. The mPD-Q has been validated in an OA population with chronic knee pain and assesses pain quality, pattern, and radiation [376].
Depression, Anxiety and Stress Scale 21 (DASS21)	The DASS is a quantitative measure of distress that evaluates depression, anxiety and stress. DASS21 is a validated and shorter version of the tool [378].

Table 38 continued

Instrument	Description
Physical function	
30 Second chair stand test (30s-CST)	This test assesses lower body strength and dynamic balance by having the participant move from a sit to stand position as many times as possible within 30 seconds. This test is a reliable measure in participants awaiting joint replacements and is suitable for the cohort of this study [379].
Quadriceps Strength Measure	The quadriceps strength measure aids to identify a functional impairment and has been previously strongly associated with knee pain[380]. For this study, quadriceps strength is measured using a digital force gauge attached to a fixed chair. Participants will be seated with hips and knees flexed to a 90° angle and have their pelvis secured using a belt. A padded cuff with a digital force gauge will be attached above their ankle. Participants will be asked to push against the lever as hard as they can manage and will be requested to complete the measure three times for 10 seconds with a 30-second interval in between[380].

Table 38 continued

Instrument	Description
Physical function	
40 Meter Fast Paced Walk Test (40m FPWT)	This test involves a patient walking at a fast pace for 4 X 10m to achieve as quick a time as possible. It is a direct measure of a patient ability to walk quickly over short distances as well as their ability to change basic body position while moving [381].
Knee range of motion (ROM)	Knee ROM will be measured by a trained researcher using a handheld goniometer while patients are in the supine position. Knee flexion, how far a patient can bend their knee within their ability, and extension, how far a patient can flatten their knee against the bed within their ability, will be measured.
Pressure Pain Threshold (PPT)	The PPT is used to measure pain reactions from patients and has been used in several OA populations [382-384]. The PPT will be carried at two sites (1 local and one remote) while patients are in the supine position. It will be performed three times at each location with a 15-second interval use a handheld algometer. The algometer will be placed perpendicular to the skin surface, and pressure will

Table 38 continued

Instrument	Description
Physical function	
	<p>be applied slowly and evenly. The participant will indicate verbally when the pressure becomes painful, and the algometer will be removed from the skin [384]. The local site for this test will be the distal patellar pole in the affected joint, and the remote location will be the non-dominant forearm. Reliability will be confirmed by comparison to a researcher with experience.</p>
Clinical	
Adiposity	<p>Adiposity will be calculated using body mass index (BMI) and waist to height ratio, which is the recommended anthropometric measure[340].</p> <p>BMI will be calculated with the standard formulae using height and weight (in meters and kilograms)</p> <p>Waist to height ratio will be measured with a standard measuring tape in centimetres for waist circumference.</p>
Ultrasound	<p>An ultrasound machine with a high-frequency probe will be used by a trained doctor to scan the synovial recesses of</p>

Table 38 continued	
Instrument	Description
Clinical	
	the knee joint to grade the degree of synovial inflammation in terms of synovial hypertrophy, Doppler signal, effusion and other findings[385]. The longitudinal and transverse planes will be utilised as required.
Serum collection	A trained phlebotomist will collect blood in a 10ml serum vacutainer tube (Becton Dickinson, New Jersey, USA). Blood will be centrifuged within 2 hours of collection for 10 minutes at 1,000 – 2,000 X g using a refrigerated centrifuge. The serum is then stored at -80°C in 200µl aliquots.

7.3.5 Surgery

Surgeons conducting the TKA will provide all IFP, bone, cartilage and soft tissue removed in the procedure as well as a 5mm² piece of subcutaneous adipose tissue from the superior section of the surgical incision in the thigh. Apart from the biopsy of subcutaneous fat, removal of all other samples is a part of routine clinical care.

7.3.6 Tissue processing

Cartilage and bone

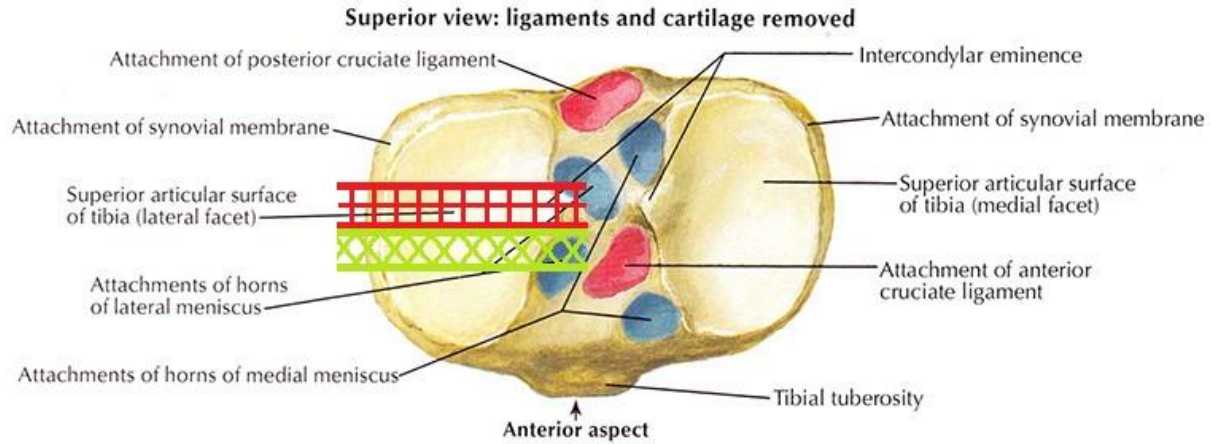


Figure 30. Tissue collection of cartilage on the tibial plateau.

The red section demarcates tissue to be frozen in liquid nitrogen while the red segment will be preserved for histology analysis

Two parts will be removed from the lateral tibial plateau (as the most well-preserved region of the joint; medial plateau usually has little or no cartilage for evaluation) (Figure 30) using established protocols[386, 387]. These samples will be processed as below, but the analysis does not form part of the current proposal. These samples could be used in future research to evaluate the association between IFP inflammation outcomes obtained from the present study and osteochondral pathology and cartilage gene expression.

- a) The cartilage from the red section will be frozen in liquid nitrogen and stored in -80°C .
- b) An osteochondral slab (the green section) will be fixed for immunohistochemistry (IHC) in 10% neutral buffered formalin (NBF), decalcified in 5% formic acid, and embedded in paraffin.

Lateral Meniscus



Figure 31. Tissue collection of the lateral meniscus.

The red section demarcates tissue to be frozen in liquid nitrogen while the red segment will be preserved for histology analysis

Two sections will also be removed from the lateral meniscus (where this is available), and as with the cartilage, analysis of the meniscus is not part of this study (Figure 31). These samples could be used in future research to evaluate the association between IFP inflammation outcomes obtained from the current study and meniscal pathology and gene expression.

- a) The red section will snap-frozen in liquid nitrogen and then stored in -80°C.
- b) The green section will be fixed for IHC in 10% neutral buffered formalin (NBF), decalcified in 5% formic acid, and embedded in paraffin[304, 363, 388].

Synovium

The abundance of synovial tissue can vary depending on the approach of surgery. Thus, to maintain consistency between samples, synovium attached to the supratrochlear fat will be used.

A 1cm² piece of tissue will be obtained and divided into three segments.

- a) One piece of tissue will be diced into smaller pieces and incubated with 2ml of sterile serum-free media (Dulbecco's Modified Eagle Medium with Insulin-Transferrin-Selenium) for 72 hours. Following termination of culture, the cultured tissue will be frozen in liquid nitrogen and then stored in -80°C for subsequent gene expression analysis by polymerase chain reaction (PCR). The conditioned medium containing the synovial secretome will be centrifuged at 1000 -2000 g for 10 minutes to particulate matter, and the resulting supernatant will be frozen at -80°C in 200µl aliquots.
- b) Snap frozen in liquid nitrogen and then stored in -80°C for subsequent PCR analysis – representing the expression profile present in vivo at the time of TKA.
- c) Fixed in 10% NBF and paraffin-embedded for histology and IHC.

IFP

The IFP will be divided into four segments and processed identically to synovium (above).

The additional piece of IFP will be processed fresh for fluorescence-activated cell sorting (FACS) analysis of inflammatory cell infiltrate. One gram of finely minced IFP will be digested in 5 units of Liberase (Sigma Aldrich, St Louis, USA) for 2 hours at 37°C on a shaker set to 220RPM. The digestion will be stopped with 5mls of digestion stop buffer (RPMI 1640 and 10% Fetal Calf Serum), filtered through a 30µm cell strainer and then centrifuged at 500g for 10 min. The resulting cell pellet will be resuspended in 3ml of phosphate-buffered saline for FACS analysis.

Subcutaneous fat

Due to the scarcity of subcutaneous adipose tissue (ScAT) and that harvesting this tissue is not part of the normal standard of care, a single piece, measuring 5mm² will be snap-frozen in liquid nitrogen and stored in -80°C for subsequent PCR analysis to represent the expression profile present in vivo at the time of surgery.

7.3.7 Laboratory analysis

Multiplex Cytokine assay

The Bio-Rad Bioplex Multiplex Cytokine assay will be used to analyse outcomes from the secretome of the synovium and the IFP, as well as serum.

The Bio-Plex Human Chemokine Panel Assay (Catalogue number: #M5000031YV, Bio-Rad Laboratories, California, USA) includes key molecules including IL-1 β , IL-6, MCP-1 and TNF α . The use of this panel will identify the following 17 chemokines with a relatively small quantity of sample:

- Granulocyte colony-stimulating factor (G-CSF)
- Granulocyte-macrophage colony-stimulating factor (GM-CSF)
- Interferon Gamma (IFN γ)
- IL-1 β
- IL-2
- IL-4
- IL-8
- IL-10
- IL-12
- IL-13
- IL-17
- Monocyte chemoattractant protein-1 (MCP-1)

- IL-5
- IL-6
- IL-7
- Macrophage Inflammatory Proteins 1 β (MIP-1 β)
- TNF α

Additionally, adiponectin and leptin will be separately assessed as adipose inflammation markers using real-time polymerase chain reaction (RT-PCR).

Fluorescence-activated cell sorting (FACS)

Using FACS analysis, we will quantify monocytes, macrophages (M1, M2,) and lymphocytes in IFP tissues to help characterise inflammatory cell populations. Antibodies for the surface staining of cells were selected based on existing evidence, and cells will be stained in two panels: 1) Monocyte and Macrophages, and 2) T Lymphocytes (Table 39).

Table 39. FACS analysis antibody selection

Panel 1	Markers
Monocyte (CD14+, CD3-)	CD3-, CD14+[389-391]
Classically activated monocytes	CD14++ CD16- [392-394]
Non-classically monocytes	CD14+CD16++ [392-394]
Intermediate monocytes	CD14++CD16+ [392-394]
Macrophage	Gated on forward scatter and side scatter

Table 39 continued	
Panel 1	Markers
Macrophage – M1	CD68, CCR2[395-397]
Macrophage – M2	CX3CR1(+)/CD163(+)/CD206[395-397]
Panel 2	Markers
T Lymphocyte (CD3+)	CD3+[398-400]
Immature/naive T cells	CD4+/CD8+[399-401]
Innate/Cytotoxic T cell	CD8+ [399-401]
Adaptive/Helper T cell	CD4+[399-401]
Th1	CXCR3[402-404]
Th2	CCR4[402-404]
Th17	CCR6[405-407]
Tregs	CD25[408-410]

Incubations will be carried out for 30 minutes at 4°C [118]. Cells will be detected with fluorophore-conjugated monoclonal antibodies to cell-surface markers versus isotype controls. After collecting a total of 10⁵ events on a fourteen-colour FACS Fortessa flow cytometer (Becton

Dickinson, San Jose, CA), cell population analysis will be performed with FlowJo software (Treestar, Ashland, OR).

Histology and Immunohistochemistry

Paraffin-embedded samples will be sectioned and stained with haematoxylin and eosin, and with antibodies to investigate the presence and immuno-localisation of inflammatory cell types including activated macrophages, CD4 (Th1 Th2 Th17 and T-reg) and CD8 lymphocytes.

The sections of synovium will also be graded for synovitis using the method described by Krenn et al. [411]. This method will consider hyperplasia of the synovial lining, synovial stroma activation and inflammatory infiltration on a 0-3 scale for each feature.

7.3.8 Statistical Methods

Sample Size Estimation

As there is no data for the correlation of IFP cytokine inflammation compared to levels of pain, MRI inflammation of the IFP is used as a proxy for sample size calculation. Ballegaard et al. showed an $r=0.4$ correlation between MRI inflammation and pain as measured by the KOOS pain subscale [106]. Accordingly, using a Fisher's z test for a correlation of 0.4, alpha of 0.05, power of 0.8 and delta of 0.4, we will require 47 participants. To account for any issues with tissue collection and analysis, we will recruit an additional 10%. Hence, we aim to recruit 52 participants, of which the evaluation of the first 30 will be a pilot of the study design.

Statistical Analysis Plan

All statistical analyses for this study will be performed using the latest available version of SPSS for Windows (SPSS Inc., Chicago, IL, USA).

Baseline demographics and characteristics will be summarised using descriptive statistics such as the number of observations (percentages), or mean (standard deviation), median (interquartile ranges) where appropriate.

The primary outcome measure will be assessed based on the distribution of outcomes. If data is normally distributed, the correlation will be evaluated using Pearson's correlation, and if the data is not normally distributed, the correlation will be assessed using Spearman's correlation. The nature of the relationship between the biomarkers and pain will be evaluated using linear regression. Histograms of the residuals will also be used to determine if the distributions are normal. This plan will also be used where appropriate in the study when analysing the relationship between other continuous variables.

In objectives that examine continuous and categorical variables, an analysis of variance will be used at the first instance to examine mean scores of the continuous variables according to the various categories. The strength of the association will be further investigated using ordinal logistic regression to explore the nature of the relationship. All analyses will be appropriately corrected for multiple testing, given the high number of evaluations to be carried out.

Statistical significance will be deemed if $\alpha < 0.05$.

Feasibility

The pilot phase of this study investigates the feasibility of the study design, and the collected data will not be used for hypothesis testing and inferential analysis.

The primary feasibility measure is the recruitment rate: the objective being at least 1 participant recruited per week on average. At three months, recruitment will be assessed, and

if rates are not met, the protocol will be modified to improve recruitment with further assessment 30 weeks after study initiation. At this stage, if a target of 30 patients recruited is not met, the study will be deemed not feasible and be closed. Otherwise, the main study will be conducted until the final sample size is achieved.

Additionally, secondary feasibility measures will assess if the length of time for the clinical visit and sample processing are suitable (less than 3 and 6 hours respectively). If the sessions are longer, then further amendments will be made to the protocol to reduce the time burden on participants and research personnel fatigue.

7.4 Preliminary Findings – study feasibility

7.4.1 Participants

The INTERLOCK study was carried out at the Royal North Shore Hospital (RNSH), Australia, with three participating surgeons as part of the study team. Recruitment of subjects began in February 2019 with one surgeon for three months. After which two additional surgeons were included for the remainder of the recruitment period that concluded in October 2019.

A total of 9 patients who visited the surgical pre-admission clinic at RNSH and had a study surgeon listed as their admitting physician were eligible for screening. Of these patients, three were not screened (2 - communication barriers, and 1- unwilling to participate due to travel concerns) and two were not eligible (1 – unwilling to attend study visit, 1 – active cancer treatment).

The remaining four patients agreed to participate. These patients were more likely to be female, and on average, 64 years of age, and a BMI of 29.8 kg/m²(Table 40).

Table 40. Demographics

	Total Screened (n=6)	Eligible (n=4)
Age (mean (SD))	71.3 (16.0)	64 (14.5)
Gender (female (%))	4 (66.7%)	3 (75%)
Affected Joint (Left/Right/Both)	1/2/2*	1/1/2
BMI (kg/m ²) (mean (SD))		29.8 (5.5)

* Missing data from one participant

7.4.2 Feasibility outcomes

The recruitment rate of this study was 0.13 participants per week. This rate was much lower than anticipated (1 patient/per week), and thus, recruitment was concluded after 30 weeks.

All study visits of the recruited participants were completed within 90 minutes, and samples processing within four hours. Hence, despite the unfeasible recruitment of participants, the secondary feasibility measures were successful.

7.4.3 Data and sample collection

Of the four participants, only 2 completed, both, the study visits and surgery/tissue collection. Surgery for the remaining two patients was postponed several times and had not occurred by the close of the study. Hence, we were unable to collect joint tissues. Measures obtained from each participant are detailed in table 41. Of the tissue samples collected, the volume of samples was sufficient for the experimental methods that were planned.

Table 41. Study milestones achieved by recruited patients

	Questionnaires	Physical Measures	Serum	Ultrasound	Tissue collection
Patient A	✓	✓#	✓	✓	✓*
Patient B	✓	✓	✓	‡	✓
Patient C	✓	✓	✓	✓	&
Patient D	✓	✓	✓	‡	&

- No quadricep strength measure due to faulty reader

* - No IFP collected due to removal at prior surgery

‡ - No ultrasound as the physician was unable

& - Surgery delayed and not completed before study closure

7.5 Discussion

Inflammation in the IFP has been increasingly investigated in knee OA in basic and clinical science. However, the role of IFP inflammation and its relationship to clinical outcomes has remained unclear. Studies have proposed, both, a pro- and anti-inflammatory role of the IFP, and while some studies have indicated a correlation of imaging surrogates to represent IFP inflammation and pain, only one has evaluated IFP tissue inflammation with pain[43, 100, 118]. Even fewer studies have assessed the role of the IFP in the other clinical manifestations of OA, such as physical function[139]. The lack of consensus about the role of IFP, absence of studies validating the use of imaging surrogates and insufficient evaluations against the clinical presentation of OA highlighted the need for a study that evaluated the IFP more comprehensively.

The INTERLOCK study aimed to address these gaps in the literature, and this chapter details the protocol along with the preliminary feasibility findings. The study identified IFP inflammation, through various measures, and related it to clinical outcomes which assessed pain, function and disability in patients with end-stage knee OA. The wide variety of outcome measures used would allow 1) the validity of imaging measures as surrogates of tissue inflammation to be established, 2) further clarify the mechanisms of IFP inflammation and 3) evaluate the associations between the inflammatory and clinical outcomes. The preliminary findings showed great success in methodological execution up to the stage of sample processing. However, the recruitment strategies were not successful, and hence, the study was unfeasible.

Using samples from the few patients that were recruited, the protocols for tissue processing were pilot tested and established. The tissue processing was divided into four main categories;

1) frozen in liquid nitrogen, 2) fixed in 10% NBF, 3) incubated with media, or 4) tissue digestion. All these methods, barring tissue digestion, were carried out using established protocols within the research group. However, due to the size and type of tissue, the tissue digestion required some further methodological refinement. Published protocols varied in the recommendations for adipose tissue digestion with durational differences (15 minutes to 2 hours) and the speed of agitation (15 rpm up to 250 rpm)[412-415]. Based on those previous studies, different combinations of time, speed and volume of digestion buffer were evaluated to identify the ideal adipose digestion process. The findings showed that 2 hours of tissue digestion at 220 RPM in 5U of Liberase was optimal to digest the fatty tissue into a creamy consistency that allowed the isolation of the stromal vascular fraction with a high yield of cells. Thus, all the tissue processing steps were deemed feasible in this study.

While the methodology up to the tissue processing phase was tested and feasible, we were unable to verify the experimental methods including the multiplex cytokine analysis kits, PCR and flow cytometry due to the low number of samples. Nevertheless, the methods chosen were not novel and have been successfully utilised in previous studies, and hence, is theoretically feasible[416, 417].

Despite, the successful pilot of the methods, the component of the study that was not feasible was the recruitment of participants. Recruitment was carried out at a single site with one surgeon initially, with the addition of two further surgeons at the same location to the protocol. The choice of one surgeon and recruitment site aimed to control for any methodological differences that might occur during surgery. Knee replacement surgery encompasses broad methodological variations in each stage of the operation, including, the approach to the joint

and implant procedure types[418, 419]. These variations create the potential for inconsistencies in the tissue samples obtained.

Additionally, factors such as tissue handling, and collection time are known to create differences in sample quality as well[419, 420]. As mentioned above, The INTERLOCK study design was limited at first to a single surgeon and then to a small pool of surgeons with similar practices within the same site to minimise these variations. However, this strategy was still met with poor recruitment numbers at both stages and did not result in an adequately sized sample pool.

Difficulties in the recruitment of surgical patients are not uncommon and have resulted in many suggestions for overcoming such challenges in the literature[421-423]. A standard recommendation that could be utilised in this study, in addition to increasing the number of surgeons, is adding new recruitment sites[423, 424]. The addition of other sites would provide a greater catchment of potential participants to recruit from and would enable greater sample diversity in terms of demographics.

However, more sites and investigators provide a different set of challenges that must be managed. The geographical location of the sites (regional versus city-based) and the volume of patients seen can vary dramatically. These factors are known to influence surgical outcomes which may indirectly imply differences in sample quality, collection, and transport time [420, 425, 426]. To improve the homogeneity of samples and preserve sample quality, protocol modifications during sample collection will be essential. These changes would include the use of RNAlater (Thermo-Fisher Scientific, Massachusetts, USA) to preserve genetic material at collection or shipping samples to the laboratory on dry ice[427].

Additionally, the practicalities of a multi-site study will also require more administration, study coordinators for recruitment and arrangements for sample transportation[428]. These changes will result in an increased financial cost to the study. Hence, while increasing the number of sites will likely make a positive impact on recruitment numbers, it is crucial to ensure adequate economic and personnel resources are available for the success of the study.

Although the recruitment rate limited this study, the experience with the first few patients provided insights into the feasibility of our study methodology. The INTERLOCK study visit collected numerous outcome measures including self-reported questionnaires, clinical measures, physical function outcomes, collection of a blood sample and an ultrasound. A strength of the study was the use of a web-based data collection instrument which allowed participants to complete the questionnaires before the face-to-face study visit and thus a reduced time burden at the research site. Another strength was the engagement of critical stakeholders such as the nursing unit manager and staff within the operating theatre unit, which allowed a seamless collection of tissues in the sample collection stage of the study.

The strengths and limitations of this study highlight the critical future steps required for a successful trial. Despite aiming for a fully comprehensive study, we were unable to include contrast-MRI evaluations of the IFP due to the study proximity to surgery. As MRI is a very common surrogate used for IFP inflammation, it is essential to validate its use against the tissue inflammation, and thus, future study designs should be structured for it to be included. Another study design consideration would be to create a multi-centre study to ensure saturation of the sample size. The combination of the described recommendation may allow the INTERLOCK

study to be carried out successfully and provide much-needed insights into the role and mechanisms of the IFP in joints with knee OA.

7.6 Conclusion

This study used a unique approach to reconcile clinical and laboratory findings to increase the understanding of how the biological state of the infrapatellar fat pad impacts the surrounding tissues relates to the disease experience of people with knee OA. The protocol evaluates multiple aspects of the disease, such as pain and disability against various conventional methods used to assess inflammation in the fat pad. The recruitment rate of this study was inadequate, but of the few participants recruited, testing of the methodology was possible. While the experimental methodology is deemed feasible, significant strides to the recruitment strategy must be made to attain the required sample size.

Chapter 8. Final considerations and conclusions

8.1 Summary of Main Findings

Osteoarthritis (OA) is a multifactorial disease that involves all joint tissues and may present with an illness that manifests with pain, physical dysfunction and associated disability in those afflicted[9]. The role of adipose tissue as an inflammatory organ, the involvement of adipose associated inflammation in OA, and the proximity of the infrapatellar fat pad (IFP) to the synovial knee joint have resulted in an increased interest in the IFP's role in recent years. This thesis aimed to contribute novel research to the field about the role of the IFP in knee OA and how it impacts clinical manifestations of the disease.

Chapter 2 systematically appraised the current literature to evaluate the relationship between IFP associated inflammation and pain, which is the predominant clinical manifestation of OA[429]. The review found a small number of studies (18) that evaluated IFP associated inflammation and pain in human trials categorised as having used either imaging or tissue-based measures and pre-clinical (animal model) studies. Due to the vast differences in the studies, the results of only three trials could be pooled with the metanalysis revealing moderate-quality evidence of a weak correlation between the measures. The strength of this review, which is the first systematic review to evaluate the relationship between IFP associated inflammation and pain, was the broad inclusion of clinical human and pre-clinical animal studies as well as studies that reported but did not evaluate the measures. By including these studies, a comprehensive evaluation of the current literature and the research opportunities were identified. This review identified a need for more tissue-based studies in humans and animals to

understand the biological interactions of IFP inflammation. Additionally, the analysis revealed a need for the validation of MOAK's Hoffa's synovitis and pain in larger samples, and that already available data in existing cohorts could be better utilized to study the role of the IFP in OA.

Having identified a need for further understanding in pre-clinical studies, **Chapter 4** utilised existing samples to evaluate the relationship between IFP adiposity, synovitis and sub-synovial fibrosis using histological methods, gene expression and pain behaviour assessments in murine models of post-traumatic OA. Firstly, this analysis demonstrated that changes in IFP adiposity were mostly driven by surgical intervention, despite efforts to reflect the IFP from the incision, rather than physically disrupting it, and to a lesser degree non-invasive mechanical ACL rupture injury. These changes indicated the involvement of the molecular responses to the insults and showed some capacity for IFP recovery, as seen in the ACL rupture model[99].

Adiposity in the IFP was negatively correlated with synovitis and sub-synovial fibrosis, indicating IFPs with more and bigger adipocytes to be associated with less severe synovial OA pathology as is consistent with current literature[99, 105, 266-268]. The most interesting histological finding was the stronger correlations between IFP adiposity and posterior synovitis and fibrosis, compared to anterior pathology. The result challenged the construct that the interaction between the IFP and surrounding tissues were due to anatomical proximity[110, 176]. One possibility is that the IFP has a higher and/or broader biological impact on the joint than previously thought. Alternatively, given the associative nature of the study, IFP adiposity could be a surrogate marker of worsening joint disease that is characterised by the increased posterior synovitis (which is where most of the articular damage occurs) that does not resolve in the pathological PTOA models used. The lack of anatomic relationship between the IFP and

posterior synovitis could also allude to synovial crosstalk within the joint as a whole with the IFP adiposity changes manifesting as a result.

Gene-expression data revealed that surgical PTOA models which resulted in lower IFP adiposity also showed acute inflammation that may be driven by CD4+ T-cells and M1 macrophage pathways evidenced by the similar temporal increases. The involvement of macrophages in models with lower adiposity is consistent with the development of crown-like structures, or a ring of macrophage cells, in the microenvironment of necrotic adipose cells[28]. Lower adiposity in the IFP was also associated with lowering CD8, leptin and adiponectin expression, which contradicted current findings that indicate increased adipokine with increased OA severity[275]. However, these differences could allude to the fact that this study investigated PTOA with IFP tissue trauma rather than spontaneous age or obesity-related OA. Despite temporal histological and gene expression differences between the various models, pain behaviours were not markedly different between the group, nor did they show any similar trends to IFP adiposity, synovitis or sub-synovial fibrosis changes.

Chapter 5 builds on the previous section by investigating the patterns of associations between IFP adiposity, sub-synovial fibrosis and the other structural features of OA within the medial tibiofemoral compartment (where the IFP was assessed). More specifically, this chapter explored the correlations to cartilage, bone (subchondral and marginal osteophyte/enthesophyte) and meniscus pathology. Additionally, the correlation analysis included adjustments for surgery, given the impact observed in the IFP synovium unit in chapter 4, in the whole sample as well as within the models that develop joint pathologies (ACL transection, ACL rupture, and sub-critical mechanical injury).

Adiposity in the IFP and sub-synovial fibrosis, both showed many correlations of varying strengths to most of the other joint-wide OA structural features. Consistent with current literature, lower adiposity and increased sub-synovial fibrosis was associated with more severe pathology[105, 121, 266, 267, 326]. However, this study found no meaningful associations between IFP adiposity or sub-synovial fibrosis and sub-chondral bone changes, despite prior research indicating strong links between sub-chondral bone and other cartilage pathologies[221, 331, 333]. A study by Zaki et al. used established models of PtOA (medial meniscal destabilisation – DMM) compared to inflammation-driven arthritis (antigen-induced arthritis – AIA) to distinguish between mechanical and inflammation-driven OA phenotypes[221, 430]. The study demonstrated that distinct signals/mechanisms drove changes in the subchondral bone and its association with cartilage damage: in DMM proteoglycan loss and AIA chondrocyte hypertrophy and apoptosis[221]. Proteoglycan loss in DMM likely alters (increases) mechanical signals to the bone, while chondrocyte differentiation and death in AIA may activate soluble biological signalling pathways. The disconnect between strong association between IFP adiposity with cartilage pathologies but the absence of correlations to subchondral bone pathologies in this thesis may mean, as Zaki et al. have suggested, separate mechanisms that drive the biological and mechanical disease process[431].

Correlations between IFP adiposity and structural OA features remained when adjusting for surgery and pathology-inducing injuries, which is consistent with suggestions that larger IFP's are protective to pathologies[121]. Additionally, reduced adiposity in the IFP was specifically associated with more severe structural damage and proteoglycan loss in the cartilage and meniscus. This finding alluded to a complex interaction between IFP adipose tissues and

cartilage proteoglycan metabolism, that is supported by ex-vivo evidence of healthy IFP's increasing proteoglycan (measured as sulphated glycosaminoglycan) production in cartilage and maintaining joint homeostasis[307].

Finally, sub-synovial fibrosis in the posterior of the joint showed stronger correlations to cartilage pathology, osteophyte and enthesophyte development and meniscal damage, indicating common mechanisms that likely involve mechanical stress[304]. Injury to the ACL results in posterior subluxation of the femur (relative to the tibia) while anterior stability remains unaffected due to the intact posterior cruciate ligament. This modulation manifests as increased strain on the posterior soft tissues resulting in increased fibrosis and other pathological responses to stress such as enthesophytes[300]. Interestingly, IFP adiposity and synovial fibrosis associations with osteophytes were anterior while those with enthesophytes were posterior. This finding not only highlights that these two marginal bone-forming OA pathologies are distinct but suggests that the more important signals in the former may be biological (e.g. growth factors released from the adjacent IFP) while in the latter altered biomechanics may be the key driver.

To build on the investigation into IFP adiposity and synovitis in the animal studies, **Chapter 6** of the thesis used the nested case-control FNIH cohort in the OAI to evaluate the associations between Hoffa-synovitis, centripetal adiposity, serum markers of synovial inflammation and pain in humans. In particular, this chapter evaluated overall pain for consistency to the existing literature and load-bearing pain (pain walking upstairs) to investigate the impact of mechanical stress, given the findings of chapter 4 and 5. Additionally, centripetal adiposity was assessed

using WHtR, which is a much better representation of adipose mass compared to the conventionally used BMI[340].

The main finding of this chapter was that increasing Hoffa-synovitis was weakly correlated with lowering centripetal adiposity. While the weak result may be classified as a negligible result, which has been previously suggested, there is evidence to support a construct that increasing IFP adiposity is protective to the joint, as seen in chapter 4[178]. Larger IFP's are associated with increased BMI, and in mice, the tissues are protected from systematic adipose driven inflammation[100, 180, 356]. These findings highlight that not all fat behaves the same with variations in adipose tissue depots/types[29, 31].

Changes in the IFP and WHtR were also correlated to the synovial serum biomarkers, which further supports the relationship observed in chapter 4. However, further analysis revealed that while both Hoffa-synovitis and centripetal adiposity affected synovial inflammation, the impacts were independent of each other.

The most interesting finding of this study was that while centripetal adiposity was associated with pain, IFP associated inflammation was not. The IFP is a highly innervated piece of tissue with highly sensitive sensory nerve fibres that have been suggested as a driver of anterior knee pain in OA[110, 179, 432]. However, as seen in the qualitative compilation of the systematic review (Chapter 2), there is evidence that both support and refute this association[106, 118, 190, 197, 198]. While there is evidence supporting our results, it was in direct contrast to the weak correlation identified in the meta-analysis in chapter 2, despite both studies using the same measures [197, 198]. The analyses in this study were carried out in a much larger sample (n = 600 vs n =243) compared to the systematic review.

Both chapters 2 and 6 highlight significant inadequacies in the current literature and databases to adequately address the role of inflammation in the IFP in OA in humans. As part of this thesis, a clinical observational study was designed to address these deficiencies and investigate the impact of IFP inflammation on clinical outcomes in an end-stage knee OA population using a mix of clinical and laboratory methodologies. **Chapter 7** presents the protocol of the proposed INTERLOCK Study and reports on its feasibility.

This observational study included one clinical research visit before total knee replacement surgery, at which point joint tissues, including the IFP, are obtained and analysed using an array of laboratory methods. The primary aim of the proposed study was to understand the association between IFP tissue inflammation, identified by cytokine levels, and pain, including neuropathic/sensitization outcomes that align with those used in pre-clinical models. The secondary objectives of the study further investigate the association of IFP inflammation to physical function (as the other primary manifestation of OA), synovitis and systemic inflammation. The study also aimed to evaluate differences in the IFP compared to subcutaneous adipose to address some of the disconnects in tissue behaviour in the present literature. Finally, the study hoped to resolve the validity of commonly used surrogate markers, such as MRI and ultrasound, in comparison to tissue inflammation level of the IFP. These questions were addressed by outcome measures which included self-reported questionnaires (KOOS, PKPM, mPD-Q, DASS21), physical function assessments (30s-CST, quadriceps strength, 40m FPWT, knee ROM, PPT) and clinical measures (WhtR, MRI, ultrasound, serum).

While the study was designed to address these questions, the recruitment strategies employed rendered the study unfeasible with only 4 participants recruited in six months at 10% of the

expected rate. This limitation was mainly attributed to the involvement of a single surgeon at a single site for recruitment, which with additional funding and resources can be overcome. Notably, it was demonstrated that the study visit was feasible in the participants recruited, despite the time taken to collect the extensive list of measures, as was the tissue processing protocol. Unfortunately, the limited number of samples prevented any evaluation of the experimental laboratory-based protocols of the study.

8.2 Strengths

8.2.1 Population

The first strength of this thesis is the population evaluated in the different studies. In the systematic review, both human clinical and animal studies were included to get a comprehensive understanding of the research field. This methodology was an unusual approach, as the population in systematic reviews are often very explicitly limited to either animal or human. However, given the lack of research in the understanding between IFP inflammation and pain, the broader approach utilised in chapter 2 was ideal. The evaluations in pre-clinical and clinical populations are built upon by the animal studies of chapter 4 and 5, the human studies (OAI database) in chapter 6, and the proposed human observational study of chapter 7. By combining the use of animal and human populations, this thesis embodies the “mechanism to medicine” or, more commonly, “bench to bedside” approach in the biomedical sciences[433, 434].

As mentioned, OA is an incredibly diverse disease with many risk factors and trajectories[9, 435]. This thesis represented that diversity by evaluating post-traumatic OA models of different stages (timepoints), injury types (surgical and mechanical), and trajectories (non-OA inducing joint injury). Additionally, the evaluation of the OAI FNIH biomarker consortium cohort represented another diverse population which included non-progressive and structural and/or pain progressive populations[349]. Finally, the target population in the final chapter was end-stage knee OA. The use of the different models and study types means that this thesis evaluated the role of the IFP across the entire OA disease cycle from injury to removal of the offending joint.

Additionally, the sample size used in the human studies were powered for the analyses in chapter 7, and the use of a large dataset meant that the questions of chapter 6 were evaluated in a cohort of 600 participants. The importance of sample size in hypothesis-testing studies is essential for the confidence in the findings[436, 437]. Often, studies are underpowered due to costs or convenience, but these studies are ultimately a waste of time and money due to the inconclusive results[437]. Chapter 4 – 6 used existing research resources such as samples from a prior study in the animals for hypothesis-generating and the OAI dataset for reducing research wastage. While the proposed research in chapter 7 proved to not be feasible in the timeframe of this thesis, it was designed based on existing research to be adequately powered for conclusive findings and included considerations of tissue sample issues[106].

Considerations for a 'Bench to Bedside' approach

The preparation of this thesis and direct involvement in pre-clinical and clinical analyses provided a unique opportunity to understand the intricacies of such an approach. The first hurdle in translating research between the bench and bedside was not all measures can be easily translated. For example, the assessment of the 'pain experience' in humans using self-reported instruments is compared to pain observations in a non-verbal species, often using difficult techniques that may not be validated[438]. Tissue obtainment is another challenge in the translation. While it is relatively easy to obtain whole joint tissue from animal models that are euthanized as part of the study, tissue collection in humans is often limited to cadaveric specimens or end-stage disease with patients undergoing joint replacement.

Additionally, the direct involvement in the studies of this thesis required a range of basic skills sets including laboratory techniques, patient communication and assessment as well as an

understanding of the different assessments to adequately analyse the outcomes. Prior experience in both basic and clinical sciences was essential to be able to carry out the studies of this thesis. However, the most important skills used was the openness to learning and the ability to ask for advice from more experienced colleagues.

8.2.2 Outcome measures

Diversity

The other main strengths of this thesis can be characterised in the measures used for outcomes. Firstly, this thesis examines the different research questions using multiple outcome measures. For instance, in the animal studies, gene expression and pain data were obtained by evaluating several gene markers, paw withdrawal in response to pain, and weight-bearing changes. Similarly, in chapter 6, the pain was assessed as an overall score as well as going upstairs, which represented pain on weight loading. By using these various measures, we were able to identify potential intricacies such as the association between IFP adiposity and posterior fibrosis which may not have been evaluated in a black and white approach that used singular measures. As part of the strategy to assess the different manifestations, a novel sub-synovial scoring tool in mice that accounted for the depth and spread of fibrosis beneath the synovial subintima was developed. The instrument addresses the low quality of histological synovial fibrosis scorings in the literature, that rather envelope it as part of synovitis despite the extensive damage and resulting joint stiffness it causes[216, 232, 233].

IFP and synovium differentiation

Another outcome strength of this study is separating the evaluations of the IFP and synovium. These two tissues are frequently analysed as one unit and treated as a surrogate for one another[96, 207]. While there is a close relationship between the IFP and synovium, they are distinct tissues with different cellular makeups and roles. The combined evaluations in current literature result in the inability to elucidate the intricate relationship. Chapter 4 evaluated the tissues separately in histology but together in gene expression, and chapter 6 included synovial biomarkers in the evaluation of Hoffa's synovitis providing some understanding of the distinct roles of the tissues while allowing a level of consistency with present literature for comparisons.

Adiposity

The final strength of this thesis is the measure of adiposity used in human studies (chapter 6 and 7). Body mass index (BMI) is a common anthropological tool used in research as a surrogate of adiposity. However, recent studies have highlighted the problematic assumption as the measure does not account of differences in body composition[338]. The measure is now well-established as a poor predictor of adiposity and recommendations have been made for the use of waist to hip or waist to height ratio, which more accurately identifies centripetal adiposity[339]. The WHtR is more highly correlated to fat mass ($r=0.706$) compared to BMI ($r = -0.003$) or waist to hip ratio ($r = -0.146$) [340]. Additionally, WHtR was also found to be more useful in metabolic syndrome, cardiovascular health and weight loss compared to other measures[340-342]. At present, there has been no published evaluation of the association between WHtR and the IFP.

8.3 Limitations

8.3.1 Inflammation

The main limitation of this thesis is the construct of “inflammation”. Inflammation is an umbrella term that encompasses physiological and biological changes and hence the measures used in the current literature are varied from the signal intensity in the IFP using MRI to the count of immune cells that had infiltrated the tissue[106, 118]. While the latter method may be the best as it is a tally of 'cellular inflammation' representing the inflammatory status of the IFP, obtaining tissues is overtly invasive with capacity for future damage and hence difficult to justify for research nor practical for routine clinical practice. However, there is little information about how well tissue inflammation translates to imaging measures used in current research, unlike pain measures, where the responsiveness of the different instruments has been validated[213]. These challenges have prevented a true 'gold-standard' for IFP inflammation to emerge, which is reflected in the variations of measures used in this thesis.

8.3.2 Animal study designs

Another challenge identified was the design of animal studies; in the systematic review and chapter 4 and 5. Measurements of IFP inflammation, molecular or histological, and pain are often obtained from different cohorts of animals due to a variety of requirements. Pre-clinical studies often include a multitude of timepoints for molecular and histological assessments which cannot be assessed in the same animal due to the tissue availability in the small joints, while pain measures require longitudinal assessments. The sample sizes necessary for combining the measures into a single cohort poses a significant logistical burden of cost, time

and resources, and is often placed in the "not feasible" pile. This approach results in findings that cannot be statistically correlated but are instead presented as trends to support a hypothesis. While in studies that are 'hypothesis testing', this would be a waste of research resources, the studies in this thesis use are designed for hypothesis generation.

8.3.3 IFP and synovium unit

Although the studies in this thesis attempted to evaluate the IFP and synovium independently as described in the strengths, this was not possible in the gene expression analysis of the animal studies. Both tissues were dissected en-bloc from the anterior of the joint with no additional sample of posterior synovium tissue. While obtaining pure synovium would have been helpful to differentiate the gene outcomes, dissecting posterior synovium is problematic due to the overlying musculature blocking access to the joint capsule in a tiny joint. While separate histological analysis of the tissues is helpful, evaluating the IFP and synovium separately for the gene expression will help provide great clarity to the differences of the tissues. Confirmation of the expression changes at a protein level will also be necessary, but again has limitations imposed by tissue proximity and size, which restrict separate extraction and proteomic/activity analysis. Immunohistology would allow spatial/tissue resolution but is limited by focal analysis (single 4 μ section across the joint width) and the soluble nature of many of the molecules of interest (e.g. cytokines, chemokines growth factors).

8.3.4 Multiple testings

The strength of evaluating several measures in chapters 4 and 5 of this thesis which allowed in-depth mechanistic interrogation, was also a limitation. These chapters involved multiple statistical tests which result in an increased risk of type 1 errors or a false-positive finding[431,

439]. While it was possible to statistically correct for this disadvantage using methods such as Bonferroni or Hochberg corrections, this study was intended to be exploratory and to facilitate the generation of hypothesis instead of being hypothesis driven[440].

8.3.5 Unfeasible study

The final limitation of this thesis was of the prospective clinical study described in chapter 7 being deemed not feasible. The INTERLOCK study was designed to answer several essential questions about the role of the IFP and clinical outcomes in patients with end-stage knee OA using a combination of methodologies. This study incorporated many of the 'gold-standards' in musculoskeletal research such as using contrast-enhanced MRIs, WHtR and the OARSI recommendations of the physical function measures. It also combined clinical and laboratory methodologies to bridge the findings from pre-clinical studies to clinical research. Given the earlier chapters, the INTERLOCK study would have assisted in testing many of the previous results. However, the unanticipated challenges of recruitment meant, despite the well-designed study visits and outcome measures and known monthly number of TKRs performed, this project could not be carried out nor modified within the resources of this thesis.

8.4 Future directions

Additional research is needed to further the current understanding of the IFP and to validate the findings of this research. The systematic review in chapter 2 identified many measures and methods of identifying IFP inflammation including the use of MRIs and ultrasounds, scoring systems such as MOAKs and WORMS, and cell counts of immune cells in the stromal vascular fractions of the tissue. While each method may have its merit, it prevents comparability between studies. Future research to validate these standard methodologies and their comparability is crucial for the research field going forward. This validation process would also be able to create a recommendation for a gold standard in measuring inflammation of the IFP.

Chapters 4 and 5 have presented novel results from an exploratory study. More research is needed to understand the relationships between IFP inflammation, synovitis and the other structural pathologies of OA. These findings need to be validated in a pre-clinical study that is statistically powered to test this hypothesis and can evaluate behavioural and molecular assessments within the same animal. Furthermore, because pain in OA is variable at different stages of disease progression, it would be important to evaluate how the IFP may contribute to the changes. The relationship could be tested in an animal study by using different timepoints in established OA models for variability in disease stage and comparing IFP inflammation (by immunohistochemistry, gene analysis). Additionally, this thesis has investigated models of PTOA based on ACL damage, and thus further research is needed to understand if the same relationship persists in other animal models such as those involving meniscal injury/destabilisation, obesity, or ageing mice. These findings should also be validated in pre-clinical studies using female mice as well as in human studies.

On that note, a well-designed observational study in humans is essential to understand the relationship between IFP inflammation and the actual clinical manifestations experienced by the OA-patient. While chapter 7 proposed a study in end-stage knee OA patients, it would not be ideal for capturing the different stages of the disease and even before disease development. Such populations may include patients with an acute ACL injury, a minor injury in athletes, or patients who are progressing beyond the early stage of OA. However, obtaining access to IFP tissues outside the TKR setting will be a challenge for ethical implications and to convince potential participants for recruitment. Based on the outcome of the INTERLOCK study, another observational study should consider the number of patients available at a site and include multiple recruitment sites to maximise inclusion of participants.

Finally, once these relationships are established, and if a strong correlation between IFP inflammation and clinical outcomes are confirmed, investigation to evaluate its potential as a therapeutic target should begin. Based on the association of higher adiposity in the IFP and lower pathologies in chapter 4 and 5, treatment to encourage adipose development could be considered. Potential treatments could also take the form of topical or injections of anti-inflammatory agents at the site of the IFP. The investigation of targeted therapies would complete the bench to bedside translation of IFP research.

8.5 Concluding remarks

The findings of this thesis highlight interactions between the IFP, other OA joint pathologies and pain. The concept that the IFP is an inert tissue designed as only a cushion for mechanical impact is difficult to reconcile given the association of adiposity and inflammatory changes within the tissue to pathological changes in the rest of the joint and systemic markers of synovial inflammation. The IFP was correlated to many pathologies features of synovitis, cartilage degradation, osteophyte and enthesophyte development, and meniscal damage, but there was a significant disconnect to changes of the sub-chondral bone indicating separate pathophysiological mechanisms. In assessments of clinical manifestations, this thesis also questions the proposed association between IFP inflammation and pain. The IFP inflammation and pain relationship was confirmed in a small meta-analysis (Chapter 2) but refuted in a nested case-control cohort of the OAI that was more than twice as large (Chapter 6). The current literature does not adequately understand the role of the IFP, and the tissue is often neglected in the treatment of OA. By further understanding the interaction of the IFP, we can potentially target the tissue to improve the disease experienced by those afflicted by OA.

References

1. Henderson, J.V., et al., *Prevalence, causes, severity, impact, and management of chronic pain in Australian general practice patients*. Pain Med, 2013. **14**(9): p. 1346-61.
2. Guccione, A.A., et al., *The effects of specific medical conditions on the functional limitations of elders in the Framingham Study*. Am J Public Health, 1994. **84**(3): p. 351-8.
3. Cross, M., et al., *The global burden of hip and knee osteoarthritis: estimates from the global burden of disease 2010 study*. Ann Rheum Dis, 2014. **73**(7): p. 1323-30.
4. Fajardo, M. and P.E. Di Cesare, *Disease-modifying therapies for osteoarthritis : current status*. Drugs Aging, 2005. **22**(2): p. 141-61.
5. Berenbaum, F., *Osteoarthritis as an inflammatory disease (osteoarthritis is not osteoarthrosis!)*. Osteoarthritis Cartilage, 2013. **21**(1): p. 16-21.
6. Sokolove, J. and C.M. Lepus, *Role of inflammation in the pathogenesis of osteoarthritis: latest findings and interpretations*. Ther Adv Musculoskelet Dis, 2013. **5**(2): p. 77-94.
7. Kraus, V.B., et al., *Call for standardized definitions of osteoarthritis and risk stratification for clinical trials and clinical use*. Osteoarthritis Cartilage, 2015. **23**(8): p. 1233-41.
8. Sarzi-Puttini, P., et al., *Osteoarthritis: an overview of the disease and its treatment strategies*. Semin Arthritis Rheum, 2005. **35**(1 Suppl 1): p. 1-10.
9. Johnson, V.L. and D.J. Hunter, *The epidemiology of osteoarthritis*. Best Pract Res Clin Rheumatol, 2014. **28**(1): p. 5-15.
10. Margetic, S., et al., *Leptin: a review of its peripheral actions and interactions*. Int J Obes Relat Metab Disord, 2002. **26**(11): p. 1407-33.

11. Scanzello, C.R. and S.R. Goldring, *The role of synovitis in osteoarthritis pathogenesis*. Bone, 2012. **51**(2): p. 249-57.
12. Hill, C.L., et al., *Synovitis detected on magnetic resonance imaging and its relation to pain and cartilage loss in knee osteoarthritis*. Ann Rheum Dis, 2007. **66**(12): p. 1599-603.
13. McCabe, P.S., et al., *Brief Report: Synovial Fluid White Blood Cell Count in Knee Osteoarthritis: Association With Structural Findings and Treatment Response*. Arthritis Rheumatol, 2017. **69**(1): p. 103-107.
14. Kaneko, S., et al., *Interleukin-6 and interleukin-8 levels in serum and synovial fluid of patients with osteoarthritis*. Cytokines Cell Mol Ther, 2000. **6**(2): p. 71-9.
15. Sohn, D.H., et al., *Plasma proteins present in osteoarthritic synovial fluid can stimulate cytokine production via Toll-like receptor 4*. Arthritis Res Ther, 2012. **14**(1): p. R7.
16. Chauffier, K., et al., *Induction of the chemokine IL-8/Kc by the articular cartilage: possible influence on osteoarthritis*. Joint Bone Spine, 2012. **79**(6): p. 604-9.
17. de Boer, T.N., et al., *Serum adipokines in osteoarthritis; comparison with controls and relationship with local parameters of synovial inflammation and cartilage damage*. Osteoarthritis Cartilage, 2012. **20**(8): p. 846-53.
18. Lago, F., et al., *Adipokines as emerging mediators of immune response and inflammation*. Nat Clin Pract Rheumatol, 2007. **3**(12): p. 716-24.
19. Clockaerts, S., et al., *The infrapatellar fat pad should be considered as an active osteoarthritic joint tissue: a narrative review*. Osteoarthritis Cartilage, 2010. **18**(7): p. 876-82.

20. Klein-Wieringa, I.R., et al., *The infrapatellar fat pad of patients with osteoarthritis has an inflammatory phenotype*. Ann Rheum Dis, 2011. **70**(5): p. 851-7.
21. Kershaw, E.E. and J.S. Flier, *Adipose tissue as an endocrine organ*. J Clin Endocrinol Metab, 2004. **89**(6): p. 2548-56.
22. Zhang, Y., et al., *Positional cloning of the mouse obese gene and its human homologue*. Nature, 1994. **372**(6505): p. 425-32.
23. Dam, V., T. Sikder, and S. Santosa, *From neutrophils to macrophages: differences in regional adipose tissue depots*. Obes Rev, 2016. **17**(1): p. 1-17.
24. Mraz, M. and M. Haluzik, *The role of adipose tissue immune cells in obesity and low-grade inflammation*. J Endocrinol, 2014. **222**(3): p. R113-27.
25. Lumeng, C.N., J.L. Bodzin, and A.R. Saltiel, *Obesity induces a phenotypic switch in adipose tissue macrophage polarization*. J Clin Invest, 2007. **117**(1): p. 175-84.
26. Wentworth, J.M., et al., *Pro-inflammatory CD11c+CD206+ adipose tissue macrophages are associated with insulin resistance in human obesity*. Diabetes, 2010. **59**(7): p. 1648-56.
27. Gordon, S., *Macrophage heterogeneity and tissue lipids*. J Clin Invest, 2007. **117**(1): p. 89-93.
28. Weisberg, S.P., et al., *Obesity is associated with macrophage accumulation in adipose tissue*. J Clin Invest, 2003. **112**(12): p. 1796-808.
29. Cinti, S., *The adipose organ*. Prostaglandins Leukot Essent Fatty Acids, 2005. **73**(1): p. 9-15.

30. Belluzzi, E., et al., *Systemic and Local Adipose Tissue in Knee Osteoarthritis*. J Cell Physiol, 2017. **232**(8): p. 1971-1978.
31. Rosen, E.D. and B.M. Spiegelman, *What we talk about when we talk about fat*. Cell, 2014. **156**(1-2): p. 20-44.
32. Giralt, M. and F. Villarroya, *White, brown, beige/brite: different adipose cells for different functions?* Endocrinology, 2013. **154**(9): p. 2992-3000.
33. Jorge, A.S., et al., *Brown and White Adipose Tissue Expression of IL6, UCP1 and SIRT1 are Associated with Alterations in Clinical, Metabolic and Anthropometric Parameters in Obese Humans*. Exp Clin Endocrinol Diabetes, 2017. **125**(3): p. 163-170.
34. Dowal, L., et al., *Intrinsic Properties of Brown and White Adipocytes Have Differential Effects on Macrophage Inflammatory Responses*. Mediators Inflamm, 2017. **2017**: p. 9067049.
35. Tilg, H. and A.R. Moschen, *Adipocytokines: mediators linking adipose tissue, inflammation and immunity*. Nat Rev Immunol, 2006. **6**(10): p. 772-83.
36. Mulder, P., et al., *Surgical removal of inflamed epididymal white adipose tissue attenuates the development of non-alcoholic steatohepatitis in obesity*. Int J Obes (Lond), 2016. **40**(4): p. 675-84.
37. Cicuttini, F.M., J.R. Baker, and T.D. Spector, *The association of obesity with osteoarthritis of the hand and knee in women: a twin study*. J Rheumatol, 1996. **23**(7): p. 1221-6.
38. Gierman, L.M., et al., *Metabolic stress-induced inflammation plays a major role in the development of osteoarthritis in mice*. Arthritis Rheum, 2012. **64**(4): p. 1172-81.

39. Griffin, T.M., et al., *Diet-induced obesity differentially regulates behavioral, biomechanical, and molecular risk factors for osteoarthritis in mice*. *Arthritis Res Ther*, 2010. **12**(4): p. R130.
40. Griffin, T.M., et al., *Induction of osteoarthritis and metabolic inflammation by a very high-fat diet in mice: effects of short-term exercise*. *Arthritis Rheum*, 2012. **64**(2): p. 443-53.
41. Mooney, R.A., et al., *High-fat diet accelerates progression of osteoarthritis after meniscal/ligamentous injury*. *Arthritis Res Ther*, 2011. **13**(6): p. R198.
42. Wu, C.L., et al., *Dietary fatty acid content regulates wound repair and the pathogenesis of osteoarthritis following joint injury*. *Ann Rheum Dis*, 2015. **74**(11): p. 2076-83.
43. Asou, Y., et al., *Pleiotropic Functions of High Fat Diet in the Etiology of Osteoarthritis*. *PLoS One*, 2016. **11**(9): p. e0162794.
44. Hamada, D., et al., *Suppressive Effects of Insulin on Tumor Necrosis Factor-Dependent Early Osteoarthritic Changes Associated With Obesity and Type 2 Diabetes Mellitus*. *Arthritis Rheumatol*, 2016. **68**(6): p. 1392-402.
45. Iwata, M., et al., *Initial responses of articular tissues in a murine high-fat diet-induced osteoarthritis model: pivotal role of the IPFP as a cytokine fountain*. *PLoS One*, 2013. **8**(4): p. e60706.
46. Louer, C.R., et al., *Diet-induced obesity significantly increases the severity of posttraumatic arthritis in mice*. *Arthritis Rheum*, 2012. **64**(10): p. 3220-30.
47. Griffin, T.M., et al., *Extreme obesity due to impaired leptin signaling in mice does not cause knee osteoarthritis*. *Arthritis Rheum*, 2009. **60**(10): p. 2935-44.

48. Gierman, L.M., et al., *Osteoarthritis development is induced by increased dietary cholesterol and can be inhibited by atorvastatin in APOE*3Leiden.CETP mice--a translational model for atherosclerosis*. *Ann Rheum Dis*, 2014. **73**(5): p. 921-7.
49. de Munter, W., et al., *High LDL levels lead to increased synovial inflammation and accelerated ectopic bone formation during experimental osteoarthritis*. *Osteoarthritis Cartilage*, 2016. **24**(5): p. 844-55.
50. Wu, C.L., et al., *Serum and synovial fluid lipidomic profiles predict obesity-associated osteoarthritis, synovitis, and wound repair*. *Sci Rep*, 2017. **7**: p. 44315.
51. Triantaphyllidou, I.E., et al., *Perturbations in the HDL metabolic pathway predispose to the development of osteoarthritis in mice following long-term exposure to western-type diet*. *Osteoarthritis Cartilage*, 2013. **21**(2): p. 322-30.
52. Collins, K.H., et al., *Relationship between inflammation, the gut microbiota, and metabolic osteoarthritis development: studies in a rat model*. *Osteoarthritis Cartilage*, 2015. **23**(11): p. 1989-98.
53. Niu, J., et al., *Metabolic Syndrome, Its Components, and Knee Osteoarthritis: The Framingham Osteoarthritis Study*. *Arthritis Rheumatol*, 2017.
54. Kalichman, L., L. Li, and E. Kobyliansky, *Prevalence, pattern and determinants of radiographic hand osteoarthritis in Turkmen community-based sample*. *Rheumatol Int*, 2009. **29**(10): p. 1143-9.
55. Qin, J., et al., *Lifetime Risk of Symptomatic Hand Osteoarthritis: The Johnston County Osteoarthritis Project*. *Arthritis Rheumatol*, 2017. **69**(6): p. 1204-1212.

56. Reginato, A.M., et al., *Osteoarthritis in Latin America: Study of Demographic and Clinical Characteristics in 3040 Patients*. J Clin Rheumatol, 2015. **21**(8): p. 391-7.
57. Reyes, C., et al., *Socio-economic status and the risk of developing hand, hip or knee osteoarthritis: a region-wide ecological study*. Osteoarthritis Cartilage, 2015. **23**(8): p. 1323-9.
58. Reyes, C., et al., *Association Between Overweight and Obesity and Risk of Clinically Diagnosed Knee, Hip, and Hand Osteoarthritis: A Population-Based Cohort Study*. Arthritis Rheumatol, 2016. **68**(8): p. 1869-75.
59. Visser, A.W., et al., *Adiposity and hand osteoarthritis: the Netherlands Epidemiology of Obesity study*. Arthritis Res Ther, 2014. **16**(1): p. R19.
60. Wen, L., et al., *Associations between body composition measurements of obesity and radiographic osteoarthritis in older adults: Data from the Dong-gu Study*. BMC Musculoskelet Disord, 2016. **17**: p. 192.
61. Carman, W.J., et al., *Obesity as a risk factor for osteoarthritis of the hand and wrist: a prospective study*. Am J Epidemiol, 1994. **139**(2): p. 119-29.
62. Yusuf, E., et al., *Association between weight or body mass index and hand osteoarthritis: a systematic review*. Ann Rheum Dis, 2010. **69**(4): p. 761-5.
63. Cho, H.J., et al., *Prevalence and Risk Factors of Spine, Shoulder, Hand, Hip, and Knee Osteoarthritis in Community-dwelling Koreans Older Than Age 65 Years*. Clin Orthop Relat Res, 2015. **473**(10): p. 3307-14.
64. Magnusson, K., et al., *Body mass index and progressive hand osteoarthritis: data from the Oslo hand osteoarthritis cohort*. Scand J Rheumatol, 2015. **44**(4): p. 331-6.

65. Strand, M.P., et al., *No association between metabolic syndrome and radiographic hand osteoarthritis: Data from the Framingham study*. Arthritis Care Res (Hoboken), 2017.
66. Frey, N., et al., *Type II diabetes mellitus and incident osteoarthritis of the hand: a population-based case-control analysis*. Osteoarthritis Cartilage, 2016. **24**(9): p. 1535-40.
67. Garessus, E.D., et al., *No association between impaired glucose metabolism and osteoarthritis*. Osteoarthritis Cartilage, 2016. **24**(9): p. 1541-7.
68. Massengale, M., et al., *The relationship between hand osteoarthritis and serum leptin concentration in participants of the Third National Health and Nutrition Examination Survey*. Arthritis Res Ther, 2012. **14**(3): p. R132.
69. Schaffler, A., et al., *Adipocytokines in synovial fluid*. JAMA, 2003. **290**(13): p. 1709-10.
70. Maeda, N., et al., *Diet-induced insulin resistance in mice lacking adiponectin/ACRP30*. Nat Med, 2002. **8**(7): p. 731-7.
71. Yamamoto, K., et al., *Production of adiponectin, an anti-inflammatory protein, in mesenteric adipose tissue in Crohn's disease*. Gut, 2005. **54**(6): p. 789-96.
72. Conde, J., et al., *Adipokines and osteoarthritis: novel molecules involved in the pathogenesis and progression of disease*. Arthritis, 2011. **2011**: p. 203901.
73. Ku, J.H., et al., *Correlation of synovial fluid leptin concentrations with the severity of osteoarthritis*. Clin Rheumatol, 2009. **28**(12): p. 1431-5.
74. Filkova, M., et al., *Increased serum adiponectin levels in female patients with erosive compared with non-erosive osteoarthritis*. Ann Rheum Dis, 2009. **68**(2): p. 295-6.
75. Pottie, P., et al., *Obesity and osteoarthritis: more complex than predicted!* Ann Rheum Dis, 2006. **65**(11): p. 1403-5.

76. Dalmas, E., K. Clement, and M. Guerre-Millo, *Defining macrophage phenotype and function in adipose tissue*. Trends Immunol, 2011. **32**(7): p. 307-14.
77. Wu, C.L., et al., *Conditional Macrophage Depletion Increases Inflammation and Does Not Inhibit the Development of Osteoarthritis in Obese Macrophage Fas-Induced Apoptosis-Transgenic Mice*. Arthritis Rheumatol, 2017.
78. Utomo, L., et al., *Cartilage inflammation and degeneration is enhanced by pro-inflammatory (M1) macrophages in vitro, but not inhibited directly by anti-inflammatory (M2) macrophages*. Osteoarthritis Cartilage, 2016. **24**(12): p. 2162-2170.
79. van der Kraan, P.M., *Age-related alterations in TGF beta signaling as a causal factor of cartilage degeneration in osteoarthritis*. Biomed Mater Eng, 2014. **24**(1 Suppl): p. 75-80.
80. Xie, L., et al., *Systemic neutralization of TGF-beta attenuates osteoarthritis*. Ann N Y Acad Sci, 2016. **1376**(1): p. 53-64.
81. Qatanani, M., et al., *Macrophage-derived human resistin exacerbates adipose tissue inflammation and insulin resistance in mice*. J Clin Invest, 2009. **119**(3): p. 531-9.
82. Wang, X., et al., *Metabolic triggered inflammation in osteoarthritis*. Osteoarthritis Cartilage, 2015. **23**(1): p. 22-30.
83. Bao, J.P., et al., *Leptin plays a catabolic role on articular cartilage*. Mol Biol Rep, 2010. **37**(7): p. 3265-72.
84. Dumond, H., et al., *Evidence for a key role of leptin in osteoarthritis*. Arthritis Rheum, 2003. **48**(11): p. 3118-29.

85. Tong, K.M., et al., *Leptin induces IL-8 expression via leptin receptor, IRS-1, PI3K, Akt cascade and promotion of NF-kappaB/p300 binding in human synovial fibroblasts*. Cell Signal, 2008. **20**(8): p. 1478-88.
86. Mutabaruka, M.S., et al., *Local leptin production in osteoarthritis subchondral osteoblasts may be responsible for their abnormal phenotypic expression*. Arthritis Res Ther, 2010. **12**(1): p. R20.
87. Yang, W.H., et al., *Leptin induces IL-6 expression through OBRI receptor signaling pathway in human synovial fibroblasts*. PLoS One, 2013. **8**(9): p. e75551.
88. Zhao, X., et al., *Leptin changes differentiation fate and induces senescence in chondrogenic progenitor cells*. Cell Death Dis, 2016. **7**: p. e2188.
89. Koskinen, A., et al., *Adiponectin associates with markers of cartilage degradation in osteoarthritis and induces production of proinflammatory and catabolic factors through mitogen-activated protein kinase pathways*. Arthritis Res Ther, 2011. **13**(6): p. R184.
90. Yusuf, E., et al., *Association between leptin, adiponectin and resistin and long-term progression of hand osteoarthritis*. Ann Rheum Dis, 2011. **70**(7): p. 1282-4.
91. Bokarewa, M., et al., *Resistin, an adipokine with potent proinflammatory properties*. J Immunol, 2005. **174**(9): p. 5789-95.
92. Gerber, M., et al., *Serum resistin levels of obese and lean children and adolescents: biochemical analysis and clinical relevance*. J Clin Endocrinol Metab, 2005. **90**(8): p. 4503-9.

93. Ke, L., et al., *Assessment of diabetes care and the healthcare system in economically and transport underdeveloped rural mountain areas of western China: A cross-sectional survey*. *J Diabetes*, 2017. **9**(5): p. 475-481.
94. Presle, N., et al., *Differential distribution of adipokines between serum and synovial fluid in patients with osteoarthritis. Contribution of joint tissues to their articular production*. *Osteoarthritis Cartilage*, 2006. **14**(7): p. 690-5.
95. Staikos, C., et al., *The association of adipokine levels in plasma and synovial fluid with the severity of knee osteoarthritis*. *Rheumatology (Oxford)*, 2013. **52**(6): p. 1077-83.
96. Macchi, V., et al., *The Infrapatellar Adipose Body: A Histotopographic Study*. *Cells Tissues Organs*, 2016. **201**(3): p. 220-31.
97. Santangelo, K.S., et al., *Pathophysiology of obesity on knee joint homeostasis: contributions of the infrapatellar fat pad*. *Horm Mol Biol Clin Investig*, 2016. **26**(2): p. 97-108.
98. Distel, E., et al., *The infrapatellar fat pad in knee osteoarthritis: an important source of interleukin-6 and its soluble receptor*. *Arthritis Rheum*, 2009. **60**(11): p. 3374-7.
99. Eymard, F., et al., *Knee and hip intra-articular adipose tissues (IAATs) compared with autologous subcutaneous adipose tissue: a specific phenotype for a central player in osteoarthritis*. *Ann Rheum Dis*, 2017. **76**(6): p. 1142-1148.
100. Barboza, E., et al., *Profibrotic Infrapatellar Fat Pad Remodeling Without M1 Macrophage Polarization Precedes Knee Osteoarthritis in Mice With Diet-Induced Obesity*. *Arthritis Rheumatol*, 2017. **69**(6): p. 1221-1232.

101. Fujisaka, S., et al., *Regulatory mechanisms for adipose tissue M1 and M2 macrophages in diet-induced obese mice*. Diabetes, 2009. **58**(11): p. 2574-82.
102. van der Kraan, P.M., *Osteoarthritis and a high-fat diet: the full 'OA syndrome' in a small animal model*. Arthritis Res Ther, 2010. **12**(4): p. 130.
103. Harasymowicz, N.S., et al., *Regional Differences Between Perisynovial and Infrapatellar Adipose Tissue Depots and Their Response to Class II and Class III Obesity in Patients With Osteoarthritis*. Arthritis Rheumatol, 2017. **69**(7): p. 1396-1406.
104. Burda, B., et al., *Variance in infra-patellar fat pad volume: Does the body mass index matter?-Data from osteoarthritis initiative participants without symptoms or signs of knee disease*. Ann Anat, 2017.
105. Han, W., et al., *Infrapatellar fat pad in the knee: is local fat good or bad for knee osteoarthritis?* Arthritis Res Ther, 2014. **16**(4): p. R145.
106. Ballegaard, C., et al., *Knee pain and inflammation in the infrapatellar fat pad estimated by conventional and dynamic contrast-enhanced magnetic resonance imaging in obese patients with osteoarthritis: a cross-sectional study*. Osteoarthritis Cartilage, 2014. **22**(7): p. 933-40.
107. Kang, H., et al., *Associations of Age, BMI, and Years of Menstruation with Proximal Femur Strength in Chinese Postmenopausal Women: A Cross-Sectional Study*. Int J Environ Res Public Health, 2016. **13**(2): p. 157.
108. Han, W., et al., *Hypointense signals in the infrapatellar fat pad assessed by magnetic resonance imaging are associated with knee symptoms and structure in older adults: a cohort study*. Arthritis Res Ther, 2016. **18**(1): p. 234.

109. Wang, J., et al., *Mass effect and signal intensity alteration in the suprapatellar fat pad: associations with knee symptoms and structure*. Osteoarthritis Cartilage, 2014. **22**(10): p. 1619-26.
110. Ioan-Facsinay, A. and M. Kloppenburg, *An emerging player in knee osteoarthritis: the infrapatellar fat pad*. Arthritis Res Ther, 2013. **15**(6): p. 225.
111. Conde, J., et al., *Identification of novel adipokines in the joint. Differential expression in healthy and osteoarthritis tissues*. PLoS One, 2015. **10**(4): p. e0123601.
112. Eymard, F., et al., *Induction of an inflammatory and prodegradative phenotype in autologous fibroblast-like synoviocytes by the infrapatellar fat pad from patients with knee osteoarthritis*. Arthritis Rheumatol, 2014. **66**(8): p. 2165-74.
113. Conde, J., et al., *Differential expression of adipokines in infrapatellar fat pad (IPFP) and synovium of osteoarthritis patients and healthy individuals*. Ann Rheum Dis, 2014. **73**(3): p. 631-3.
114. Clockaerts, S., et al., *Cytokine production by infrapatellar fat pad can be stimulated by interleukin 1beta and inhibited by peroxisome proliferator activated receptor alpha agonist*. Ann Rheum Dis, 2012. **71**(6): p. 1012-8.
115. Bastiaansen-Jenniskens, Y.M., et al., *Stimulation of fibrotic processes by the infrapatellar fat pad in cultured synoviocytes from patients with osteoarthritis: a possible role for prostaglandin f2alpha*. Arthritis Rheum, 2013. **65**(8): p. 2070-80.
116. Gross, J.B., et al., *The infrapatellar fat pad induces inflammatory and degradative effects in articular cells but not through leptin or adiponectin*. Clin Exp Rheumatol, 2017. **35**(1): p. 53-60.

117. He, J., et al., *Infrapatellar fat pad aggravates degeneration of acute traumatized cartilage: a possible role for interleukin-6*. *Osteoarthritis Cartilage*, 2017. **25**(1): p. 138-145.
118. Klein-Wieringa, I.R., et al., *Inflammatory Cells in Patients with Endstage Knee Osteoarthritis: A Comparison between the Synovium and the Infrapatellar Fat Pad*. *J Rheumatol*, 2016. **43**(4): p. 771-8.
119. Fu, Y., et al., *Effect of Aging on Adipose Tissue Inflammation in the Knee Joints of F344BN Rats*. *J Gerontol A Biol Sci Med Sci*, 2016. **71**(9): p. 1131-40.
120. Chuckpaiwong, B., et al., *Age-associated increases in the size of the infrapatellar fat pad in knee osteoarthritis as measured by 3T MRI*. *J Orthop Res*, 2010. **28**(9): p. 1149-54.
121. Pan, F., et al., *A longitudinal study of the association between infrapatellar fat pad maximal area and changes in knee symptoms and structure in older adults*. *Ann Rheum Dis*, 2015. **74**(10): p. 1818-24.
122. Tang, T., T. Muneta, and I. Sekiya, *Fibrous change of the infrapatellar fat pad due to strenuous running exercise and its treatment with intraarticular hyaluronan injection in a rat model*. *J Med Dent Sci*, 2008. **55**(1): p. 163-73.
123. Apostolaki, E., et al., *MRI appearances of the infrapatellar fat pad in occult traumatic patellar dislocation*. *Clin Radiol*, 1999. **54**(11): p. 743-7.
124. Murakami, S., et al., *Immunohistologic analysis of synovium in infrapatellar fat pad after anterior cruciate ligament injury*. *Am J Sports Med*, 1995. **23**(6): p. 763-8.
125. Zhang, J.M. and J. An, *Cytokines, inflammation, and pain*. *Int Anesthesiol Clin*, 2007. **45**(2): p. 27-37.

126. Malfait, A.M. and T.J. Schnitzer, *Towards a mechanism-based approach to pain management in osteoarthritis*. Nat Rev Rheumatol, 2013. **9**(11): p. 654-64.
127. Miller, R.E., R.J. Miller, and A.M. Malfait, *Osteoarthritis joint pain: the cytokine connection*. Cytokine, 2014. **70**(2): p. 185-93.
128. Malfait, A.M. and R.J. Miller, *Emerging Targets for the Management of Osteoarthritis Pain*. Curr Osteoporos Rep, 2016. **14**(6): p. 260-268.
129. Rechartd, M., et al., *Associations of metabolic factors and adipokines with pain in incipient upper extremity soft tissue disorders: a cross-sectional study*. BMJ Open, 2013. **3**(8): p. e003036.
130. Younger, J., et al., *Association of Leptin with Body Pain in Women*. J Womens Health (Larchmt), 2016. **25**(7): p. 752-60.
131. Perruccio, A.V., et al., *Plasma adipokine levels and their association with overall burden of painful joints among individuals with hip and knee osteoarthritis*. J Rheumatol, 2014. **41**(2): p. 334-7.
132. Cuzdan Coskun, N., et al., *Adiponectin: is it a biomarker for assessing the disease severity in knee osteoarthritis patients?* Int J Rheum Dis, 2015.
133. Massengale, M., et al., *Adipokine hormones and hand osteoarthritis: radiographic severity and pain*. PLoS One, 2012. **7**(10): p. e47860.
134. Gandhi, R., et al., *The synovial fluid adiponectin-leptin ratio predicts pain with knee osteoarthritis*. Clin Rheumatol, 2010. **29**(11): p. 1223-8.

135. Song, Y.Z., et al., *Possible Involvement of Serum and Synovial Fluid Resistin in Knee Osteoarthritis: Cartilage Damage, Clinical, and Radiological Links*. J Clin Lab Anal, 2016. **30**(5): p. 437-43.
136. Bas, S., et al., *Adipokines correlate with pain in lower limb osteoarthritis: different associations in hip and knee*. Int Orthop, 2014. **38**(12): p. 2577-83.
137. Atukorala, I., et al., *Is There a Dose-Response Relationship Between Weight Loss and Symptom Improvement in Persons With Knee Osteoarthritis?* Arthritis Care Res (Hoboken), 2016. **68**(8): p. 1106-14.
138. Henriksen, M., et al., *Is increased joint loading detrimental to obese patients with knee osteoarthritis? A secondary data analysis from a randomized trial*. Osteoarthritis Cartilage, 2013. **21**(12): p. 1865-75.
139. Messier, S.P., et al., *Effects of intensive diet and exercise on knee joint loads, inflammation, and clinical outcomes among overweight and obese adults with knee osteoarthritis: the IDEA randomized clinical trial*. JAMA, 2013. **310**(12): p. 1263-73.
140. Paans, N., et al., *Effect of exercise and weight loss in people who have hip osteoarthritis and are overweight or obese: a prospective cohort study*. Phys Ther, 2013. **93**(2): p. 137-46.
141. Christensen, R., et al., *Effect of weight maintenance on symptoms of knee osteoarthritis in obese patients: a twelve-month randomized controlled trial*. Arthritis Care Res (Hoboken), 2015. **67**(5): p. 640-50.

142. Richette, P., et al., *Benefits of massive weight loss on symptoms, systemic inflammation and cartilage turnover in obese patients with knee osteoarthritis*. *Ann Rheum Dis*, 2011. **70**(1): p. 139-44.
143. Chen, S.X., et al., *Knee osteoarthritis improvement and related biomarker profiles are sustained at 24 months following bariatric surgery*. *Osteoarthritis and Cartilage*. **25**: p. S57.
144. Bartholdy, C., et al., *The role of muscle strengthening in exercise therapy for knee osteoarthritis: A systematic review and meta-regression analysis of randomized trials*. *Semin Arthritis Rheum*, 2017. **47**(1): p. 9-21.
145. Nguyen, C., et al., *Rehabilitation (exercise and strength training) and osteoarthritis: A critical narrative review*. *Ann Phys Rehabil Med*, 2016. **59**(3): p. 190-5.
146. Allen, J., et al., *Effects of Treadmill Exercise on Advanced Osteoarthritis Pain in Rats*. *Arthritis Rheumatol*, 2017. **69**(7): p. 1407-1417.
147. Cormier, J., et al., *Exercise reverses pain-related weight asymmetry and differentially modulates trabecular bone microarchitecture in a rat model of osteoarthritis*. *Life Sci*, 2017.
148. McAlindon, T.E., et al., *OARSI guidelines for the non-surgical management of knee osteoarthritis*. *Osteoarthritis Cartilage*, 2014. **22**(3): p. 363-88.
149. Gersing, A.S., et al., *Is Weight Loss Associated with Less Progression of Changes in Knee Articular Cartilage among Obese and Overweight Patients as Assessed with MR Imaging over 48 Months? Data from the Osteoarthritis Initiative*. *Radiology*, 2017: p. 161005.

150. Anandacoomarasamy, A., et al., *Weight loss in obese people has structure-modifying effects on medial but not on lateral knee articular cartilage*. *Ann Rheum Dis*, 2012. **71**(1): p. 26-32.
151. Hunter, D.J., et al., *The Intensive Diet and Exercise for Arthritis (IDEA) trial: 18-month radiographic and MRI outcomes*. *Osteoarthritis Cartilage*, 2015. **23**(7): p. 1090-8.
152. Aaboe, J., et al., *Effects of an intensive weight loss program on knee joint loading in obese adults with knee osteoarthritis*. *Osteoarthritis Cartilage*, 2011. **19**(7): p. 822-8.
153. Messier, S.P., et al., *Weight loss reduces knee-joint loads in overweight and obese older adults with knee osteoarthritis*. *Arthritis Rheum*, 2005. **52**(7): p. 2026-32.
154. Beavers, K.M., et al., *Effects of total and regional fat loss on plasma CRP and IL-6 in overweight and obese, older adults with knee osteoarthritis*. *Osteoarthritis Cartilage*, 2015. **23**(2): p. 249-56.
155. Pogacnik Murillo, A.L., et al., *Impact of Diet and/or Exercise Intervention on Infrapatellar Fat Pad Morphology: Secondary Analysis from the Intensive Diet and Exercise for Arthritis (IDEA) Trial*. *Cells Tissues Organs*, 2017. **203**(4): p. 258-266.
156. Lavery, C.A., et al., *miR-34a(-/-) mice are susceptible to diet-induced obesity*. *Obesity (Silver Spring)*, 2016. **24**(8): p. 1741-51.
157. Pendas, A.M., et al., *Diet-induced obesity and reduced skin cancer susceptibility in matrix metalloproteinase 19-deficient mice*. *Mol Cell Biol*, 2004. **24**(12): p. 5304-13.
158. O'Connor, C.J., et al., *Increased susceptibility of Trpv4-deficient mice to obesity and obesity-induced osteoarthritis with very high-fat diet*. *Ann Rheum Dis*, 2013. **72**(2): p. 300-4.

159. Liu, J., et al., *Genetic deficiency and pharmacological stabilization of mast cells reduce diet-induced obesity and diabetes in mice*. Nat Med, 2009. **15**(8): p. 940-5.
160. Liu, S., et al., *SRA gene knockout protects against diet-induced obesity and improves glucose tolerance*. J Biol Chem, 2014. **289**(19): p. 13000-9.
161. Petersen, P.S., et al., *Immunomodulatory roles of CTRP3 in endotoxemia and metabolic stress*. Physiol Rep, 2016. **4**(5).
162. Little, C.B. and A.J. Fosang, *Is cartilage matrix breakdown an appropriate therapeutic target in osteoarthritis--insights from studies of aggrecan and collagen proteolysis?* Curr Drug Targets, 2010. **11**(5): p. 561-75.
163. Little, C.B. and D.J. Hunter, *Post-traumatic osteoarthritis: from mouse models to clinical trials*. Nat.Rev.Rheumatol., 2013. **9**(8): p. 485-497.
164. Little, C.B. and S. Zaki, *What constitutes an "animal model of osteoarthritis"--the need for consensus?* Osteoarthritis Cartilage, 2012. **20**(4): p. 261-7.
165. Verschuren, L., et al., *MIF deficiency reduces chronic inflammation in white adipose tissue and impairs the development of insulin resistance, glucose intolerance, and associated atherosclerotic disease*. Circ Res, 2009. **105**(1): p. 99-107.
166. Heard, B.J., et al., *The infrapatellar fat pad is affected by injury induced inflammation in the rabbit knee: use of dexamethasone to mitigate damage*. Inflamm Res, 2016. **65**(6): p. 459-70.
167. Ailixiding, M., et al., *Pivotal role of Sirt6 in the crosstalk among ageing, metabolic syndrome and osteoarthritis*. Biochem Biophys Res Commun, 2015. **466**(3): p. 319-26.

168. Jiang, M., et al., *Oral Administration of Resveratrol Alleviates Osteoarthritis Pathology in C57BL/6J Mice Model Induced by a High-Fat Diet*. *Mediators Inflamm*, 2017. **2017**: p. 7659023.
169. Gu, H., et al., *Oral Resveratrol Prevents Osteoarthritis Progression in C57BL/6J Mice Fed a High-Fat Diet*. *Nutrients*, 2016. **8**(4): p. 233.
170. Scotece, M., et al., *Adiponectin and leptin: new targets in inflammation*. *Basic Clin Pharmacol Toxicol*, 2014. **114**(1): p. 97-102.
171. Daghestani, H.N., C.F. Pieper, and V.B. Kraus, *Soluble macrophage biomarkers indicate inflammatory phenotypes in patients with knee osteoarthritis*. *Arthritis Rheumatol*, 2015. **67**(4): p. 956-65.
172. Furman, B.D., et al., *Targeting pro-inflammatory cytokines following joint injury: acute intra-articular inhibition of interleukin-1 following knee injury prevents post-traumatic arthritis*. *Arthritis Res Ther*, 2014. **16**(3): p. R134.
173. Kraus, V.B., et al., *Effects of intraarticular IL1-Ra for acute anterior cruciate ligament knee injury: a randomized controlled pilot trial (NCT00332254)*. *Osteoarthritis Cartilage*, 2012. **20**(4): p. 271-8.
174. Kraus, V.B., et al., *Direct in vivo evidence of activated macrophages in human osteoarthritis*. *Osteoarthritis Cartilage*, 2016. **24**(9): p. 1613-21.
175. Oliveria, S.A., et al., *Body weight, body mass index, and incident symptomatic osteoarthritis of the hand, hip, and knee*. *Epidemiology*, 1999. **10**(2): p. 161-6.
176. Urban, H. and C.B. Little, *The role of fat and inflammation in the pathogenesis and management of osteoarthritis*. *Rheumatology (Oxford)*, 2018. **57**(suppl_4): p. iv10-iv21.

177. Cuzdan Coskun, N., et al., *Adiponectin: is it a biomarker for assessing the disease severity in knee osteoarthritis patients?* Int J Rheum Dis, 2017. **20**(12): p. 1942-1949.
178. Li, S., et al., *Visceral adiposity is associated with pain, but not structural osteoarthritis.* Arthritis Rheumatol, 2020.
179. Belluzzi, E., et al., *Contribution of Infrapatellar Fat Pad and Synovial Membrane to Knee Osteoarthritis Pain.* Biomed Res Int, 2019. **2019**: p. 6390182.
180. Burda, B., et al., *Variance in infra-patellar fat pad volume: Does the body mass index matter?-Data from osteoarthritis initiative participants without symptoms or signs of knee disease.* Ann Anat, 2017. **213**: p. 19-24.
181. de Vries, R.B.M., et al., *A protocol format for the preparation, registration and publication of systematic reviews of animal intervention studies.* Evidence-based Preclinical Medicine, 2015. **2**(1): p. e00007.
182. Stang, A., *Critical evaluation of the Newcastle-Ottawa scale for the assessment of the quality of nonrandomized studies in meta-analyses.* Eur J Epidemiol, 2010. **25**(9): p. 603-5.
183. Modesti, P.A., et al., *Panethnic Differences in Blood Pressure in Europe: A Systematic Review and Meta-Analysis.* PLoS One, 2016. **11**(1): p. e0147601.
184. Guyatt, G.H., et al., *GRADE guidelines: a new series of articles in the Journal of Clinical Epidemiology.* J Clin Epidemiol, 2011. **64**(4): p. 380-2.
185. Guyatt, G.H., et al., *GRADE: an emerging consensus on rating quality of evidence and strength of recommendations.* BMJ, 2008. **336**(7650): p. 924-6.

186. Guyatt, G.H., et al., *GRADE guidelines: 4. Rating the quality of evidence--study limitations (risk of bias)*. J Clin Epidemiol, 2011. **64**(4): p. 407-15.
187. Viechtbauer, W., *Conducting Meta-Analyses in R with the metafor Package*. Journal of Statistical Software, 2010. **36**(3): p. 1-48.
188. Higgins, J.P.T. and Cochrane Collaboration, *Cochrane handbook for systematic reviews of interventions*. Second edition. ed. Cochrane book series. 2020, Hoboken, NJ: Wiley-Blackwell. pages cm.
189. Bernardo-Bueno, M.M., et al., *Stratifying Minimal Versus Severe Pain in Knee Osteoarthritis Using a Musculoskeletal Ultrasound Protocol*. J Ultrasound Med, 2019. **38**(6): p. 1411-1423.
190. Carotti, M., et al., *Relationship between magnetic resonance imaging findings, radiological grading, psychological distress and pain in patients with symptomatic knee osteoarthritis*. Radiol Med, 2017. **122**(12): p. 934-943.
191. Collins, J.E., et al., *Semiquantitative Imaging Biomarkers of Knee Osteoarthritis Progression: Data From the Foundation for the National Institutes of Health Osteoarthritis Biomarkers Consortium*. Arthritis Rheumatol, 2016. **68**(10): p. 2422-31.
192. Cowan, S.M., et al., *Infrapatellar fat pad volume is greater in individuals with patellofemoral joint osteoarthritis and associated with pain*. Rheumatol Int, 2015. **35**(8): p. 1439-42.
193. Gudbergson, H., et al., *Weight loss is effective for symptomatic relief in obese subjects with knee osteoarthritis independently of joint damage severity assessed by high-field MRI and radiography*. Osteoarthritis Cartilage, 2012. **20**(6): p. 495-502.

194. Kaukinen, P., et al., *Associations between MRI-defined structural pathology and generalized and localized knee pain - the Oulu Knee Osteoarthritis study*. *Osteoarthritis Cartilage*, 2016. **24**(9): p. 1565-76.
195. Lo, G.H., et al., *Bone marrow lesions and joint effusion are strongly and independently associated with weight-bearing pain in knee osteoarthritis: data from the osteoarthritis initiative*. *Osteoarthritis Cartilage*, 2009. **17**(12): p. 1562-9.
196. Mahler, E.A.M., et al., *Effectiveness of low-dose radiation therapy on symptoms in patients with knee osteoarthritis: a randomised, double-blinded, sham-controlled trial*. *Ann Rheum Dis*, 2019. **78**(1): p. 83-90.
197. Petersen, K.K., et al., *Sensitization and Serological Biomarkers in Knee Osteoarthritis Patients With Different Degrees of Synovitis*. *Clin J Pain*, 2016. **32**(10): p. 841-8.
198. Radojicic, M.R., et al., *Biomarker of extracellular matrix remodelling C1M and proinflammatory cytokine interleukin 6 are related to synovitis and pain in end-stage knee osteoarthritis patients*. *Pain*, 2017. **158**(7): p. 1254-1263.
199. Roemer, F.W., et al., *From Early Radiographic Knee Osteoarthritis to Joint Arthroplasty: Determinants of Structural Progression and Symptoms*. *Arthritis Care Res (Hoboken)*, 2018. **70**(12): p. 1778-1786.
200. Sofat, N., et al., *Biomarkers in Painful Symptomatic Knee OA Demonstrate That MRI Assessed Joint Damage and Type II Collagen Degradation Products Are Linked to Disease Progression*. *Front Neurosci*, 2019. **13**: p. 1016.

201. Wu, J., et al., *Associations between serum ghrelin and knee symptoms, joint structures and cartilage or bone biomarkers in patients with knee osteoarthritis*. *Osteoarthritis Cartilage*, 2017. **25**(9): p. 1428-1435.
202. Hoshino, T., et al., *Persistent synovial inflammation plays important roles in persistent pain development in the rat knee before cartilage degradation reaches the subchondral bone*. *BMC Musculoskelet Disord*, 2018. **19**(1): p. 291.
203. Inomata, K., et al., *Time course analyses of structural changes in the infrapatellar fat pad and synovial membrane during inflammation-induced persistent pain development in rat knee joint*. *BMC Musculoskelet Disord*, 2019. **20**(1): p. 8.
204. Ruan, G., et al., *Associations between serum IL-8 and knee symptoms, joint structures, and cartilage or bone biomarkers in patients with knee osteoarthritis*. *Clin Rheumatol*, 2019. **38**(12): p. 3609-3617.
205. Oo, W.M., et al., *Superb Microvascular Imaging in Low-Grade Inflammation of Knee Osteoarthritis Compared With Power Doppler: Clinical, Radiographic and MRI Relationship*. *Ultrasound Med Biol*, 2020. **46**(3): p. 566-574.
206. Loeuille, D., et al., *Magnetic resonance imaging in osteoarthritis: which method best reflects synovial membrane inflammation? Correlations with clinical, macroscopic and microscopic features*. *Osteoarthritis Cartilage*, 2009. **17**(9): p. 1186-92.
207. Hunter, D.J., et al., *Evolution of semi-quantitative whole joint assessment of knee OA: MOAKS (MRI Osteoarthritis Knee Score)*. *Osteoarthritis Cartilage*, 2011. **19**(8): p. 990-1002.

208. Fernandez-Madrid, F., et al., *Synovial thickening detected by MR imaging in osteoarthritis of the knee confirmed by biopsy as synovitis*. Magn Reson Imaging, 1995. **13**(2): p. 177-83.
209. Hunter, D.J., et al., *The reliability of a new scoring system for knee osteoarthritis MRI and the validity of bone marrow lesion assessment: BLOKS (Boston Leeds Osteoarthritis Knee Score)*. Ann Rheum Dis, 2008. **67**(2): p. 206-11.
210. Roemer, F.W., et al., *Hoffa's Fat Pad: Evaluation on Unenhanced MR Images as a Measure of Patellofemoral Synovitis in Osteoarthritis*. AJR Am J Roentgenol, 2009. **192**(6): p. 1696-700.
211. Roos, E.M. and L.S. Lohmander, *The Knee injury and Osteoarthritis Outcome Score (KOOS): from joint injury to osteoarthritis*. Health Qual Life Outcomes, 2003. **1**: p. 64.
212. Bellamy, N., et al., *Validation study of WOMAC: a health status instrument for measuring clinically important patient relevant outcomes to antirheumatic drug therapy in patients with osteoarthritis of the hip or knee*. J Rheumatol, 1988. **15**(12): p. 1833-40.
213. Zampelis, V., et al., *A simple visual analog scale for pain is as responsive as the WOMAC, the SF-36, and the EQ-5D in measuring outcomes of revision hip arthroplasty*. Acta Orthop, 2014. **85**(2): p. 128-32.
214. Dobson, F., et al., *OARSI recommended performance-based tests to assess physical function in people diagnosed with hip or knee osteoarthritis*. Osteoarthritis Cartilage, 2013. **21**(8): p. 1042-52.
215. Oehler, S., et al., *Subtyping of osteoarthritic synoviopathy*. Clin Exp Rheumatol, 2002. **20**(5): p. 633-40.

216. McNulty, M.A., et al., *A Comprehensive Histological Assessment of Osteoarthritis Lesions in Mice*. *Cartilage*, 2011. **2**(4): p. 354-63.
217. Cake, M.A., et al., *Synovial pathology in an ovine model of osteoarthritis: effect of intraarticular hyaluronan (Hyalgan)*. *Clin Exp Rheumatol*, 2008. **26**(4): p. 561-7.
218. Sanders, T.L., et al., *Incidence of Anterior Cruciate Ligament Tears and Reconstruction: A 21-Year Population-Based Study*. *Am J Sports Med*, 2016. **44**(6): p. 1502-7.
219. Nicholls, M., et al., *Nationwide study highlights a second peak in ACL tears for women in their early forties*. *Knee Surgery, Sports Traumatology, Arthroscopy*, 2018. **26**(2): p. 648-654.
220. Blaker, C.L., E.C. Clarke, and C.B. Little, *Using mouse models to investigate the pathophysiology, treatment, and prevention of post-traumatic osteoarthritis*. *J Orthop Res*, 2017. **35**(3): p. 424-439.
221. Zaki, S., et al., *Differential patterns of pathology in and interaction between joint tissues in long-term osteoarthritis with different initiating causes: phenotype matters*. *Osteoarthritis Cartilage*, 2020. **28**(7): p. 953-965.
222. Little, C.B. and M.M. Smith, *Animal Models of Osteoarthritis*. *Current Rheumatology Reviews*, 2008. **4**(3): p. 175-182.
223. Little, C.B. and S. Zaki, *What constitutes an "animal model of osteoarthritis" – the need for consensus?* *Osteoarthritis and Cartilage*, 2012. **20**(4): p. 261-267.
224. Glasson, S.S., T.J. Blanchet, and E.A. Morris, *The surgical destabilization of the medial meniscus (DMM) model of osteoarthritis in the 129/SvEv mouse*. *Osteoarthritis Cartilage*, 2007. **15**(9): p. 1061-9.

225. Christiansen, B.A., et al., *Musculoskeletal changes following non-invasive knee injury using a novel mouse model of post-traumatic osteoarthritis*. *Osteoarthritis Cartilage*, 2012. **20**(7): p. 773-82.
226. Blaker, C.L., C.B. Little, and E.C. Clarke, *Joint loads resulting in ACL rupture: Effects of age, sex, and body mass on injury load and mode of failure in a mouse model*. *J Orthop Res*, 2017. **35**(8): p. 1754-1763.
227. Gilbert, S.J., et al., *Inflammatory and degenerative phases resulting from anterior cruciate rupture in a non-invasive murine model of post-traumatic osteoarthritis*. *J Orthop Res*, 2018.
228. Satkunanathan, P.B., et al., *In vivo fluorescence reflectance imaging of protease activity in a mouse model of post-traumatic osteoarthritis*. *Osteoarthritis Cartilage*, 2014. **22**(10): p. 1461-9.
229. Poulet, B., et al., *Characterizing a novel and adjustable noninvasive murine joint loading model*. *Arthritis Rheum*, 2011. **63**(1): p. 137-47.
230. Wu, P., et al., *Early response of mouse joint tissue to noninvasive knee injury suggests treatment targets*. *Arthritis Rheumatol*, 2014. **66**(5): p. 1256-65.
231. Poulet, B., et al., *Spontaneous osteoarthritis in Str/ort mice is unlikely due to greater vulnerability to mechanical trauma*. *Osteoarthritis Cartilage*, 2013. **21**(5): p. 756-63.
232. Krieg, T., D. Abraham, and R. Lafyatis, *Fibrosis in connective tissue disease: the role of the myofibroblast and fibroblast-epithelial cell interactions*. *Arthritis Res Ther*, 2007. **9 Suppl 2**: p. S4.

233. Draghi, F., et al., *Hoffa's fat pad abnormalities, knee pain and magnetic resonance imaging in daily practice*. Insights Imaging, 2016. **7**(3): p. 373-83.
234. Scanzello, C.R., et al., *The influence of synovial inflammation and hyperplasia on symptomatic outcomes up to 2 years post-operatively in patients undergoing partial meniscectomy*. Osteoarthritis Cartilage, 2013. **21**(9): p. 1392-9.
235. Bapat, S., et al., *Pros and cons of mouse models for studying osteoarthritis*. Clin Transl Med, 2018. **7**(1): p. 36.
236. Zhang, W., et al., *EULAR evidence-based recommendations for the diagnosis of knee osteoarthritis*. Ann Rheum Dis, 2010. **69**(3): p. 483-9.
237. Smith, M.D., *The normal synovium*. Open Rheumatol J, 2011. **5**: p. 100-6.
238. Goldenberg, D.L., M.S. Egan, and A.S. Cohen, *Inflammatory synovitis in degenerative joint disease*. J Rheumatol, 1982. **9**(2): p. 204-9.
239. Soren, A., W. Klein, and F. Huth, *THE SYNOVIAL CHANGES IN POST-TRAUMATIC SONOVITIS AND OSTEOARTHRITIS*. Rheumatology, 1978. **17**(1): p. 38-45.
240. Roemer, F.W., et al., *Presence of MRI-detected joint effusion and synovitis increases the risk of cartilage loss in knees without osteoarthritis at 30-month follow-up: the MOST study*. Ann Rheum Dis, 2011. **70**(10): p. 1804-9.
241. Wang, X., et al., *The importance of synovial inflammation in osteoarthritis: current evidence from imaging assessments and clinical trials*. Osteoarthritis Cartilage, 2018. **26**(2): p. 165-174.

242. Prieto-Potin, I., et al., *Characterization of multinucleated giant cells in synovium and subchondral bone in knee osteoarthritis and rheumatoid arthritis*. BMC Musculoskelet Disord, 2015. **16**: p. 226.
243. de Lange-Brokaar, B.J., et al., *Synovial inflammation, immune cells and their cytokines in osteoarthritis: a review*. Osteoarthritis Cartilage, 2012. **20**(12): p. 1484-99.
244. Millerand, M., F. Berenbaum, and C. Jacques, *Danger signals and inflammaging in osteoarthritis*. Clin Exp Rheumatol, 2019. **37 Suppl 120**(5): p. 48-56.
245. Conaghan, P.G., et al., *MRI and non-cartilaginous structures in knee osteoarthritis*. Osteoarthritis Cartilage, 2006. **14 Suppl A**: p. A87-94.
246. Torres, L., et al., *The relationship between specific tissue lesions and pain severity in persons with knee osteoarthritis*. Osteoarthritis Cartilage, 2006. **14**(10): p. 1033-40.
247. Baker, K., et al., *Relation of synovitis to knee pain using contrast-enhanced MRIs*. Ann Rheum Dis, 2010. **69**(10): p. 1779-83.
248. Wang, X., et al., *Cross-sectional and Longitudinal Associations between Knee Joint Effusion Synovitis and Knee Pain in Older Adults*. J Rheumatol, 2016. **43**(1): p. 121-30.
249. Zhang, Y., et al., *Fluctuation of knee pain and changes in bone marrow lesions, effusions, and synovitis on magnetic resonance imaging*. Arthritis Rheum, 2011. **63**(3): p. 691-9.
250. Brown, T.D., et al., *Posttraumatic osteoarthritis: a first estimate of incidence, prevalence, and burden of disease*. J Orthop Trauma, 2006. **20**(10): p. 739-44.
251. Majewski, M., H. Susanne, and S. Klaus, *Epidemiology of athletic knee injuries: A 10-year study*. Knee, 2006. **13**(3): p. 184-8.

252. Swenson, D.M., et al., *Epidemiology of knee injuries among U.S. high school athletes, 2005/2006-2010/2011*. Med Sci Sports Exerc, 2013. **45**(3): p. 462-9.
253. Lohmander, L.S., et al., *The long-term consequence of anterior cruciate ligament and meniscus injuries: osteoarthritis*. Am J Sports Med, 2007. **35**(10): p. 1756-69.
254. Carbone, A. and S. Rodeo, *Review of current understanding of post-traumatic osteoarthritis resulting from sports injuries*. J Orthop Res, 2017. **35**(3): p. 397-405.
255. Sono, T., et al., *Perivascular Fibro-Adipogenic Progenitor Tracing during Post-Traumatic Osteoarthritis*. Am J Pathol, 2020. **190**(9): p. 1909-1920.
256. Warmink, K., et al., *High-fat feeding primes the mouse knee joint to develop osteoarthritis and pathologic infrapatellar fat pad changes after surgically induced injury*. Osteoarthritis Cartilage, 2020. **28**(5): p. 593-602.
257. Jackson, M.T., et al., *Depletion of protease-activated receptor 2 but not protease-activated receptor 1 may confer protection against osteoarthritis in mice through extracartilaginous mechanisms*. Arthritis Rheumatol, 2014. **66**(12): p. 3337-48.
258. Shu, C.C., et al., *The relationship between synovial inflammation, structural pathology, and pain in post-traumatic osteoarthritis: differential effect of stem cell and hyaluronan treatment*. Arthritis Res Ther, 2020. **22**(1): p. 29.
259. Taber, K.S., *The Use of Cronbach's Alpha When Developing and Reporting Research Instruments in Science Education*. Research in Science Education, 2018. **48**(6): p. 1273-1296.

260. Haubruck, P., et al., *Flow Cytometry Analysis of Immune Cell Subsets within the Murine Spleen, Bone Marrow, Lymph Nodes and Synovial Tissue in an Osteoarthritis Model*. J Vis Exp, 2020(158).
261. Miller, R.E., et al., *CCR2 chemokine receptor signaling mediates pain in experimental osteoarthritis*. Proc Natl Acad Sci U S A, 2012. **109**(50): p. 20602-7.
262. Dixon, W.J., *The Up-and-Down Method for Small Samples*. Journal of the American Statistical Association, 1965. **60**(312): p. 967-978.
263. Dixon, W.J., *Efficient analysis of experimental observations*. Annu Rev Pharmacol Toxicol, 1980. **20**: p. 441-62.
264. Chaplan, S.R., et al., *Quantitative assessment of tactile allodynia in the rat paw*. J Neurosci Methods, 1994. **53**(1): p. 55-63.
265. Akoglu, H., *User's guide to correlation coefficients*. Turk J Emerg Med, 2018. **18**(3): p. 91-93.
266. Cai, J., et al., *Association Between Infrapatellar Fat Pad Volume and Knee Structural Changes in Patients with Knee Osteoarthritis*. J Rheumatol, 2015. **42**(10): p. 1878-84.
267. Teichtahl, A.J., et al., *A large infrapatellar fat pad protects against knee pain and lateral tibial cartilage volume loss*. Arthritis Res Ther, 2015. **17**: p. 318.
268. Favero, M., et al., *Infrapatellar fat pad features in osteoarthritis: a histopathological and molecular study*. Rheumatology (Oxford), 2017. **56**(10): p. 1784-1793.
269. Onuma, H., et al., *Fibrotic changes in the infrapatellar fat pad induce new vessel formation and sensory nerve fiber endings that associate prolonged pain*. J Orthop Res, 2020. **38**(6): p. 1296-1306.

270. Yoon, K.H., et al., *Association of fibrosis in the infrapatellar fat pad and degenerative cartilage change of patellofemoral joint after anterior cruciate ligament reconstruction*. *Knee*, 2017. **24**(2): p. 310-318.
271. Zhang, Z., et al., *Dermal adipose tissue has high plasticity and undergoes reversible dedifferentiation in mice*. *J Clin Invest*, 2019. **129**(12): p. 5327-5342.
272. Braune, J., et al., *IL-6 Regulates M2 Polarization and Local Proliferation of Adipose Tissue Macrophages in Obesity*. *J Immunol*, 2017. **198**(7): p. 2927-2934.
273. Cho, K.W., D.L. Morris, and C.N. Lumeng, *Flow cytometry analyses of adipose tissue macrophages*. *Methods Enzymol*, 2014. **537**: p. 297-314.
274. Kratz, M., et al., *Metabolic dysfunction drives a mechanistically distinct proinflammatory phenotype in adipose tissue macrophages*. *Cell Metab*, 2014. **20**(4): p. 614-25.
275. Gandhi, R., et al., *Microarray analysis of the infrapatellar fat pad in knee osteoarthritis: relationship with joint inflammation*. *J Rheumatol*, 2011. **38**(9): p. 1966-72.
276. Macchi, V., et al., *The infrapatellar fat pad and the synovial membrane: an anatomic-functional unit*. *J Anat*, 2018. **233**(2): p. 146-154.
277. Srikanth, V.K., et al., *A meta-analysis of sex differences prevalence, incidence and severity of osteoarthritis*. *Osteoarthritis Cartilage*, 2005. **13**(9): p. 769-81.
278. Boyan, B.D., et al., *Addressing the gaps: sex differences in osteoarthritis of the knee*. *Biol Sex Differ*, 2013. **4**(1): p. 4.
279. Zhang, W., et al., *OARSI recommendations for the management of hip and knee osteoarthritis: part III: Changes in evidence following systematic cumulative update of*

- research published through January 2009. *Osteoarthritis Cartilage*, 2010. **18**(4): p. 476-99.
280. Adebayo, O.O., et al., *Kinematics of meniscal- and ACL-transected mouse knees during controlled tibial compressive loading captured using roentgen stereophotogrammetry*. *J Orthop Res*, 2017. **35**(2): p. 353-360.
281. Gregory, M.H., et al., *A review of translational animal models for knee osteoarthritis*. *Arthritis*, 2012. **2012**: p. 764621.
282. Andrianakos, A.A., et al., *Prevalence of symptomatic knee, hand, and hip osteoarthritis in Greece. The ESORDIG study*. *J Rheumatol*, 2006. **33**(12): p. 2507-13.
283. Peat, G., et al., *Clinical classification criteria for knee osteoarthritis: performance in the general population and primary care*. *Ann Rheum Dis*, 2006. **65**(10): p. 1363-7.
284. van der Kraan, P.M., *Osteoarthritis year 2012 in review: biology*. *Osteoarthritis Cartilage*, 2012. **20**(12): p. 1447-50.
285. Buckwalter, J.A., V.C. Mow, and A. Ratcliffe, *Restoration of Injured or Degenerated Articular Cartilage*. *J Am Acad Orthop Surg*, 1994. **2**(4): p. 192-201.
286. Wong, M. and D.R. Carter, *Articular cartilage functional histomorphology and mechanobiology: a research perspective*. *Bone*, 2003. **33**(1): p. 1-13.
287. Goldring, M.B. and K.B. Marcu, *Cartilage homeostasis in health and rheumatic diseases*. *Arthritis Res Ther*, 2009. **11**(3): p. 224.
288. Hardingham, T., *Extracellular matrix and pathogenic mechanisms in osteoarthritis*. *Curr Rheumatol Rep*, 2008. **10**(1): p. 30-6.

289. Garnero, P., J.C. Rousseau, and P.D. Delmas, *Molecular basis and clinical use of biochemical markers of bone, cartilage, and synovium in joint diseases*. *Arthritis Rheum*, 2000. **43**(5): p. 953-68.
290. Mononen, M.E., et al., *Alterations in structure and properties of collagen network of osteoarthritic and repaired cartilage modify knee joint stresses*. *Biomech Model Mechanobiol*, 2011. **10**(3): p. 357-69.
291. Milz, S. and R. Putz, *Quantitative morphology of the subchondral plate of the tibial plateau*. *J Anat*, 1994. **185 (Pt 1)**: p. 103-10.
292. Young, D.R., et al., *Mechanical and morphometric analysis of the third carpal bone of Thoroughbreds*. *Am J Vet Res*, 1991. **52**(3): p. 402-9.
293. Durand, M., et al., *Monocytes from patients with osteoarthritis display increased osteoclastogenesis and bone resorption: the In Vitro Osteoclast Differentiation in Arthritis study*. *Arthritis Rheum*, 2013. **65**(1): p. 148-58.
294. Findlay, D.M. and G.J. Atkins, *Osteoblast-chondrocyte interactions in osteoarthritis*. *Curr Osteoporos Rep*, 2014. **12**(1): p. 127-34.
295. Muratovic, D., et al., *Bone marrow lesions detected by specific combination of MRI sequences are associated with severity of osteochondral degeneration*. *Arthritis Res Ther*, 2016. **18**: p. 54.
296. Muratovic, D., et al., *Bone matrix microdamage and vascular changes characterize bone marrow lesions in the subchondral bone of knee osteoarthritis*. *Bone*, 2018. **108**: p. 193-201.

297. Philp, A.M., et al., *Resistin promotes the abnormal Type I collagen phenotype of subchondral bone in obese patients with end stage hip osteoarthritis*. *Sci Rep*, 2017. **7**(1): p. 4042.
298. van der Kraan, P.M. and W.B. van den Berg, *Osteophytes: relevance and biology*. *Osteoarthritis Cartilage*, 2007. **15**(3): p. 237-44.
299. Bechtold, T.E., et al., *Osteophyte formation and matrix mineralization in a TMJ osteoarthritis mouse model are associated with ectopic hedgehog signaling*. *Matrix Biol*, 2016. **52-54**: p. 339-354.
300. Xu, Z., et al., *Cartilaginous Metabolomic Study Reveals Potential Mechanisms of Osteophyte Formation in Osteoarthritis*. *J Proteome Res*, 2017. **16**(4): p. 1425-1435.
301. Andrews, S.H.J., et al., *Current concepts on structure-function relationships in the menisci*. *Connect Tissue Res*, 2017. **58**(3-4): p. 271-281.
302. Englund, M., et al., *Meniscus pathology, osteoarthritis and the treatment controversy*. *Nat Rev Rheumatol*, 2012. **8**(7): p. 412-9.
303. Hough, A.J., Jr. and R.J. Webber, *Pathology of the meniscus*. *Clin Orthop Relat Res*, 1990(252): p. 32-40.
304. Melrose, J., E.S. Fuller, and C.B. Little, *The biology of meniscal pathology in osteoarthritis and its contribution to joint disease: beyond simple mechanics*. *Connect Tissue Res*, 2017. **58**(3-4): p. 282-294.
305. Krupkova, O., et al., *The Pathobiology of the Meniscus: A Comparison Between the Human and Dog*. *Front Vet Sci*, 2018. **5**: p. 73.

306. Masaki, T., et al., *Volume change in infrapatellar fat pad is associated not with obesity but with cartilage degeneration*. J Orthop Res, 2019. **37**(3): p. 593-600.
307. Nishimuta, J.F., M.F. Bendernagel, and M.E. Levenston, *Co-culture with infrapatellar fat pad differentially stimulates proteoglycan synthesis and accumulation in cartilage and meniscus tissues*. Connect Tissue Res, 2017. **58**(5): p. 447-455.
308. Glasson, S.S., et al., *The OARSI histopathology initiative - recommendations for histological assessments of osteoarthritis in the mouse*. Osteoarthritis Cartilage, 2010. **18 Suppl 3**: p. S17-23.
309. Kwok, J., et al., *Histopathological analyses of murine menisci: implications for joint aging and osteoarthritis*. Osteoarthritis Cartilage, 2016. **24**(4): p. 709-18.
310. Hayami, T., et al., *Inhibition of cathepsin K reduces cartilage degeneration in the anterior cruciate ligament transection rabbit and murine models of osteoarthritis*. Bone, 2012. **50**(6): p. 1250-9.
311. Pritzker, K.P., et al., *Osteoarthritis cartilage histopathology: grading and staging*. Osteoarthritis Cartilage, 2006. **14**(1): p. 13-29.
312. O'Connor, K.M., *Unweighting accelerates tidemark advancement in articular cartilage at the knee joint of rats*. J Bone Miner Res, 1997. **12**(4): p. 580-9.
313. Voros, G., et al., *Expression of aggrecan(ases) during murine preadipocyte differentiation and adipose tissue development*. Biochim Biophys Acta, 2006. **1760**(12): p. 1837-44.
314. Hudetz, D., et al., *The Effect of Intra-articular Injection of Autologous Microfragmented Fat Tissue on Proteoglycan Synthesis in Patients with Knee Osteoarthritis*. Genes (Basel), 2017. **8**(10).

315. Desando, G., et al., *Regenerative Features of Adipose Tissue for Osteoarthritis Treatment in a Rabbit Model: Enzymatic Digestion Versus Mechanical Disruption*. Int J Mol Sci, 2019. **20**(11).
316. Fontanella, C.G., et al., *Investigation of biomechanical response of Hoffa's fat pad and comparative characterization*. J Mech Behav Biomed Mater, 2017. **67**: p. 1-9.
317. Murata, D., R. Fujimoto, and K. Nakayama, *Osteochondral Regeneration Using Adipose Tissue-Derived Mesenchymal Stem Cells*. Int J Mol Sci, 2020. **21**(10).
318. Griffin, M.F., et al., *Chemical group-dependent plasma polymerisation preferentially directs adipose stem cell differentiation towards osteogenic or chondrogenic lineages*. Acta Biomater, 2017. **50**: p. 450-461.
319. Guerrero, J., et al., *Fractionated human adipose tissue as a native biomaterial for the generation of a bone organ by endochondral ossification*. Acta Biomater, 2018. **77**: p. 142-154.
320. Sakaguchi, Y., et al., *Comparison of human stem cells derived from various mesenchymal tissues: superiority of synovium as a cell source*. Arthritis Rheum, 2005. **52**(8): p. 2521-9.
321. De Bari, C., F. Dell'Accio, and F.P. Luyten, *Human periosteum-derived cells maintain phenotypic stability and chondrogenic potential throughout expansion regardless of donor age*. Arthritis Rheum, 2001. **44**(1): p. 85-95.
322. do Amaral, R., et al., *Infrapatellar Fat Pad Stem Cells: From Developmental Biology to Cell Therapy*. Stem Cells Int, 2017. **2017**: p. 6843727.

323. Yue, R., et al., *Leptin Receptor Promotes Adipogenesis and Reduces Osteogenesis by Regulating Mesenchymal Stromal Cells in Adult Bone Marrow*. *Cell Stem Cell*, 2016. **18**(6): p. 782-96.
324. Histing, T., et al., *Obesity does not affect the healing of femur fractures in mice*. *Injury*, 2016. **47**(7): p. 1435-44.
325. Yamanaka, J.S., et al., *A high-fat diet can affect bone healing in growing rats*. *J Bone Miner Metab*, 2018. **36**(3): p. 255-263.
326. Smith, M.M., et al., *Significant synovial pathology in a meniscectomy model of osteoarthritis: modification by intra-articular hyaluronan therapy*. *Rheumatology (Oxford)*, 2008. **47**(8): p. 1172-8.
327. Duthon, V.B., et al., *Anatomy of the anterior cruciate ligament*. *Knee Surg Sports Traumatol Arthrosc*, 2006. **14**(3): p. 204-13.
328. Louboutin, H., et al., *Osteoarthritis in patients with anterior cruciate ligament rupture: a review of risk factors*. *Knee*, 2009. **16**(4): p. 239-44.
329. Felson, D.T., *Osteoarthritis as a disease of mechanics*. *Osteoarthritis Cartilage*, 2013. **21**(1): p. 10-5.
330. Benjamin, M., et al., *Where tendons and ligaments meet bone: attachment sites ('entheses') in relation to exercise and/or mechanical load*. *J Anat*, 2006. **208**(4): p. 471-90.
331. Madry, H., C.N. van Dijk, and M. Mueller-Gerbl, *The basic science of the subchondral bone*. *Knee Surg Sports Traumatol Arthrosc*, 2010. **18**(4): p. 419-33.

332. Pan, J., et al., *In situ measurement of transport between subchondral bone and articular cartilage*. J Orthop Res, 2009. **27**(10): p. 1347-52.
333. Li, G., et al., *Subchondral bone in osteoarthritis: insight into risk factors and microstructural changes*. Arthritis Res Ther, 2013. **15**(6): p. 223.
334. McIlroy, G.D., et al., *Female adipose tissue-specific Bsc12 knockout mice develop only moderate metabolic dysfunction when housed at thermoneutrality and fed a high-fat diet*. Sci Rep, 2018. **8**(1): p. 17863.
335. Bohnsack, M., et al., *Distribution of substance-P nerves inside the infrapatellar fat pad and the adjacent synovial tissue: a neurohistological approach to anterior knee pain syndrome*. Arch Orthop Trauma Surg, 2005. **125**(9): p. 592-7.
336. Garcia, J., et al., *Obesity does not affect the size of infrapatellar fat pad adipocytes: implications for the pathogenesis of knee osteoarthritis*. Osteoarthritis and Cartilage, 2016. **24**: p. S334-S335.
337. de Jong, A.J., et al., *Lack of high BMI-related features in adipocytes and inflammatory cells in the infrapatellar fat pad (IFP)*. Arthritis Res Ther, 2017. **19**(1): p. 186.
338. Pasco, J.A., et al., *Body mass index and measures of body fat for defining obesity and underweight: a cross-sectional, population-based study*. BMC Obes, 2014. **1**: p. 9.
339. Swainson, M.G., et al., *Prediction of whole-body fat percentage and visceral adipose tissue mass from five anthropometric variables*. PLoS One, 2017. **12**(5): p. e0177175.
340. Ashtary-Larky, D., et al., *Waist Circumference to Height Ratio: Better Correlation with Fat Mass Than Other Anthropometric Indices During Dietary Weight Loss in Different Rates*. Int J Endocrinol Metab, 2018. **16**(4): p. e55023.

341. Yang, H., et al., *Waist-to-height ratio is better than body mass index and waist circumference as a screening criterion for metabolic syndrome in Han Chinese adults.* *Medicine (Baltimore)*, 2017. **96**(39): p. e8192.
342. van Dijk, S.B., et al., *Different anthropometric adiposity measures and their association with cardiovascular disease risk factors: a meta-analysis.* *Neth Heart J*, 2012. **20**(5): p. 208-18.
343. Loeuille, D., et al., *Macroscopic and microscopic features of synovial membrane inflammation in the osteoarthritic knee: correlating magnetic resonance imaging findings with disease severity.* *Arthritis Rheum*, 2005. **52**(11): p. 3492-501.
344. Bondeson, J., et al., *The role of synovial macrophages and macrophage-produced mediators in driving inflammatory and destructive responses in osteoarthritis.* *Arthritis Rheum*, 2010. **62**(3): p. 647-57.
345. Turan, Y., et al., *Serum hyaluronan levels in patients with knee osteoarthritis.* *Clin Rheumatol*, 2007. **26**(8): p. 1293-8.
346. Hunter, D.J., et al., *Biomarkers for osteoarthritis: current position and steps towards further validation.* *Best Pract Res Clin Rheumatol*, 2014. **28**(1): p. 61-71.
347. Petersson, I.F., et al., *Radiographic osteoarthritis of the knee classified by the Ahlback and Kellgren & Lawrence systems for the tibiofemoral joint in people aged 35-54 years with chronic knee pain.* *Ann Rheum Dis*, 1997. **56**(8): p. 493-6.
348. Wirth, W., et al., *Regional analysis of femorotibial cartilage loss in a subsample from the Osteoarthritis Initiative progression subcohort.* *Osteoarthritis Cartilage*, 2009. **17**(3): p. 291-7.

349. Roemer, F.W., et al., *Semi-quantitative MRI biomarkers of knee osteoarthritis progression in the FNIH biomarkers consortium cohort - Methodologic aspects and definition of change*. BMC Musculoskelet Disord, 2016. **17**(1): p. 466.
350. Kraus, V.B., et al., *Predictive validity of biochemical biomarkers in knee osteoarthritis: data from the FNIH OA Biomarkers Consortium*. Ann Rheum Dis, 2017. **76**(1): p. 186-195.
351. Sun, S., et al., *The active form of MMP-3 is a marker of synovial inflammation and cartilage turnover in inflammatory joint diseases*. BMC Musculoskelet Disord, 2014. **15**: p. 93.
352. Tamer, T.M., *Hyaluronan and synovial joint: function, distribution and healing*. Interdiscip Toxicol, 2013. **6**(3): p. 111-25.
353. Kronmal, R.A., *Spurious Correlation and the Fallacy of the Ratio Standard Revisited*. Journal of the Royal Statistical Society. Series A (Statistics in Society), 1993. **156**(3): p. 379-392.
354. Li, S., et al., *Visceral adiposity is associated with pain, but not structural osteoarthritis*. Arthritis & Rheumatology. **n/a**(n/a).
355. Harasymowicz, N.S., et al., *Regional Differences Between Perisynovial and Infrapatellar Adipose Tissue Depots and Their Response to Class II and Class III Obesity in Patients With Osteoarthritis*. Arthritis & Rheumatology, 2017. **69**(7): p. 1396-1406.
356. Berenbaum, F., T.M. Griffin, and R. Liu-Bryan, *Review: Metabolic Regulation of Inflammation in Osteoarthritis*. Arthritis Rheumatol, 2017. **69**(1): p. 9-21.
357. Bredella, M.A., et al., *Increased bone marrow fat in anorexia nervosa*. J Clin Endocrinol Metab, 2009. **94**(6): p. 2129-36.

358. Deveza, L.A., et al., *Is synovitis detected on non-contrast-enhanced magnetic resonance imaging associated with serum biomarkers and clinical signs of effusion? Data from the Osteoarthritis Initiative*. Scand J Rheumatol, 2018. **47**(3): p. 235-242.
359. Shakoor, D., et al., *Are contrast-enhanced and non-contrast MRI findings reflecting synovial inflammation in knee osteoarthritis: a meta-analysis of observational studies*. Osteoarthritis Cartilage, 2020. **28**(2): p. 126-136.
360. Crema, M.D., et al., *Peripatellar synovitis: comparison between non-contrast-enhanced and contrast-enhanced MRI and association with pain. The MOST study*. Osteoarthritis Cartilage, 2013. **21**(3): p. 413-8.
361. Weiss, E., *Knee osteoarthritis, body mass index and pain: data from the Osteoarthritis Initiative*. Rheumatology (Oxford), 2014. **53**(11): p. 2095-9.
362. Rogers, M.W. and F.V. Wilder, *The association of BMI and knee pain among persons with radiographic knee osteoarthritis: a cross-sectional study*. BMC Musculoskelet Disord, 2008. **9**: p. 163.
363. Melrose, J., et al., *Fragmentation of decorin, biglycan, lumican and keratocan is elevated in degenerate human meniscus, knee and hip articular cartilages compared with age-matched macroscopically normal and control tissues*. Arthritis Res Ther, 2008. **10**(4): p. R79.
364. Hertzog, C., et al., *Enrichment Effects on Adult Cognitive Development: Can the Functional Capacity of Older Adults Be Preserved and Enhanced?* Psychol Sci Public Interest, 2008. **9**(1): p. 1-65.

365. Field, J., et al., *GM-CSF-induced autoimmune gastritis in interferon alpha receptor deficient mice*. J Autoimmun, 2008. **31**(3): p. 274-80.
366. Zhao, W., et al., *A conserved IFN-alpha receptor tyrosine motif directs the biological response to type I IFNs*. J Immunol, 2008. **180**(8): p. 5483-9.
367. Stine-Morrow, E.A., et al., *Self-regulated reading in adulthood*. Psychol Aging, 2008. **23**(1): p. 131-53.
368. Bennett, G.W., et al., *Search for Lorentz and CPT violation effects in Muon spin precession*. Phys Rev Lett, 2008. **100**(9): p. 091602.
369. Peterson, J.A., B.C. Yates, and M. Hertzog, *Heart and soul physical activity program: social support outcomes*. Am J Health Behav, 2008. **32**(5): p. 525-37.
370. Hertzog, M.A., *Considerations in determining sample size for pilot studies*. Res Nurs Health, 2008. **31**(2): p. 180-91.
371. Crack, P.J., et al., *The genomic profile of the cerebral cortex after closed head injury in mice: effects of minocycline*. J Neural Transm (Vienna), 2009. **116**(1): p. 1-12.
372. Altman, R., et al., *Development of criteria for the classification and reporting of osteoarthritis. Classification of osteoarthritis of the knee. Diagnostic and Therapeutic Criteria Committee of the American Rheumatism Association*. Arthritis Rheum, 1986. **29**(8): p. 1039-49.
373. Roos, E.M. and S. Toksvig-Larsen, *Knee injury and Osteoarthritis Outcome Score (KOOS) - validation and comparison to the WOMAC in total knee replacement*. Health Qual Life Outcomes, 2003. **1**: p. 17.

374. Elson, D.W., et al., *The photographic knee pain map: locating knee pain with an instrument developed for diagnostic, communication and research purposes*. *Knee*, 2011. **18**(6): p. 417-23.
375. Van Ginckel, A., et al., *Location of knee pain in medial knee osteoarthritis: patterns and associations with self-reported clinical symptoms*. *Osteoarthritis Cartilage*, 2016. **24**(7): p. 1135-42.
376. Hochman, J.R., et al., *Neuropathic pain symptoms in a community knee OA cohort*. *Osteoarthritis Cartilage*, 2011. **19**(6): p. 647-54.
377. Freynhagen, R., et al., *painDETECT: a new screening questionnaire to identify neuropathic components in patients with back pain*. *Curr Med Res Opin*, 2006. **22**(10): p. 1911-20.
378. Henry, J.D. and J.R. Crawford, *The short-form version of the Depression Anxiety Stress Scales (DASS-21): construct validity and normative data in a large non-clinical sample*. *Br J Clin Psychol*, 2005. **44**(Pt 2): p. 227-39.
379. Gill, S. and H. McBurney, *Reliability of performance-based measures in people awaiting joint replacement surgery of the hip or knee*. *Physiother Res Int*, 2008. **13**(3): p. 141-52.
380. O'Reilly, S.C., et al., *Quadriceps weakness in knee osteoarthritis: the effect on pain and disability*. *Ann Rheum Dis*, 1998. **57**(10): p. 588-94.
381. Wright, A.A., et al., *A comparison of 3 methodological approaches to defining major clinically important improvement of 4 performance measures in patients with hip osteoarthritis*. *J Orthop Sports Phys Ther*, 2011. **41**(5): p. 319-27.

382. Kuni, B., et al., *Pain threshold correlates with functional scores in osteoarthritis patients*. Acta Orthop, 2015. **86**(2): p. 215-9.
383. Goode, A.P., et al., *Associations between pressure-pain threshold, symptoms, and radiographic knee and hip osteoarthritis*. Arthritis Care Res (Hoboken), 2014. **66**(10): p. 1513-9.
384. Arendt-Nielsen, L., et al., *Sensitization in patients with painful knee osteoarthritis*. Pain, 2010. **149**(3): p. 573-81.
385. Bruyn, G.A., et al., *An OMERACT reliability exercise of inflammatory and structural abnormalities in patients with knee osteoarthritis using ultrasound assessment*. Ann Rheum Dis, 2016. **75**(5): p. 842-6.
386. Young, A.A., et al., *Dynamic biomechanics correlate with histopathology in human tibial cartilage: a preliminary study*. Clin Orthop Relat Res, 2007. **462**: p. 212-20.
387. Young, A.A., et al., *Regional assessment of articular cartilage gene expression and small proteoglycan metabolism in an animal model of osteoarthritis*. Arthritis Res Ther, 2005. **7**(4): p. R852-61.
388. Fuller, E.S., et al., *Zonal differences in meniscus matrix turnover and cytokine response*. Osteoarthritis Cartilage, 2012. **20**(1): p. 49-59.
389. Crilly, A., et al., *PAR(2) expression in peripheral blood monocytes of patients with rheumatoid arthritis*. Ann Rheum Dis, 2012. **71**(6): p. 1049-54.
390. Kramski, M., et al., *Role of monocytes in mediating HIV-specific antibody-dependent cellular cytotoxicity*. J Immunol Methods, 2012. **384**(1-2): p. 51-61.

391. Jeong, J.H., et al., *CD14(+) Cells with the Phenotype of Infiltrated Monocytes Consist of Distinct Populations Characterized by Anti-inflammatory as well as Pro-inflammatory Activity in Gouty Arthritis*. *Front Immunol*, 2017. **8**: p. 1260.
392. Gjelstrup, M.C., et al., *Subsets of activated monocytes and markers of inflammation in incipient and progressed multiple sclerosis*. *Immunol Cell Biol*, 2018. **96**(2): p. 160-174.
393. Boyette, L.B., et al., *Phenotype, function, and differentiation potential of human monocyte subsets*. *PLoS One*, 2017. **12**(4): p. e0176460.
394. Wildgruber, M., et al., *The "Intermediate" CD14(++)CD16(+) monocyte subset increases in severe peripheral artery disease in humans*. *Sci Rep*, 2016. **6**: p. 39483.
395. Fadini, G.P., et al., *Monocyte-macrophage polarization balance in pre-diabetic individuals*. *Acta Diabetol*, 2013. **50**(6): p. 977-82.
396. Fadini, G.P., et al., *An unbalanced monocyte polarisation in peripheral blood and bone marrow of patients with type 2 diabetes has an impact on microangiopathy*. *Diabetologia*, 2013. **56**(8): p. 1856-66.
397. Fadini, G.P., et al., *Pro-inflammatory monocyte-macrophage polarization imbalance in human hypercholesterolemia and atherosclerosis*. *Atherosclerosis*, 2014. **237**(2): p. 805-8.
398. Kundu-Raychaudhuri, S., C. Abria, and S.P. Raychaudhuri, *IL-9, a local growth factor for synovial T cells in inflammatory arthritis*. *Cytokine*, 2016. **79**: p. 45-51.
399. Autissier, P., et al., *Evaluation of a 12-color flow cytometry panel to study lymphocyte, monocyte, and dendritic cell subsets in humans*. *Cytometry A*, 2010. **77**(5): p. 410-9.

400. Heath, W.R., *T Lymphocytes*, in *Encyclopedia of Immunology (Second Edition)*, P.J. Delves, Editor. 1998, Elsevier: Oxford. p. 2341-2343.
401. Lurati, A., et al., *Effects of hyaluronic acid (HA) viscosupplementation on peripheral Th cells in knee and hip osteoarthritis*. *Osteoarthritis Cartilage*, 2015. **23**(1): p. 88-93.
402. Toldi, G., et al., *Human Th1 and Th2 lymphocytes are distinguished by calcium flux regulation during the first 10 min of lymphocyte activation*. *Immunobiology*, 2012. **217**(1): p. 37-43.
403. Silva, M.T., et al., *Severity of atopic dermatitis and Ascaris lumbricoides infection: an evaluation of CCR4+ and CXCR3+ helper T cell frequency*. *Rev Soc Bras Med Trop*, 2012. **45**(6): p. 761-3.
404. Musha, H., et al., *Selective infiltration of CCR5(+)CXCR3(+) T lymphocytes in human colorectal carcinoma*. *Int J Cancer*, 2005. **116**(6): p. 949-56.
405. Ramesh, R., et al., *Pro-inflammatory human Th17 cells selectively express P-glycoprotein and are refractory to glucocorticoids*. *J Exp Med*, 2014. **211**(1): p. 89-104.
406. Komatsu, N., et al., *Pathogenic conversion of Foxp3+ T cells into TH17 cells in autoimmune arthritis*. *Nat Med*, 2014. **20**(1): p. 62-8.
407. Oo, Y.H., et al., *CXCR3-dependent recruitment and CCR6-mediated positioning of Th-17 cells in the inflamed liver*. *J Hepatol*, 2012. **57**(5): p. 1044-51.
408. Kusano, J., et al., *Vitamin K1 and Vitamin K2 immunopharmacological effects on the peripheral lymphocytes of healthy subjects and dialysis patients, as estimated by the lymphocyte immunosuppressant sensitivity test*. *J Clin Pharm Ther*, 2018.

409. Huang, S., W. Wang, and L. Chi, *Feasibility of up-regulating CD4(+)CD25(+) Tregs by IFN-gamma in myasthenia gravis patients*. BMC Neurol, 2015. **15**: p. 163.
410. Hardy, M.Y., et al., *A flow cytometry based assay for the enumeration of regulatory T cells in whole blood*. J Immunol Methods, 2013. **390**(1-2): p. 121-6.
411. Krenn, V., et al., *Grading of chronic synovitis--a histopathological grading system for molecular and diagnostic pathology*. Pathol Res Pract, 2002. **198**(5): p. 317-25.
412. Zachar, V., J.G. Rasmussen, and T. Fink, *Isolation and growth of adipose tissue-derived stem cells*. Methods Mol Biol, 2011. **698**: p. 37-49.
413. Pilgaard, L., et al., *Comparative analysis of highly defined proteases for the isolation of adipose tissue-derived stem cells*. Regen Med, 2008. **3**(5): p. 705-15.
414. Doornaert, M., et al., *Xenogen-free isolation and culture of human adipose mesenchymal stem cells*. Stem Cell Res, 2019. **40**: p. 101532.
415. Wankhade, U.D. and S.G. Rane, *Flow Cytometry Assisted Isolation of Adipose Tissue Derived Stem Cells*. Methods Mol Biol, 2017. **1566**: p. 17-24.
416. Smith, M.M., et al., *A hexadecylamide derivative of hyaluronan (HYMOVIS(R)) has superior beneficial effects on human osteoarthritic chondrocytes and synoviocytes than unmodified hyaluronan*. J Inflamm (Lond), 2013. **10**: p. 26.
417. Karsten, E., E. Breen, and B.R. Herbert, *Red blood cells are dynamic reservoirs of cytokines*. Sci Rep, 2018. **8**(1): p. 3101.
418. Reddy, G., et al., *Can the Surgical Approach to Total Knee Arthroplasty Influence Early Postoperative Outcomes? - A Comparative Study between Trivector and Medial Parapatellar Approaches*. Int J Appl Basic Med Res, 2020. **10**(1): p. 25-29.

419. David, K.A., et al., *Surgical procedures and postsurgical tissue processing significantly affect expression of genes and EGFR-pathway proteins in colorectal cancer tissue*. *Oncotarget*, 2014. **5**(22): p. 11017-28.
420. Jewell, S.D., et al., *Analysis of the molecular quality of human tissues: an experience from the Cooperative Human Tissue Network*. *Am J Clin Pathol*, 2002. **118**(5): p. 733-41.
421. Thoma, A., et al., *Practical tips for surgical research: how to optimize patient recruitment*. *Can J Surg*, 2010. **53**(3): p. 205-10.
422. Cook, J.A., *The challenges faced in the design, conduct and analysis of surgical randomised controlled trials*. *Trials*, 2009. **10**: p. 9.
423. Thoma, A., et al., *How to optimize patient recruitment*. *Canadian Journal of Surgery*, 2010. **53**(3): p. 205-210.
424. Thomas, A.J., et al., *Recruitment and screening for a randomized trial investigating Roux-en-Y gastric bypass versus intensive medical management for treatment of type 2 diabetes*. *Obes Surg*, 2014. **24**(11): p. 1875-80.
425. Panageas, K.S., et al., *The effect of clustering of outcomes on the association of procedure volume and surgical outcomes*. *Ann Intern Med*, 2003. **139**(8): p. 658-65.
426. Singh, J.A., et al., *Hospital volume and surgical outcomes after elective hip/knee arthroplasty: a risk-adjusted analysis of a large regional database*. *Arthritis Rheum*, 2011. **63**(8): p. 2531-9.
427. Mutter, G.L., et al., *Comparison of frozen and RNALater solid tissue storage methods for use in RNA expression microarrays*. *BMC Genomics*, 2004. **5**(1): p. 88.

428. Kidd, T.J., et al., *Multi-centre research in Australia: analysis of a recent National Health and Medical Research Council-funded project*. *Respirology*, 2009. **14**(7): p. 1051-5.
429. Hunter, D.J., J.J. McDougall, and F.J. Keefe, *The symptoms of osteoarthritis and the genesis of pain*. *Rheum Dis Clin North Am*, 2008. **34**(3): p. 623-43.
430. Vincent, T.L., et al., *Mapping pathogenesis of arthritis through small animal models*. *Rheumatology*, 2012. **51**(11): p. 1931-1941.
431. Noble, W.S., *How does multiple testing correction work?* *Nature Biotechnology*, 2009. **27**(12): p. 1135-1137.
432. Kennedy, J.C., I.J. Alexander, and K.C. Hayes, *Nerve supply of the human knee and its functional importance*. *Am J Sports Med*, 1982. **10**(6): p. 329-35.
433. Woolf, S.H., *The meaning of translational research and why it matters*. *JAMA*, 2008. **299**(2): p. 211-3.
434. Fontanarosa, P.B. and C.D. DeAngelis, *Basic science and translational research in JAMA*. *JAMA*, 2002. **287**(13): p. 1728.
435. Tormalehto, S., et al., *Eight-year trajectories of changes in health-related quality of life in knee osteoarthritis: Data from the Osteoarthritis Initiative (OAI)*. *PLoS One*, 2019. **14**(7): p. e0219902.
436. Nayak, B.K., *Understanding the relevance of sample size calculation*. *Indian J Ophthalmol*, 2010. **58**(6): p. 469-70.
437. Moher, D., C.S. Dulberg, and G.A. Wells, *Statistical power, sample size, and their reporting in randomized controlled trials*. *Jama*, 1994. **272**(2): p. 122-4.

438. Sharkey, M., *The challenges of assessing osteoarthritis and postoperative pain in dogs*. AAPS J, 2013. **15**(2): p. 598-607.
439. Sainani, K.L., *The problem of multiple testing*. PM R, 2009. **1**(12): p. 1098-103.
440. Nichols, T.E., *Multiple testing corrections, nonparametric methods, and random field theory*. Neuroimage, 2012. **62**(2): p. 811-5.